

**IMPROVING PERFORMANCE OF DISCHARGE  
EQUIPMENT FOR COALS WITH POOR HANDLING  
CHARACTERISTICS**

by

**KAROL ARIZA-ZAFRA**

This thesis is submitted in partial fulfilment of the requirements for the award of the Degree of Doctor of Philosophy under the conditions of the award of higher degrees of the University of Greenwich

This research was undertaken at the Wolfson Centre for Bulk Solids Handling Technology in collaboration with the British Coal Utilization Research Association (BCURA)

April 2015

## DECLARATION

---

I certify that this work has not been accepted in substance for any degree, and is not concurrently being submitted for any degree other than that of Doctor of Philosophy being studied at the University of Greenwich. It is also declared that this work is the result of my own investigations except where otherwise identified by references and that I have not plagiarised the work of others. Please note that some extracts of this thesis, data, analysis and figures have been included as part of internal reports for the University of Greenwich, the industrial sponsor (BCURA) and the publications arising from the project:

K. Ariza-Zafra, R.J. Berry and M. Bradley, Review of Models for Predicting the Discharge Rates of Bulk Particulates from Silos and Bins. Proceedings of RELPOFLOW IV, 2008.

R.J. Berry, M.S.A. Bradley, K. Ariza-Zafra, Interpretation of Stick-Slip Powder Flowability Measurements, 6th International Conference for Conveying and Handling of Particulate Solids, Brisbane, Australia, 3rd - 7th August 2009.

K. Ariza-Zafra, R.J. Berry, M. Bradley and J. Santana, Study of Discharge Behaviour in a Silo Retrofitted with Flow-Promoting Inserts. Proceedings of WCPT6, 2010.

K. Ariza-Zafra, R.J. Berry and M. Bradley, Achieving Mass Flow in Silos with Shallow Converging Sections Using Inverted Cones. Proceedings of Bulk Solids Europe, 2010.

---

Karol Ariza-Zafra, Candidate

---

Dr Robert Berry, First Supervisor

---

Professor Michael Bradley, Second Supervisor

## ACKNOWLEDGEMENTS

---

Acknowledgement is made to the British Coal Utilisation Research Association and the UK Department of Trade and Industry for a grant in aid of this research, but the views expressed are those of the author, and not necessarily those of BCURA or the Department of Trade and Industry. I would also like to thank my industrial supervisor Dr Ruth Poultney for her guidance and her effort to make this project as enriching as possible for me.

I would like to thank the staff of the Wolfson Centre not just for their support and knowledge but more important for becoming my family from the moment I first arrived. To Rob for all his help and always being there for me to the last second of every deadline. To Mike for believing in me and being always willing to share his knowledge. To Richard for making me a better engineer and also being there as a friend. To Caroline for everything, life would have been a lot more difficult and less enjoyable without her. To Jon, Trevor and Jose for all their help and friendship. And to Oscar my great friend who introduced me to the Wolfson Centre and has always been there no matter what.

Finally, I would like to thank my parents and my brother for all their affection, support and always believing in me. And to my beautiful wife Emiliana, for her patience on the long and lonely hours, her encouragement in the difficult moments and her love at all times.

## ABSTRACT

---

The accepted design techniques for bulk solids handling equipment are frequently overlooked during the installation of industrial process plants. As a result, flow unreliability is often observed in silos in the form of flow stoppages, product bulk density variations, formation of rat-holes, flushing, flooding and product segregation. In most cases when these problems are detected in silos, they are the result of a discharge pattern known as core flow, where localised flow channels promote the preferential draw of material from certain zones of the silo, with the rest of the material remaining stagnant. Coal handling is not the exception and process equipment is not always designed to cope with the often variable characteristics of the coal, which is frequently processed in a large variety of forms, with particle sizes ranging from fine dust to a top size several inches and other parameter like moisture content varying from completely dry to dripping wet.

In order to solve the problems caused by core flow, the discharge behaviour of the silo needs to be modified to produce a uniform movement of all the material, to achieve a flow pattern known as mass flow. Static inserts have been proved to be an effective method of modifying the discharge patterns in silos, but their use and design procedures are not well understood or are well hidden behind patents and trade secrecy. This research project aims to produce practical guidelines for the design and positioning of static insert to improve flow in silos.

The work presented in this thesis follows an experimental approach where the performance of an insert is first evaluated at bench scale in a 3 litre model silo and then validated at semi-industrial scale in a 400 litre test rig. The bench scale model allows the evaluation of numerous changes in insert morphology and positioning at relatively low costs, facilitating the development of practical rules for their design. Following this approach a design procedure for inverted cone inserts is proposed as a modification of a method developed by J. Johanson [Johanson, 1965]. A performance comparison was undertaken both at bench and semi-industrial scales with inserts designed following Johanson's method and the modified method proposed by the author. The results

showed that both inserts were capable of producing mass flow in an otherwise core flow silo, but the modified insert produced more consistent results, particularly with lower heights of powder bed.

This experimental approach was also followed to develop a novel type of insert called open double cone which maximizes the area of influence of the insert inside the silo facilitating flow. For this insert, three design procedures were proposed with each of them producing inserts capable of achieving mass flow in the bench scale model. The main difference between the inserts produced by the three procedures, was the size of the insert in relation to the volume of the silo hopper. In a similar way, two procedures were also proposed for the design of double cone inserts, with the resulting inserts capable of achieving mass flow in the bench scale silo. Then, a prototype of an inverted cone designed with the modified method, a prototype of the open double cone and a prototype of a double cone were tested in the semi-industrial scale test rig. The results at both scales showed that the open double cone and the double cone inserts outperformed the inverted cone, by producing more uniform velocity profiles across the silo and also producing more consistent flow rates. Although the performance between the open double cone and the double cone was very similar, the open double cone was more consistent in producing flatter velocity profiles and also the double cone was more prone to produce slightly off centre discharges.

The procedures proposed for insert design provide the tools needed to apply insert technology to industrial processes. This is demonstrated with the design of double cones which successfully eliminated rat-holing problems in conical silos from an industrial pneumatic conveying system. The bench scale methodology is also employed to try to solve flow unreliability issues experienced in an industrial coal silo. For this case, a bespoke type of insert was developed to respond to the complex geometry and mode of operation of the silo. The proposed insert produced very positive results at bench and semi-industrial scales, laying the bases for a solution for the full scale silo.

# CONTENTS

---

<b>DECLARATION.....</b>	<b>II</b>
<b>ACKNOWLEDGEMENTS.....</b>	<b>III</b>
<b>ABSTRACT .....</b>	<b>IV</b>
<b>CONTENTS.....</b>	<b>VI</b>

## **CHAPTER ONE: INTRODUCTION**

1.1	Project Objectives .....	2
1.2	Project Overview .....	2

## **CHAPTER TWO: LITERATURE REVIEW**

2.1	Silo Discharge Patterns .....	4
2.1.1	Mass Flow .....	5
2.1.2	Core Flow .....	7
2.1.3	Mixed Flow .....	9
2.2	Effect of Discharge Patterns on Wall Stresses.....	10
2.3	Bulk Solids Handling Problems and their Relationship to Discharge Patterns .....	14
2.4	The Use of Inserts .....	20
2.4.1	Inverted Cones .....	20
2.4.2	Flat Plates .....	25
2.4.3	Cone in Cone.....	26
2.4.4	Double Cone .....	28
2.4.5	V Tents .....	29
2.4.6	Discharge Tubes.....	30
2.4.7	Internal Divisions .....	33
2.4.8	Wall Liners.....	34
2.4.9	Twisted Tape .....	34

2.4.10	Other Inserts .....	35
2.5	Insert Design for Flow Promotion .....	37
2.5.1	Design of Inverted Cones as Flow Promotion Devices for Discharging Bulk Solids .....	39
2.5.1.1	Johanson Design Method for Insert Placement.....	45
2.5.2	Design of Cone in Cone Inserts as Flow Promotion Devices for Discharging Bulk Solids .....	52
2.5.2.1	Johanson's Design Method .....	56
2.5.2.2	Enstad's Design Method .....	59
2.5.3	Design of Double Cone Inserts as Flow Promotion Devices for Discharging Bulk Solids .....	62
2.6	Loads on Inserts .....	64
2.6.1	Stress Analysis in a Vertical Channel .....	66
2.6.2	Calculation of Vertical Stress.....	68
2.6.3	Calculation of Total Vertical Force.....	70
2.7	Impact of the Literature Review on the Objectives of the Project.....	71
2.8	Summary .....	72

### **CHAPTER THREE: EARLY TEST RIG DEVELOPMENT**

3.1	Test Rig design and Construction .....	75
3.2	Commissioning of the Test Rig .....	78
3.3	Results and Discussion .....	79
3.3.1	Flow Behaviour Observed During Discharge .....	79
3.3.2	Influence of the height of the Vertical Section on the Stress Distribution.....	84
3.3.3	Insert Load Measurement.....	85
3.3.4	Vertical Load at the Outlet.....	97
3.4	Summary .....	97

### **CHAPTER FOUR: STUDY OF INVERTED CONES AS FLOW PROMOTION INSERTS AT BENCH AND SEMI-INDUSTRIAL SCALES**

4.1	Semi-Industrial Test Rig Design and Construction .....	99
4.1.1	Vertical Section .....	100

4.1.2	Converging Section .....	103
4.1.3	Discharge Pattern Tracer System .....	103
4.1.4	Inserts .....	105
4.2	Bench Scale Model for Insert Development.....	108
4.2.1	Design and Construction .....	109
4.2.2	Insert Design .....	110
4.2.3	Test Method and Results.....	113
4.2.4	Modified Method for the Design of Inverted Cone Inserts.....	116
4.3	Commissioning of the Semi-Industrial Test Rig .....	119
4.3.1	Silo Allowed to Drain After Filling .....	119
4.3.2	Silo with additional material fed during discharge .....	121
4.4	Results and Discussion .....	121
4.4.1	Expected Results .....	121
4.4.2	Silo Allowed to Drain After Filling .....	124
4.4.3	Silo with additional material fed during discharge .....	132
4.4.4	Vertical Load Acting on the Cylindrical Section of the Bin.....	137
4.4.5	Vertical Load Acting on the Inserts .....	142
4.5	Summary .....	145

**CHAPTER FIVE: INSERT CONFIGURATION TO OPTIMIZE DISCHARGE FROM SILOS: A STUDY AT BENCH AND SEMI-INDUSTRIAL SCALES**

5.1	Bench Scale Test Rig Modification .....	147
5.2	Initial Steps in Insert Development .....	150
5.2.1	Concentric Cylinders.....	150
5.2.2	Concentric Cylinders with Inverted Cone.....	152
5.2.3	Concentric Truncated Cones with Inverted Cone .....	152
5.3	Open Double Cones – The Proposal of a Novel Type of Static Insert .....	154
5.3.1	Evaluation of Cone in Cone Inserts .....	156
5.3.2	Open Double Cone Insert: First Generation.....	161
5.3.3	Open Double Cone Insert: Second Generation .....	165
5.3.4	Open Double Cone Insert: Third Generation.....	168
5.4	Double Cone Inserts.....	172

5.4.1	Double Cone Inserts: First Generation.....	173
5.4.2	Double Cone Inserts: Second Generation .....	176
5.5	Performance Comparison at Bench Scale.....	179
5.6	Performance Evaluation of Inserts at Semi-Industrial Scale .....	189
5.6.1	Test Material .....	189
5.6.2	Test Rig .....	190
5.6.3	Inserts .....	190
5.6.3.1	Inverted Cone .....	191
5.6.3.2	Open Double Cone .....	191
5.6.3.3	Double Cone .....	192
5.6.4	Test Method .....	193
5.6.5	Results and Discussion.....	194
5.7	Summary .....	203

## **CHAPTER SIX: INDUSTRIAL APPLICATIONS**

6.1	Granular Coal Silo with Multiple Outlets.....	205
6.1.1	Description of the Process.....	205
6.1.2	Product Quality Study .....	207
6.1.3	Proposed Feeding Interface Solutions.....	209
6.1.4	Study at Bench-Scale .....	212
6.1.4.1	Bench-Scale Model Fabrication.....	212
6.1.4.2	Half Silo Test Rig .....	213
6.1.4.3	Complete Silo Test Rig .....	215
6.1.5	Insert Validation at 1:10 Scale .....	221
6.1.5.1	Test Rig Description .....	221
6.1.5.2	Test Material .....	222
6.1.5.3	Test Procedure.....	223
6.1.5.4	Results and Discussion.....	225
6.2	Rat-Holing in Conical Hopper .....	242
6.2.1	Description of the Process.....	242
6.2.2	Insert Design .....	243
6.2.3	Problems Encountered with the Performance of the Inserts .....	245
6.2.3.1	Incorrect Insert support .....	245

6.2.3.2	Chemical Attack to Insert Surface .....	248
6.3	Low Headroom Drum Tipper .....	249
6.3.1	Description of the Process.....	249
6.3.2	Drum Tipper and Insert Design.....	250
6.4	Summary .....	254
<b>CHAPTER SEVEN: CONCLUSIONS .....</b>		<b>256</b>
<b>CHAPTER EIGHT: RECOMMENDATIONS FOR FURTHER WORK.....</b>		<b>265</b>
<b>NOMENCLATURE.....</b>		<b>266</b>
<b>GLOSSARY.....</b>		<b>268</b>
<b>REFERENCES.....</b>		<b>271</b>
<b>APPENDIX.....</b>		<b>ERROR! BOOKMARK NOT DEFINED.</b>

## CHAPTER ONE: INTRODUCTION

---

Some coals handled in the UK have variable or poor flow properties, owing to near-critical moisture contents and/or substantial fines contents. Unreliable flow and variable discharge rates are commonplace when handling these coals through existing equipment, much of which was not designed using the appropriate techniques for determining optimum plant geometry. Inappropriate silo design often results in the granular material discharging through a flow channel above the outlet of the silo, creating stagnant zones near the walls. This type of discharge is known as core flow and is in most cases, the cause of the problems mentioned above. To obtain best results in terms of reliability and consistency, it is desirable for the solids to discharge in a mass flow pattern. In this type of flow pattern, the solids slip at the walls of the silo and there is an even movement throughout the cross section of the bin. Achieving mass flow eliminates the formation of ratholes and dead regions in the hopper, minimizes segregation, produces fairly constant values of bulk density eliminating flooding and flushing, plus smaller hopper outlets can be used without creating flow stoppages. Whereas the drawbacks include reduced storage capacity within given headroom values and higher wear on the silo walls due to the shearing of the material.

Although through the use of standard techniques it is possible to ensure silos are designed to discharge in mass flow and cope with any given set of flow properties, the redesign and rebuilding of existing hoppers and associated equipment are rarely justifiable on economic grounds. It is therefore desirable to have available a range of retro-fit techniques which can be applied to existing silos (and designed into new equipment), to enable the handling of coals with a wider range of flow properties. Research on the use of static inserts inside bunkers has shown them to be a simple and cost-effective retro-fit method to improve discharge, by modifying the discharge pattern developed in the silo. They consume no energy and have little to go wrong, compared with mechanical flow-assisting devices. However, in most cases there are no quantitative-based guidelines for the selection of the size, shape or position of the insert that could maximize the benefits produced.

## **1.1 Project Objectives**

- To develop an understanding that supports the use of inserts in existing storage silos to improve discharge performance, allowing them to handle coals that exhibit problematic flow properties reliably.
- To develop practical procedures for the design and installation of static inserts for the promotion of flow in bulk solids handling equipment.

## **1.2 Project Overview**

The work presented in this thesis is based on a practical approach for the development of static insert technology using coal and other bulk solids. The thesis is divided in six chapters as follows:

Chapter 1 presents the project objectives and thesis structure

Chapter 2 presents a review of the current state of insert technology. The chapter introduces the types of flow patterns developed in silos during discharge as well as advantages and disadvantages of each of them. Then an overview is presented of the most common types of inserts and their applications. The focus is then placed on static inserts for the flow promotion of bulk solids, where a review is presented on the existing methods and research studies for the design and positioning of the inserts.

Chapter 3 describes the first practical steps undertaken for the study of the flow promoting properties of static inserts. The chapter includes the construction and commissioning of a test rig for the study of the performance of flat plate inserts using granular coal as test material.

Chapter 4 introduces the design of a bench scale model for the development of static inserts and proposal of a methodology for the design of inverted cone inserts. The chapter also describes the construction of a test rig at semi-industrial scale which was then used to validate the results obtained at bench scale and the evaluation of the design method proposed.

Chapter 5 describes the development of a novel type of insert called open double cone, presents three practical procedures for their design and positioning in a silo as well as the experimental validation of these procedures at bench scale. Two procedures are also presented for the design and positioning of double cone inserts as well as the experimental validation at bench scale. Then, the performances of inverted cones, open double cones and double cones are compared at semi-industrial scale by testing a prototype of each type of insert.

Chapter 6 presents three industrial case studies where the knowledge developed through this project is applied. In the first case study, a trouser leg insert is developed to try to improve the discharge and product quality consistency of an industrial coal silo featuring multiple outlets. In the second case study, double cone inserts are installed to eliminate rat-holing problems observed in conical silos. Finally, in the third case study, a drum tipper is designed including a double cone insert to produce reliable flow in a plant with very restricted headroom.

## CHAPTER TWO: LITERATURE REVIEW

---

This chapters presents an overview of the discharge behaviour of bulk solids in silos and the impact that static inserts can have on that behaviour. A review of the most common types of inserts and their applications is also presented as well as the current state on insert technology for flow promotion.

### 2.1 Silo Discharge Patterns

Some of the earliest studies that classify the discharge patterns in a silo were made by Takhtamishev between 1938 and 1941 (Ravenet, 1977, Sudgen, 1980). According to his observations, Takhtamishev defined two types of flow patterns depending on the profile evolution of the upper surface of the material in the silo during discharge. From this he concluded that the pattern developed during discharge was a consequence of the method used for filling the silo. He explained that when the silo was “gently” filled (minimizing the compaction of the particles) the material slid at the wall and the upper surface did not change during discharge, he called this pattern dynamic flow (see Figure 2.1). When the material achieved a higher compaction during filling, there was not movement in the vicinity of the wall and a conical depression formed in the upper surface during discharge. He called this type of pattern non-dynamic flow (see Figure 2.1).

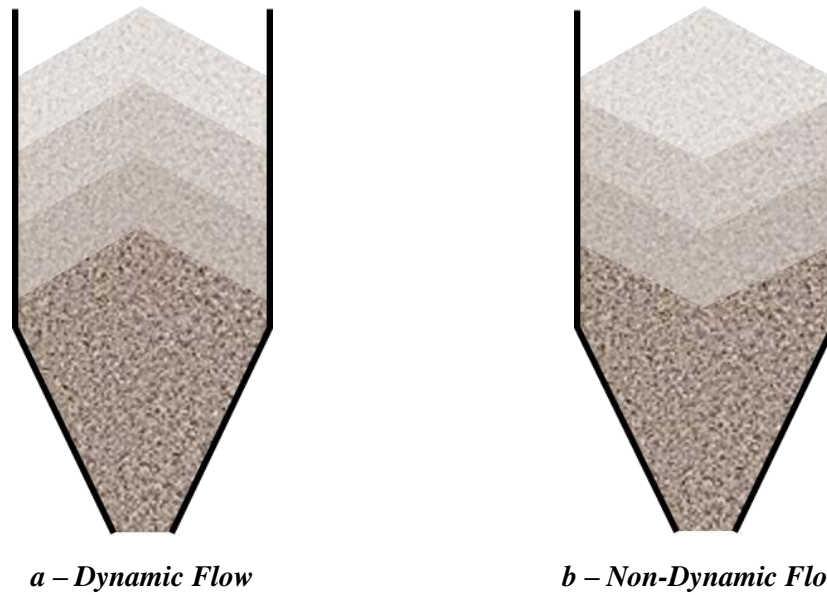


**Figure 2.1** *Profile Evolution of the Upper Surface of a Silo During Discharge*

Dynamic and non-dynamic flow patterns are better known as mass flow and core flow respectively, terms made popular by the work of A. Jenike in the sixties (Jenike, 1961 and Jenike, 1964). Jenike’s work forms the basis for the current theories of gravity flow of bulk solids, and the concepts of core flow and mass flow play a key role in Jenike’s work. For Jenike, the reason behind the development of a particular flow pattern is the interaction between the characteristics of the material, the geometry of the silo and the frictional properties between the bulk solid and the walls of the silo.

### **2.1.1 Mass Flow**

The concept of mass flow in a discharging silo is based on a very simple principle: “all particles must remain in motion at all times during discharge”. Even if this statement sounds extremely simplistic, it has powerful implications over the phenomenological behaviour of the bulk contents of the silo, furthermore, most of the characteristics commonly attributed to mass flow can be derived from it.

As it was mentioned above, a flow pattern is the result of an interaction between the geometry of the silo, the properties of the material and the frictional properties between the material and the walls of the silo. For mass flow to occur, the walls of

the silo must be steep and smooth enough to allow the material to move at that boundary (and not to contradict the definition). When slipping at the wall is achieved, stagnant zones inside the silo are eliminated and the whole contents of the silo become “live” (see Figure 2.2a)

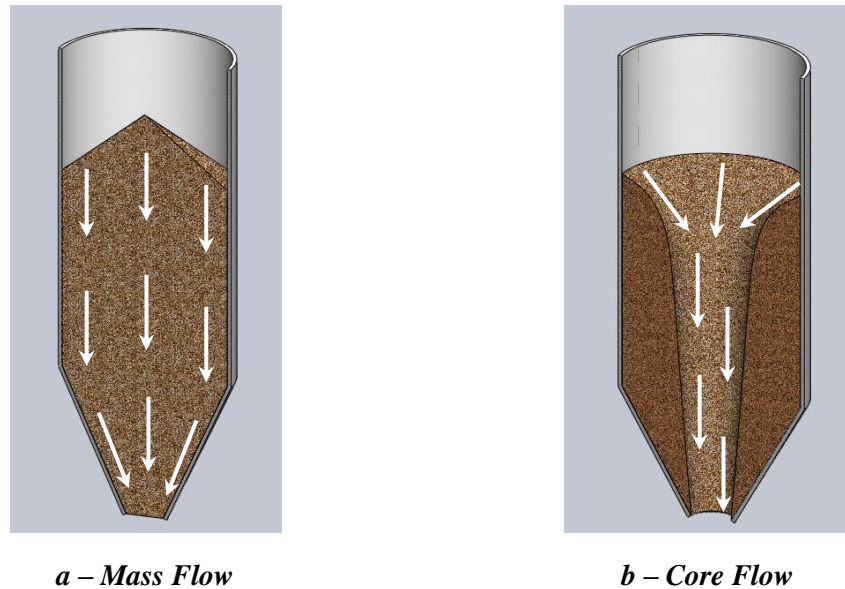
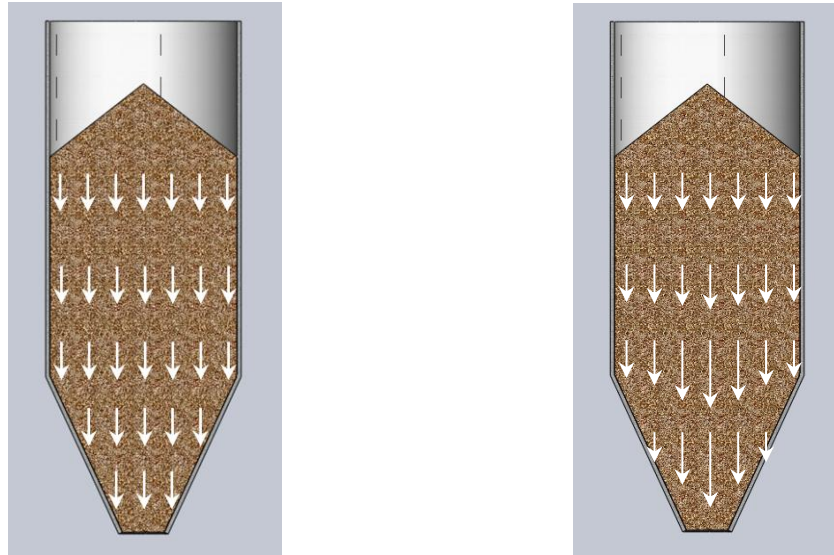


**Figure 2.2**      **Flow Patterns**

An important point to note from the definition statement is that it does not make reference to the velocity of the particles (apart from saying that it must not be equal to zero). This is important because a common misconception about mass flow is that all particles in a cross sectional area of the silo move at the same vertical speed. In fact, this is practically impossible because, it implies that all the particles in that cross sectional area would come out through the outlet at the same time, however, in most cases the diameter of outlet is several times smaller than the diameter of the silo and would not be able accommodate the same number of particles in its area. Due to this generalization about the speed of the particles, mass flow is also known as “first in first out discharge” (Bates, 2012).

Even though it is not possible to obtain an ideal mass flow as shown in Figure 2.3a, a velocity distribution as shown in Figure 2.3b can be achieved with a practical result very close to first in first out discharge. Figure 2.3b shows that in the converging section of the silo, the particles located above the outlet move with a higher velocity than those near the walls. This velocity gradient reduces with the vertical distance

from the outlet and becomes close to zero in the non-converging section of the silo (cylindrical or rectangular section). As a result, the upper surface of the material in a mass flow silo remains unchanged until it approaches the transition of the bin.



*a – Ideal Mass Flow*

*b – Achievable Mass Flow (Schulze, 2008<sub>1</sub>)*

**Figure 2.3** Vertical Velocity Profiles in a Mass Flow Silo

### 2.1.2 Core Flow

In the previous section mass flow was defined as a discharge pattern where all particles remain in motion at all times. When this principle is not fulfilled a different type of discharge pattern develops in the bin, this type of pattern is known as core flow, funnel flow or pipe flow. Therefore, core flow could be defined as a pattern where some of the particles remain static for some time during discharge. In fact, depending on how many particles and for how long they remain static the performance of the bin during discharge can vary greatly.

The most common mechanism that causes a silo to core flow, takes place when the converging walls of that silo are not steep or smooth enough to allow the material in contact with them to move. When this occurs, the static particles create a high friction surface that will stop other particles from moving, creating stagnant zones of material in the silo.

However, this is not the only mechanism that produces core flow in a silo. Similarly, a static region is formed when the outlet of a “mass flow silo” is partially blocked during discharge, for example when a slide valve at the outlet is not fully open or when a feeder does not draw material from the entire area of the outlet. Core flow can also be a result of changes in the characteristics of the material during storage, for example the phenomenon of caking or agglomeration due to migration of moisture in a water soluble bulk solid that has free moisture. This phenomenon is driven by the temperature cycles the silo experience between day and night during long term storage. The presence of free moisture creates liquid bridges between particles partially dissolving their surfaces. During the day an increase in the ambient temperature heats the silo walls driving moisture towards the centre of the vessel. As the moisture migrates the liquid bridges crystallise causing the agglomeration of the particulates. During the night as the temperature cools the moisture migrates back to walls, dissolving the surfaces of the crystal bridges already formed (thus on the next cycle the crystal bridge will thicken increasing the strength of the agglomeration). This cycling causes a crust of caked non-flowing material to initially form adjacent to the walls of the silo, but over time it increases in strength and propagates from the walls towards the centre of the vessel restricting the flow channel.

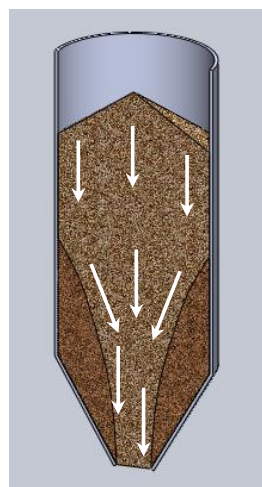
A typical example of core flow is shown in Figure 2.2b. When the outlet of the silo is opened, the material located directly above the outlet discharges forming a channel which extends to the top free surface. Then, the material on the top surface cascades down the channel while the rest of the silo contents remain static, if at this point fresh material is fed into the silo it would flow directly into the discharge zone. For this reason core flow is also known as “first in last out discharge”. The characteristics of the flow channel and stagnant zones depend on many variables primarily including: flow characteristics of the bulk material, geometry of the silo, method of filling, materials of construction of the silo and surface finish and the presence of valves or feeders that prevent the flow over the full cross sectional area of the outlet.

### 2.1.3 Mixed Flow

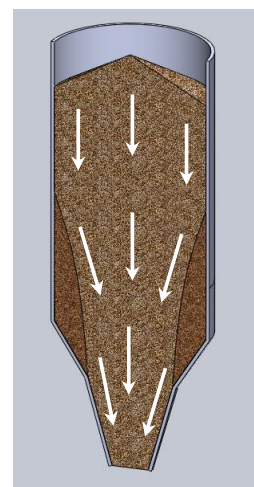
As it was mentioned above, the discharge performance of the silo heavily depends on the characteristics of the stagnant zones and discharge channel. A particular case of core flow (of special interest for industry) is known as mixed flow.

Mixed flow occurs when in a section of the silo the particles in contact with the walls move at all times during discharge, while in the rest of the silo the particles near the walls remain static. An example is shown in Figure 2.4a where the discharge channel formed above the outlet widens enough to reach the walls of the silo. When this happens, the contents above the height of the static regions move in a mass flow like pattern, whereas below that height the pattern continues to be core flow. This type of pattern, known as internal mass flow, is generally a natural occurrence for some bulk solids / bin geometry combinations. It is very difficult to predict or model and in some cases completely undesired (as it will be explained in the following sections).

Another type of mixed flow, known as expanded flow, can be the target pattern for the bulk solids engineer during the process design. In that case, the silo can be designed with a steep converging section to produce flow at the wall and a shallower one where no flow at the wall would occur, as shown in Figure 2.4b. This is also a common retrofit method applied when it is desired to modify the flow pattern in a core flow silo.



*a. Internal Mass Flow*



*b. Expanded Flow*

**Figure 2.4** *Types of Mixed Flow*

## 2.2 Effect of Discharge Patterns on Wall Stresses

The pressure exerted by a liquid on the walls of a tank is a linear function of the depth of the liquid as shown in Figure 2.5. This linearity is the consequence of two properties of Newtonian fluids: their inability to transmit shear stresses when at rest and the fact that the magnitude of the stresses, acting on an infinitesimal element, is the same in all directions. The stresses resulting from a bulk solid stored in a container are significantly different from those of a liquid, because bulk solids at rest do transmit shear stresses (due to friction between particles) and also because the stresses acting on an infinitesimal element are not the same in all directions. The difference in the first property results in a reduced increment rate of stress with depth, which is a consequence of the walls of the container supporting part of the weight of the material through friction. The effect of the wall support increases with depth until the stresses become almost independent of the depth and their magnitudes approach an asymptotic value.

As a consequence of the second property, more than one function is needed to define the stresses exerted by the bulk solid, as shown in Figure 2.5, where two functions are used to indicate the stresses in the vertical direction and the stresses in the direction perpendicular to the wall respectively.

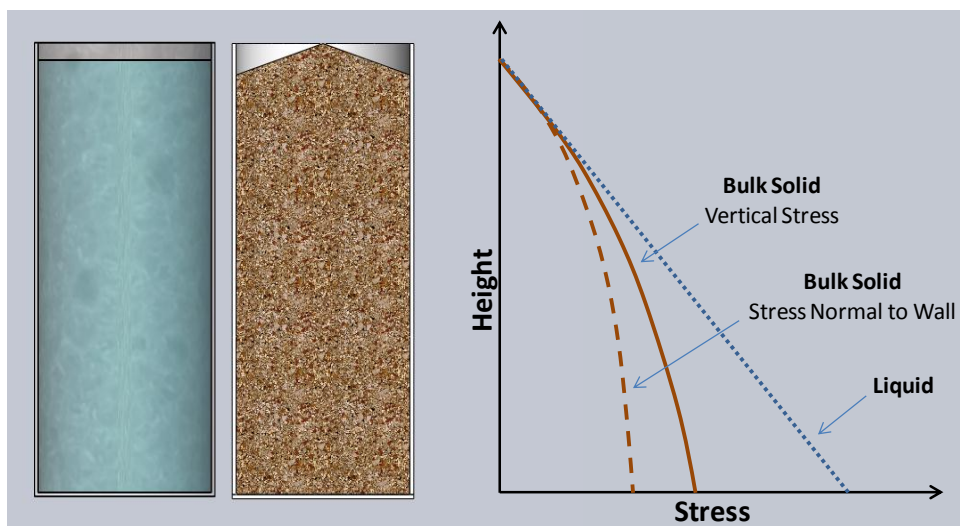


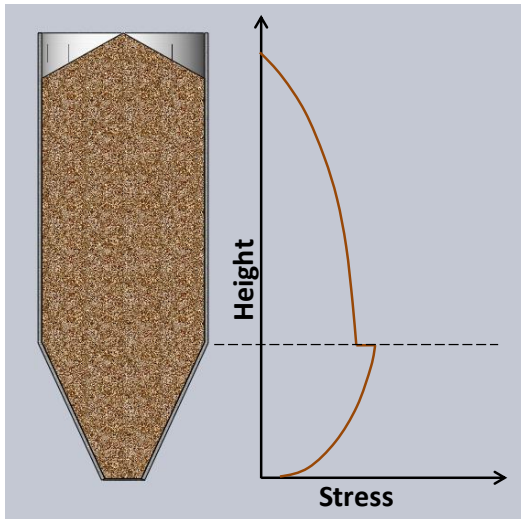
*Figure 2.5 Stresses Exerted by Liquids and Bulk Solids in a Flat Bottom Container*

The case illustrated in Figure 2.5 is just a particular example where a flat bottom container filled with a bulk solid and it is not a generalization. In fact, the wall stress profile along the depth of silo depends on many variables including: geometry of the silo, properties of the material, if the silo is been filled or discharged and the flow pattern developed during discharge. The effect the discharge pattern has on the normal stress exerted on the wall will be the focus point for the rest of this section.

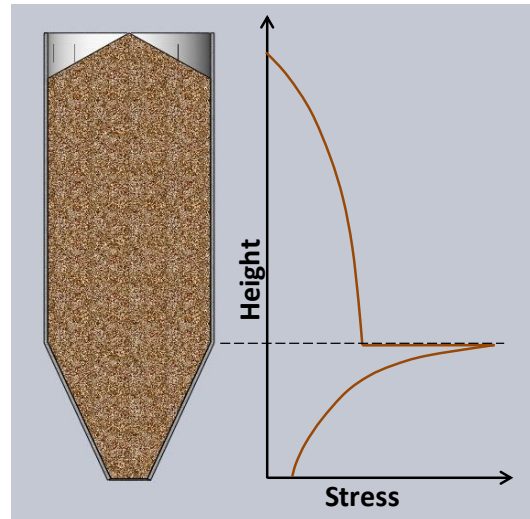
When a silo with a converging section is filled, the normal wall stress presents a profile like the one shown in Figure 2.6a. Please notice that in the vertical section of the silo the stress has a profile with the same shape shown in Figure 2.5, however, at the transition of the bin the magnitude of the stress increases. This is caused by the change in geometry of the silo walls, suddenly the normal stress has a vertical component supporting a larger share of the weight of the material. The magnitude of the stress reduces towards the outlet where it reaches its minimum value.

If the outlet of the silo is opened and its contents discharge following a mass flow pattern, the wall normal stress will develop a profile as shown in Figure 2.6b. Here it can be seen that in the vertical section of the silo, the profile remains similar to the profile during filling (slight increase in magnitude due to mobilisation of wall friction, potential imperfections in geometry), however, at the transition of the bin there is a large increment in the magnitude of the stress. This sudden peak is caused by the change in direction of the stress field in the material, or to put it simply, the particles distributed in the constant cross sectional area of the vertical section, are flowing downwards into the reducing cross section area of the hopper getting “squeezed” in the horizontal direction, producing a larger reaction load on the converging walls as a result. If the flow pattern developed during discharge is core flow instead of mass flow, the wall stress profile will resemble that of Figure 2.6c. It is important to notice that in this case the profile of the stress during discharge will be very close to the profile developed during filling. This is due to the fact that any changes in the stress field will be produced just within the flowing channel, therefore, if there is any incremental change in the stress in that region it would be relatively small and it would be dissipated within the bulk of material. Figure 2.6d illustrates the stress profile developed when the flow channel extends to the walls of the silo producing an internal mass flow pattern. For this pattern, the stress profile in

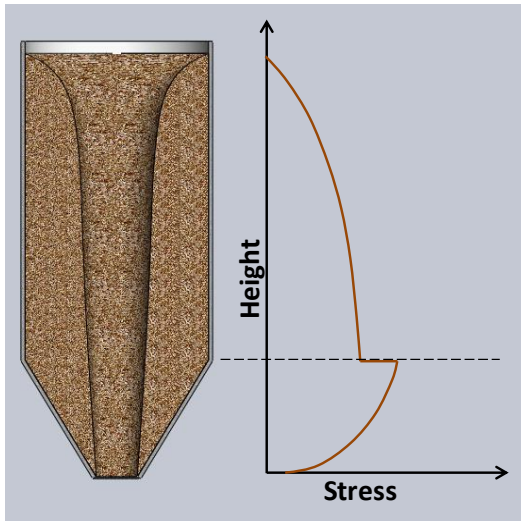
the top part of the vertical section remains mostly unchanged with respect to filling, but only down to the point where the flow channel intersects the walls. This intersection creates an effective convergence in the vertical section producing a spike in the magnitude of the wall stress due to the reasons explained earlier for mass flow. It is important to emphasize that the location of this spike in the wall normal stress cannot be reliably predicted (other than a range of probable heights) and is in fact, transient and generally asymmetric. The magnitude of the stress then reduces approaching the filling profile and it continues following a profile close to that until the outlet is reached. When the silo has been designed or modified to produce an expanded flow pattern, the stress profile developed is illustrated in Figure 2.6e. In this case, the stress profile closely resembles the filling profile down to the second transition of the bin, where the angle of the convergence changes to produce mass flow. At this point an increment in the magnitude of the stress is observed, however the value of the peak is not as high as those produced in mass flow bins or at the intersection of the flow channel with the walls of the silo. It is important to note that with this type of pattern the flow channel might also expand to the walls, as shown in Figure 2.6f, where three peaks are produced one at each critical point, namely intersection of flow channel and walls, transition from vertical to converging and change on the angle of convergence.



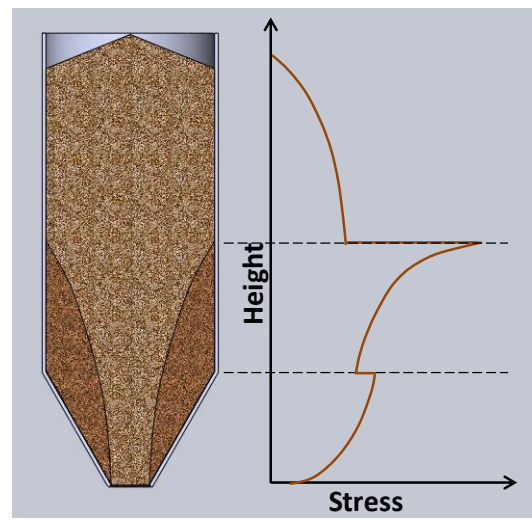
*a. Filling Stress*



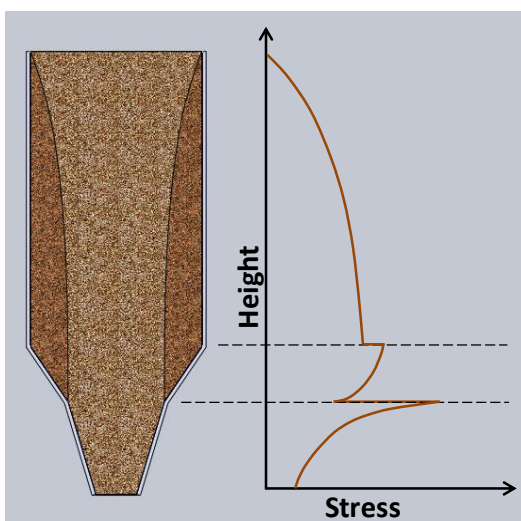
*b. Mass Flow*



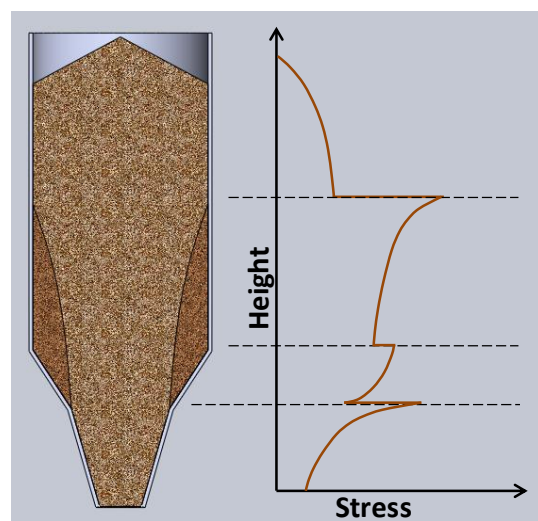
*c. Core Flow*



*d. Internal Mass Flow*



*e. Expanded Flow*



*f. Expanded Flow*

**Figure 2.6** *Effect of Discharge Pattern on Normal Wall Stress*

### **2.3 Bulk Solids Handling Problems and their Relationship to Discharge Patterns**

In the early 60's Andrew Jenike published his work on the design of hopper and silos to obtain reliable gravity flow. Jenike identified the characteristics of the main flow patterns and developed both theoretical and practical procedures for the design of mass flow silos and core flow silos for reliable discharge. Even though these techniques have been successfully used for over fifty years, many bulk solids handling equipment manufacturers are not familiar with them or simply choose not to use them. As a result a large proportion of the silos and hoppers used in industry exhibit flow reliability and material quality problems. Some of these problems will be briefly explained below, in order to identify the relationship that might exist between these problems and the discharge patterns presented in Section 2.1.

#### **Arching**

Arching or bridging occurs when the material above the outlet of a silo forms a stable domed structure supporting the weight of the material above, therefore, obstructing the discharge. Two forms are considered as outlined below:

Mechanical arching (Figure 2.7b) occurs when the particles are large compared to diameter of the silo outlet (typically,  $d_{\text{outlet}} \leq 5 \cdot d_{\text{particle}}$ ). The techniques developed by Jenike for silo design allow the calculation for the minimum outlet size to avoid cohesive arching in mass flow silos. To avoid mechanical arching the diameter outlet needs to be at least five to seven times bigger than the diameter of the largest particles to be handled.

Cohesive arching occurs when the interparticle forces are large relative to gravity forces. In cohesive arching (see Figure 2.7a) , several factors including moisture content, particle size, vibration and time consolidation, can contribute to increasing the strength of the material allowing the formation of stable arches.

### **Rat-holing**

When the contents of a silo discharge following a core flow pattern, the zones of stagnant material can consolidate over time (adjacent particles move closer together increasing the inter-particle forces) which result in an increased cohesive strength so it can form stable structures unable to flow under gravity (Figure 2.7c). When the discharge starts the material above the outlet flows out of the silo followed by the material at the top of the silo, at some point the consolidated material is unable to flow into the discharge channel and the silo does not drain completely. To avoid rat-holes developing, the outlet of the silo needs to be significantly larger than that required to avoid arching, and it can be calculated using Jenike's techniques. Please note that by definition rat-holing cannot take place in mass flow silos and even though it can appear in expanded flow silos these can be design/modified to avoid this problem, without the inconvenience of a very large outlet.

### **Flooding/Flushing**

When fine powders are allowed to dilate in the presence of air (conveying, falling stream, etc.) they can retain air and their flow behaviour becomes close to that of a fluid. However, if the material is left to rest for a period of time, the particles will settle and the bulk material will recover its original flow characteristics. If a core flow silo is used to handle a material of this type, fresh powder fed into the silo will flow directly into the preferential flow channel and the residence time is insufficient for deaeration. When this happens, the material will behave like a fluid and most feeders will not be able to control the flow causing spillages, dust, etc. If a mass flow silo is used instead, the first in, first out flow pattern ensures the entire inventory has relative constant residence time, significantly longer than that of a similar size core flow silo. Thus the material will have more time to deaerate and will be exposed to higher consolidation pressures thus minimising the potential for this problem to occur. Expanded flow will also allow some settling time, but it will be shorter than in mass flow silos, therefore in some extreme cases it might not be enough to avoid flooding.

## Bulk Density Variation

Please note that a very similar mechanism causes bulk density variability in the discharged product, which might have a negative impact in processes where a volumetric feeder is used (rotary valve, screw feeder) and a constant dose is needed.

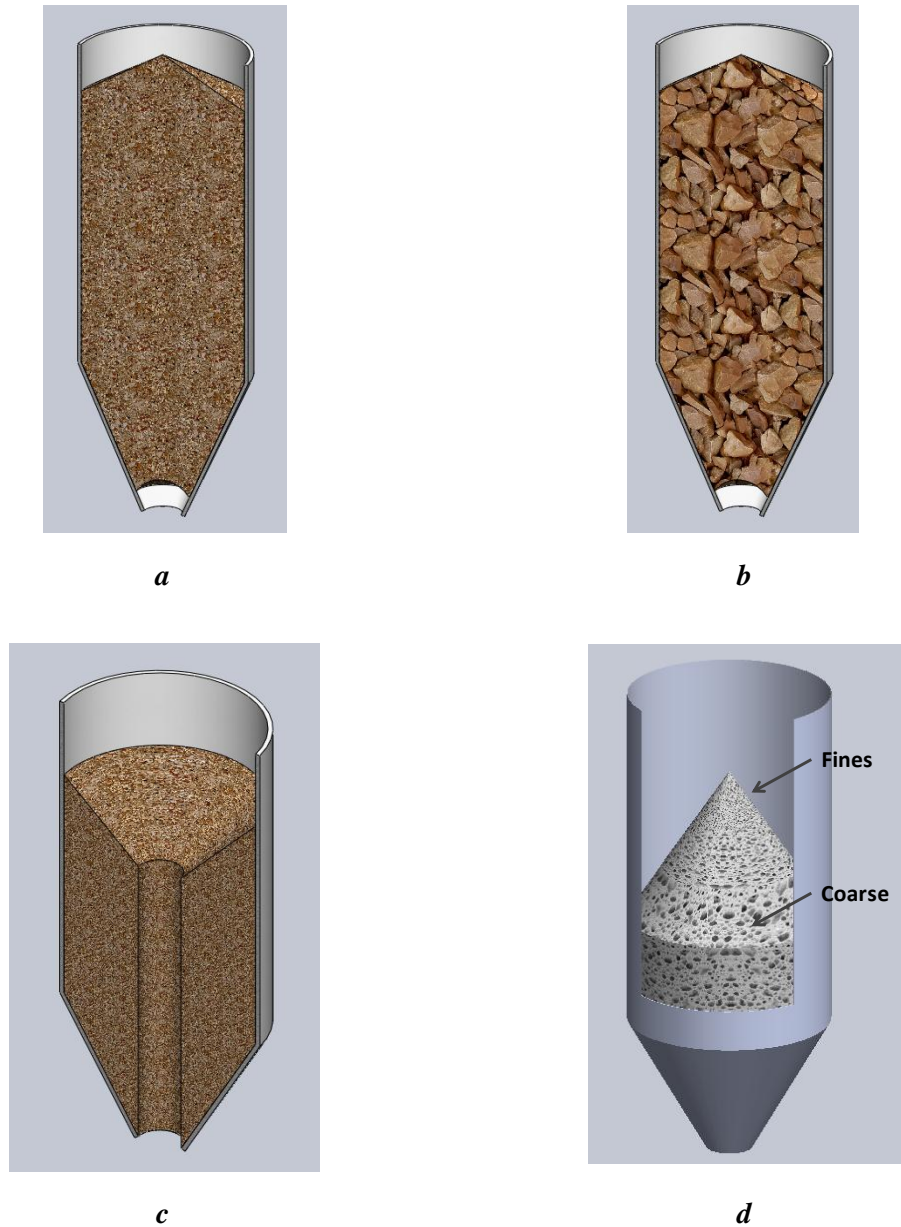


*Figure 2.7 Common Bulk Solids Handling Problems*

## **Silo Quaking and Honking**

The flow of granular materials in silos is not a continuous process like a liquid flowing from a tank. For bulk solid to discharge from a silo, discrete regions of material accelerate and decelerate producing pulses and vibration. Depending on their frequency and amplitude these pulses can cause loud noises (honking) or shock waves (quaking) which could compromise the structural integrity of the silo. The mechanisms that produce this pulsation are complex and not completely well understood and can occur both in mass flow and core flow silos.

## **Segregation**

The term segregation in bulk solids makes reference to the process through which particles separate due to differences in physical properties. These properties include particle size, density, shape and inter-particle forces. Segregation produces variability in the characteristics of the bulk material which can have serious implications for downstream processes and end users. For example: in the pharmaceutical industry segregation can generate ineffective drug doses with little API content, while other doses could be highly concentrated, which could produce negative health effects and in some cases even death. Segregation can take place through several mechanisms:

Rolling Segregation: when a bulk solid is discharged into a container or a flat surface it forms a conical pile, as the particles fall and hit the apex of the pile, those with larger size continue rolling down the slope of the pile while the finer particles stop near the apex. This is due to the larger particles having a larger momentum but also to the smaller particles ability to fill crevices of smaller size between the static particles. The result from this process is a larger concentration of fines in the centre of the pile and a larger concentration of coarse particle towards the sides (near the walls in a silo centrally fed) as shown in Figure 2.7d. When a material is segregated inside a core flow silo according to the mechanism described above, the effects of segregation will be intensified. When the discharge starts the flow channel forms above the outlet, drawing first material with a very high concentration of fines. This is followed by alternating layers of different compositions. In a mass flow silo there

is some degree of remixing of the segregated material due to the small difference in residence time between the particles in the centre and those near the walls. For expanded flow silos it is more difficult to generalize, as in some cases some reduction in segregation could be observed, however, if segregation is likely to generate problems downstream, only mass flow silos are recommended.

**Elutriation:** elutriation is the separation of particles (typically 50µm and below) due to drag forces generated from the relative movement between the bulk solid and a fluid (typically a gas, air). When a stream of gas crosses a stream of particles, the fines are dragged by the gas producing segregation. For example: when a powder falls through a vertical chute into a closed container, it displaces air which moves through the solids carrying the finer particles upwards. The product from this process will have a top layer rich in fines and a bottom layer rich in coarse particles.

**Percolation:** when a bed of solids is disturbed, the relative movement between the particles allows fines to move downwards filling voids. This produces a larger concentration of fines towards the bottom and a larger concentration of coarse at the top. The most common cause of percolation is vibration, this can be produced by transport of the container, or from mechanical links with equipment with moving parts, or tapping/hitting the container, etc.

## **Product Degradation**

Bulk solids handling equipment can have a significant impact on the quality of the material handled and the segregation section above is a clear example. Particles can break, get squashed or crushed, biodegrade, react with other particles, react with other substances etc. Particle breakage in silos can occur by impact during filling, by friction between particles when discharging a core flow silo, by friction with the wall when discharging a mass flow silo, the weight of the bed of material above can crush or squash the particles, etc. Biological degradation commonly occurs in core flow silos that are not completely emptied on a regular basis, the material in the stagnant zones simply stays too long in the silo producing degradation. The same occur with

products that self-heat, or produce reactions between particles. In these cases is important to use mass flow silos.

### **Loads on Feeders**

The vertical stress generated by the bed of solids acts on the feeding equipment located at the outlet of the silo, depending on the magnitude of that stress the feeder may need a larger drive (i.e. screw feeders, belt feeders). Mass flow silos also tend to suffer higher wall loads and wear due to the slippage of material on the walls.

### **Structural Failure**

The flow behaviour of the contents of a silo has a large impact on the structural integrity of the silo. Some causes of silo failure are presented below.

*Collapsing Arches:* arches formed inside silos can in many cases span over several hundreds of millimetres, leaving a large void underneath. When that arch collapses the bed of material flows suddenly impacting the lower part of the convergence of the silo, this can cause the rupture of the converging section (cone, wedge). At the same time, the sudden movement of the bed will create a void at the top of the silo producing vacuum and if there is not sufficient means for air to ingress the top of the silo, it could implode.

*Switch Stress on Vertical Section:* the largest stress exerted on the walls of a silo is expected to occur at the transition of the bin (as shown in Figure 2.6b) and this area is commonly reinforced accordingly. However, if the flow pattern is core flow and the channel reaches the walls of the silo, the peak stress will be acting somewhere on the vertical section (as it was previously shown in Figure 2.6d) which is not normally designed to resist stresses of that magnitude. Additionally, because predicting the place where the channel might intersect the walls is very difficult and unreliable, reinforcement of the structure would need to be done over the entire vertical section.

*Wear:* wear is generally observed in mass flow silos handling abrasive materials, the fact that the material slips at the wall (and high wall loads) over time causes thinning and weakening of the walls increasing the possibilities of structural damage.

*Eccentric Flow:* when the discharge channel in a core flow silo is not central but runs through one side and along a section of the wall, it produces non uniform stresses on the wall creating bending moments which can buckle the structure of the silo.

## **2.4 The Use of Inserts**

During the design of new plants, bulk solids discharge from silos is often regarded a fairly simple process which does not require much consideration. However, it is not until problems start to appear (like those from the previous section), that attention is paid to the design of the handling equipment. For decades static inserts have been used as a means of getting over these shortcomings because they often represent an economic and easy to retrofit method to improve handling of bulk solids. Additionally, inserts can also be included in the original design of the equipment to enhance their capabilities. In bulk solids handling, inserts can be defined as any device installed inside handling equipment with the object of modifying its performance. Inserts can have many different shapes, be placed in different parts of the equipment and aim to achieve a variety of purposes. Below, an introduction is made to some of the different types of static inserts and the purposes for their use.

### **2.4.1 Inverted Cones**

An inverted cone is one of the simplest yet most versatile and commonly used types of inserts. They can be used as a single unit, as clusters, or as multiple independent units to address different issues. They can be positioned at the inlet of a hopper, near the outlet, in the vertical section, or in combinations of these places. Depending on the size, position and number of inserts a variety of effects can be achieved.

Probably, the most common use of inverted cones is to promote flow. When an insert of this type is correctly designed and positioned in a core flow hopper, the

discharge pattern in the silo can be transformed into mass flow (Figure 2.8a). In the nineteen sixties, Jerry Johanson developed a method for the design and positioning of inverted cones to achieve mass flow in core flow silos [Johanson, 1965; Johanson and Kleysteuber, 1966; Johanson, 1968]. An insight into Johanson's work is presented in section 2.5.3. According to Johanson, the insert changes the flow channel into an annulus and the flow behaviour resembles a plane flow hopper, which can support mass flow with shallower walls than conical hoppers. If mass flow is achieved, a large number of problems associated to core flow can be avoided (as explained in section 2.3), for example: effects of segregation can be reduced, more consistent properties of product can be achieved, rat-holing would be avoided as well as flushing and flooding. However, if the material has tendency to rat-hole and a stable channel is formed underneath the insert, the contents of the silo will simply not discharge. For materials that could present this behaviour, Johanson recommends installing an additional inverted cone of smaller size between the outlet and the main insert (as shown in Figure 2.8b). The small insert widens the discharge channel impeding the formation of the rat-hole.

If obtaining mass flow is not desired, then inverted cones can still be used to improve the performance of core flow silos. The insert acts as a support for the material above, reducing the magnitude of the consolidating stresses acting on the regions near the outlet, as a result it reduces the possibilities of a cohesive arch forming. Rat-holing can still be avoided as mentioned above, if the group of inserts produce a wide enough discharge channel.

Figure 2.8c and d show a cone valve and a bin activator respectively, two commercial applications of inverted cones. Even though these two applications are not strictly static inserts, it is still worth mentioning them. Cone valves have an inverted cone which acts as flow promoter during discharge and it closes the outlet when it is required to stop. Bin activators are commonly used as flow promoting devices to discharge cohesive materials and where headroom is a concern. Bin activators are generally vibrated to encourage flow and have a very shallow convergence underneath to save space.

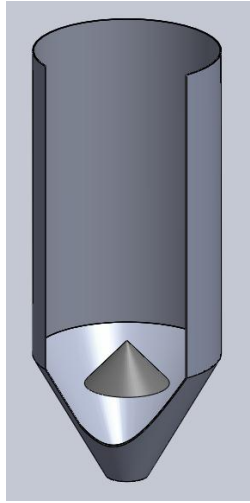
By changing the position of the insert in the bin a completely different issue can be addressed. In section 2.3 the mechanism of rolling segregation was explained, from there it can be extracted that the longer the slope of the pile formed during filling, the more potential for segregation. By fitting an inverted cone at the place where the material is fed into the silo, the stream can be redistributed to form an annular pile reducing the length of the slope produced (see Figure 2.8e). This reduces the tendency for segregation to occur, rather than seeking to rectify its effect. This objective can be enhanced by placing more than one inverted cone. In this case groups of concentric cones can be fitted to produce several annular piles, reducing further the slopes of the piles. Figure 2.8f shows the effect obtained by placing two inverted cones at the inlet of the silo, please note that only the inner insert retains its apex whereas the outer cone has been truncated to allow a section of the stream to flow through it.

An additional benefit obtained by this type of configurations, is that a higher filling level can be achieved during filling increasing the effective storage capacity of the silo. The installation of this inserts however, must not be taken lightly because the wrong set up can increase segregation instead of preventing it. If the incoming stream does not hit the insert uniformly around the apex, the stream will be directed preferentially towards a side of the silo as shown in Figure 2.8g (thus increasing slope length aiding segregation and limiting filling efficiency). This problem is more evident when the velocity of the stream in the horizontal direction is different from zero, for example streams coming from inclined chutes and belt conveyors. In these cases it is recommended that the stream is redirected using additional chutes and fed vertically onto the apex of the cone.

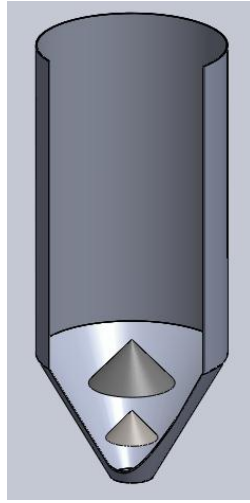
Inverted cones can also be used to reduce the consolidation stresses in silos. This can be achieved by placing groups of small inserts along the vertical section of the bin as shown in Figure 2.8h. There are many reasons why a reduction of the magnitude of the stresses might be desirable. It could be to avoid particle degradation when handling friable particles, or particles that might be flattened by the weight of the bed, or particles storing a fluid like detergent sachets. Another reasons to reduce vertical loads include avoid caking caused by overpressures, reduce loads acting on feeders, avoid arching and rat-holing, reduce intensity of quaking and honking. In

any case it needs to be considered that the loads taken by the inserts will be transferred “somewhere”, and that somewhere is the insert mount. Therefore if the inserts are hung from the silo top plate or supported on the walls of the bin these areas might need to be reinforced accordingly.

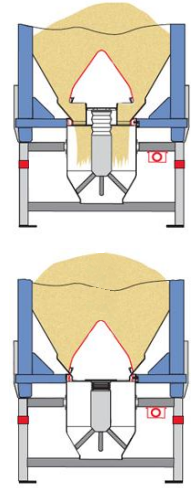
Please note that the solutions presented above are not exclusive from each other and could be combined to obtain a synergistic result. Figure 2.8i shows a combination of three different applications of inverted cones which could be used for processes where minimizing segregation is mandatory.



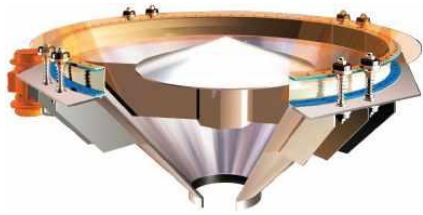
*a*



*b*



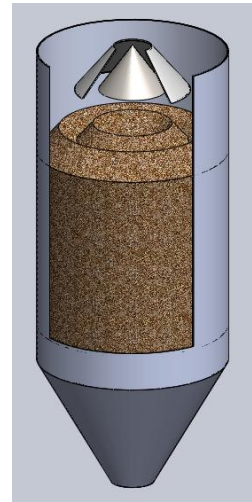
*c. [Servolift, 2013]*



*d. [Polimak, 2013]*



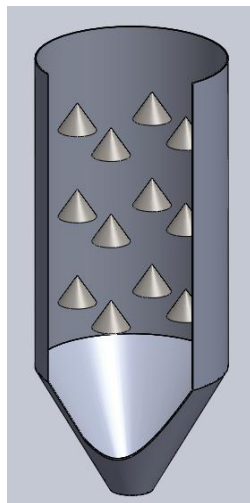
*e*



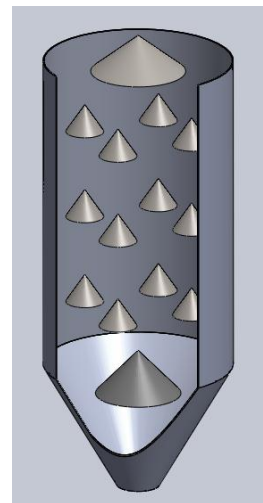
*f*



*g*



*h*



*i*

**Figure 2.8 Use of Inverted Cone Inserts**

## 2.4.2 Flat Plates

If a round flat plate is placed in a horizontal plane so it opposes flow, material will build up on top of it forming an inverted cone as shown in Figure 2.9a. The result from this is that most of the benefits and applications explained for inverted cones in the previous section are also valid for flat plates. However, an important difference that needs to be highlighted is that inverted cones are self-draining whereas flat plates are not. Most of the material that builds up on top of the plate will remain there after the silo has been emptied. This is an important detail because it limits the applicability of flat plates i.e. they are not suitable for time dependent materials (food industry), processes where cross contamination must be avoided (pharmaceutical industry) and processes handling high value materials (precious metals industry).

In addition to the applications where flat plates work as inverted cones, Figure 2.9b to f show examples of other applications of this type of inserts. Figure 2.9b presents an invention patented by Lyndon Bates in 1998 [Bates, 1998] where elongated flat plates (can also be curved) are directed inwards towards the outlet at an angle that allows the material to slip at its surface. The plates provide stress relief promoting mass flow in otherwise core flow hoppers. Figure 2.9c shows flat rings fitted to the vertical walls of a silo to reduce vertical loads in the lower regions of the bin and inhibit quaking, these rings can also be slanted to allow the material to drain at the end of the discharge (Figure 2.9d). Vertical ribs (as shown in Figure 2.9e) are also used to increase the load transferred to the walls of the silo reducing the magnitude of the stresses exerted in the lower part of the silo (Bates, 2010). Figure 2.9f shows a flat plate used to obtain a central feeding of the silo. In this particular case the material is pneumatically conveyed into the silo in the radial direction, the particles enter the silo and continue travelling across until they hit the plate and fall towards the centre of the bin. If the plate is removed, the particles would continue travelling towards the opposite wall where a pile with a long slope would be formed (a similar effect was shown in Figure 2.8g).

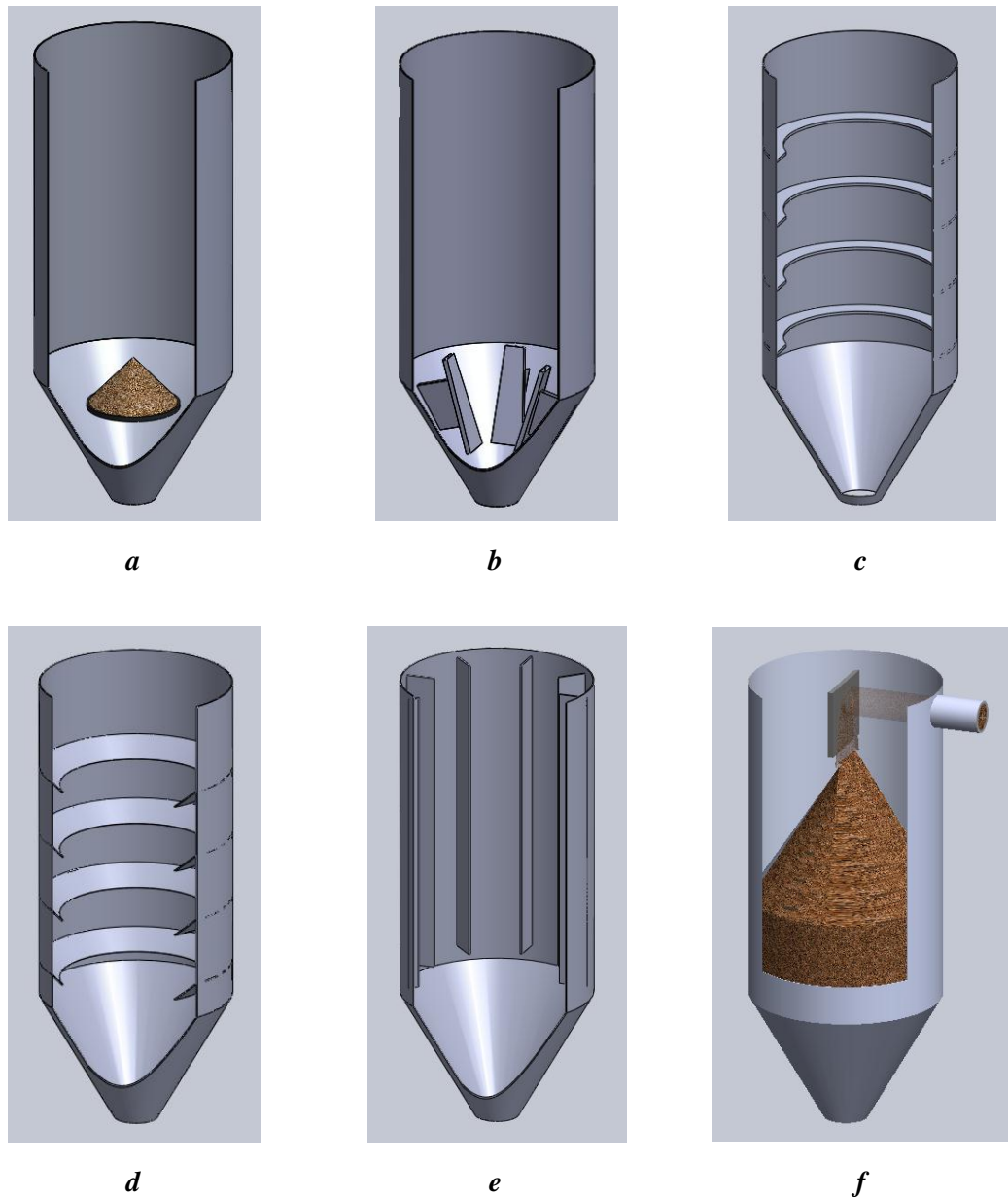


**Figure 2.9 Use of Flat Plates**

### 2.4.3 Cone in Cone

A cone in cone insert consists of a hopper within a hopper as shown in Figure 2.10a. Retrofitting this type of inserts is usually done with two main purposes, achieving mass flow and/or producing static blending.

The concept of installing internal hoppers to improve discharge performance of silos has been used for over half a century, in 1958 Gael M. Williams patented an invention which included a cone in cone insert to promote discharge and reduce

particle segregation. Even though this patent precedes the concepts of mass flow and core flow, from its description becomes clear that achieving mass flow was the target. The patent states that the invention aims to keep a more uniform upper surface avoiding the formation of a funnel and achieving more consistent discharge rates. However, the work that made popular the use of cone in cone inserts was developed by Jerry R. Johanson and presented in the patent for a blending apparatus for bulk solids in 1981; this device is better known as Binsert (see Figure 2.10b). A Binsert consists of a mass flow hopper installed inside a hopper which would not be able to support mass flow without the insert. The area between the insert and the silo wall becomes an annulus and the flow resembles plane flow, which can mass flow at shallower geometries. This means that it can be retrofitted into core flow hoppers to achieve mass flow or it can be incorporated in the design of new mass flow silos increasing storage capacity with limited headroom requirements. The use of this insert also enables the control of the velocity profile in the lower part of the silo which is used to obtain particle blending. The velocity profile is controlled by the way the solids are extracted for the section that contains the insert, if the solids are allowed to flow out unrestricted or a stand pipe is interfaced below the outlet, the resulting velocity profile would be fairly uniform. However if a mass flow cone is directly interfaced to the outlet of the section that contains the insert, the velocity gradient across the lower part of the silo will be increased. The magnitude of the gradient can be controlled by the angle of the mass flow section interfaced and the inclusion of any stand pipe. The gradient obtained is the characteristic that allows this invention to be used as a blending device. More recent patents [Fisher, 1985; Jackson, 1989] and a number of research projects undertaken at the POSTEC centre in Norway [Karlsen, 1998; Enstad, 1998; Schuricht, 2001; Xiao, 2008; Hartl, 2008; Schuricht, 2008], also look at the use of cone in cone inserts to achieve mass flow and the main difference between them is the design procedure which will be discussed in section 2.5.2.

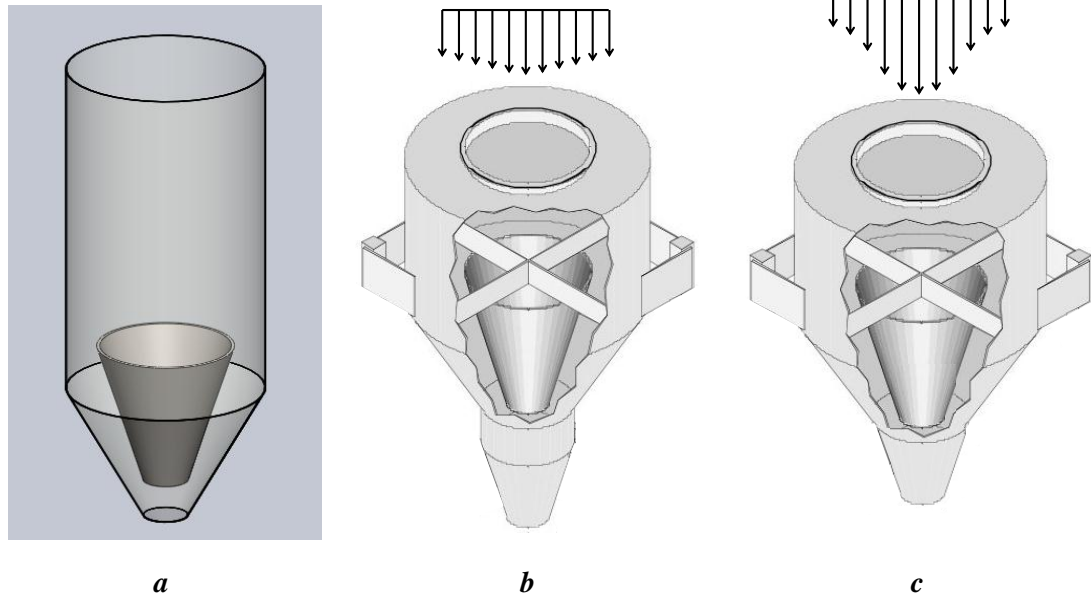


**Figure 2.10** *Use of Cone in Cones*

#### 2.4.4 Double Cone

Double cone inserts consist of two truncated cones joined at the base and with opposing apexes as shown in Figure 2.11a. When one of these inserts is installed in a conical hopper, the flow channel is changed into an annulus. The stress field then resembles a plane flow hopper where mass flow can be supported by shallower geometries. With a double cone insert this effect is obtained in two stages [Bates, 2010], the upper part works in the same way that an inverted cone whereas the lower part of the insert can work like the external part of a cone in cone insert. The material moving in the upper region of the insert converges at a relative high convergence rate, due to the “large” angle between the walls of the insert and the walls of the silo, whereas in the lower region the rate of convergence is reduced as the inclusive angle is acuter. This ability to modify the flow channel and stress field enables double cone inserts to achieve mass flow in otherwise core flow silos. However, if mass flow is not desired for the process but the material handled has tendency to form rat-holes, double cones can still be used as a solution to that problem. In that case a smaller insert (as shown in Figure 2.11b) can be installed to expand the flow channel beyond the maximum dimension that would support a stable rat-hole, producing reliable flow. Examples of the use of inverted cones to promote flow can be found in the

following references [Jenike, 2013<sub>10</sub>; Enstad, 1998; Ding, 2002; Ding, 2003; Ding, 2004<sub>1</sub>; Ding, 2004<sub>2</sub>; Ding, 2005; Wójcik, 2007; Ding, 2008; Xiao, 2008]

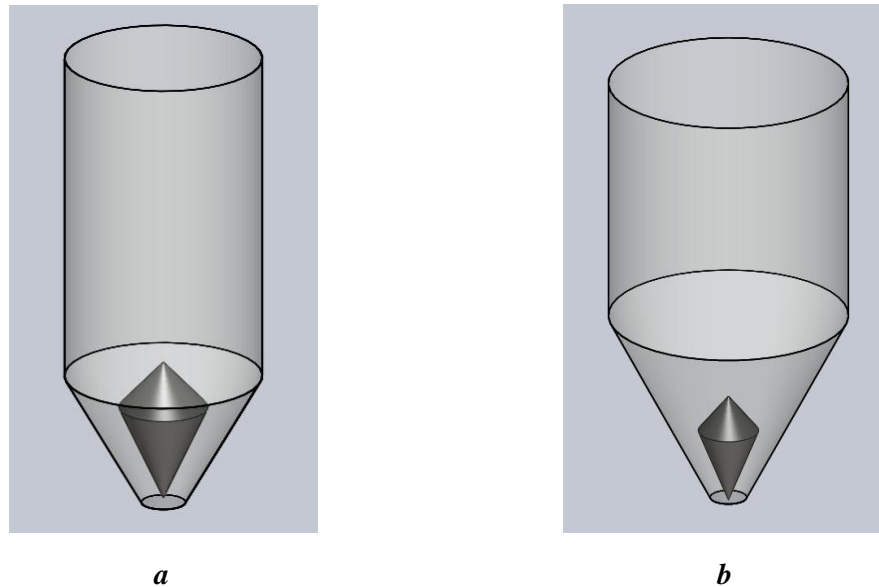


*Figure 2.11 Use of Double Cones*

#### **2.4.5 V Tents**

The most common application for V tents is to fit them above the slotted outlet of silos interfaced to screw feeders and belt feeders (as shown in Figure 2.12a), where the insert produces a double effect in benefit of the performance of the system. The first objective of this type of installation is to reduce the vertical load on the feeder, which allows the use of smaller drive motors reducing both capital and operating costs. Additionally, wear of the feeder is also reduced, providing further savings in maintenance costs. The second benefit of installing V tents above feeders is to allow dilation of the powder bed during discharge. A granular material under stress needs to dilate to be able to commence flow, in a silo interfaced to a feeder this dilation occurs at the void space left by the movement of the feeder. However, this dilation is restricted by the consolidation of the material and the efficiency of the feeder might be reduced. By placing a V tent, flow initiates between the insert and the silo walls and the bed expands towards the void under the tent easing the flow into the feeder [Bates, 2010].

V tents can also be installed in pair forming a cross (as shown in Figure 2.12b) to reduce consolidation of the material in the lower part of the silo which reduces the possibilities of the formation of arches and rat-holes. This reduction of stresses in the silo also reduces wear and particle degradation. This configuration can also be used to inject gases into the bed to promote flow or to promote gas solids interaction for example for chemical reactions and heat transfer [Royal, 1995].

As it was explained for inverted cones and illustrated in Figure 2.8h, V tents can also be suspended in the vertical section of the silo to reduce further the consolidation stresses acting on the material [Bates, 2010].

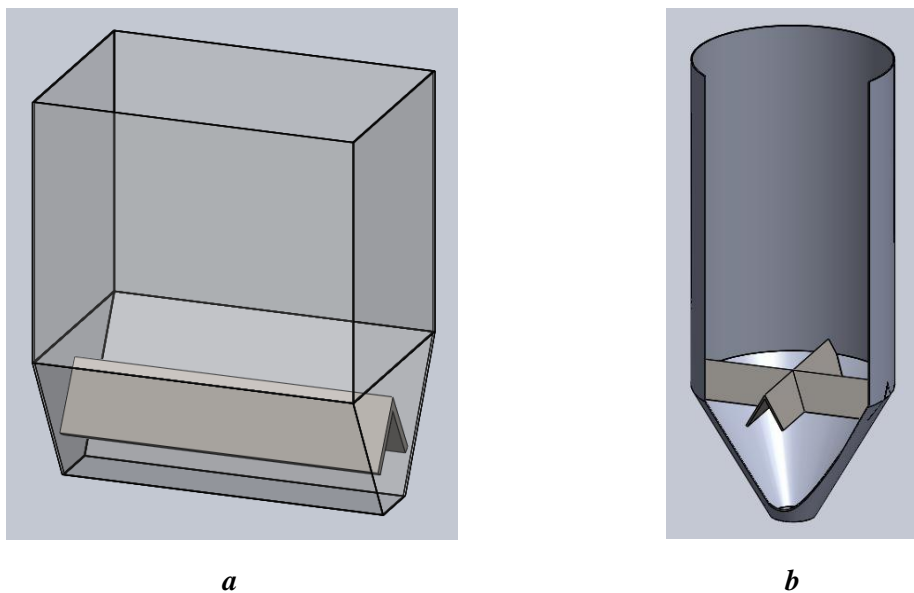


*Figure 2.12 Use of V Tents*

#### **2.4.6 Discharge Tubes**

Some of the main applications of the inserts explained above promote the flow of particles in silos reducing stagnant zones; achieving mass flow could be considered the ultimate goal. The use of discharge tubes however, aims in general to obtain exactly the opposite: pure core flow [Reimbert, 1983]. Core flow can be beneficial

for many processes because it eliminates switch stresses, reduces wear and reduces quaking and honking, among others.

The most common type of discharge tube is a perforated vertical tube located above the outlet of a silo as shown in Figure 2.13a. During discharge, the material from the top of the silo flows into the tube and the rest of the contents remain static. When the level of material falls below the top aperture, particles start flowing into the tube through the upper most set of lateral perforations. The difference in magnitude of the stresses does not allow flow through the lower apertures until material positioned higher in the silo has been discharged [Schulze, 2008<sub>1</sub>]. However, this is only true if the discharge rate is controlled in such a way that it is lower than the maximum achievable rate through a set of lateral openings (the tube is choked fed). If the tube is allowed to discharge without restriction, the particles flowing through a set of openings would not fill the tube and material would be allowed to discharge through the lower apertures as shown in Figure 2.13b. The extraction of material at multiple depths in the silo as explained above, paves the way for another common application of discharge tubes: solids mixing. Taking advantage of that effect many designs of mixers have been created as shown in Figure 2.14.

There are however designs of discharge tubes that aim to achieve mass flow. An example of this is an insert created by Lyndon Bates [Bates, 1998] and shown in Figure 2.13c. The insert obstructs the discharge through the centre of the bin and promotes a skewed discharge, the material under the insert is consolidated to a lower stress and flows more readily. The continuity of the hoop stress is broken and the material in the conical section flows in a horseshoe shaped channel towards the region sheltered by the tube [Bates, 2010].

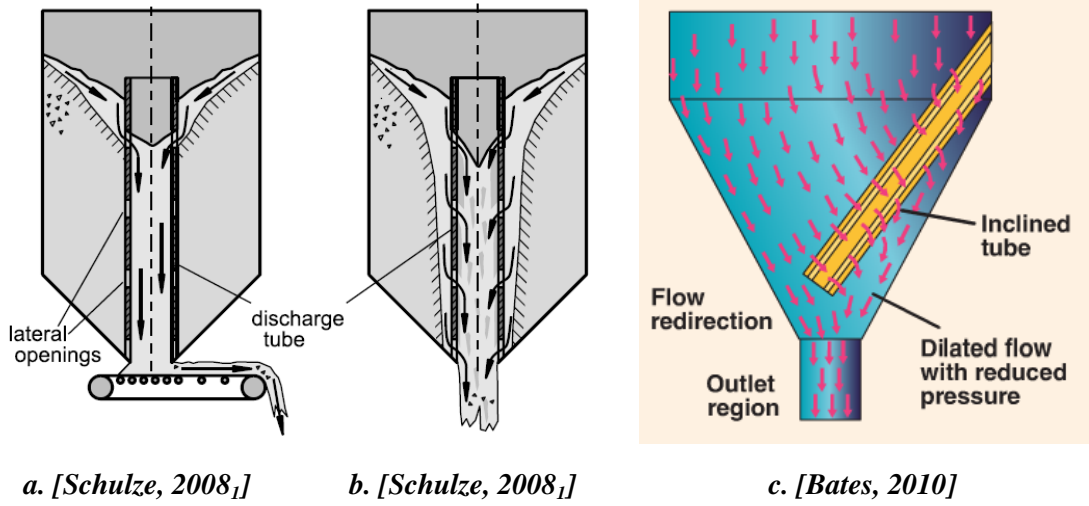


Figure 2.13 Discharge Tubes

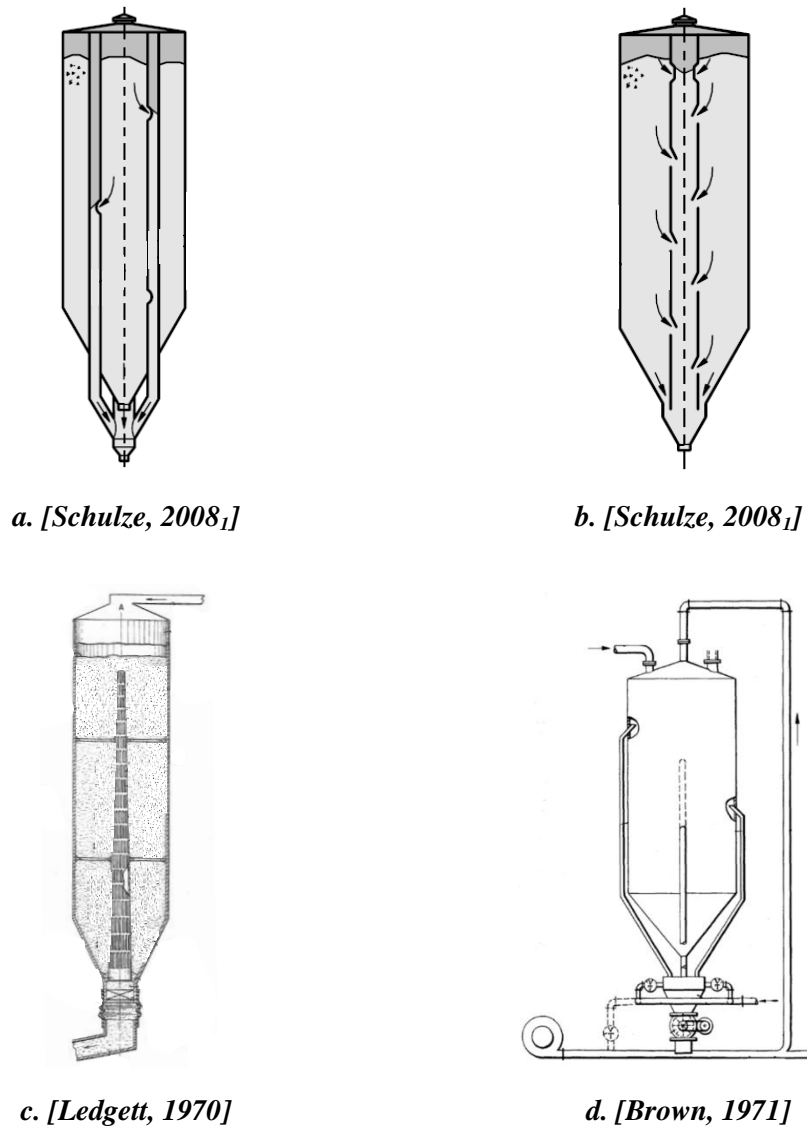
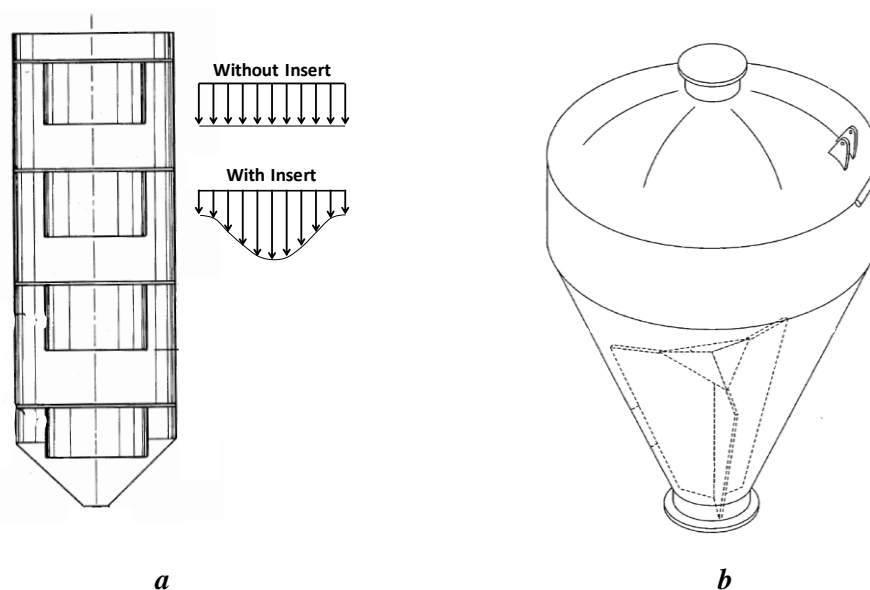


Figure 2.14 Discharge Tubes Mixers

### 2.4.7 Internal Divisions

This type of inserts consists in arrangements of vertical walls that divide the internal flow of material in a silo and depending on their configuration a variety of effects can be achieved. An invention created by Johanson uses short cylindrical wall segments located along the vertical section of the silo to improve mixing [Johanson, 1989]. The segments are used to increment the velocity gradients along the cross sectional area of the silo as shown in Figure 2.15a, this is particularly useful in mass flow and expanded flow bins where the velocity profile in the upper section of the silo is fairly uniform.

A different application of internal divisions is presented in an invention by Vaynshteyn as shown in Figure 2.15b [Vaynshteyn, 2006], where the purpose of the divisions is to reduce the possibility of arching and rat-holing. During discharge, instead of a central funnel forming, three channels will form expanding the width of the discharge area. The baffle located above the junction of the divisions helps to reduce consolidation by impact during filling, reducing as a result the probability of rat-holing. The author claims that the risk of arching is diminished by the fact there are not opposing converging walls in each section, but two vertical walls and one converging wall instead. A similar claim is made by Coleman in an invention to avoid arching in plane flow hoppers [Coleman, 2001].



**Figure 2.15 Use of Internal Divisions**

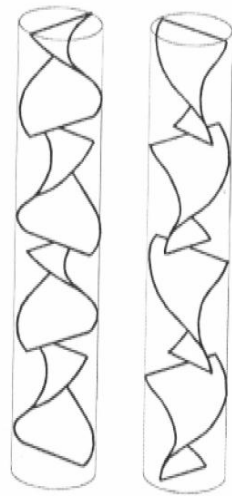
#### **2.4.8 Wall Liners**

Wall liners might not be considered inserts in the traditional use of the word for bulk solids in the sense that they are not an obstruction in the solids flow path. However, wall liners are devices installed inside silos to modify their performance (definition of insert). Depending on the application different materials of construction and surface finishes might be selected. For example, ultra-high molecular weight polyethylene (i.e. Tivar 88) has shown to reduce wall friction for some powders when compared to mild and stainless steel, this reduction promotes mass flow [Bradley, 2000; Goldberg, 1991]. A porous material (plastic, metal or ceramic) can be used to inject air (or other gas) to reduce wall friction, fluidize the material, increase flow rate, promote chemical reactions, etc [Beckschulte, 2013, Dewitz, 1990]. Other uses of wall liners include: ceramic liners to reduce wear when handling abrasive materials [Ding, 2003], plastic or ceramic liners to prevent corrosion of the silo walls and rough liners to increase wall friction which would reduce consolidating stresses or reduce intensity of silo quaking and honking.

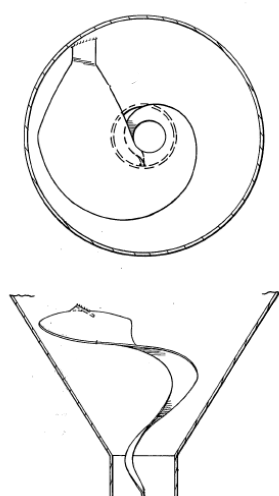
#### **2.4.9 Twisted Tape**

A common application of twisted tape inserts is as static mixers [Bauman, 2001; Gyenis, 2002; Denis, 2006] as shown in Figure 2.16a. The sections of tape create multiple motion paths for the solids, which promotes inter-particle interaction and residence time differences resulting in mixing of the material. It is important to note that this type of mixers should only be used for free flowing particles because the tape sections create narrow channels where cohesive materials could produce blockages.

A different application for this type of insert uses a helical tape running along the depth of a silo as illustrated in Figure 2.16b. The tape imparts a circular component of motion to the material as it moves towards the outlet improving discharge and reducing chance of bridging [Watson, 1976]. This particular type of twisted tape is also used to reduce particle breakage when handling friable materials. During silo filling, the solid slide along the tape reducing impact forces that could cause breakage.



*a. [Denis, 2006]*

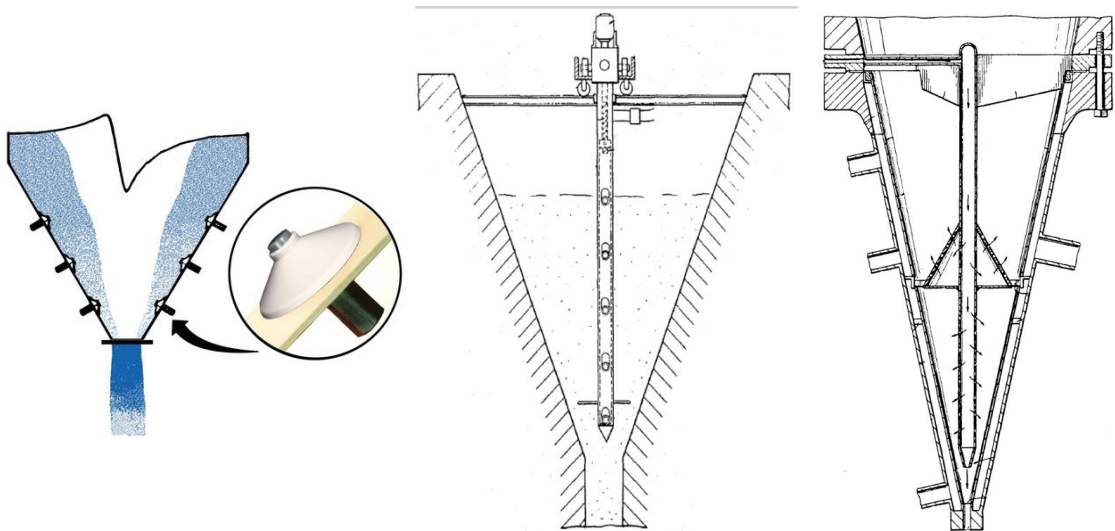


*b. [Watson, 1976]*

**Figure 2.16 Twisted Tape Inserts**

#### **2.4.10 Other Inserts**

In addition to the devices presented above, a large number of inserts are used in industry for two particular applications: solids mixing and solids aeration (gasification). Aeration devices can be used for a variety of purposes including: reduction of wall friction, cohesive arch breaking, flow rate control, powder fluidization, promoting/inhibiting chemical reactions, drying and temperature control. The single most common kind of aeration device used in industry is the mushroom type aeration pad, of which an example is shown in Figure 2.17a. Additional examples of aeration inserts are shown in Figure 2.17b and Figure 2.17c.



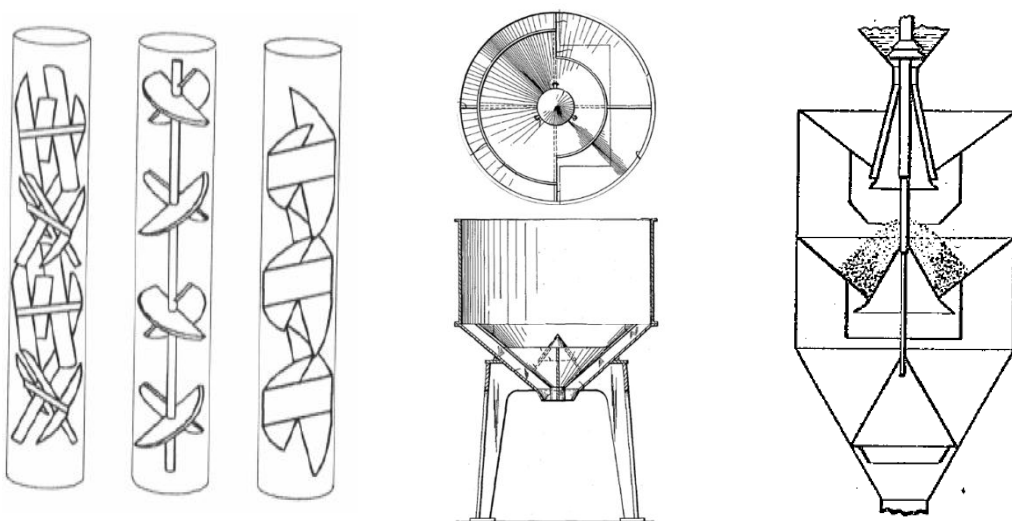
a. [BinMaster, 2013]

b. [Lucas, 1968]

c. [Dirkse, 1992]

Figure 2.17 Other Aeration Inserts

In the case of solids mixing a type of device widely used is the tube mixer. An example of this was presented in section 2.4.9, where segments of twisted tape were used as inserts to promote blending. A similar effect can be achieved changing the shape of the inserts as shown in Figure 2.18a. Other mixing devices use a combination inserts presented previously to modify the velocity profile of the particles in the silo and produce the blending effect, for example the inventions by Matthews and McCandliss which combine internal hoppers and inverted cones as shown in Figure 2.18b and Figure 2.18c respectively.



a. [Denis, 2006]

b. [Matthews, 1961]

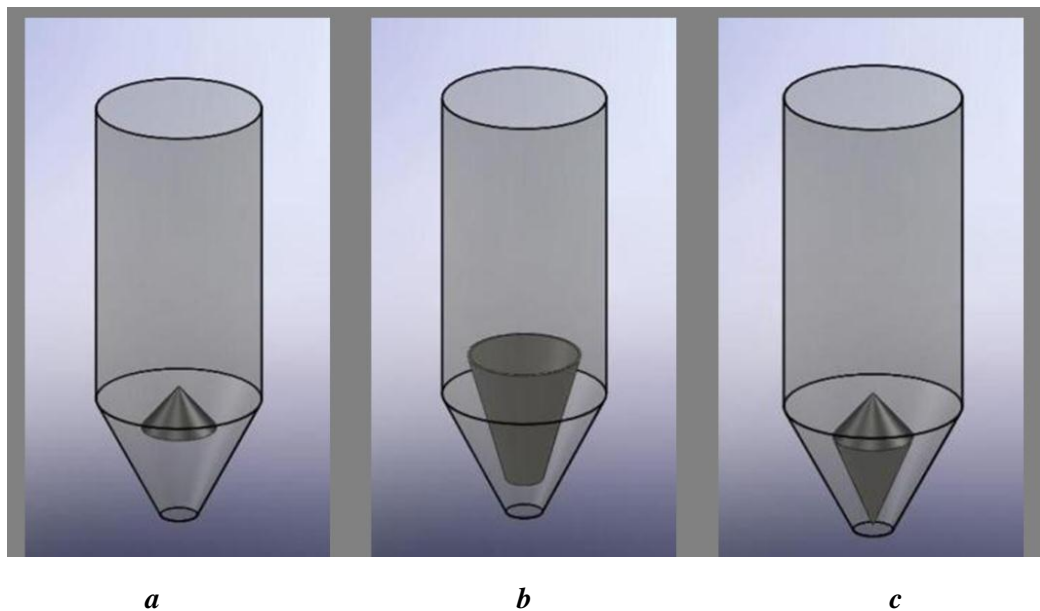
c. [McCandliss, 1917]

Figure 2.18 Other Static Mixers

## 2.5 Insert Design for Flow Promotion

As it was shown in section 2.4, static inserts can be used for a large number of industrial applications, however, in most of cases the rules for their design and optimum positioning are well hidden as trade secrets, whereas industrial applications are well protected behind patents. For this reason the design of inserts is still considered a field for specialists and those who adventure into the construction and installation of these devices, more often than not carry out a design based on intuition or “gut feel”.

This research work focuses on the use of inserts to improve discharge performance of hoppers and silos, therefore the purpose of this section is to present an overview of techniques that have been developed to design static inserts to promote reliable flow. However, the number of inserts used for this purpose is too large to make it practical for the author to address each of them on their own, therefore three main types have been chosen due to the fact that between them embrace most of the research work published on this subject. These insert types are: inverted cones, cone in cones and double cones as shown in Figure 2.19.



**Figure 2.19** Common Shapes of Inserts; *a – Inverted Cone, b – Cone-in-Cone and c – Double-Cone*

Research on the use of inserts has been carried out for nearly five decades. In one of the earliest publications [Johanson, 1965], Johanson made a theoretical approach to determine the optimum size and position of the inverted cones inside conical hoppers. He developed a procedure to calculate the geometry of the insert and its placement to widen the discharge channel in core flow hoppers. Later, Johanson and Kleysteuber [Johanson, 1966] studied the pressures exerted on inserts (inverted cones) and the way they should be supported inside the hoppers to avoid structural failure. In the early nineteen eighties, a cone in cone insert was developed by Johanson, which was part of a patented blending apparatus for bulk solids [Johanson, 1981]. This insert, known as Binsert, is a conical hopper designed to obtain mass flow, which is installed in a silo and is capable of changing the discharge pattern in the entire bin from core flow to mass flow [Johanson, 1982].

In the mid-nineteen eighties, Tuzun and Nedderman [Tuzun, 1985<sub>1</sub>; Tuzun, 1985<sub>2</sub>], studied the effect that triangular and cubic inserts had on the shape of streamlines of particles when discharging in a silo, as well as the effect of the inserts on the stress profiles on the walls of the silo. However, this study was focused more towards modelling the phenomena, than towards industrial application or flow promotion. A decade later, Strusch and Schwedes [Strusch, 1994; Strusch, 1998] measured wall stress distribution and forces on inserts inside plane flow hoppers and developed a mathematical model based on slice element methods.

During the last fifteen years, a large percentage of the research done on inserts has been carried out at the POSTEC institute, where several projects [Klonteig, 1997; Karlsen, 1998; Enstad, 1998; Schuricht, 2001; Ding, 2002; Ding, 2003; Ding, 2004<sub>1</sub>; Ding, 2004<sub>2</sub>; Ding, 2005; Wójcik, 2007; Ding, 2008; Xiao, 2008; Hartl, 2008; Schuricht, 2008, Wójcik, 2012] have been conducted on the use of cone-in-cone and double-cone inserts aiming to obtain mass flow in core flow silos. In 2006, Chou and Chang [Chou, 2006], following the approach made by Strusch and Schwedes [Strusch, 1994; Strusch, 1998] for plane flow hoppers, developed a theoretical model for the prediction of wall stresses and insert loads in a conical hopper with a inverted cone insert. Also in 2006 Kerry Johanson presented a methodology to predict blending performance through Binserts, calculating the velocity gradients across the

different sections of the silo [Johanson, 2006]. This methodology also explains how a cone in cone can promote mass flow in otherwise core flow silos.

### **2.5.1 Design of Inverted Cones as Flow Promotion Devices for Discharging Bulk Solids**

The first research study on the use of inserts to promote flow from silos was presented by Johanson in 1965 [Johanson, 1965]. He developed a practical procedure for the design of inserts aiming to obtain mass flow in silos that would otherwise discharge in core flow pattern. The introduction of an inverted cone in a shallow conical hopper creates an annular gap between the edge of the insert and the wall of the silo, in this way according to Johanson, the silo would behave in fact as a wedge silo. The solids are expected to fail at the annulus between the insert and the silo walls and the outlet shape changes from circular to an annular slot.

The fact is that for a given powder and wall material, the converging sections of wedge-shaped silos can be shallower than those required for conical hoppers to obtain mass flow. This is one of the conclusions from the silo design theory and practical procedure developed by Jenike for reliable flow [Jenike, 1961]. Figure 2.20 shows the graphical representation of numerical solutions to Jenike's work, these charts are commonly used for silo design. From the charts it becomes evident that a wedge hopper (plane flow) can sustain mass flow at shallower angles than conical hoppers. For example, for a system handling a powder with internal friction angle equal to 50 degrees and wall friction angle of 22 degrees, the angle of the walls of a conical hopper cannot be larger than 24 degrees from the vertical if mass flow is to be achieved, whereas for a wedge hopper that maximum angle is just over 30 degrees.

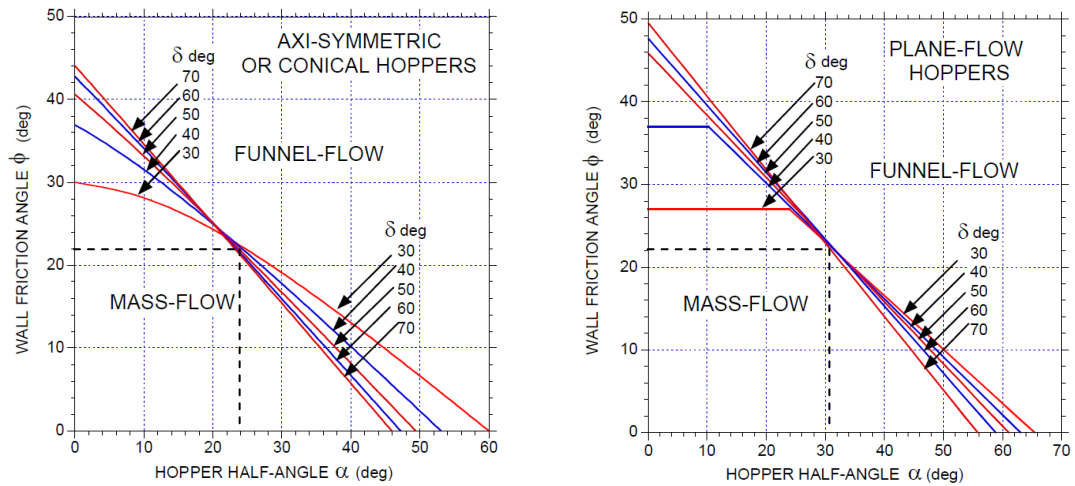


**Figure 2.20** Design Charts for Mass Flow [Roberts, 2009]

To help explain this phenomenon it is important to understand the difference in the way a material converges in a wedge hopper and in a conical hopper. In a wedge hopper, only two of the walls converge while the other two remain vertical (in some cases can also present a small convergence or divergence), therefore when the material moves towards the outlet, the area of the hopper reduces in only one direction and compressing stresses that hinder flow are also produced in only one direction (as shown in Figure 2.21a). By contrast in a conical hopper, the cross sectional area reduces in two directions and the solids are compressed both in the radial and angular directions producing higher resistance to flow (Figure 2.21b). A simple way to visualize this difference is that the solids in a wedge hopper converge towards a line, whereas the solids in a conical hopper converge towards a single point.

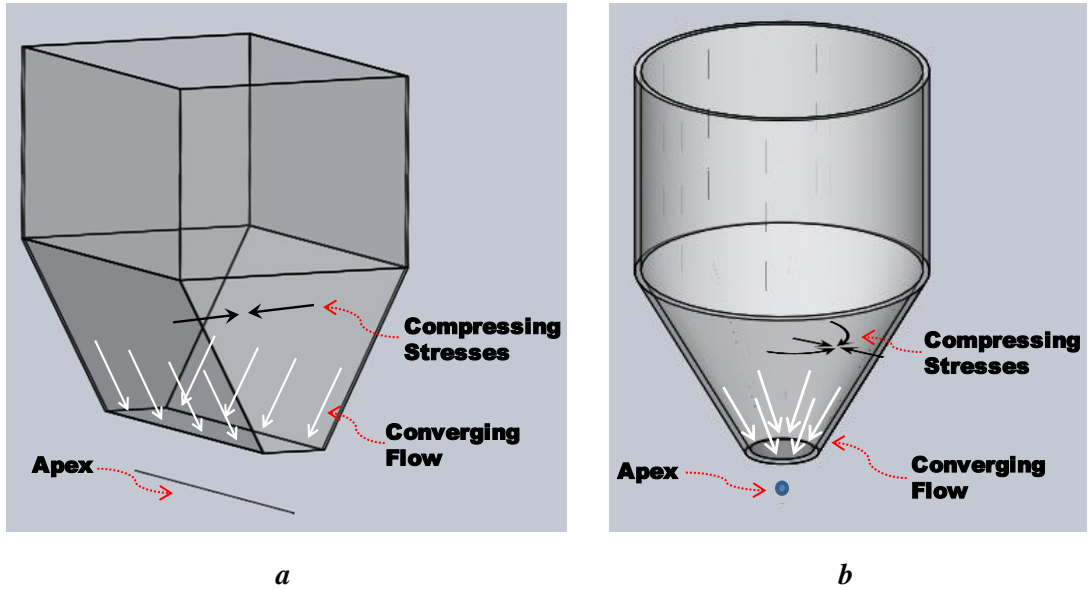


**Figure 2.21** *Flow Convergence in Wedge and Conical Hoppers*

As the insert modifies the behaviour of the silo from axi-symmetric to pseudo plane flow, the hopper can then develop mass flow in the region influenced by the insert, therefore the position of this influenced area would determine the behaviour of the solids in the upper part of the silo. As shown in Figure 2.22, flow along the insert AB causes Flow at the hopper wall between D and C.

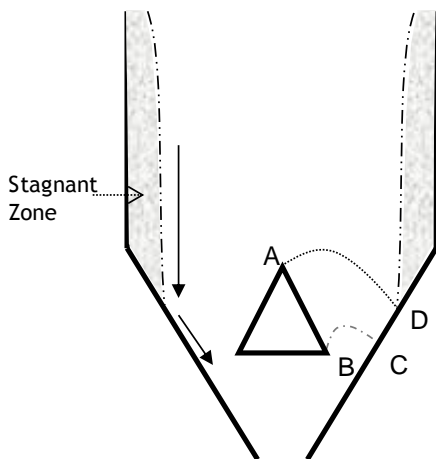


**Figure 2.22a** *Region Influenced by the Insert Below the Transition of the Bin*

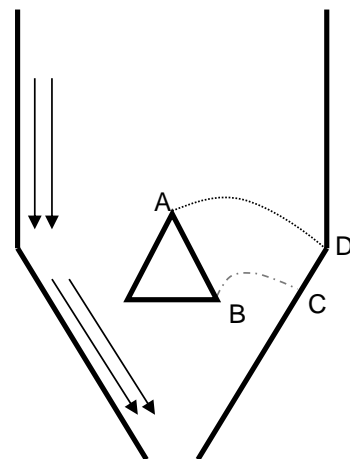


**Figure 2.22b** *Region Influenced by the Insert Above the Transition of the Bin*

If the area influenced by the insert is located below the transition of the silo (see Figure 2.22a), there will be a stagnant zone propagating upwards from the point just before where the solids slip at the wall. However, if the insert influences the wall at the point of transition from the cylindrical to conical part of the bin (see Figure 2.22b), the material will be mobilized at the wall on the whole surface of the cone and there will not be stagnant zones present.

In order to predict the region influenced by the insert, Johanson assumed that the solids behave as an ideal Coulomb material (cohesionless materials that present a linear relationship between normal stress and shear stress) under conditions of steady flow (stress and velocity at any point are unchanged with time). In this case, equations of equilibrium in a conical hopper take the form of a set of hyperbolic-partial-differential equations [Johanson, 1964]:

For the stress field:

$$\begin{aligned} (1 + \sin\delta\cos2\omega)\frac{\partial\sigma}{\partial x} + \sin\delta\sin2\omega\frac{\partial\sigma}{\partial y} - 2\sigma\sin\delta\sin2\omega\frac{\partial\omega}{\partial x} \\ + 2\sigma\sin\delta\cos2\omega\frac{\partial\omega}{\partial y} = \gamma - \frac{\sigma}{y}\sin\delta\sin2\omega \end{aligned} \quad (2-1)$$

$$\begin{aligned} (1 - \sin\delta\cos2\omega)\frac{\partial\sigma}{\partial y} + \sin\delta\sin2\omega\frac{\partial\sigma}{\partial x} + 2\sigma\sin\delta\sin2\omega\frac{\partial\omega}{\partial y} \\ + 2\sigma\sin\delta\cos2\omega\frac{\partial\omega}{\partial x} = \frac{\sigma}{y}\sin\delta(1 + \cos2\omega) \end{aligned} \quad (2-2)$$

Where

$$\sigma = \frac{\sigma_1 + \sigma_2}{2} = \frac{\sigma_x + \sigma_y}{2} \quad (2-3)$$

The velocity field is obtained from the continuity of the solid with constant density and with the condition of coincidence of principal stress and strain-rate directions [Johanson, 1964].

$$\frac{\partial u}{\partial x} + \frac{\partial v}{\partial y} + \frac{v}{y} = 0 \quad (2-4)$$

$$\tan 2\omega = \frac{\frac{\partial u}{\partial y} + \frac{\partial v}{\partial x}}{\frac{\partial u}{\partial x} - \frac{\partial v}{\partial y}} \quad (2-5)$$

However, as it was also assumed that the insert changes the geometry from axial-symmetry to plane strain, therefore these equations are simplified to produce:

For the stress field:

$$\begin{aligned} (1 + \sin\delta\cos 2\omega) \frac{\partial \sigma}{\partial x} + \sin\delta\sin 2\omega \frac{\partial \sigma}{\partial y} - 2\sigma\sin\delta\sin 2\omega \frac{\partial \omega}{\partial x} \\ + 2\sigma\sin\delta\cos 2\omega \frac{\partial \omega}{\partial y} = \gamma \end{aligned} \quad (2-6)$$

$$\begin{aligned} (1 - \sin\delta\cos 2\omega) \frac{\partial \sigma}{\partial y} + \sin\delta\sin 2\omega \frac{\partial \sigma}{\partial x} + 2\sigma\sin\delta\sin 2\omega \frac{\partial \omega}{\partial y} \\ + 2\sigma\sin\delta\cos 2\omega \frac{\partial \omega}{\partial x} = 0 \end{aligned} \quad (2-7)$$

For the velocity field:

$$\frac{\partial u}{\partial x} + \frac{\partial v}{\partial y} = 0 \quad (2-8)$$

$$\tan 2\omega = \frac{\frac{\partial u}{\partial y} + \frac{\partial v}{\partial x}}{\frac{\partial u}{\partial x} - \frac{\partial v}{\partial y}} \quad (2-9)$$

Where:

$\delta$ : *Effective angle of internal friction*

$\omega$ : Angle between  $x$ -axis and direction of major principal stress

$\sigma_1$ : Major principal stress

$\sigma_2$ : Minor principal Stress

$u$ : Velocity component in  $x$  direction

$v$ : Velocity component in  $y$  direction

The common way of solving these equations is using the method of characteristics [Johanson, 1964; Nedderman, 1992]. This method is a way of solving first and second order partial differential equations, reducing them to ordinary differential equations along particular lines known as the characteristics. Where the characteristic lines intercept, the ordinary differential equations can be solved simultaneously given sufficient boundary conditions.

The characteristics for the equation systems (2-6),(2-7) and (2-8),(2-9) are:

For the stress field:

$$\frac{dy}{dx} = \tan(\omega \pm \mu) \quad (2-10)$$

Where

$$\mu = \frac{\pi}{4} - \frac{\delta}{2} \quad (2-11)$$

For the velocity field:

$$\frac{dy}{dx} = \tan\left(\omega \pm \frac{\pi}{4}\right) \quad (2-12)$$

The major principal stress trajectory ( $\omega$ ) is determined by the stress field, hence the velocity and stress fields are bonded; however, the boundary conditions of the velocity field are not determined by the boundary conditions of the stress field.

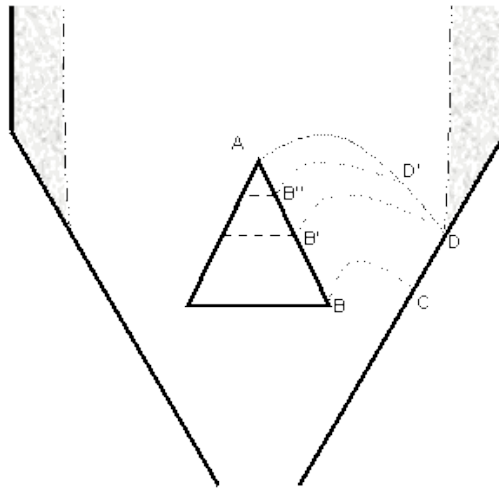


**Figure 2.23** *Region of influence of a conical insert [Johanson, 1965]*

The region influenced by the wall of the insert, shown in Figure 2.23, is the region ABCD where AD and BC are the first and second stress characteristics from points A and B. The influence of the insert AB will propagate flow along the bin walls when at least one point on the wall is included in the region of influence. The limiting condition occurs when points C and D are the same. Such a condition occurs when the lower portion of the insert from B' to B is removed. The flow pattern for this limiting case would be essentially the same as with the larger insert; flow would occur along the hopper wall up to point D. [Johanson, 1965]

If the lower section of the insert is removed up to point B'', the characteristic lines will intersect at point D' and the region of influence will not be big enough to change the flow pattern at the wall of the bin. In this case, the width of the discharge channel is likely to be widen and the extension of stagnant areas is likely to be reduced, however, mass flow will not be achieved.

### **2.5.1.1 Johanson Design Method for Insert Placement**

According to the discussion above, the success of a design method for inverted cone inserts will depend on whether it is capable of fulfilling the following two conditions:

- The insert needs to be large enough to ensure that the first stress characteristic from its apex and the second stress characteristic from its base, do not intersect before the wall of the hopper.
- The apex of the insert needs to be located in such a way that the first stress characteristic from it intersects the wall at the transition of the silo or above.

Please note that the first condition guarantees that the insert produces movement of the solids at a region of the wall of the hopper and the second one guarantees that the influenced region includes the transition of the silo eliminating the possibility of stagnant zones developing.

The previously discussed assumption of geometry change from axial-symmetric to plane strain also simplifies the solution of the stress field, as it can be approximated to the radial stress field proposed by Jenike [Jenike, 1961]. Using this approximation, Johanson calculated a critical ratio  $W/R$  (annulus width / insert radius) which would fulfil the first condition, and presented the results in a graphical form as shown in Figure 2.24.

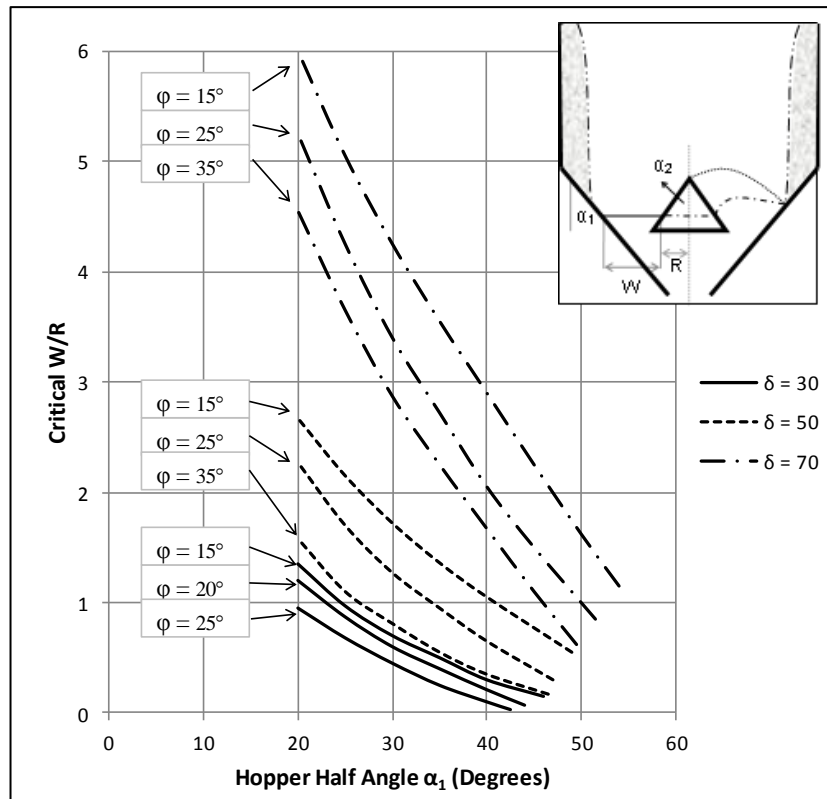


**Figure 2.24** *Approximate critical W/R for inserts and hoppers with the same slope [Johanson, 1965]*

The results presented in Figure 2.24 were obtained assuming a symmetric, wedge-shaped hopper, and hence these results are only applicable when the insert and the hopper have the same half angle. However, Johanson found experimentally that the critical W/R-values are essentially independent of the slope of the insert. Thus, Figure 2.24 gives acceptable values for any half angle of the insert.

Johanson calculated the location of the point D, then defined  $\psi$  as the angle between the line AD and the wall of the insert and presented values of  $\psi$  in terms of the effective angle of internal friction of the bulk solid ( $\delta$ ), the half angle of the hopper ( $\alpha_1$ ) and the half angle of the insert ( $\alpha_2$ ) (see Figure 2.25), the angle  $\psi$  can then be used to fulfil the second condition as it will be shown in the design procedure below.

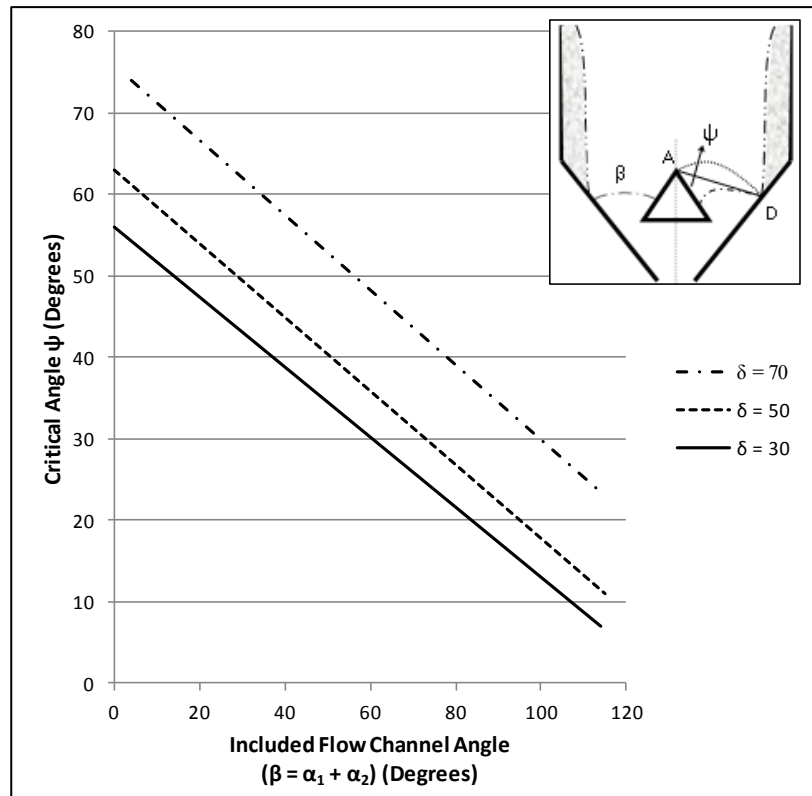


**Figure 2.25** *Approximate angle  $\psi$  to determine limit of flow along hopper walls [Johanson, 1965]*

As with the W/R ratio, the results for the angle  $\psi$  were obtained for symmetrical, wedge-shaped hoppers and would be valid only when the hopper and the insert have the same slope, but again these results seem to be valid for any slope angle of the insert wall, according to Johanson's experimental observations.

With the information obtained above, Johanson developed the following design procedure to retrofit inverted cones into existing silos performing in core flow pattern. See Figure 2.26.

- a. The first step consists of selecting the half angle ( $\alpha_2$ ) of the insert.  $30^\circ$  is recommended for most materials, however when cleanout is not necessary, (i.e. materials which are not time-sensitive) a flat plate could be used instead. When the bin is discharging, material will build up on the flat plate effectively forming an inverted cone and in that case for design purposes, the angle  $\alpha_2$  is calculated as:

$$\alpha_2 = \frac{\pi}{4} + \frac{\delta}{2} \quad (2-13)$$

- b. To continue to the next step, the flow properties of the bulk solid must be known. If that is not the case the effective angle of internal friction ( $\delta$ ) and the wall friction angle ( $\phi$ ) between the bulk solid and the material of the hopper wall have to be measured. These properties can be obtained through the use of a powder shear test.
- c. Once the flow properties are known, the values for the critical W/R ratio and angle  $\psi$  can be obtained from Figure 2.24 and Figure 2.25 respectively.
- d. Make a scale drawing of the existing silo.
- e. Draw a line from the transition of the silo at an angle  $\pi/2 - \psi - \alpha_2$  from the horizontal until it intersects the central axis of the hopper (see Figure 2.26, line DA). This intersection (point A) represents the apex of the inverted cone.
- f. Draw a line from the apex of the hopper at angle  $\eta$  from the vertical, such as:

$$\tan\eta = \frac{\tan\alpha_1}{1 + W/R} \quad (2-14)$$

This line represents the critical ratio W/R (see Figure 2.26, line EF).

- g. Draw a line from the apex of the inverted cone at an angle  $\alpha_2$  from the vertical, until it intersects the critical W/R line (see Figure 2.26, line AB). The intersection point (point B) represents the bottom of the insert; thus the size and location of the insert are determined. However, it may be desirable to make a 10% reduction on the critical W/R value as a factor of safety.

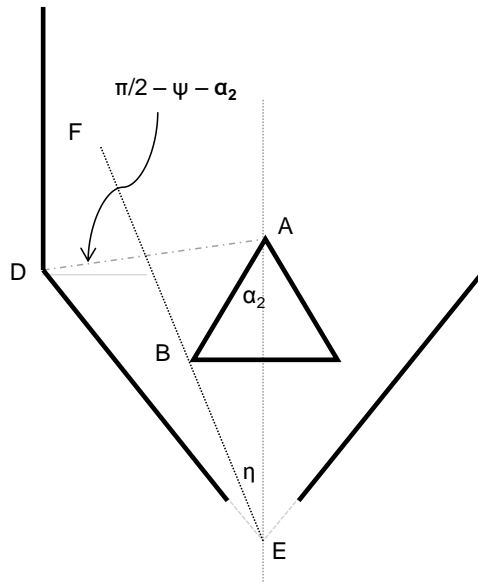


**Figure 2.26** Proper placement of inserts [Johanson, 1965]

It is worth noting that for convenience of the procedure, the line DA has been drawn at an angle  $\pi/2 - \psi - \alpha_2$  from the horizontal. However, simple geometry would show that the angle ADB is in effect  $\psi$ . This means that at the point D the solids will slip at the wall and that in fact will make the whole silo discharge in the mass flow pattern, fulfilling the second condition for the design method.

The procedure described above assumes that the material is continuously discharged from the bin without stoppages occurring, if the powder tends to form arches or rat-holes in the silo, the insert could become completely ineffective. For systems where these types of problems are likely to happen, Johanson presented an extension of the design method in order to avoid flow stoppages in the silo, including the following additional steps.

- h. Calculate the minimum arching dimension ( $W_c$ ) for the annular ring between the insert and the hopper wall. This can be obtained following standard silo design procedures for plane flow hoppers [Arnold, 1979; Jenike, 1961; Jenike, 1964<sub>1</sub>; Schulze, 2008<sub>1</sub>; Roberts, 2009].

- i. Locate the point G, Figure 2.27, at which the distance between the wall and the line EF equals the minimum arching dimension  $W_c$ . Be aware that no insert should be placed below point G as it will cause arching.
- j. Check that point B is above point G. If that is not the case, the insert will need to be raised and its size increased. If this is not possible to achieve, an inverted cone insert cannot be used to solve the problems of the system.
- k. Measure the angle of repose of the material ( $\theta_r$ ).
- l. Check if a rat-hole is likely to form below the upper insert. To achieve this, draw a line downwards from the base of the insert until it intersects the axis of the bin, at an angle from the horizontal equal to the angle of repose of the material; line BH. If the distance h between the point H and the outlet is larger than the outlet of the silo, rat-holing is likely to occur.
- m. Include an additional insert between the outlet of the silo and the upper insert, with the base starting above point G as shown in Figure 2.27.

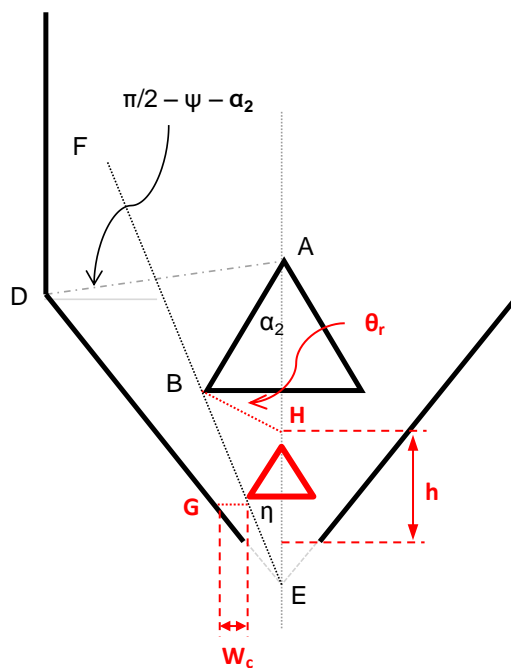


**Figure 2.27** Design Method to Avoid Arching and Rat-Holing [Johanson, 1965]

## 2.5.2 Design of Cone in Cone Inserts as Flow Promotion Devices for Discharging Bulk Solids

In the case of the design and use of cone-in-cone inserts, there are two main design approaches (one by J. Johanson [Johanson, 1981] and the other one by G. Enstad [Enstad, 2008]) which hold multiple similarities, but also have important differences that make them perform in distinct fashions. However, the published works by these two authors do not include the mathematical deduction and modelling for the design of cone-in-cone inserts. Nonetheless, in 2006 K. Johanson presented a theoretical model that supports the use of this type of inserts to achieve mass flow in hoppers with shallow converging walls [Johanson, 2006].

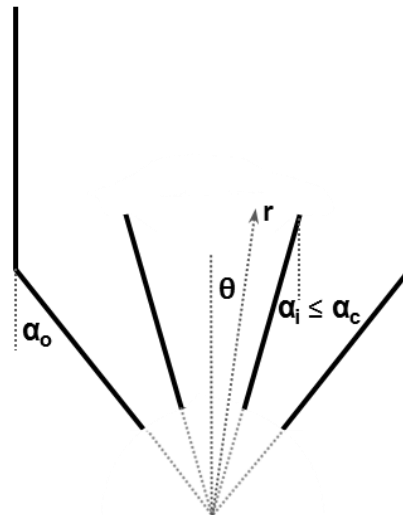


*Figure 2.28 Cone in Cone Insert Schematic*

K. Johanson based his theoretical development in the radial stress theory for Coulomb materials and for this he assumes that the internal cone have a common apex with the external hopper. He also assumes that the internal cone is capable of discharging in mass flow as shown in Figure 2.28, where the insert half angle is set to be smaller than the critical angle for mass flow. Using spherical coordinates with the radial direction starting at the common apex of the cones, the equations of motion for slow moving conditions (acceleration terms neglected) can be written as follows:

$$\frac{1}{r^2} \cdot \frac{\partial(r^2 \cdot \sigma_r)}{\partial r} + \frac{1}{r \cdot \sin\theta} \cdot \frac{\partial(\tau_{r\theta} \cdot \sin\theta)}{\partial \theta} + \frac{1}{r \cdot \sin\theta} \frac{\partial \tau_{r\varphi}}{\partial \varphi} - \frac{\sigma_\theta + \sigma_\varphi}{r} = \rho \cdot g_r \quad (2-15)$$

$$\frac{1}{r^2} \cdot \frac{\partial(r^2 \cdot \tau_{r\theta})}{\partial r} + \frac{1}{r \cdot \sin\theta} \cdot \frac{\partial(\sigma_\theta \cdot \sin\theta)}{\partial \theta} + \frac{1}{r \cdot \sin\theta} \frac{\partial \tau_{\theta\varphi}}{\partial \varphi} + \frac{\tau_{r\theta}}{r} - \frac{\cot\theta}{r} \cdot \sigma_\varphi = \rho \cdot g_\theta \quad (2-16)$$

Please note that K. Johanson's work also includes terms for gas pressure gradients but these have been omitted to simplify the explanation of the method.

According to the Haar-Von Karman hypothesis the normal stress ( $\sigma_\varphi$ ) is either a major or minor principal stress. Normal hoop stress ( $\sigma_\theta$ ) equals major principal stress if the material flows through converging geometries, and equals the minor principal stress when flowing through diverging geometries. In either case, the shear stresses ( $\tau_{r\varphi}$ ) and ( $\tau_{\theta\varphi}$ ) equal zero. Taking this into account equations (2-15) and (2-16) can be simplified to:

$$\frac{1}{r^2} \cdot \frac{\partial(r^2 \cdot \sigma_r)}{\partial r} + \frac{1}{r \cdot \sin\theta} \cdot \frac{\partial(\tau_{r\theta} \cdot \sin\theta)}{\partial \theta} - \frac{\sigma_\theta + \sigma_\varphi}{r} = \rho \cdot g_r \quad (2-17)$$

$$\frac{1}{r^2} \cdot \frac{\partial(r^2 \cdot \tau_{r\theta})}{\partial r} + \frac{1}{r \cdot \sin\theta} \cdot \frac{\partial(\sigma_\theta \cdot \sin\theta)}{\partial \theta} + \frac{\tau_{r\theta}}{r} - \frac{\cot\theta}{r} \cdot \sigma_\varphi = \rho \cdot g_\theta \quad (2-18)$$

Then, from the Mohr-Coulomb yield criteria for steady flow:

$$\sigma_r = \sigma \cdot (1 - \sin\delta \cdot \cos 2\omega) \quad (2-19)$$

$$\sigma_\theta = \sigma \cdot (1 + \sin\delta \cdot \cos 2\omega) \quad (2-20)$$

$$\tau_{r\theta} = -\sigma \cdot \sin\delta \sin 2\omega \quad (2-21)$$

$$\sigma_\varphi = \sigma \cdot (1 + \sin\delta) \quad (2-22)$$

And from the radial stress field:

$$\sigma = \gamma \cdot g \cdot r \cdot s(\theta) \quad (2-23)$$

Substituting equations (2-19) to (2-23) into (2-17) and (2-18) and simplifying:

$$\frac{ds}{d\theta} = \frac{(\sin 2\omega + \sin \delta \cdot \cot \theta \cdot \cos 2\omega - \sin \delta \cdot \cot \theta - \sin \delta \cdot \sin 2\varphi)s}{\cos 2\omega + \sin \delta} \quad (2-24)$$

$$\frac{d\omega}{d\theta} = \frac{1}{2} \frac{\left[ \cos \delta^2 - \sin \delta \cdot \left( \frac{\sin 2\omega \cdot \cot \theta}{\cos 2\omega + 1} \right) \cdot (\sin \delta + 1) \right] s + (\cos 2\omega \cdot \cos \theta - \sin 2\omega \cdot \sin \theta) \cdot \sin \delta + \cos \theta}{s \cdot \sin \delta \cdot \cos 2\omega + \sin \delta} - 1 \quad (2-25)$$

The equations above are valid for the conical region inside the internal cone and for the annular region between the two cones, the difference between them lies on the boundary conditions. For the region inside the internal cone the boundary conditions are given by:

$$\omega = 0 \text{ at } \theta = 0 \quad (2-26)$$

$$\omega = \frac{1}{2} \cdot \left( \varphi_w + a \sin \left( \frac{\sin \varphi_w}{\sin \delta} \right) \right) \text{ at } \theta = \alpha_i \quad (2-27)$$

And for the annular region between the cones:

$$\omega = \frac{1}{2} \cdot \left( \varphi_{wo} + a \sin \left( \frac{\sin \varphi_w}{\sin \delta} \right) \right) \text{ at } \theta = \alpha_o \quad (2-28)$$

$$\omega = -\frac{1}{2} \cdot \left( \varphi_{wi} + a \sin \left( \frac{\sin \varphi_w}{\sin \delta} \right) \right) \text{ at } \theta = \alpha_i \quad (2-29)$$

Equations (2-22) and (2-23) are then integrated using the boundary conditions given above to produce radial stress solutions for both the conical and the annular region. The solutions for the conical region are normally presented as a family of curves marking the limit of the variables for which a solution exists as it was shown in Figure 2.20. The bold line marked as conical mass flow limit in Figure 2.29 is an example of these limit lines, for a powder with 50 degrees internal friction angle. In the region to the right of the line there are no solutions to the radial stress field and it has been found experimentally that these lines are also the limit between mass flow and core flow. Figure 2.29 also presents solutions for the annular region depending on the half angle of the internal cone, therefore for a given insert the maximum half angle of the external hopper can be calculated. Conversely, for an existing external hopper the adequate half angle of the internal insert to achieve mass flow can be calculated. The curve marked as balanced friction limiting mass flow line represents the mass flow limit of the cone in cone system when the wall friction angle is the same at the walls of the internal and external cones. Please note that although solutions exist beyond the balanced friction limit and therefore mass flow could still be achieved in the annular region, core flow would develop inside the inner cone creating regions of stagnant material.

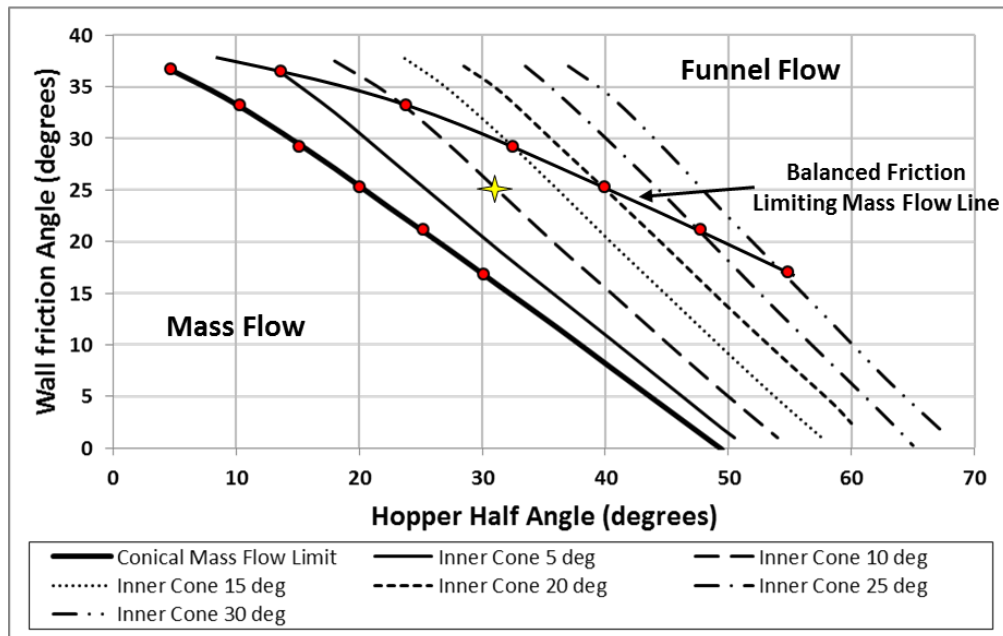


Figure 2.29 *Balanced Friction Mass Flow limit for a Cone in Cone System for  $\delta=50^\circ$  [Johanson, 2006]*

To illustrate the benefits of installing a cone in cone insert, consider a powder with 50 degrees internal friction angle which is to be handled in a hopper with a wall friction angle of 25 degrees and mass flow is required. In that case from Figure 2.29 it can be seen that the maximum inclination of the hopper is 20 degrees from the vertical. However, if a 20 degree half angle cone in cone insert is used, the walls of the hopper can have a 40 degrees angle from the vertical and still produce mass flow. In the same way, if a 30 degrees half angle hopper is used for the example above, installing an insert with 10 degrees half angle will be enough to produce mass flow in the entire system. However, if for the same hopper a 25 degrees half angle insert is used, mass flow will be achieved in the annular region but the material inside the insert will discharge following a core flow pattern.

#### **2.5.2.1 Johanson's Design Method**

Johanson presented his design as part of a patented blending machine for bulk solids, where the insert is placed in a core flow bin and develops a mass flow pattern inside itself and around it. Depending on the operation of the machine, the velocity of the solids inside the insert could be different to that of the solids flowing around it, producing a mixing effect, or both velocities could be similar, producing a standard mass flow pattern. The insert designed by Johanson is known as Binsert and has been used to overcome segregation and unreliable flow problems [Jenike, 2008<sub>1</sub>; Jenike, 2008<sub>2</sub>; Arnold, 2001; Bates, 2001, Jenike, 2013<sub>1</sub>; Jenike, 2013<sub>2</sub>; Jenike, 2013<sub>3</sub>; Jenike, 2013<sub>4</sub>; Jenike, 2013<sub>5</sub>; Jenike, 2013<sub>6</sub>; Jenike, 2013<sub>7</sub>; Jenike, 2013<sub>8</sub>].

A procedure for the design of the insert can be deduced from the patent. However, some aspects are not fully specified, therefore a complete design is not entirely possible.

The inserts has to be capable of developing mass flow in its interior. For that reason, the walls of the insert must have a half angle no bigger than the critical half angle for mass flow ( $\alpha_c$ ). Johanson states that to obtain mass flow in the annular channel between the walls of the insert and the walls of the bin, the difference between the

half angles of these walls must not exceed the critical angle for mass flow ( $\alpha_c$ ) either. See Figure 2.30.

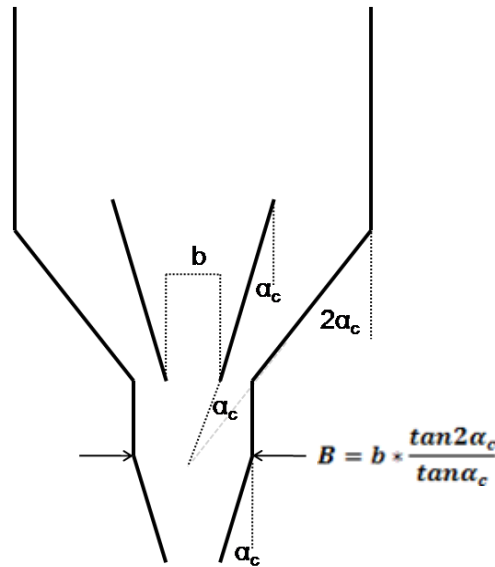


**Figure 2.30** Design of a Cone in Cone insert in accordance with Johanson

The limit imposed on these two angles fixes the maximum slope, which the walls of the hopper can have in order to obtain mass flow. Consequently, mass flow could not be achieved in a hopper with a half angle bigger than twice the value of the critical angle for mass flow ( $\alpha_c$ ), if only one insert is installed. However, more than one cone in cone insert can be installed in a silo to achieve mass flow when the hopper walls have a half angle exceeds twice the value of  $\alpha_c$ . For example, if two inserts are installed in a silo, the half angle of the hopper walls can be up to three times the value of  $\alpha_c$ , as shown in Figure 2.31. Reference [Jenike, 2013<sub>1</sub>] presents an industrial application where a double Binsert was installed in a hopper.

The insert should be placed in such a fashion that its apex coincides with the apex of the hopper and for the moment it will be assumed that both outlets are be at the same level (this however, is not necessarily a requirement as it will be explained below). The outlet size for the insert should be at least equal to the arching dimension of the bulk solid ( $b$ ); no information is given on the outlet size of the hopper ( $B$ ), but a simple mathematical deduction would yield:

$$B = b * \frac{\tan 2\alpha_c}{\tan \alpha_c} \quad (2-30)$$

For values of  $\alpha_c$  commonly varying between  $12^\circ$  and  $30^\circ$ , the ratio  $B/b$  varies between 2.3 and 2.0 approximately; then the outlet of the silo would be at least twice the arching dimension of the bulk solid. This in many cases would be too large to be directly interfaced on to a feeding device, and an additional converging section would have to be added to reduce the outlet size.

The additional section should be capable of performing in mass flow; therefore its half angle should be no bigger than the critical angle for mass flow ( $\alpha_c$ ) and its outlet size no smaller than the arching dimension ( $b$ ). However, if this section is installed right at the outlet of the silo, the insert will produce the mixing effect mentioned above; for that reason a cylindrical segment has to be fitted between the outlet of the silo and the new converging section. See Figure 2.30.

As can be seen, there are still features of the design which have not been fully described. There is no mention in the document about the length of the cylindrical section, nor the length or upper diameter of the insert, which would be necessary to obtain the complete design of the device.

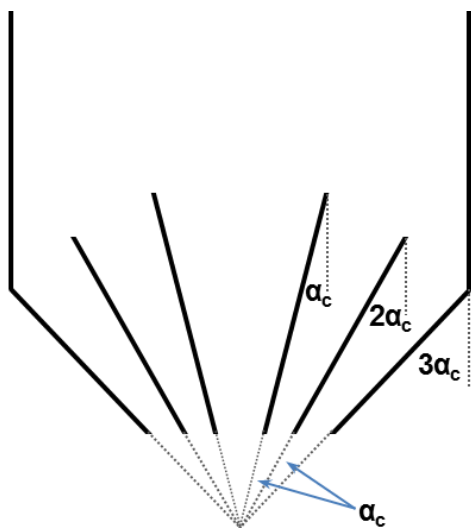


**Figure 2.31** Multiple Cone in Cone Insert

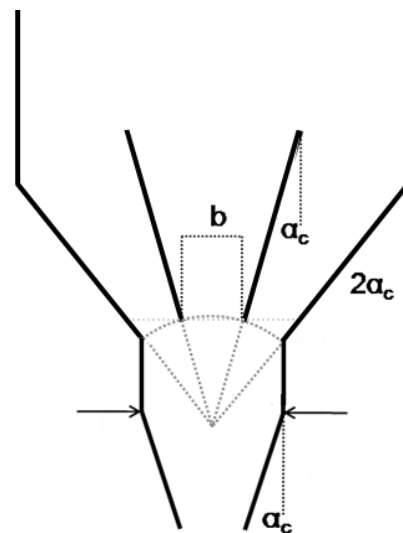


**Figure 2.32** Insert and Hopper Outlets at Different Levels

The outlet of the insert and the outlet of the hopper do not need to be at the same level as it was mentioned before, in fact the wall of the hopper can be extended downwards until it intersects an arc struck from the apex of the cones and passing through the outlet of the insert, as shown in Figure 2.32. This presents the advantage of a reduction on the minimum outlet of the silo which as it was shown above had to be at least twice the arching dimension of the bulk solid. The wall of the silo must not be extended past the intersection with the arc, otherwise mass flow will not be achieved in that section and the stagnant zone produced could propagate upwards rendering the insert ineffective.

### **2.5.2.2 Enstad's Design Method**

Several articles have been published on different research aspects related to cone-in-cone inserts at POSTEC [Karlsen, 1998; Enstad, 1996; Enstad, 1997; Enstad, 1998; Schuricht, 2001; Xiao, 2008; Hartl, 2008; Schuricht, 2008; Wójcik, 2008 and Wójcik, 2012 among others]. However, design guidelines are not presented in most of the publications above, except for [Enstad, 1996] where the experimental results are analysed based on some insert design variables.

The design procedure presented below was obtained from a personal interview with Professor Gisle G. Enstad, at the POSTEC laboratories in Porsgrunn - Norway in August 2008. The author would like to express his most sincere gratitude to Professor Enstad and POSTEC team for their time, affability and willingness to help.

Enstad proposes a design in essence similar to Johanson's, the relationship between the half angles of the hopper and insert is maintained. Consequently, the insert must have a maximum half angle equal to the value of the critical angle for mass flow ( $\alpha_c$ ), and the hopper cannot be shallower than twice the value of the said angle.

In order to avoid bridging inside the insert, the size of its outlet should be at least equal to the arching dimension of the bulk solid ( $b$ ), yet it is recommended to make the outlet slightly bigger; a safety factor of ten percent is usually applied.

The key element that differentiates both designs lies in the placement of the insert inside the hopper. For Enstad, the optimum position would be such, that the area of the insert outlet equals 10% of the cross sectional area of the hopper at the height where it is placed, see Figure 2.33. That is, the area of the insert outlet should be 10% of the hopper cross sectional area at point D.

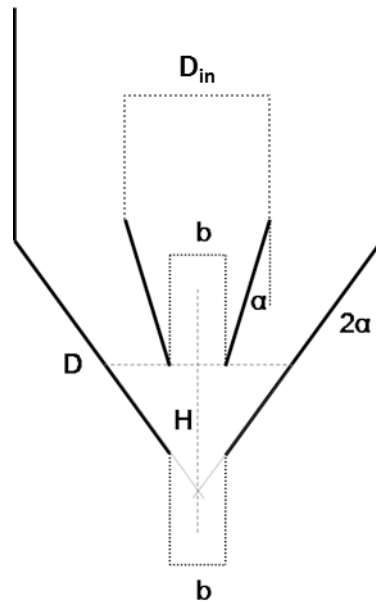


*Figure 2.33 Design of a Cone in Cone insert in accordance with Enstad*

It is not difficult to calculate the position of the point D, it can be done playing with the areas and angles as follows:

$$\frac{A_{ins}}{A_{hop}} = \frac{\frac{\pi b^2}{4}}{\frac{\pi d^2}{4}} = \frac{b^2}{d^2} = 0.1 \quad (2-31)$$

$$\tan 2\alpha = \frac{d/2}{H} \quad (2-32)$$

Where H is the distance between the apex of the hopper and the outlet of the insert and d is the diameter of the hopper cross sectional area at point D.

From (2-32) and (2-33)

$$H = \frac{b}{2\sqrt{0.1}\tan 2\alpha} \quad (2-33)$$

Thus, the position of the insert will be a function of the arching dimension and the critical half angle. The insert is then extended upwards with an angle from the vertical equal to the value of the critical angle for mass flow ( $\alpha_c$ ), until the area of the insert inlet equals 50% of the cross sectional area of the silo cylindrical section. The calculation for the inlet diameter of the insert produces:

$$D_{in} = \sqrt{0.5} D_{silo} \quad (2-34)$$

Finally, the outlet of the hopper should be the same size as the outlet of the insert, or just slightly bigger. With this, Enstad's design requires less headroom than Johanson's.

When the half angle of the hopper exceeds twice the value of the critical angle for mass flow ( $\alpha_c$ ), Enstad also recommends the use of multiple inserts as shown in Figure 2.34. Please note that a comparison between Figure 2.34 and Figure 2.31 makes evident the differences between both design methods.

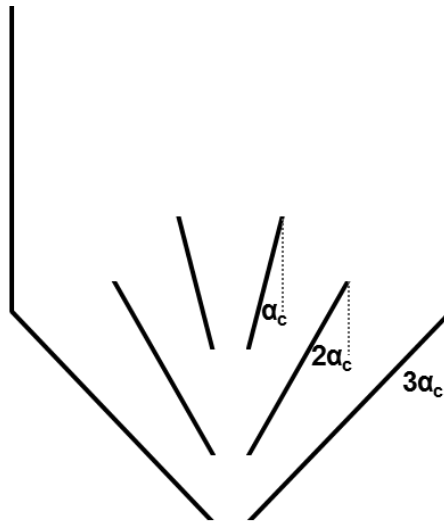


**Figure 2.34** Multiple Cone in Cone insert in accordance with Enstad

### **2.5.3 Design of Double Cone Inserts as Flow Promotion Devices for Discharging Bulk Solids**

Most of the research on the use of double cones to promote flow has been carried out by the POSTEC team in Norway [Enstad, 1998; Ding, 2002; Ding, 2003; Ding, 2004<sub>1</sub>; Ding, 2004<sub>2</sub>; Ding, 2005; Wójcik, 2007; Ding, 2008; Xiao, 2008]. In these publications, it is possible to find some indications that would lead to the design of a double cone insert. However, most of the information related to the design procedures was obtained from the interview sustained in Norway with the POSTEC team.

Basically, two different design approaches have been followed in POSTEC, one derived from the cone-in-cone concept and the other one developed through experimentation and simulation.

Enstad has designed and successfully installed cone-in-cone inserts in industrial silos in the past [Enstad, 2008]. However, in applications where time consolidation has a high effect on the flow properties of the material, a stable arch could develop inside the insert. Should this happen, it would be a very difficult problem to overcome. Whilst thinking about a solution for these types of processes, Enstad decided to cover the insert with an inverted cone so the solids would only flow on the exterior of the insert. Covering the insert with an inverted cone theoretically presents a great advantage, as the benefits of inverted cones could be added to those of the cone-in-cone insert. In this way, the hopper will not be limited to a maximum half angle of twice the critical half angle for mass flow.

The general procedure design for this approach would be as follows:

The lower part of the insert will be a cone with a half angle equal to the critical half angle for mass flow ( $\alpha_c$ ). The apex of this cone should be placed at the outlet of the existing silo, see Figure 2.35. The lower cone would extend upwards up to a point just below the transition of the silo.

An inverted cone with  $30^\circ$  half angle and diameter equal to the largest diameter of the lower cone would complete the design.

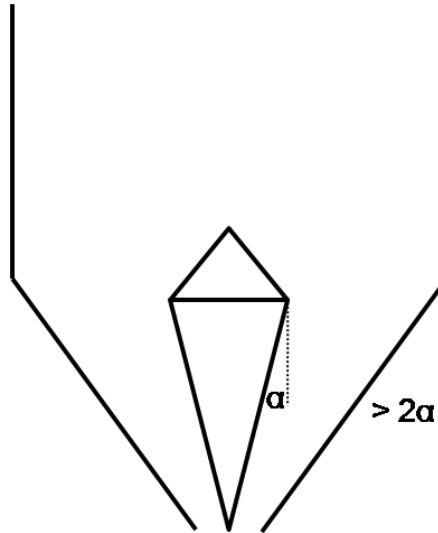


*Figure 2.35 Design of a Double Cone Insert, Method Derived from the Cone in Cone Concept*

The second method for the design of double cone inserts relies more on the experimental results obtained through the numerous projects carried out in POSTEC and the results from finite element method (FEM) and discrete element method (DEM) simulations.

Several configurations of the double cone, in one way or another, have been studied in POSTEC, these include: steep top cone and shallow bottom cone, shallow top cone and steep top cone, both cones steep, both cones shallow, lower cone extending to the outlet of the silo or extending to different places inside the bin, among others [Enstad, 1997; Ding, 20042; Wójcik, 2007].

So far the best results have been obtained with an insert designed as follows [Wójcik, 2007]:

An inverted cone is made with a half angle of  $30^\circ$ , its diameter ( $D_{ins}$ ) would be 25% of the diameter of the vertical section of the silo ( $D_{silo}$ ). This insert should be located so that its lower part stands just below the transition of the silo.

From the lower part of the inverted cone, a cone is built extending down to the outlet of the silo, see Figure 2.36.

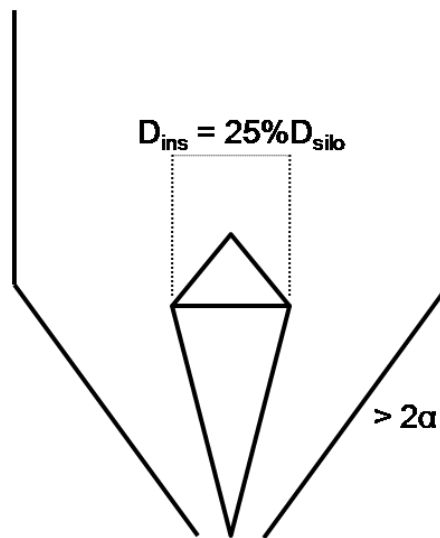


**Figure 2.36** *Design of a Double Cone Insert, from experimental and simulated results*

Although the design methods are different, both approaches produce similar inserts. Nevertheless, the configuration of the insert is still being developed by the POSTEC team and a definitive recommendation for industrial application does not seem to be available yet.

## 2.6 Loads on Inserts

An important aspect to bear in mind when installing an insert, is the force that the granular material above is applying on its surface. If the insert is not supported adequately and cannot resist the load exerted, failure is inevitable.

Johanson carried out an experimental investigation on the loads exerted on inverted cones of different sizes and positions. Typical results from that study are presented in Figure 2.37.

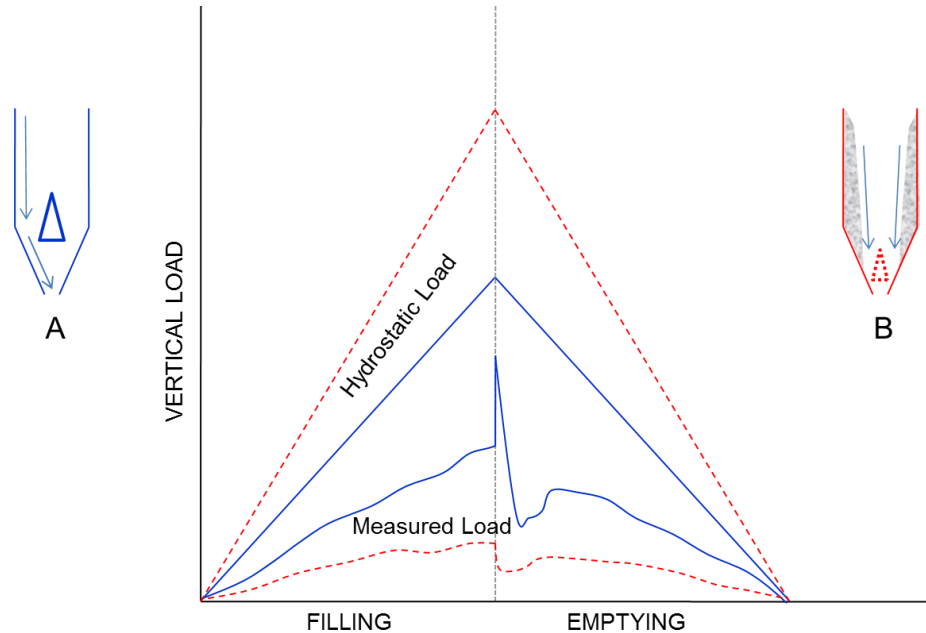


**Figure 2.37** Vertical Stress on Inserts, Johanson [Johanson, 1966]

The solid lines in Figure 2.37 show the results for the insert A and the dashed lines for insert B. It can be seen that when the insert is positioned high in the hopper, there is a sudden increase in the load when the silo starts discharging. However, this peak is not present when the insert is positioned low in the hopper closer to the converging walls. This is due to the walls supporting a larger part of the load exerted by the powder.

When the silo starts discharging, flow is not completely developed on the insert walls, the coefficient of friction is not fully mobilised and the stress exerted is higher, which explains the presence of the peak. Once the flow is fully developed, the stress decreases and can be modelled applying concepts for converging channels.

### 2.6.1 Stress Analysis in a Vertical Channel

Before proceeding to the calculation of loads on inserts it is important to analyse the stresses acting in a vertical channel, as this will be later used for the calculation of those loads. In 1895 Janssen introduced a method to calculate stresses in vertical channels with parallel walls, which was later known as the method of differential slices [Nedderman, 1992; Arnold, 1979; Schulze, 2008]. The analysis considered a cylindrical silo containing a cohesionless granular material and included the following assumptions:

- a. Stresses are constant across any horizontal section of the material.
- b. The ratio of vertical to horizontal stress is constant and independent of the magnitude of stress.
- c. The wall friction is fully mobilized at every point along the wall.
- d. The bulk density is independent of stress.

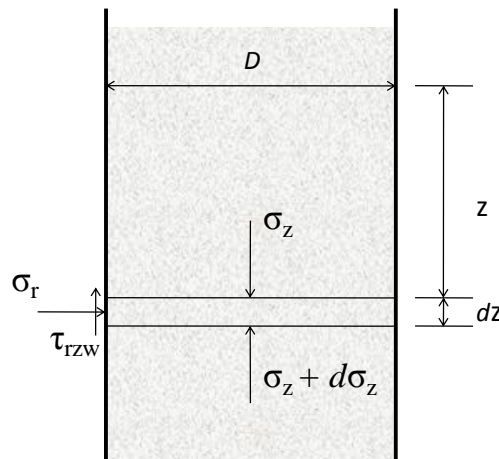


*Figure 2.38 Stresses Acting on a Differential Slice [Arnold, 1979]*

$D$ : Diameter of the silo

$z$ : Head of powder

$\tau_{rzw}$ : Shear stress at the wall

$\sigma_z$ : Vertical stress

$\sigma_r$ : Radial stress

A force balance in the vertical direction, carried out on the differential slice of Figure 2.38 yields [Arnold, 1979]:

$$\frac{\pi D^2}{4}(\sigma_z + d\sigma_z) + \pi D\tau_{rzw}dz = \frac{\pi D^2}{4}\sigma_z + \rho g \frac{\pi D^2}{4}dz \quad (2-35)$$

*Neglecting second order terms and dividing by  $\frac{\pi D^2}{4} dz$ :*

$$\frac{d\sigma_z}{dz} + \frac{4}{D}\tau_{rzw} = \rho g \quad (2-36)$$

From assumption b:

$$\frac{\sigma_r}{\sigma_z} = K_j \quad (2-37)$$

From assumption c:

$$\mu = \tan\varphi = \frac{\tau_{rzw}}{\sigma_r} \quad (2-38)$$

Where  $K_j$  is the Janssen constant,  $\mu$  is the coefficient of friction between the powder and the wall and  $\varphi$  is the angle of wall friction. Substituting (2-37) and (2-38) in (2-36) gives:

$$\frac{d\sigma_z}{dz} = \rho g - \frac{4\mu K_j}{D}\sigma_z \quad (2-39)$$

Equation (2-39) can be integrated between the limits of  $\sigma_z = 0$  at  $z = 0$  and  $\sigma_z = \sigma_z$  at  $z = z$  yielding:

$$\sigma_z = \frac{\rho g D}{4\mu K_j} \left[ 1 - e^{-4\mu K_j \frac{z}{D}} \right] \quad (2-40)$$

One of the most important results derived from Equation (2-40) can be found when taking the limit when  $z/D$  becomes large. In that case the term in the brackets tends to 1 and therefore:

$$\sigma_z = \frac{\rho g D}{4\mu K_j} \quad \text{when } \frac{z}{D} \rightarrow \infty \quad (2-41)$$

Equation (2-41) shows that in tall silos the stresses are not dependent on depth of powder, but are dependent on the width of the silo; that is the reason why silos usually have a high height to diameter ratio, contrary to what happens with fluid tanks, where that ratio is small due to stress being a strong function of depth.

Equation (2-37) is identical to an equation developed by Rankine, so it is common to take  $K_j$  as follows:

$$K_j = \frac{1 - \sin\delta}{1 + \sin\delta} \quad (2-42)$$

Although it can be shown that the assumptions made by Janssen are incorrect [Nedderman, 1992], this method is still commonly used due to its simplicity. Other models have been developed to overcome the inconsistencies of Janssen's method [Nedderman, 1992; Arnold, 1979], however these models are more complex and the results are usually very close to Janssen's.

### 2.6.2 Calculation of Vertical Stress

Johanson assumed that the flow around the insert is basically a vertical cylinder, therefore for tall silos, the maximum vertical stress could be calculated using Equation (2-41), which can be rewritten as:

$$\sigma_z = \frac{\rho g D (1 + \sin\delta)}{4 \tan\phi (1 - \sin\delta)} \quad (2-43)$$

However, Johanson proposed the following alternative equation to calculate the maximum vertical stress on the insert when the flow has not fully developed.

$$\sigma_z = \frac{\rho g D (1 + \sin \delta)}{4 \sin \delta \cdot \sin \left( \sin^{-1} \left[ \frac{\sin \varphi}{\sin \delta} \right] - \varphi \right)} \quad (2-44)$$

Depending on the size and position of the insert, the parameters of Equation (2-44) might be different.

The diameter  $D$  in the equation refers to the diameter of the flow channel, therefore if the transition of the silo is contained in the area influenced by the insert, as in Figure 2.37a (large insert positioned near the transition), the flow channel will have the same diameter as the vertical section of the silo. However, if the insert is small and positioned low in the hopper, the diameter of the flow channel would be smaller (see Figure 2.37b) and should be calculated with the help of the procedure presented in section 2.5.1.

Attention should be paid to the value of the wall friction angle ( $\varphi$ ), when the insert is positioned low, as in Figure 2.37b. The powder does not slip at the wall at any point and  $\varphi$  should be replaced by the angle of internal friction ( $\delta$ ), as the friction would be produced through powder against powder.

When the insert produces the effect shown in Figure 2.37a, the powder would slip at the wall along the total height of the silo and  $\varphi$  can be used. A third case has to be considered, where the insert produces a flow channel not wide enough to obtain mass flow, but which touches the wall of the silo at some point. Shear would occur, powder against powder below this point, and powder against the wall above it; thus a value between  $\delta$  and  $\varphi$  should be used.

The analysis above applies for tall silos, that is, when the depth of powder over the insert is at least four or five times the diameter of the bin. When this is not the case,

Johanson recommends the use of hydrostatic stress for the head of powder, thus  $\sigma_z$  would be equal to  $\rho gz$ , where  $z$  is the head of material.

### 2.6.3 Calculation of Total Vertical Force

The total vertical force applied on the insert will be given by the maximum vertical stress  $\sigma_z$  from Equations (2-43) or (2-44) multiplied by the effective area of the insert. When the material is free flowing, the effective area will be a circle of radius  $r$  equal to the radius of the insert. However for less free flowing materials, an arch would tend to form between the insert and the surrounding material, see Figure 2.39.

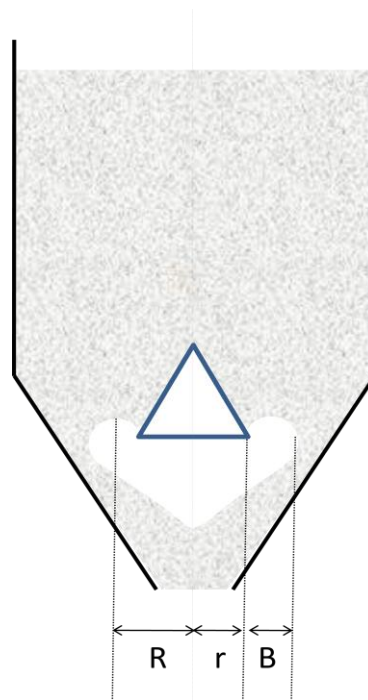


*Figure 2.39 Arching Effect Around the Insert, Johanson [Johanson, 1966]*

Although the arch will probably fail, it causes the inserts to receive additional force. This effect is obviously more notorious when the discharge starts. In Figure 2.13,  $B$  represents the arching dimension of the material, thus the effective area will be a circle of radius  $r$  plus half the arching dimension.

## **2.7 Impact of the Literature Review on the Objectives of the Project**

Section 2.5 presented a review of the main types of insert used as flow promotion devices including the information available for their design. The inserts presented were inverted cones, cone in cones and double cones which represent the vast majority of the research published on the subject. Although other insert configurations are also used for flow promotion, the design information about them is in general very limited and for that reason have not been discussed further.

From the inserts reviewed, the reference material on inverted cones contains the most detailed information both for their design and positioning, with a fully design method published by J. Johanson in 1965 [Johanson, 1965]. The method takes into account the geometry of the silo and the flow properties of the material which produces an insert that is specific for each application. However, an area of concern for the author is that the method has been developed for steady state conditions of stress in the vicinity of the insert. This implies that it would only be valid for silos with tall vertical sections i.e. where the head of material is at least 3 times larger than the diameter of the silo. Therefore, the validity of the method with low heads of material is questionable and could represent a good starting point for the familiarisation of insert performance for this research project. Another issue with the design method is that for silos with shallow convergences and depending on the flow properties of the material, the design procedure might not produce a practical solution. The insert produced could be so large that the material would arch over the annulus between the hopper walls and the insert base, stopping flow altogether.

Cone in cone is another type of insert where some design information can be found in the literature. From this, the best known application was developed by J. Johanson and presented as part of a patent for a static powder mixer. Although some of the design features of the insert can be deduced from the patent, it does not include all the information to produce a full design. A second approach for the design of cone in cone inserts has been developed at the POSTEC institute. A fully detailed procedure for the design of the insert has been include in section 2.5, which was obtained from the published work and also through a personal interview with the members of POSTEC. However, the author would like to state his concerns with the

insert produced by this design method, particularly with the relationship between the out of the insert and the outlet of the silo. The design procedure recommends the insert outlet to be the same size as the outlet of the silo, which the author would suggest should create a preferential draw of material for the interior of insert which very little movement (if any) in the annular region between the insert and the hopper walls. This is however, just the author opinion which would need to be supported by experimental data.

In the case of double cone inserts, most of the information available comes from the research undertaken at POSTEC, where two main approaches have been followed for the design of the inserts. One approach is based on experimental development whereas the second one is based on software modelling and simulation. The data published so far does not suggest that a reliable design procedure has been produced through either approach and the development of mass flow in core flow silos has not consistent with the use of this insert.

The points above clearly present the knowledge gap that currently exists in the application of static inserts as flow promotion devices. Therefore, that gap has been identified as the main target of this research project, with the idea of providing engineers with the practical tools necessary to improve the discharge performance from silos through the use of inserts.

## **2.8 Summary**

### **Silo Discharge Behaviour and Operation Problems**

When a granular material stored in a silo is discharged, the flow behaviour of the solids would depend on the properties of the bulk solid, the geometry of the silo and the frictional characteristics between the solids and the materials of construction of the silo walls. If all the particles in the silo are in motion at all times during discharge, the flow pattern developed in the silo is known as mass flow. If regions of stagnant material develop during discharge, the silo is said to discharge in core flow. A large number of bulk solids handling problems in industry are associated to core

flow discharge, some of these include: flow stoppages, segregation, flooding, and particle degradation. Mass flow could be the preferred flow pattern for the larger number of industrial applications because it minimizes some of the problems associated with core flow, however, other types of problems are associated with mass flow including: silo quaking and honking, high structural stresses and wear.

### **Insert Solution to Silo Discharge Problems**

Inserts of a variety of shapes and sizes have been used in industry to overcome the problems mentioned above. In many cases, the best way to address these problems is by changing the discharge pattern of the silo. The use of inserts for this purpose has been the subject of several studies during the last five decades and research has focused mainly on the development of three types of insert: inverted cones, cone in cones and double cones. In 1965, Jerry Johanson presented a method for the design and positioning of inverted cones to achieve mass flow in conical core flow bins. The method provides practical guidelines for the design of the inserts according to the flow properties of the material and the configuration of the existing bin.

### **Current Standards for Insert Design**

It was also Johanson who first published research results on the use of cone in cone inserts to promote flow in 1981. In more recent years cone in cone inserts have also been the object of study for the POSTEC research group in Norway led by Professor Gisle Enstad. They have generated numerous publications on this subject and have produced a design method slightly different from that of Johanson's. Most of the published work on double cone inserts, has also been done by the POSTEC group and two main design approaches have been followed, one derived from the cone-in-cone concept and the other one developed through experimentation and simulation.

## **The Inadequacies of the Current Insert Methods and the Challenge for this Thesis**

Although in some cases it is possible to achieve mass flow in core flow bins with the help of the methods explained in this chapter, this is not always the case. If an inverted cone is designed to work with cohesive materials, in some instances it will be found that in order to achieve mass flow the insert needs to be so large that there will be not enough space, between the insert and the walls of the hopper, for the powder to flow making the design unviable. The use of a cone in cone could be the answer to the problem, however, it needs to be remembered that the outlet of the silo will have to be at least twice the arching dimension of the material. Additionally, if the convergence of the silo is shallow more than one insert needs to be fitted making the outlet three or four times the arching dimension of the material. This means that the silo through put could be larger than the process requirement which would necessitate enlargement of the downstream equipment increasing the capital and operational costs. Therefore, this case presents an ideal scenario for the use of double cones. However, the understanding of this type of inserts is still inadequate making the technology unreliable. This example presents just one of the opportunities still available where progress can be made with the use of inserts but the technology is not quite there yet to produce a robust solution, paving the way for the objectives of this thesis.

## CHAPTER THREE: EARLY TEST RIG DEVELOPMENT

---

This chapter illustrates the first practical steps taken towards meeting the objectives of the project. The aim of this initial test programme was to gain familiarity with the way inserts work and also the equipment and methodology needed for their study. The work presented below includes the design, construction and commissioning of a 0.1 m<sup>3</sup> storage capacity test rig; as well as the results and analysis of the effect produced by installing flat plate inserts in a core flow hopper.

### 3.1 Test Rig design and Construction

The first step undertaken was to design and build a fairly basic test rig to try to understand the way the static inserts affect the discharge of bulk solids. The rig should at least provide the opportunity to observe a granular material discharging from a bin, both in the presence and absence of inserts. For this purpose, the test rig shown in Figure 3.1 was designed.

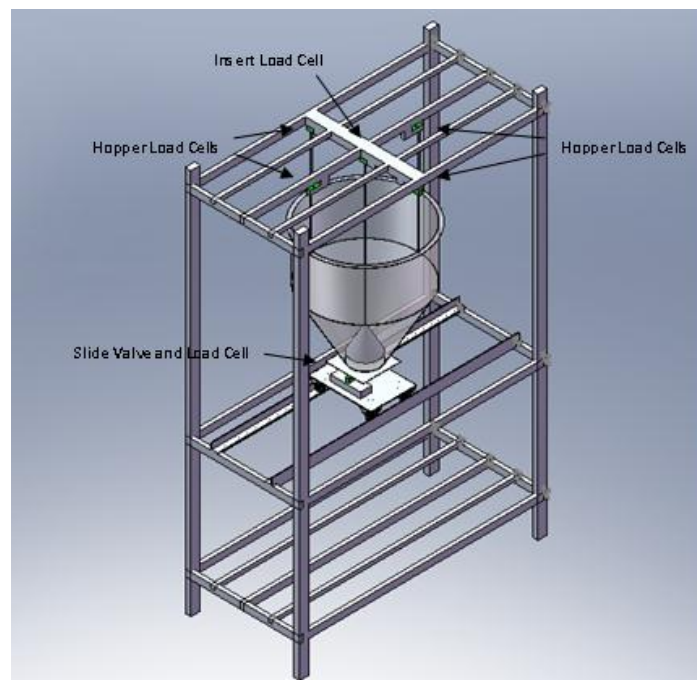


*Figure 3.1 Schematic Design of the Initial Test Rig*

The rig consisted of a conical hopper of 30° half angle hanging from load cells, a slide valve with an attached load cell and a bracket supported on another load cell, where various inserts could be mounted. A three level modular steel frame was used for the supporting structure as shown in Figure 3.1. The top level supported the load cells used to hold the silo and insert bracket, the middle level had two rails used as guides for the movement of the outlet slide valve and the bottom level was used as a shelf to support the containers collecting the discharge materials from the tests. An existing silo – property of The Wolfson Centre for Bulk Solids Handling Technology – was used as the storage silo for the tests. The conical silo made of stainless steel, had a half angle of 30° (measured from the vertical) and vertical section diameter of 550 mm. The height of the vertical section was 270 mm and the silo outlet diameter was 150 mm. However, the size of the outlet was reduced to 100 mm by installing a stainless steel extension cone on the lower part of the hopper, in order to slow down the discharge rate of the test material. The hopper was suspended from three LCM Systems-BF2 beam load cells (with a range spanning from 0 to 30 kg  $\pm 0.1\%$ ) [LCM Systems, 2015], using 6mm stainless steel threaded studs, which allowed fine adjustment of the hopper level and weight distribution.

The outlet slide valve consisted of a trolley with an attached 0-30 kg ( $\pm 0.1\%$ ) LCM Systems-BF2 beam load cell [LCM Systems, 2015], which supported a 150 mm square mild steel plate (as shown in Figure 3.2). The valve rolled on a pair of steel rails welded onto the middle module of the frame. When the trolley was placed under the hopper, the metal plate closed the hopper outlet acting as a valve and at the same time, measuring the vertical load on the outlet area.

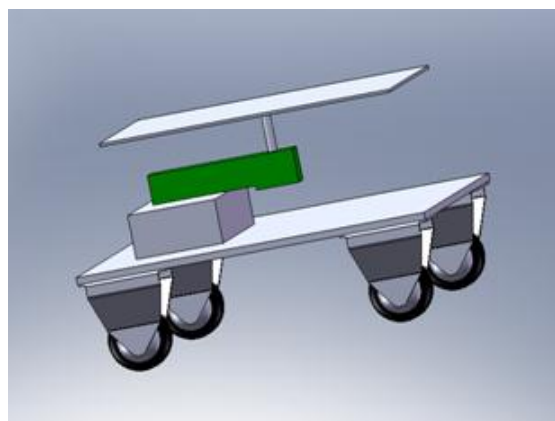


*Figure 3.2 Slide Valve*

The bracket for the inserts consisted of a 6 mm stainless steel stud hanging from a 0-30 kg ( $\pm 0.1\%$ ) LCM Systems-BF2 beam load cell [LCM Systems, 2015], which was mounted on the upper most module of the frame. The stud gave the possibility of modifying the vertical position of the inserts, allowing study of the effect of relative insert position on the discharge of solids. Additionally, the reading obtained from the load cell holding the stud would provide a measurement of the vertical load acting on the inserts, which is an important design feature from a structural point of view. Figure 3.3 shows the finished test rig.



**Figure 3.3** *Initial Test Rig*

In order to collect the data from the tests, a data acquisition system was designed and built. Three ADAM 4016 [Advantech, 2015<sub>1</sub>] I/O units were used to condition and acquire the signal from the load cells and a software application was developed to store and display the data using the ADAMView 1<sup>st</sup> Edition development tool [Advantech, 2015<sub>2</sub>].

### 3.2 Commissioning of the Test Rig

The experiments were carried out using granulated coal as a test material. The flow properties of the coal were measured using a Brookfield Powder Flow Tester and the results can be found in Table 3-1. The half angle and arching dimension shown in Table 3-1 are the result of silo design calculations for mass flow following the procedure developed by Jenike (Jenike, 1961).

**Table 3-1** *Flow Properties of the Coal Used as Test Material*

Wall Friction Angle for Stainless Steel (Deg)	Internal Friction Angle (Deg)	Bulk Density (kg/m <sup>3</sup> )	$\alpha_c$ (Deg)	Arching dimension (mm)
24	42	641	19	40
$\alpha_c$ : Maximum half angle of a cylindrical hopper to obtain mass flow				

Two flat discs made of aluminium were used as inserts. One of the discs was 220 mm in diameter, equivalent to 40% of the silo diameter. The size of this insert was calculated following the procedure developed by Johanson and presented in section 2.5.1. The second insert was 138 mm in diameter, equivalent to 25% of the bin diameter and was designed according to the work carried out by Enstad for inverted cones and double cones (Enstad, 1997; Enstad, 1998; Wójcik, 2007). The discs were located concentrically within the silo and the vertical position was varied according to Table 3-2. Figure 3.4 shows the larger insert in the middle position B.

**Table 3-2** *Inserts Vertical Position*

Distance from the outlet of the silo (mm)		
Position	Insert Diameter 220 mm	Insert Diameter 138 mm
A	300	330
B	240	240
C	190	120

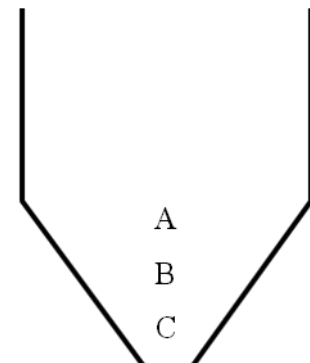




*Figure 3.4 Flat Plate Insert*

The silo was manually filled up to approximately 95% of its depth and then emptied, allowing gravity discharge. The change in weight of the hopper and the vertical force acting on the insert were recorded both when filling and discharging. Several repetitions were carried out for each insert at every position and also for the silo discharge without an insert.

### **3.3 Results and Discussion**

#### **3.3.1 Flow Behaviour Observed During Discharge**

Due to the characteristics of the test rig, the only indication that could be obtained to identify the type of flow pattern developed during discharge, was the change in the shape of the top surface of the solids. When the coal was charged into the silo it naturally formed a conical pile as shown in Figure 3.5. However, once the discharge started a funnel was rapidly formed in the centre of the upper surface and the surrounding material cascaded into it, then, the only material in motion was that in the funnel and no movement was observed near the silo walls. As the discharge continued and the level of material decreased, the shape of the coal surface remained as a funnel, as shown in Figure 3.5, where the variation in colour intensity represents the material surface at different inventory levels in the silo. This behaviour is typical of a core flow discharge pattern, which was expected due to the geometry of the silo and the characteristics of the coal. This is explained by the results of the silo design

presented in Table 3-1, where it can be seen that in order to obtain mass flow, the hopper should not have had a half angle larger than 19 degrees, whereas the half angle of the hopper used for the tests was 30 degrees.

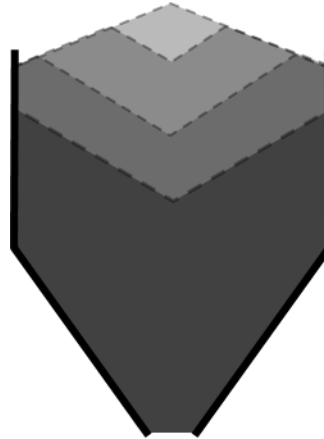


*Figure 3.5 Observed Flow – No Insert*

When the flat plate inserts were installed in the hopper the flow behaviour changed significantly, the flow behaviour became dependant both of the size and the position of the plates. When the large insert was fitted in position A, the material was observed to slip at the wall and the shape of superficial conical pile remained unchanged for a short period of time at the start of the discharge. This was followed by the formation of an annular channel concentric with the hopper, which coincided with the end of material movement in the vicinity of the walls. Therefore, the materials started cascading from the stagnant regions along the axis of the hopper and near the walls, into the annular channel. It is worth explaining that position A was calculated following Johanson's procedure to obtain mass flow (section 2.5.1). However, even though the material was observed to slip at the wall at the beginning of the discharge, it would not be correct to assume that mass flow was achieved at that moment. Conversely, it would also be incorrect to assume that mass flow was not achieved at the start of the discharge, the fact is, that observation of the top surface of the discharging material alone is not a sufficient method to infer the discharge pattern in a silo. Mass flow could be a possible explanation to the behaviour of the particles, but it is also possible that the insert widened the discharge channel in the hopper until it reached the walls of the silo, therefore producing a mixed flow type discharge pattern. In any case it is clear how the installation of the

insert produces a positive impact on the discharge of the solids by reducing (or possibly eliminating) the regions of stagnant material in the silo. Figure 3.6a shows the evolution of the upper surface profile for the test explained above, starting with the conical pile which remains unchanged for a small period, followed by the formation of the annular channel.

When the position of the insert was lowered to level B, the results were very similar to those explained above for level A and it would be difficult to differentiate the flow pattern produced by these two setups. By contrast, when the insert was positioned at level C, the annular channel appeared immediately after the start of the discharge and the material was never seen to slip at the wall (see Figure 3.6b). Another difference found for the insert at level C was that for some of the tests, the material seemed to move slightly faster through a section of the annular channel as shown in Figure 3.6c, this resulted in a slightly skewed discharge. It was also observed that when this happened, the stud holding the plate insert would bend lightly moving away from the section of faster material movement.

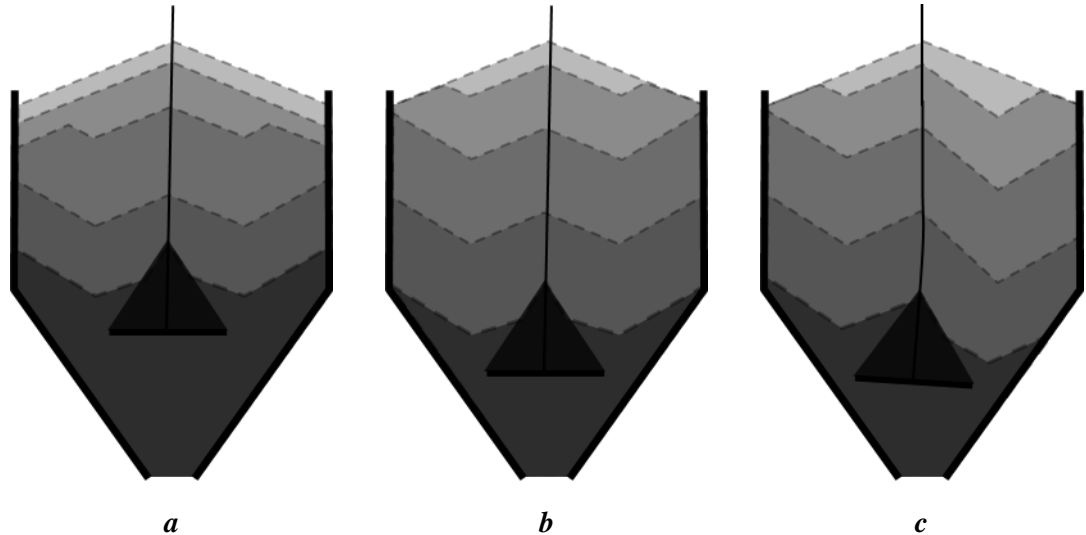


**Figure 3.6** *Observed Flow – Large Insert*

When the small insert was installed the resulting flow behaviour was different from the one obtained using the larger insert. When the flat plate was positioned at level A, the annular discharge channel was formed immediately after commencing the discharge (as shown in Figure 3.7a), in a similar way as it was described for the large flat plate positioned at level A (Figure 3.6b). However, in contrast to the larger insert

which produced similar flow behaviours when positioned at levels A and B, when the small insert was lowered to level B the result was different from that at position A (see Figure 3.7b). In fact, the discharge resembled the asymmetric one obtained with the large insert at the bottom position (Figure 3.6c). However, in this case, the difference in the rate of flow between the fast and slow moving section of the annular channel was more pronounced than what was observed for the large insert and the holding stud also seemed to bend more, but always moving away from the faster moving section. It should be noted, that the position of this faster moving section seemed to be fairly random and did not seem to follow any pattern, across the multiple repetitions.

Moving the insert to the lower level C produced an even more significant effect on the flow behaviour of the material. Instead of an annular channel forming on the surface (as it was observed for the other test setups), for the majority of the repetitions carried out with this configuration an off centre funnel was observed. As the inventory of material would go down, the discharge channel would take the shape of an incomplete annulus with the side opposite to the faster flowing region remaining stagnant (as shown in Figure 3.7c and Figure 3.7d), the holding stud would also bend significantly more than with the other configurations (see Figure 3.7e) but always bending towards the opposite side where the discharge channel was formed. Then, after most of the material would have been already discharged, the insert would return towards the centre of the bin allowing the stagnant material to be discharged.

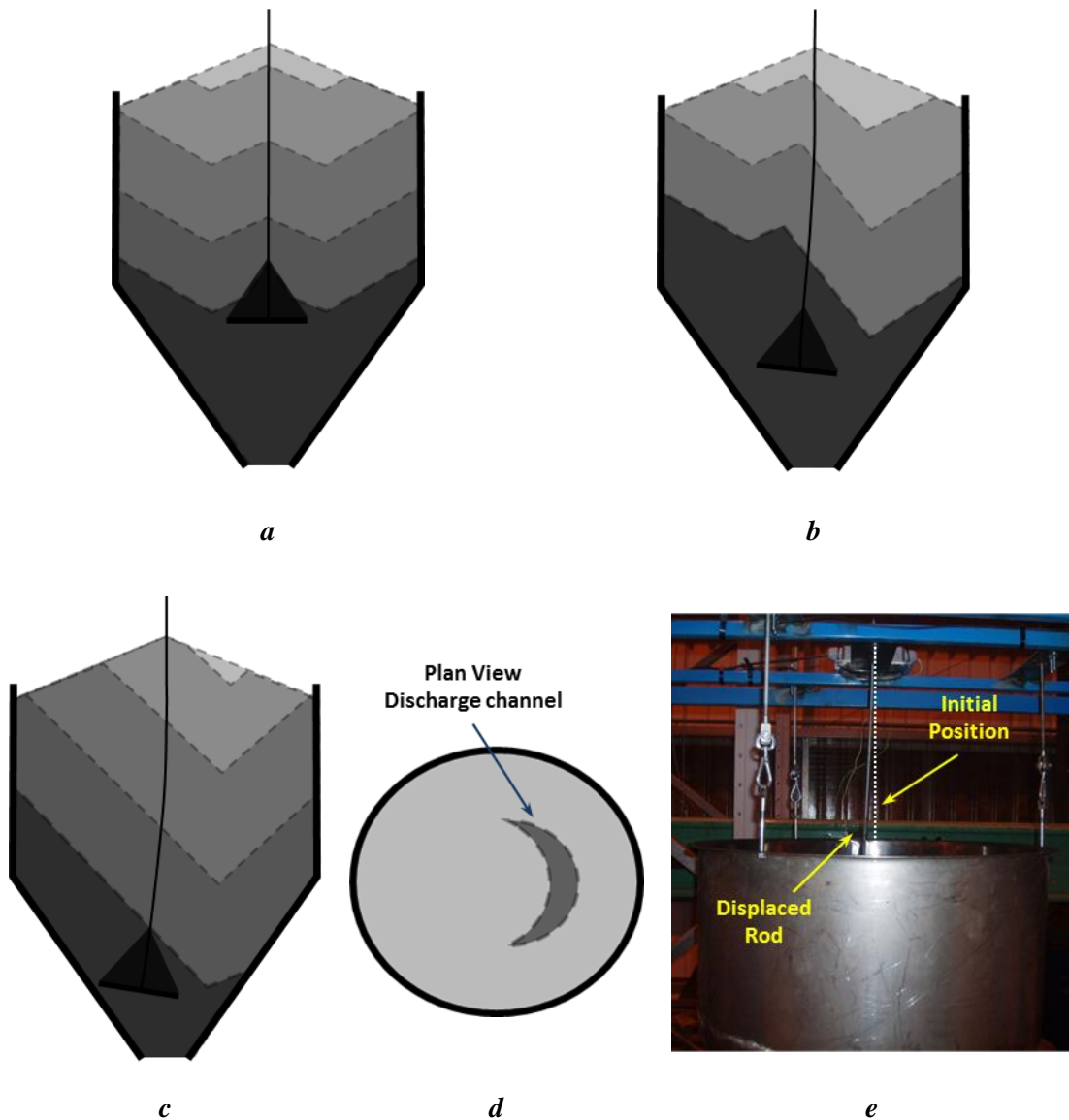


**Figure 3.7** *Observed Flow – Small Insert*

From the description given above it is clear that mass flow was not achieved when the small insert was used, the fact that the material was never seen to move in the vicinity of the walls is sufficient to support that statement. Nonetheless, the insert changed the shape of the flow channel from a central funnel to an annulus reducing the size of the stagnant regions in the bin, which for some application could be enough of a benefit to warrant installing the insert. However, as it could be seen from the results, in order to realize the benefits of installing a flat plate insert for flow promotion it is important to keep the insert central with a stable support, otherwise the displacement of the insert can cause off centre discharge channels that could even represent a risk for the structure of the silo.

Comparing the results obtained with both inserts at the different positions it is clear that the best performance was produced by the large insert located at the middle and top levels, which was actually the configuration recommended by the design procedure developed by Johanson for inverted cones and flat plates. However, as it mentioned previously, the development of mass flow in the hopper cannot be inferred from the observations carried out. For future tests, a system needs to be put in place that allows the monitoring of material motion inside the hopper, therefore allowing the inference of the flow pattern developed during discharge. Another important aspect that needs to be taken into account for the construction of a future rig is the support of the insert in the silo, because as the above results demonstrate, the lack of a stable support could diminish the potential benefits produced by the insert.

### **3.3.2 Influence of the height of the Vertical Section on the Stress Distribution**

As it was mentioned in section 3.1 the outlet of the existing hopper was reduced from 150 mm internal diameter to 100 mm internal diameter. However, during the test it was noticed that the discharge took place over a fairly short period of time which made more difficult the observation of the different stages of the discharge process. Therefore it is recommended to reduce further the size of the hopper outlet to be used without falling below the minimum arching dimension of the test material. An additional characteristic that could also be improved is the height of the vertical section of the bin, because the hopper used for these tests had a vertical section with a height to diameter ratio just under 0.5. This low value means that any change in the head of material would have a significant effect on the stress condition in the area around the insert (as it can be seen in Figure 3.8) and it would be beneficial to carry out tests with more stable conditions of stress which can be achieved with ratio values of equal to or larger than 3 where the magnitude of the stresses approach the asymptotic value (see Figure 3.8).

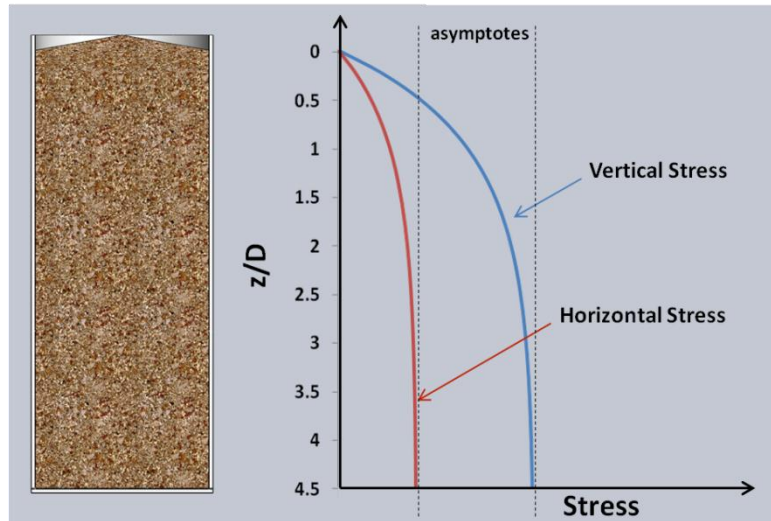
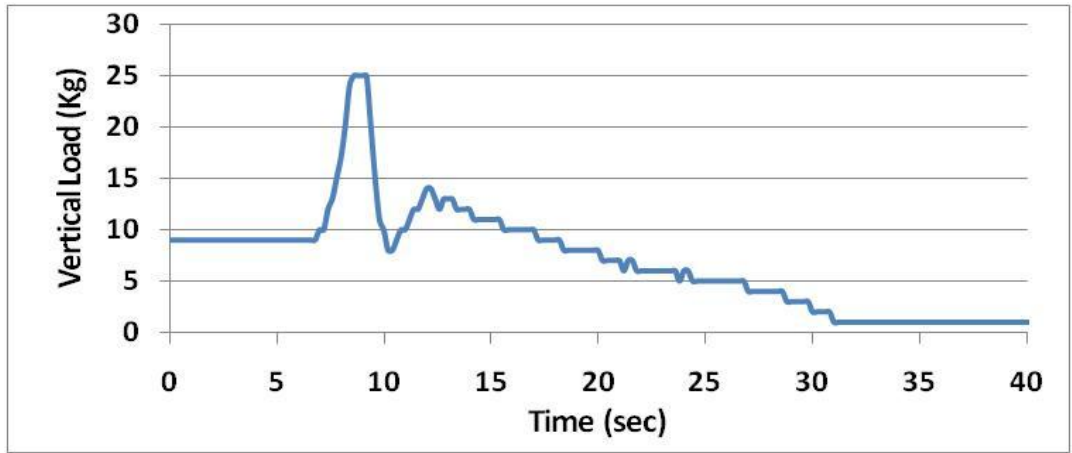


**Figure 3.8** *Stress Variation with Material Bed Depth – Bin Diameter Ratio ( $z/D$ )*

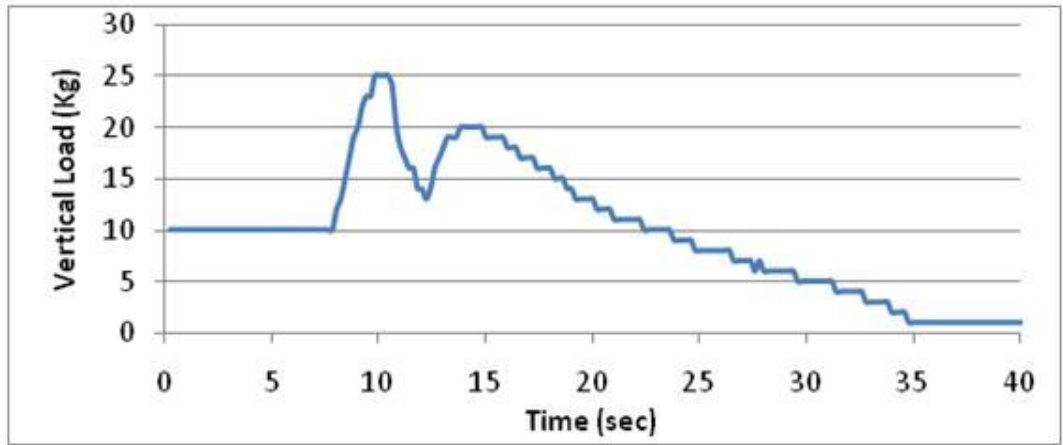
### 3.3.3 Insert Load Measurement

The results obtained from the tests for the loads on inserts are presented in Figure 3.9 and Figure 3.10. Although the load exerted on the insert during the filling process was recorded, it has not been presented in the results because for the purposes of this project the objective of the tests was to find the maximum value of that load which always occurred during the discharge phase.

a Position A



b Position B



c Position C

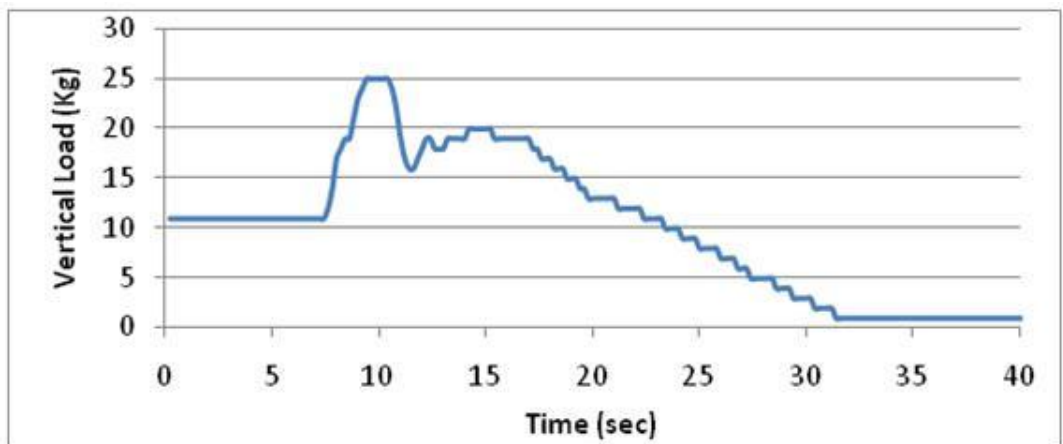
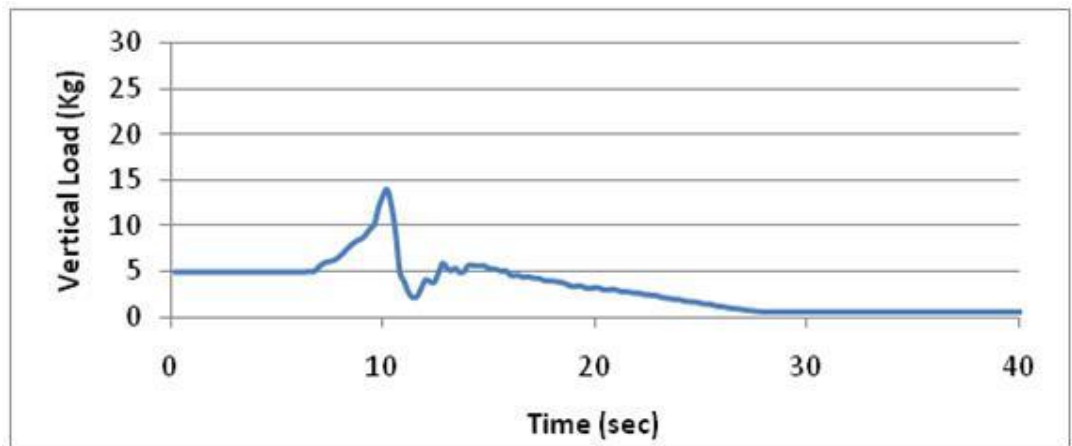
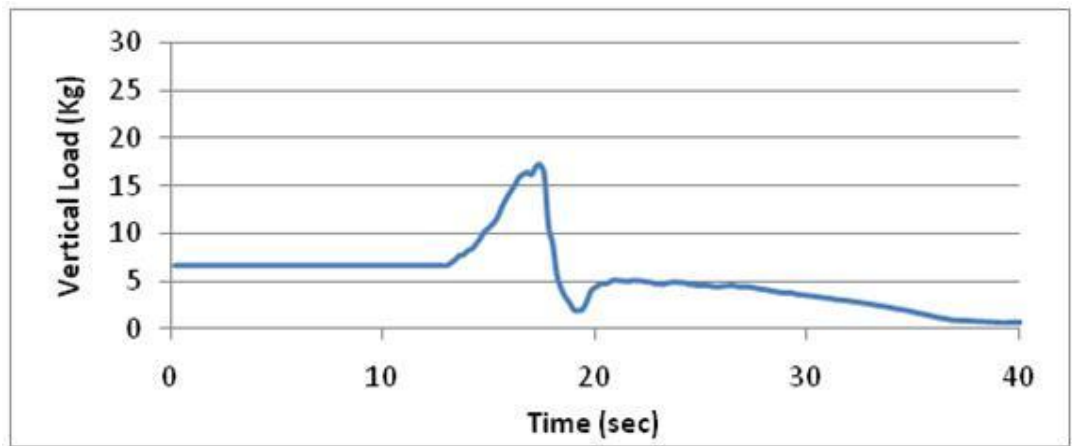


Figure 3.9 Measurements of the Vertical Load Acting on the Large Insert

a Position A



b Position B



c Position C

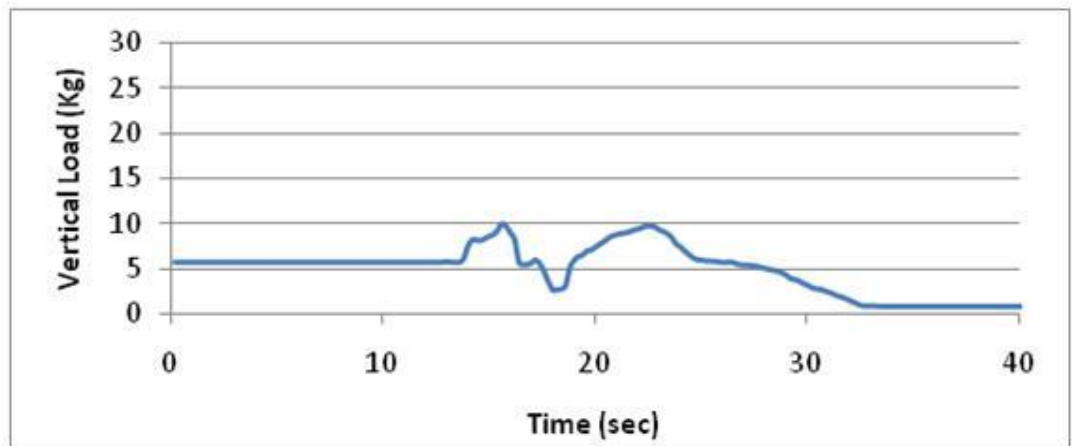
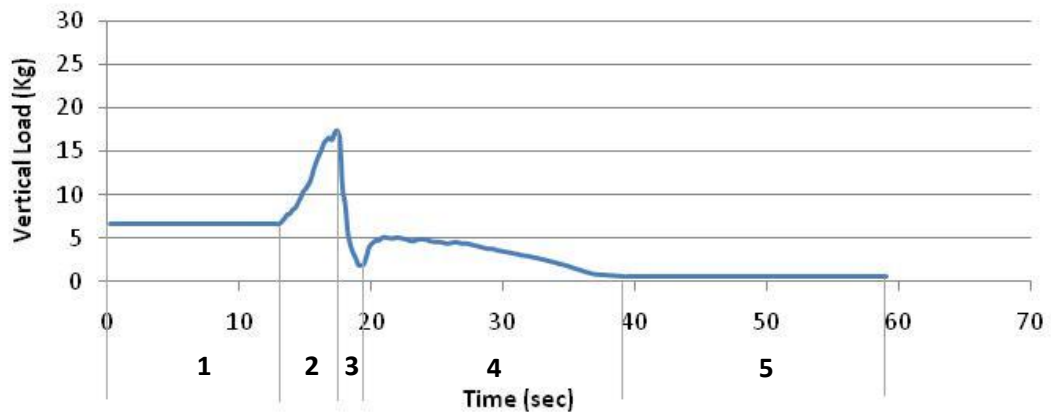


Figure 3.10 Measurements of the Vertical Load Acting on the Small Insert

From Figure 3.9 and Figure 3.10 it can be observed that the data follows a similar pattern, and some common regions can be identified as shown in Figure 3.11.



**Figure 3.11** *Discharge Process Stages*

Region 1 in Figure 3.11 represents the end of the filling process. The value of the vertical load is the maximum that can be reached during that process. This value can be affected by the filling method, as variables like the mass flow rate and relative position of the filling stream, produce changes in the bulk density of the material and in the distribution of stresses.

Region 2 is the time period from the initiation of flow to the peak vertical load. It was this region that was the most important for the objectives of this project, as it represents the highest load the insert will support during operation of the silo, and it is the parameter that should be taken into account when carrying out a structural design. During the filling process of a wedge silo fitted with a tent insert and provided no material is discharged, the direction of the major principal consolidating stress follows the lines shown in Figure 3.12a (Schulze, 2008<sub>1</sub>). The direction of the principal stress is vertical at the axis of the silo and deviates towards the silo walls where its horizontal component increases. When the outlet of the bin opens and the discharge starts, the material moves downwards through a reducing transversal area forming a transitory arch which collapses to produce flow. As a result, the material is compacted in the horizontal direction and dilated in vertical direction changing the direction of the major consolidating stress which becomes almost horizontal. This effect propagates upwards as the material starts moving until it reaches the vicinity of the insert (as shown in Figure 3.12b) where the material around the insert forms an

arch. This arch is supported on the edge of the insert and part of the load acting on the arch gets transferred to the insert increasing the total load exerted.

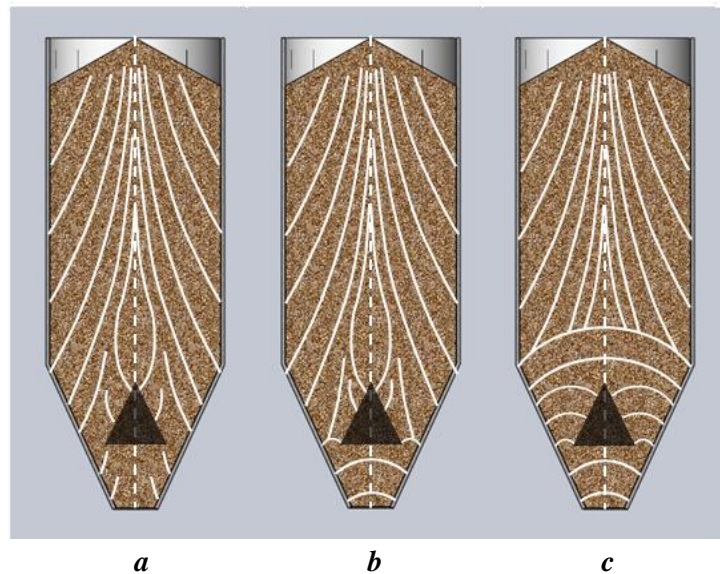


**Figure 3.12** Major Consolidating Stress lines and Vertical Stress Magnitude in a Silo Fitted with an Insert

As this effect continues propagating upwards, the vertical component of the stress acting on the insert reduces due to change of the direction of the major consolidating stress lines which take the form of an arch. This causes a progressive reduction on the load acting on the insert as it can be seen in region 3. The propagation of major consolidating stress lines change stops at the transition of the silo where the area perpendicular to the direction of flow becomes constant and the filling stress distribution is maintained in the cylindrical section. After the initial effect of vertical dilation is finished the material reaches conditions of steady state flow, moving with near to constant values of bulk density until it fails at the annulus around the insert. The change of direction of the major consolidating stress and the fact that friction has not been fully mobilised on the insert surface, produce a reduction of the vertical load under the steady state value. The vertical load then increases as the material reaches the flow-equilibrium state, and then a constant value of the vertical load is maintained if the head of material in the silo is not allowed to drop under a certain level ( $z \approx 3D$ ) or there will be a smooth reduction if the silo is allowed to empty, as shown in region 4.

Region 5 indicates the end of the discharge. However, as can be seen in Figure 3.11, in this case the vertical load does not drop down to zero. This is because the insert was a flat plate and there was remnant material above it at the end of the process.

It is noticeable that some of the loads exerted exceeded the capacity of the instrumentation. The load cell used for the measurements had a range up to 30 kg ( $\pm 0.1\%$ ). However, it can be seen in Figure 3.9a, Figure 3.9b and Figure 3.9c that the measurements stop at 25 kg, while the trend of the graph would suggest a higher peak value.

Initially, a load cell with a capacity up to 30 kg ( $\pm 0.1\%$ ) was considered adequate as the calculated loads were below these values when using both Janssen's analysis, Equation (2-43) and the equivalent hydrostatic pressure as recommended by Johanson. The calibration of the load cells was carried out according to the expected load values and the upper capacity limits of the load cells were not tested. Comparing the results for the large insert Figure 3.9 and for the small one Figure 3.10, the resolution of the data was increased, giving smoother measurements. This was achieved through development of the acquisition software. It is worth noting that although the resolution of the data for the first tests was lower, the trend and key values of the results were not significantly affected by it.

An aspect that did affect the results was the way the inserts were attached to the load cell. These types of load cells generally have a thread for a 6 mm stud, so the inserts were suspended using a long stud of this diameter. The problem was that any side force applied on the insert would flex the stud, causing the insert to move away from the centre of the bin. This was noticed both during the filling and discharging stages (as it was mentioned in the previous section). Movement of the insert away from the centre line would cause preferential draw from one side of the bin, redistributing the stresses on the powder unevenly and asymmetrically.

From the results of the large insert, it can be seen that the steady state value is similar for the positions B and C in Figure 3.9b and Figure 3.9c respectively. However for position A, Figure 3.9a, the vertical load is lower. This is not unexpected because at position A the insert was at the highest position in the bin and by the time the load

reaches the “steady state value” a significant proportion of the head of powder above the insert had been lost, whereas for the other positions the head of powder would be higher when reaching the steady state value.

What happens with the small insert is interesting. In the lowest position, the value of the peak is fairly small (see Figure 3.10c), in fact, the value of the peak is the same as the steady state value. Then there is a considerable increment on value of the peak when the insert is placed in the middle position Figure 3.10b, and when the insert is raised further up, the peak value decreases, Figure 3.10a.

The head of material would explain the difference between the peak values for the highest and middle position, as stated above. However, contrary to what happens with the large insert, the value of the peak for the small insert at the lowest position decreases with respect to the other two positions, although subject to a taller head of material. This is explained by the fact that when the small insert is placed low down, there will be higher interaction with the wall, which will support part of the vertical load exerted.

In general the test results obtained agree with the results presented by Johanson in Figure 2.37. The trend of the data for large inserts and the reduction of the peak for small inserts are similar, but Johanson’s results showed no peak at all. However, the results presented by Johanson do not show explicit values of the position and size of the inserts and it could be that measurements without a peak would be found, if tests with a smaller insert at a lower position were carried out with the test rig of this project. However, the author finds little value in trying to replicate these results.

The results from the load measurements on the inserts have been compared with the predictions made by the procedure recommended by Johanson and presented in section 2.6. However, depending on the characteristics of the material, the geometry of the silo and the installation of the insert, the procedure could produce different load values. First, the procedure suggests the use of one of two methods according to the geometry of the silo. The first method should be chosen to calculate the vertical stress exerted on the insert when the head of powder acting on the inserts is significantly bigger than the diameter of the silo, in other words, when the vertical

stress in the vicinity of the insert is independent of the head of material. As it was explained in the previous section, this condition is considered fulfilled when the head of powder is at least three times the diameter of the silo. When that is the case this method can be applied using equation (2-44). If the head of powder is less than three times the diameter of the silo, the stresses near the insert become highly dependent on the head of material, therefore, the calculation of the load needs to take into account the depth of the powder bed and Johanson recommends using the equivalent hydrostatic pressure ( $\rho gh$ ) instead.

Another parameter whose selection will influence the predicted value of maximum load exerted on the insert is the diameter of the flow channel. Depending on the region of the hopper that the insert influences, mass flow could be achieved for the entire contents of the silo. In this case the diameter of the flow channel equals the diameter of the bin, as all the material is in movement, this is achieved when the area of influence of the insert includes the transition of the bin. If the area of influence of the insert does not include the transition of the silo, regions of stagnant material will be developed during discharge and the discharge channel will not span across the whole diameter of the silo. For this case, the diameter of the flow channel need to be calculated with the help of the insert design procedure presented in section 2.5.1.

Finally, the selection for the value of the effective diameter of the insert also influences the final value of the stress and needs to be chosen according to the characteristics of the material. When the material employed is cohesive, an arch would tend to form round the insert and the force applied onto the arch would effectively be transferred to the surface of the insert. Therefore to calculate the total load exerted on the insert, the arching dimension of the material should be added to the diameter of the insert. When the material is very free flowing, any arch trying to form would be very weak and unable to transfer additional loads onto the insert, therefore the original insert diameter should be used.

The silo used during the test program had a short vertical section compared to its width. Hence, the condition to use equation (2-44) would not be fulfilled in any case and the equivalent hydrostatic pressure would be the logical choice. For the diameter of the flow channel, as explained in section 3.3.1, mass flow might have been

achieved only with the large insert at the top two positions. For any of the other experiments, it was clear from the observations that mass flow was not achieved, therefore the diameter of the flow channel would need to be calculated using the procedure presented in section 2.5.1. Finally, for effective diameter of the insert it needs to be remembered that the arching dimension of the coal was 40 mm and it should not be considered as very free flowing, therefore the arching dimension should be added to the diameter of the insert. Nonetheless, the maximum load has been calculated using the equivalent hydrostatic pressure and Janssen's method for all combinations of these parameters and the results are presented in Table 3-3, to Table 3-6. Table 3-3 and Table 3-4 present the results obtained using Janssen's method, Equation (2-40). Table 3-5 and Table 3-6 present the results calculated using the equivalent hydrostatic pressure ( $\rho gh$ ).

As it can be seen from Table 3-3 and Table 3-4, the vertical loads predicted by Janssen's method are far from the measurements obtained during the experimental programme. In fact, none of the predictions calculated using the extended method were close to the measured values and in every case the experimental value was at least twice the predicted load. A very similar conclusion can be drawn after studying the results obtained with the equivalent hydrostatic pressure and presented in Table 3-5 and Table 3-6. These results are higher in value as expected, however, they still are nowhere near the values measured during the tests.

It is clear that the theoretical methods did not produce accurate predictions of the loads acting on the inserts. However, the test rig employed did not provide the best condition for the measurement of the vertical loads due the shortcomings already discussed. It should be noted that the experimental loads presented in Table 3-3, Table 3-4, Table 3-5 and Table 3-6 were obtained from the experiments that seem more stable and showed less displacement of the inserts. However, it is not possible to discount the possibility of some movement of the insert and therefore horizontal stresses influencing the vertical measurements. In order to make a more informed decision on the use of this theoretical procedure, the test rig needs to be improved to include a more robust mechanism for the measurement of insert loads.

**Table 3-3 Calculated Force Acting on the Large Insert Using the Janssen Method**

<b>Insert and Method</b>	<b>Diameter of the Insert: 220 mm - Janssen Method, Equation (2-40)</b>											
<b>Position (m)</b>	<b>A z = 0.36</b>				<b>B z = 0.42</b>				<b>C z = 0.47</b>			
<b>Flow channel diameter</b>	Same as Vertical Section		Procedure 2.5.1		Same as Vertical Section		Procedure 2.5.1		Same as Vertical Section		Procedure 2.5.1	
<b>Vertical Stress <math>\sigma_z</math> (Pa)</b>	2019		1920		2313		2235		2549		2388	
<b>Insert effective diameter</b>	Insert	Insert + B	Insert	Insert + B	Insert	Insert + B	Insert	Insert + B	Insert	Insert + B	Insert	Insert + B
<b>Vertical Load (Kg)</b>	7.83	10.94	7.45	10.40	8.97	12.53	8.67	12.11	9.9	13.81	9.2	12.94
<b>Measured Vertical Load (Kg)</b>	25+				25+				25+			

**Table 3-4** *Calculated Force Acting on the Small Insert Using Janssen's Method*

<b>Insert and Method</b>	<b>Diameter of the insert: 138 mm - Janssen Method, Equation (2-40)</b>											
<b>Position (m)</b>	<b>A z = 0.33</b>				<b>B z = 0.42</b>				<b>C z = 0.54</b>			
<b>Flow channel diameter</b>	Same as Vertical Section		Procedure 2.5.1		Same as Vertical Section		Procedure 2.5.1		Same as Vertical Section		Procedure 2.5.1	
<b>Vertical Stress <math>\sigma_z</math> (Pa)</b>	1868		864		231		2234		2867		2499	
<b>Insert effective diameter</b>	Insert	Insert + B	Insert	Insert + B	Insert	Insert + B	Insert	Insert + B	Insert	Insert + B	Insert	Insert + B
<b>Vertical Load (Kg)</b>	2.85	4.74	2.84	4.73	3.53	5.87	3.41	5.67	4.38	7.28	3.81	6.34
<b>Measured Vertical Load (Kg)</b>	10				17				14			

**Table 3-5** *Calculated Force Acting on the Large Insert Using Johanson's Method*

Insert and Method	Diameter of the Insert: 220 mm Johanson's Method, $\sigma_z = \rho gh$					
	A z = 0.36		B z = 0.42		C z = 0.47	
Vertical Stress $\sigma_z$ (Pa)	2261		2638		2952	
Insert effective diameter	Insert	Insert + B	Insert	Insert + B	Insert	Insert + B
Vertical Load (Kg)	8.77	12.25	10.23	14.29	11.45	16.00
Measured Vertical Load (Kg)	25+		25+		25+	

**Table 3-6** *Calculated Force Acting on the Small Insert Using the Simplified Method*

Insert and Method	Diameter of the Insert: 138 mm Johanson's Method, $\sigma_z = \rho gh$					
	A z = 0.33		B z = 0.42		C z = 0.54	
Vertical Stress $\sigma_z$ (Pa)	2037		2638		3392	
Insert effective diameter	Insert	Insert + B	Insert	Insert + B	Insert	Insert + B
Vertical Load (Kg)	3.16	5.26	4.03	6.70	5.18	8.61
Measured Vertical Load (Kg)	10		17		14	

### **3.3.4 Vertical Load at the Outlet**

The construction of the test rig included a slide valve mounted on a load cell with the purpose of measuring the load exerted through the outlet which, for example, could affect the performance of a feeder. The maximum load that could be exerted on the slide valve was calculated as 2 kg and for that reason, a load cell capable of measuring up to 5 kg was employed. However, when the experimental tests were undertaken, the measured load was well above upper limit of the load cell and for this reason a comparison and analysis of results was not possible. It is the belief of the author that the large loads exerted on the slide valve were the product of coal particle lodging between the edge of the hopper outlet and the slide valve. These particles would act as support for the hopper transferring additional vertical force to the load cell. An indication of this was that when trying to slide the valve open to initiate discharge, it appeared jammed and a larger force than expected had to be applied. If this was the case, it is possible that measurement of the insert loads could have also been affected by the valve.

### **3.4 Summary**

A test rig was designed and built as a first approach to familiarize with the use of inserts to promote flow in core flow silos. The test rig consisted of a core flow hopper with a support for flat plates to be used as static inserts. One of the inserts was made following the design method developed by Johanson (larger insert) and the second one according to the work carried out by Enstad (smaller insert). The test rig also provided the possibility of measuring the vertical load acting on the flat plates. The experimental results showed that when the hopper was discharged without fitting an insert the powder formed a funnel on the top surface which is a typical characteristic of core flow. When the large insert was installed material was observed to slip at the wall of the silo, which could indicate the development of mass flow. However, the performance of the insert was affected by its position within the hopper and when it was lowered past a certain level an annular channel formed during discharge indicating core flow. The use of the smaller insert produced less successful results as the material was never seen to move at the wall, from this it can be concluded that mass flow was never achieved with that insert. In any case, the

performance of the smaller insert was also dependent of the position inside the hopper and it was more susceptible to side forces which laterally displaced the insert affecting the discharge pattern.

The measurement of the vertical forces on the insert showed that the maximum load is exerted just after the discharge has commenced. This is thought to be the effect of the formation of a temporary arch supported on the edge of the insert, which increases its effective area, increasing the load acting on it. The prediction of this maximum value is important for structural purposes and Johanson proposed a methodology for its calculation. The calculations obtained were compared with the experimental measurements, but the resulting values were very different, with the experimental values being at least twice as large as the theoretical predictions. The large load values obtained during the tests could be the result of forces transferred from the hopper to the slide valve, due to lodged material in the gap between them. Once the valve is removed, part of the supported load is transferred to the insert due to the inertia of the system therefore increasing the total vertical force exerted.

For future experiments it was necessary to develop the test rig to incorporate a higher vertical section, a system for the identification of the flow pattern, a more stable support for the placement of the inserts and a load cell with a higher load rating

## **CHAPTER FOUR: STUDY OF INVERTED CONES AS FLOW PROMOTION INSERTS AT BENCH AND SEMI-INDUSTRIAL SCALES**

---

This chapter presents the design, construction and commissioning of a semi-industrial scale test rig (0.4 m<sup>3</sup>) for the study of static inserts as flow promoting devices. The test rig was designed taking into account the experience acquired from the previous experiments and the limitations identified on the equipment used. Inverted cone was the type of insert chosen as the subject of study. Their selection and development was undertaken first at bench scale and then scaled up for use on the semi-industrial rig. The experimental results and the performance analysis of the inserts are also included in this chapter.

### **4.1 Semi-Industrial Test Rig Design and Construction**

Chapter 3 presented the design and commissioning of a test rig for the study of inserts in silos. However, the practical work revealed several limitations of the equipment which impeded the collection of meaningful data for the evaluation of the performance of the inserts employed. These limitations included insufficient length of the cylindrical section of the bin, lack of system for the identification of flow pattern and inadequate insert support, among others. The sections below present the modifications carried out over the original test rig to enable a more profound study of inserts as flow promotion devices. Figure 4.1 illustrates the differences between the two test rigs.



*a*



*b*

**Figure 4.1** Differences Between original rig (a) and modified rig (b)

#### 4.1.1 Vertical Section

The first difference that can be observed in Figure 4.1 is the height of the vertical sections of the silos. The original rig had a very short cylindrical section with a height to diameter ratio ( $z/D$ ) of just 0.5, which meant that stress values were strongly dependant on the depth of material in the vertical section and achieving steady state conditions was practically impossible. As it was explained in section 2.6, the stresses in the vertical section of a silo can be calculated using the following equations:

$$\sigma_z = \frac{\rho g D}{4\mu K_j} \left[ 1 - e^{-4\mu K_j \frac{z}{D}} \right] \quad (4-1)$$

$$\sigma_r = \frac{\rho g D}{4\mu} \left[ 1 - e^{-4\mu K_j \frac{z}{D}} \right] \quad (4-2)$$

$$\tau_{rzw} = \frac{\rho g D}{4} \left[ 1 - e^{-4\mu K_j \frac{z}{D}} \right] \quad (4-3)$$

As it can be seen from Equations (4-1) (4-2) and (4-3), the stresses in the vertical section of a silo increase with the depth of material not linearly like in a liquid, but with a decreasing gradient which tends asymptotically towards a maximum. When the ratio  $z/D > 3$ , the exponential term in Equations (4-1) (4-2) and (4-3) becomes small and can be neglected, therefore, the stresses acting on the lower part of the silo are close to the asymptotic values and can be considered approximately constant. Taking this into account, it was decided to extend the vertical section of the rig to obtain a  $z/D$  ratio of 3; although a higher ratio value was desirable, it was not achievable in practice due to headroom restrictions in the laboratory and the lifting equipment available for the tests.



**Figure 4.2** *Modified Vertical Section*

The extended vertical section (as shown in Figure 4.2) was 500 mm in diameter, 1500 mm in height, made of mild steel with a 2B inside finish and was mounted on three 0 – 150 kg ( $\pm 0.05\%$ ) Tedeo-Huntleigh load cells model 1260 [Tedeo, 2015]. Three ADAM 4016 [Advantech, 2015<sub>1</sub>] I/O units were used to condition and acquire the signal from the load cells and a software application was developed to store and display the data using the ADAMView 1<sup>st</sup> Edition development tool [Advantech, 2015<sub>2</sub>].

The rig has been set up, so that the vertical section and the converging section were independently mounted on the support frame. This is important as it gives the opportunity to measure the traction force acting on the walls of the cylindrical section, which can be related to the coefficient of friction and therefore to the wall friction angle. At any point during discharge, the only force acting on the independent cylindrical section is the friction force exerted by the material due to the stress perpendicular to the walls. The reading of the load cells would therefore be a measurement of the total traction force acting over the whole internal area of the vertical section. Therefore:

$$F_{Load\ Cells} = \iint \tau_{rzw} dA \quad (4-4)$$

However, as the area is equal to  $\pi Dz$  and the diameter is constant along the depth of the vertical section, then the double integral becomes a simple integral as follows:

$$F_{Load\ Cells} = \pi D \int_0^z \tau_{rzw} dz \quad (4-5)$$

Then replacing Equations (4-3) and (4-4) into (4-5).

$$F_{Load\ Cells} = \pi D \int_0^z \left( \frac{\rho g D}{4} \left[ 1 - e^{-4\mu K_j \frac{z}{D}} \right] \right) dz \quad (4-6)$$

The integration of Equation (4-6) produces:

$$F_{Load\ Cells} = \frac{\pi \rho g D^2 z}{4} + \frac{\pi \rho g D^3}{16\mu K_j} e^{-4\mu K_j \frac{z}{D}} - \frac{\pi \rho g D^3}{16\mu K_j} \quad (4-7)$$

Equation can then be numerically solved to calculate the value of the friction coefficient ( $\mu$ ) which can be compared to those obtained through traditional wall friction characterisation techniques.

### 4.1.2 Converging Section

An inconvenience found during the test programme undertaken with the original rig, was the short residence time of the material in the hopper. Besides the extension of the vertical section (which increases the capacity of the silo), it was decided to reduce the outlet of the hopper to achieve a lower flow rate of material. For this purpose, an extension to the lower part of the converging section was installed, which had the same half angle as the conical hopper and reduced the diameter of the outlet from 150mm to 50mm. Additionally, a slide valve was fitted at the outlet of the hopper. The modifications are illustrated in Figure 4.3.

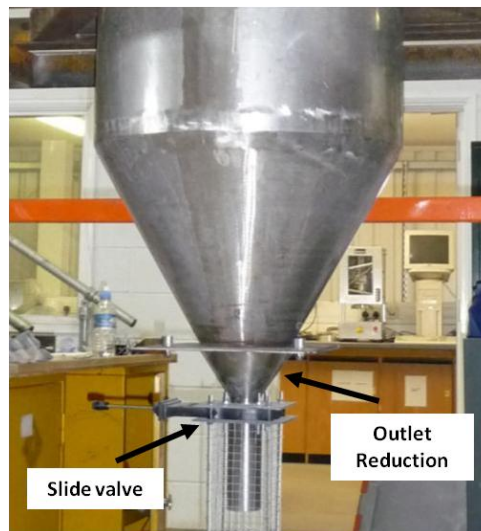


*Figure 4.3 Modified Converging Section*

### 4.1.3 Discharge Pattern Tracer System

The ideal performance of a silo is achieved when its contents discharge in a mass flow pattern. Therefore, determining the discharge behaviour of a silo has played an important role in bulk solids research. Through the years, different methods have been used to identify the type of pattern developed inside a silo during discharge, from these methods the most widely employed is the use of tracers [Karlsen, 1998; Schuricht, 2001; Ding, 2004<sub>2</sub>; Enstad, 2007; Ding, 2008; Hartl, 2008].

A tracer system basically consists of measuring the residence time of markers placed at known points inside a silo, which are allowed to discharge with the stored

material. With the residence time and the position of each tracer, a flow pattern can be deduced. Thus in a silo with central discharge, if mass flow is developed, tracers placed at the same depth should have similar residence times, and the lower the position, the lower the residence time. In contrast, if core flow is developed, markers placed at the same depth will have different residence times, increasing with the horizontal distance from the centre and the lower the position, the higher the residence time, except for the tracers placed in the channel above the outlet, which will have the shortest residence times of all.

For this purpose, a tracer system was designed comprising two main parts, the tracer positioning tool and the tracer detection device. The positioning tool consisted of a guide made with nine 24 mm ID mild-steel tubes of 600 mm in length. The tubes determined the horizontal positions of the markers, so they were evenly distributed in the pattern of a cross. Through each guide tube, a placement tube 20 mm OD mild-steel could slide independently, allowing the tracers to be dropped at different depths inside the bin (see Figure 4.4). Note that the length of the placement tubes varied depending on their position relative to the centre of the bin and the insert used. An additional marker was positioned just above the outlet to be used as a reference.



*Figure 4.4 Tracer Positioning Tool*

The tracer detection device consisted of a 10 mm opening mesh used to screen out the tracers from the discharge stream, and feed them into a funnel where a DB1Cherry Standard V4 micro-switch for the detection of the tracers, a 0 - 0.6 kg

( $\pm 0.007\%$ ) Tedeo-Huntleigh load cell Model 1004 [Tedeo, 2015<sub>2</sub>] used as back up detection device and a collection hose, used to store the tracers in the same order that they were discharged (see Figure 4.5). 14 mm diameter individually marked stainless steel balls were used as tracers.

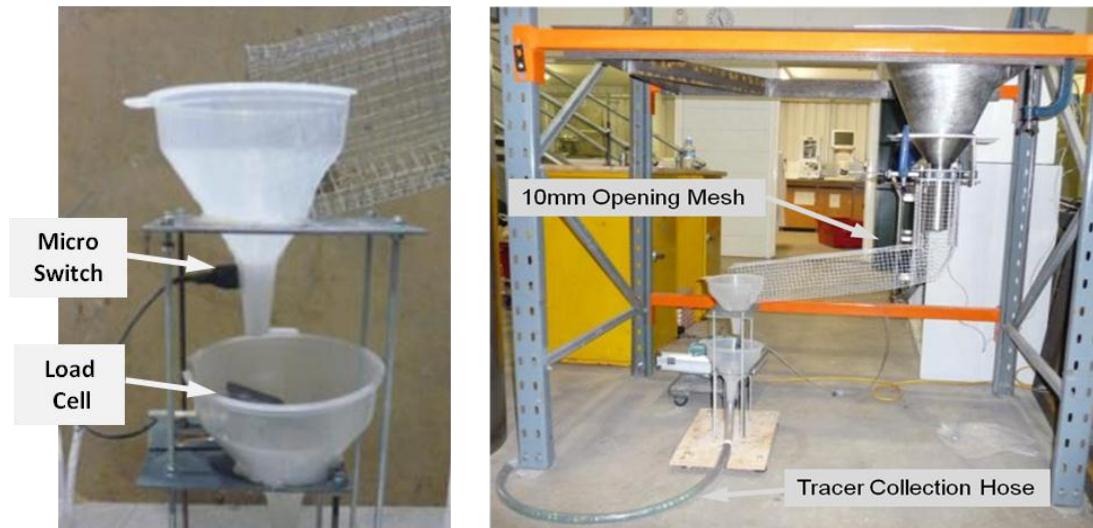


**Figure 4.5** *Tracer Detection Device*

#### 4.1.4 Inserts

The method proposed by Johanson for the design of inverted cones as flow promoting devices is explained in section 2.5. In this method, Johanson designs the insert in such a manner that the apex of the inverted cone (A in Figure 4.6) influences the transition of the silo (D) and the base (B) influences a point on the wall below the transition, so that the silo will operate in mass flow. If the influenced zone does not contain the transition point (D), a stagnant zone will appear propagating upwards and core flow will develop. The problem with the method developed by Johanson is that the stress field in the vicinity of the insert will affect the extension of the area of influence of the insert, therefore the head of material above the insert will play an important role on its performance. In order for the insert to produce a consistent effect on the discharge, the stress field around the insert also needs to be consistent. This only can be achieved when the stress field is independent of the head of material, in other words, when the height of the vertical section of the silo is larger than its diameter ( $z/D > 3$  at least). However, when the height of the vertical section

of the silo, or the head of material contained in it is less than three times the magnitude of the diameter of the bin, the stress field near the transition of the silo is no longer independent of the amount of material above and the insert might no longer be as effective. To account for the changes in the stress field a slight modification of the method was proposed. The two main aspects addressed were the size of the insert and the position of its apex, both relative to the original method. A slightly larger insert was obtained and the apex was located slightly higher than what was recommended by Johanson. The intention was to avoid two types of problems that can occur as consequences of the reduction in magnitude of the stress field. The first considers a displacement of the influenced zone to just below the transition causing a stagnant zone to appear propagating upwards, and the second a reduction of the area of influence in a way that it no longer reaches the wall and therefore does not facilitate the flow of stagnant material.

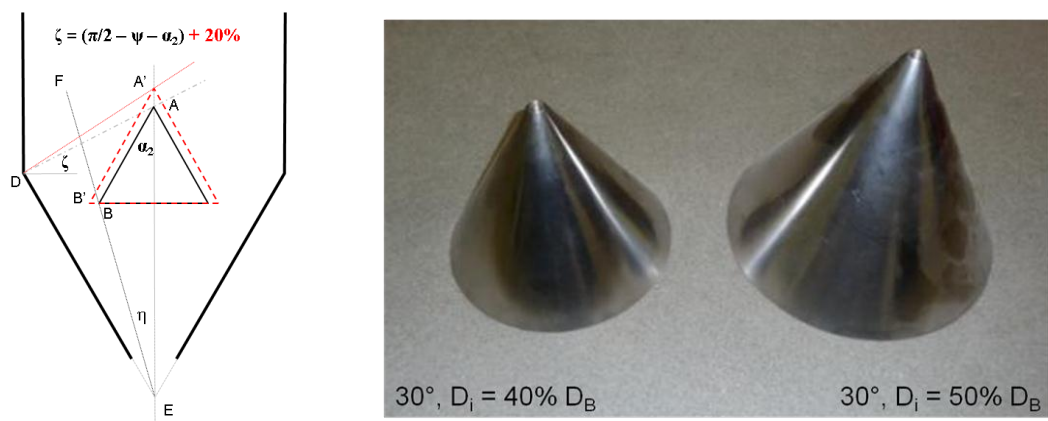


**Figure 4.6** *Insert Design*

Two inverted cone inserts made of mild steel with a 2B finish were designed and built, one of them (200 mm in diameter, 40% of the diameter of the bin) following Johanson's method and the other one (250 mm in diameter, 50% of the diameter of the bin) introducing a safety factor for the point influenced by the apex of the insert. For this purpose, the angle from the horizontal of the line DA in Figure 4.6 was increased by 20%, locating the apex of the insert at a slightly higher position. The base line was kept at the same level and the half angle was conserved resulting in a larger insert. This design method was developed from experimental results which are presented in section 4.2

One of the features of the original rig that caused significant problems was the way the inserts were located inside the silo. The insert was held in position by a long stud connected to a load cell at the top of the rig, this made its position very sensitive to side loads, so it was common to see it moving sideways during the filling and discharge processes. The lateral movement of the insert was the main cause for the offset discharge obtained. An additional problem caused by this mechanism was that the mounting and bracket obstructed the inlet of the silo complicating the loading of material. Taking these factors into account, a support device was designed attempting to simulate the manner in which the insert would be supported in an industrial installation.

The support device had to be easy to install and remove to undertake tests with and without inserts, but stable and strong enough to support the forces acting on the insert with minimum interference to the flow of material. The device built (see Figure 4.7) comprised a central mild steel disc with three horizontal arms that sat on the walls of the converging section of the bin, the load cell was attached to the disc with a 12 mm studding and another 12 mm studding coupled the load cell and the insert. The cable of the load cell was passed through a stainless steel tube welded underneath one of the arms of the device, and then through a small orifice on the wall of the hopper.



*Figure 4.7 Insert Support Device*

## 4.2 Bench Scale Model for Insert Development

As it was explained in the previous section, the aim of the method developed by Johanson was to produce an insert that influences the wall of the silo in such a manner, that all the contents of the bin discharge in mass flow. For this to occur, the insert needs to be large enough to influence the wall of the silo and the apex of the insert needs to be positioned high enough to influence a point on the wall just above the transition of the bin. However, the position and extension of the influenced areas are not only function of the size and position of the inverted cone, but also of the magnitude of the stresses in the vicinity of the insert. This means that when the bed of material above is tall enough to produce nearly constant stresses around the insert ( $z/D > 3$  at least), the calculations obtained by Johanson have the best chance of producing an effective design. However, as the head of material reduces, the stresses around the insert become dependent of the amount of powder above and the performance of the insert changes. After certain level, the point influenced by the apex of the insert is no longer located above the transition of the silo and stagnant zones appear as a result. Then as the level of powder continues descending, the area of insert influence no longer reaches the wall and movement near the walls of the hopper stops all together.

Within his design method, Johanson proposes the introduction of a safety factor which results in an incremental increase of the insert diameter. This increase in the size of the insert enhances the possibilities for the area of influence to reach the walls of the hopper at low levels of head of material. However, the safety factor does not affect the position of the apex and therefore, neither does it affect the point of influence of the insert apex. As a result of this, it is possible that at low levels of material inventory, the insert could produce flow at a section of the wall of the hopper but stagnant regions would appear near the transition. After carrying out this analysis, the author hypothesized that introducing a safety factor for the position of the insert apex should enhance the performance of inverted cones at low levels of material inventory. In order to test that theory it was decided to build a bench scale model of the test rig presented in section 4.1. This model silo would give the opportunity of studying multiple insert sizes and positions, without incurring in high

costs which could have compromised the budget for the further development of the project.

#### **4.2.1 Design and Construction**

In section 4.1 a method of discharge pattern identification using tracers was described. However, to employ the same type of technique at the scale proposed for the test rig would be impractical. For that reason, it was decided to build the test rig using transparent material to observe the behaviour of the granular material in the vicinity of the walls.

The model comprised a 120mm ID, 500mm tall Perspex tube, mounted on a support frame to which different converging sections could be attached (see Figure 4.8). For this case, the converging section consisted of a polypropylene conical hopper with 30 degrees half angle and 20 mm outlet. This configuration produced model which resembled the test rig described in section 4.1 at 1:4.2 scale, when filled to the right level. A slide valve under the outlet of the hopper was used to control the material discharge.

The inserts were designed using the CAD tool SolidWorks from Dassault Systèmes SolidWorks Corp. Then, they were built using a rapid prototype machine which “takes virtual designs from computer aided design (CAD) or animation modelling software, transforms them into thin, virtual, horizontal cross-sections and then creates successive layers until the model is complete” [Social, 2013].



**Figure 4.8** *Bench Scale Model for Insert Development*

#### **4.2.2 Insert Design**

In order to test the hypothesis presented by the author regarding the position of the insert apex, a series of tests were carried out using multiple configurations of inverted cones obtained through variations of the method developed by Johanson. The tests also included the use of an inverted coned designed following the original method.

To produce a design, the original method calculates the angle from the horizontal of the line DA (angle  $\zeta$  in Figure 4.9), which starting from the transition of the silo (point D) marks the apex of the insert when it intersects the axis of the hopper (point A). The method then calculates the angle from the vertical of the line EF (angle  $\eta$  in Figure 4.9) which starts at the apex of the hopper (point E). The design is completed by drawing a line from point A until it intersects the line EF at point B, which marks the base of the insert.

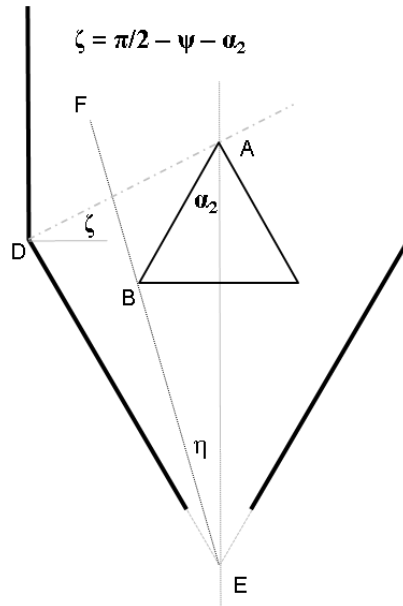
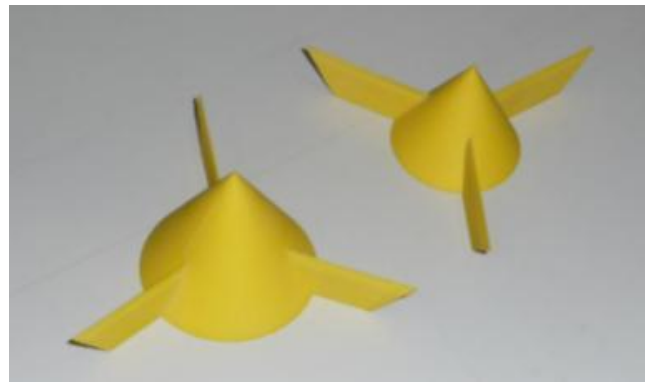
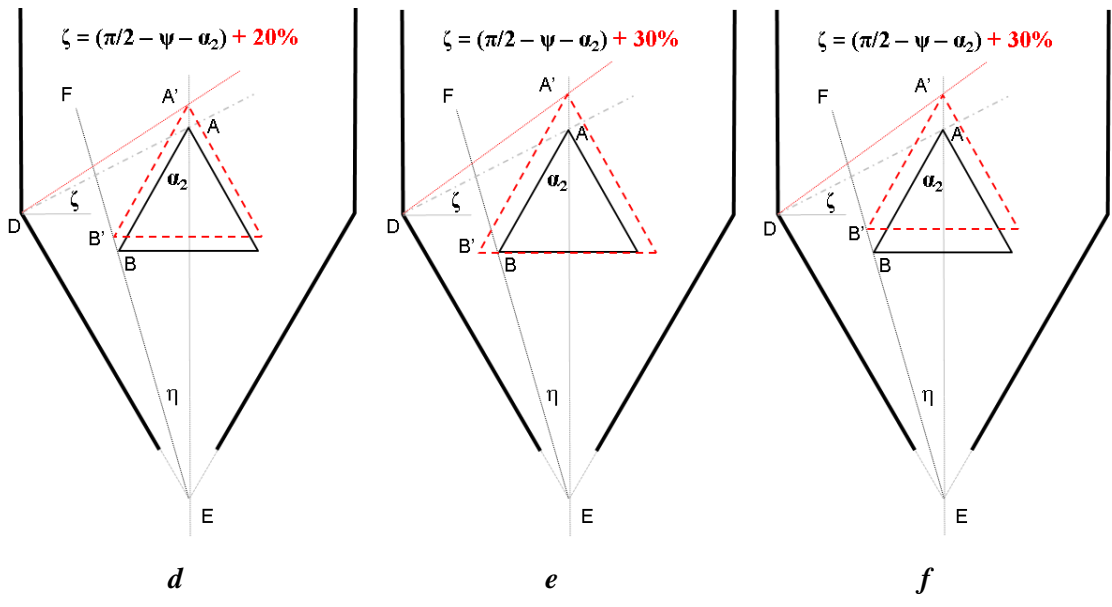
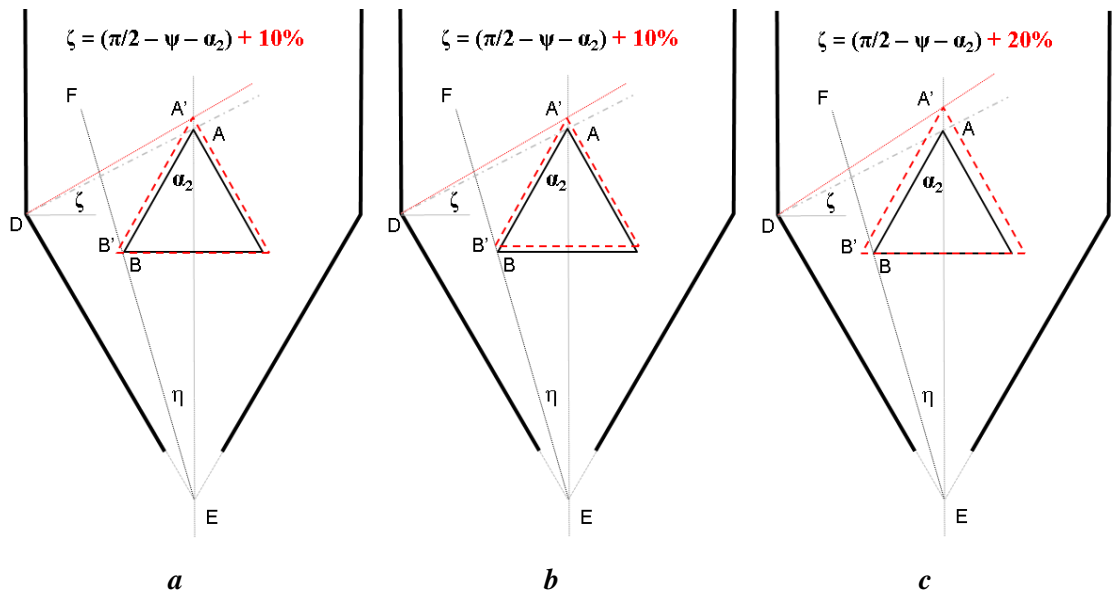


**Figure 4.9** *Bench Scale Insert Design*

To obtain the different designs for the tests, both the position of the apex and the diameter of the insert were modified and the different possibilities were combined. To add a safety factor to the position of the insert apex, the angle  $\zeta$  was increased by 10%, 20% and 30%. In each case the base of the insert was obtained either at the intersection between the 30 degrees angle line from A and the line EF (B' in Figure 4.10b, Figure 4.10d and Figure 4.10f) or extending the 30 degrees angle line from A until it reached the level of the base of the insert obtained with the original method (B' in Figure 4.10a, Figure 4.10c and Figure 4.10e). Figure 4.10g shows an illustration of two of the inserts used for the tests.



**g**

**Figure 4.10** *Alternative Inverted Cone Designs Tested*

### 4.2.3 Test Method and Results

To undertake the tests, the model was filled with sub 400 micron olivine sand to a total height of 360 mm from the transition of the bin and then allowed to discharge. In this way, an initial ratio  $z/D = 3$  was obtained which resembled the conditions of the larger test rig. Tests were also carried out filling the model to the top obtaining a ratio  $z/D > 4$ .

In general there was not noticeable difference between the results of the test starting with ratio  $z/D = 3$  and those starting with ratio  $z/D > 4$ . In both cases, mass flow was achieved with all the seven insert designs tested (the original Johanson design plus the six configurations presented in Figure 4.10). In every case, the material was observed to flow at the wall of the model and also, the upper surface profile of bed of powder was maintained for a period of time as the level of material decreased. As the inventory of powder continued descending, differences in the discharge behaviour for the model started to appear depending on the insert that was tested, as it is explained below.

When the model was discharged without fitting any insert, the behaviour observed was typical of a core flow pattern. A central channel was rapidly formed after the start of the discharge, the material at the top cascaded down into the central funnel and the upper surface profile resembled the illustration presented in Figure 4.11a. Additionally, movement of the particles at the wall was never observed, therefore the development of core flow was the obvious conclusion.

The introduction of the insert designed following Johanson's method, completely changed the discharge behaviour of the solids. Material was observed to slip at the walls of the silo and the profile of the surface at the top of the powder bed remained undisturbed for a significant part of the discharge, as shown in Figure 4.11b. Then, at a certain point during the discharge a central funnel started to form on the surface of the material, the movement at the walls seemed to slow down and in some of the repetitions it was observed to stop altogether.

The behaviour described above was however not consistent throughout all the repetitions, and in fact accounted just for around 40% of them. For the other 60% of the repetitions, although the start of the discharge was the same, with mass flow developing in the silo, the behaviour was different at lower levels of material. Instead of continuing to flow at the walls and later form a central channel, material would start discharging preferentially through a side of the bin with parts of the opposite side remaining static, as shown in Figure 4.11c

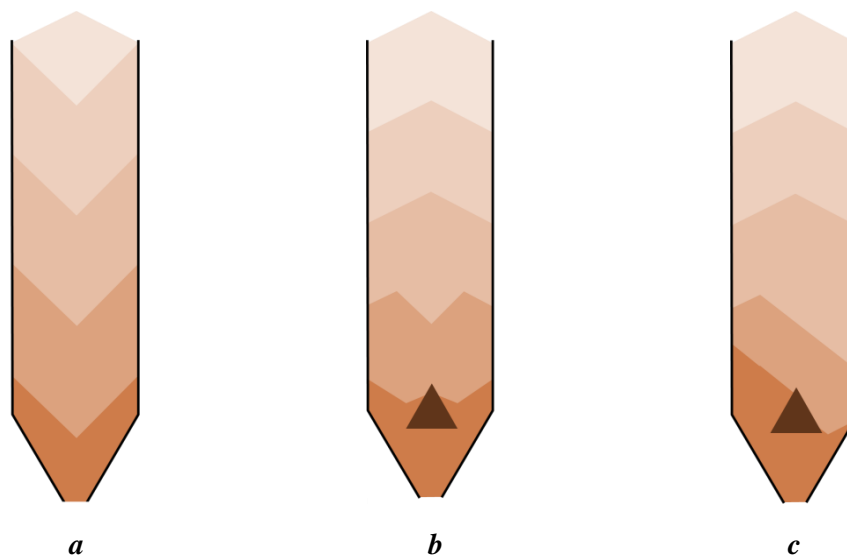


**Figure 4.11** *Observed Flow Patterns During Tests*

When the inserts designed with a 10% safety factor were fitted (Figure 4.10a and Figure 4.10b) the general performance obtained was fairly similar between them and to that of Johanson's insert. In fact for the insert from Figure 4.10b the results were so close to those obtained with Johanson's insert that it would be difficult to try to point out any differences. However, when using the insert from Figure 4.10a a slight improvement was noticed across the multiple repetitions. It was observed that the number of repetitions where off centre discharge developed, reduced slightly when compared with the other two inserts and the overall percentage of this behaviour went from 60% down to 50%.

By contrast, the use of the inserts designed with a 20% safety factor (Figure 4.10c and Figure 4.10d) produced a more pronounced improvement in the quality of the

discharge from the model silo. The insert from Figure 4.10d produced a further reduction in the number of repetition were off centre discharge was observed, taking that percentage down to 40%. It was however the insert from Figure 4.10c which really made a difference in terms of performance. Not only the number of repetitions with off centre discharge was reduced to 20%, but the severity of the problem was also diminished. For comparison, in some of the cases when off centre discharge was observed using Johanson's insert, the material was noticed to stop moving at the wall on the opposite side. This however, was never observed with the insert from Figure 4.10c where the material on one side of the bin was seen to move slightly faster than that on the opposite side. In general when comparing the profile of the upper surface of material after the off centre discharge started, the result obtained with the insert from Figure 4.10c produced a slope considerably shallower than the one observed when using Johanson's insert as shown in Figure 4.12.

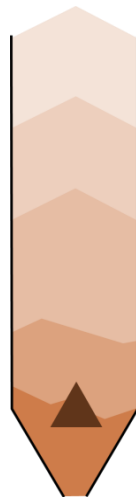


**Figure 4.12** *Observed Off Centre Discharge Using the Insert from Figure 4.10c*

The inserts designed with a 30% safety factor (Figure 4.10e and Figure 4.10f) produced the most particular set of results, in the sense that the performance obtained with each of them was very different from one another. The insert from Figure 4.10e produced results very similar to the best insert designed with 20% safety factor and even reduced further the occurrence of off centre discharge, where it was only observed in around 10% of the repetitions. By contrast, when the insert from Figure 4.10f was installed, the number of repetitions presenting off centre discharge rose

considerably to a total of 50% and with more severe differences in velocity between the fast and slow moving regions.

#### **4.2.4 Modified Method for the Design of Inverted Cone Inserts**

The results presented in the previous section seem to support the hypothesis formulated by the author, which suggested the design method developed by Johanson for the design of inverted cones, could benefit from the introduction of a safety factor for the position of the insert apex and also for the overall size of the insert (as suggested by Johanson as well). The results showed that the best performance was produced by the insert designed with 30% safety factor for the apex position and with the base kept at the level of the original design. However, the insert designed with 20% safety factor also produced very good results improving the discharge of the solids from the model and its performance was very close to that of the 30% safety factor insert. The additional 10% increase in the safety factor produces an insert considerably larger which could be counterproductive for silos with shallow converging angles or for cohesive materials (as it will be explained at the end of this section). For these reasons it was decided to select the 20% as the safety factor recommended for the design of the insert to be tested in the semi-industrial scale silo.

Taking this into account, the author proposes the following design procedure as an alternative to the method presented by Johanson:

- a. Select  $30^\circ$  as the half angle ( $\alpha/2$ ) of the insert.
- b. Obtain the values of the effective angle of internal friction ( $\delta$ ) of the bulk solid and the wall friction angle ( $\varphi$ ) between the bulk solid and the material of the hopper wall. These properties can be obtained through the use of a powder shear test.
- c. Obtain the values for the critical W/R ratio and angle  $\psi$  from Figure 2.24 and Figure 2.25 respectively.

- d. Make a scale drawing of the existing silo.
- e. Draw a line from the transition of the silo at an angle  $\pi/2 - \psi - \alpha_2$  from the horizontal until it intersects the central axis of the hopper (line DA in Figure 4.13).
- f. Draw a line from the apex of the hopper at angle  $\eta$  from the vertical, such as:

$$\tan \eta = \frac{\tan \alpha_1}{1 + W/R} \quad (4-8)$$

This line represents the critical ratio W/R (line EF in Figure 4.13)

- g. Draw a line from the apex of the inverted cone at an angle  $\alpha_2$  from the vertical, until it intersects the critical W/R line (line AB in Figure 4.13).
- h. Draw a second line from the transition of the silo at an angle  $(\pi/2 - \psi - \alpha_2) + 20^\circ$  from the horizontal until it intersects the central axis of the hopper (see Figure 2.9, line DA'). This intersection (point A') represents the apex of the inverted cone.
- i. Draw line A'B' at an angle  $\alpha_2$  from the vertical, making the bottom of the new insert coincide with the bottom of the insert previously drawn.

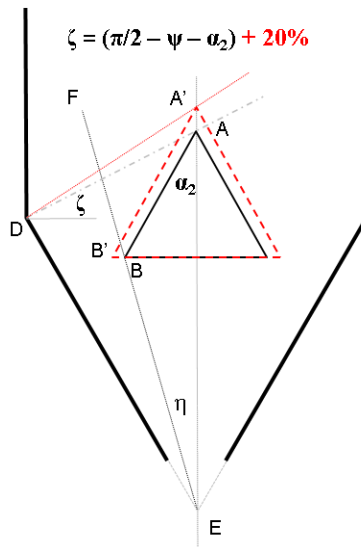


**Figure 4.13** *Modified Method for the Design of Inverted Cone Inserts*

Attention needs to be paid when using this method for certain silo geometry and material characteristics combinations. For example, if an inverted cone insert were to be designed for silo with 45° half angle, the size of the insert could be so large that the width of the annulus between the edge of the insert and the hopper wall (line B’G in Figure 4.14) could be less than the arching dimension of the material. If that were to happen, an arch would form above the annulus impeding the flow of material, rendering the solution worse than the initial problem. It is therefore evident that if the safety factor for the apex was 30% instead of 20% the size of the insert would be larger, the gap between the edge of the insert and the hopper wall would be smaller, and the likelihood of supporting a stable arch would increase.

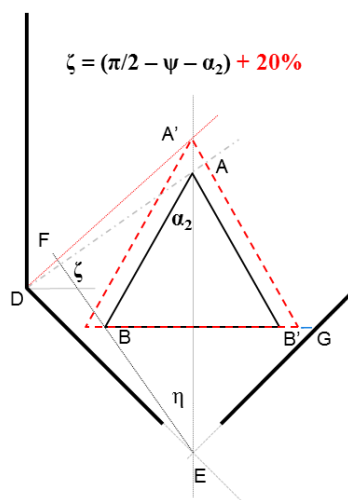


**Figure 4.14** *Inverted Cone in 45° Hopper*

### 4.3 Commissioning of the Semi-Industrial Test Rig

The experiments were carried out using sub-400 micron olivine sand as a test material. The flow properties of the sand were measured using a Brookfield Powder Flow Tester and the results can be found in Table 4-1.

*Table 4-1 Flow Properties of the Sand Used as Test Material*

Wall Friction Angle for Stainless Steel (Deg)	Wall Friction Angle for Mild Steel (Deg)	Internal Friction Angle (Deg)	Bulk Density (Kg/m <sup>3</sup> )
25	29	39	1950

Two polished mild steel inserts with a 30° half angle to the vertical were evaluated, one designed with the method developed by Johanson and the other with the modified method proposed by the author. Johanson's insert was 0.2 m in diameter, 40% of the diameter of the bin and its apex was positioned at 0.12 m upwards from the transition of the bin, the modified insert was 0.25 m in diameter, 50% of the diameter of the bin and its apex was positioned at 0.16 m upwards from the transition of the bin. To facilitate silo filling and the collection of discharged material, 0.5 m<sup>3</sup> polypropylene bulk bags were used and handled with an overhead crane. Two types of test were undertaken, in the first type the silo was filled with sand and then left to drain completely. In the second type of test, the silo was filled and then additional material was fed into the silo while discharging, to maintain a constant head of material.

#### 4.3.1 Silo Allowed to Drain After Filling

The tests were carried out without the insert, with Johanson's insert and with the modified insert, respectively. In each case, the tracer guide and tubes were placed in position, one tracer was placed at the outlet of the hopper (to act as reference for the residence time) and then the bin was filled with 550 Kg of olivine sand. The tracers were positioned according to Figure 4.15 and Figure 4.16. Level B was located at a depth of 1730 mm, level C at a depth of 1500 mm (transition of the bin), level D at a depth of 1200 mm, level E at a depth of 900 mm, level F at a depth of 600 mm and

level G at the surface of the material approximately 100 mm from the upper edge of the silo.

Once the silo had been filled, a tracer would be dropped through a tube positioning it at the deepest level. The tube would then be pulled upwards for a certain distance until its lower end would reach the following level, where another tracer would be dropped. This process would then be repeated for each tube and for every level. At each level nine tracers were placed, with the exception of level B were only five were positioned. The slide valve was then opened and the bin left to discharge completely, the complete process is illustrated in Figure 4.17.

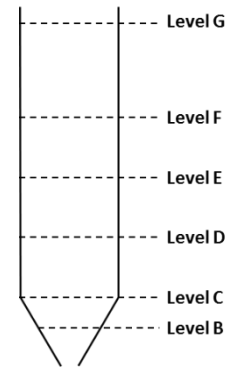
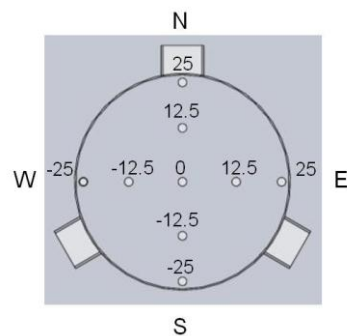


**Figure 4.15** *Horizontal Tracer Location*    **Figure 4.16** *Vertical Tracer Location*



**Figure 4.17** *Bin Filling and Tracer Positioning Process*

### 4.3.2 Silo with additional material fed during discharge

The tests were carried out without the insert, with the small insert and with the large insert respectively. The bin was loaded and the tracers positioned following the procedure described in the previous section. Then another bag with 550 Kg of olivine sand was placed and opened on top of the material already in the bin (see Figure 4.18). The slide valve was opened and, while material was being discharged, fresh material was fed into the bin keeping the head constant until the upper bag ran empty, then the bin was left to discharge completely.



*Figure 4.18 Additional Material Fed During Discharge*

## 4.4 Results and Discussion

### 4.4.1 Expected Results

The tracer system installed for the identification of the flow pattern developed in the silo measures the time it takes for each marker to be discharged. With the time and position of each tracer, a map of the movement of material inside the bin can be obtained and from this map the flow pattern can be deduced. In order to explain the process for the deduction of the flow pattern, the three general pattern types (mass flow, core flow and mixed flow) will be illustrated which will also facilitate the comparison and analysis of the experimental results.

As is has been explained previously, when mass flow is developed in a silo all its contents are in motion during discharge and the material should discharge in the same order that was charged into the bin. Therefore, the material charged first should come out first. Figure 4.19 shows the residence time map for the test rig should its contents developed an ideal mass flow pattern. In this case it can be seen how the tracers located at the deepest level B have the lowest residence time of them all (these are the first discharged), then the second deepest level C have the second lowest residence time, meaning that are discharged next and it continues in succession until the top layer of tracers is discharged last. This illustrates the first in first out discharge expected for mass flow. In addition to this, please note how all the tracers located at the same level have the same residence time, this represents ideal discharge behaviour without velocity gradients in the radial direction. However, in a real process some difference in residence time is anticipated, with the tracers located near the centre of the bin having slightly lower values of residence time.

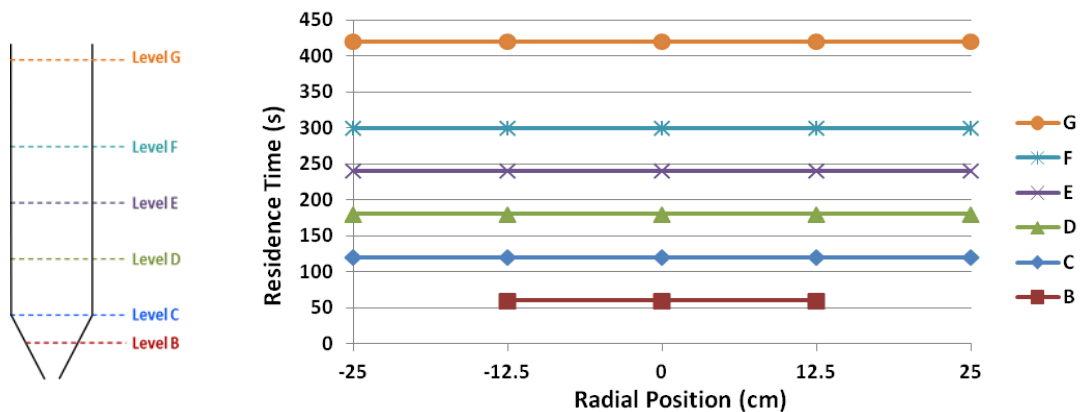


**Figure 4.19** *Ideal Mass Flow Pattern*

By contrast, Figure 4.20 presents the residence time map for the test rig if its contents were to be discharge following a core flow pattern. In this case it can be seen how the tracers located along the symmetry axis of the silo (throughout all the different levels) have the lowest residence time, which illustrates the formation of a central channel at the beginning of the discharge while the rest of the contents remain static. Then, instead of the tracers located at the deepest level, the next tracers discharged are those located at the upper most level (level G), which illustrates the material from

the top of the silo cascading into the central channel as the rest of the material remains stagnant. This trend continues until the tracers located at the deepest level (level B) come out last. This map clearly represents a first in last out discharge typical of core flow.

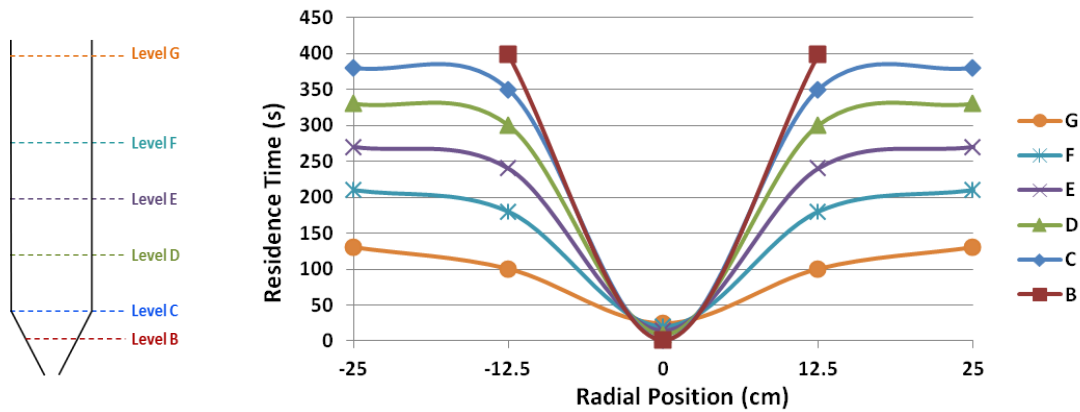


**Figure 4.20** Typical Core Flow Pattern

Figure 4.21 shows the residence time map for the silo discharging in a mixed flow pattern. In this case the first tracers to come out are those located along the symmetry axis of the silo but only through the three deepest levels B, C and D; which indicates the formation of a central channel. The next tracers discharged are those located at the intermediate radial position at level D, which indicates that the central channel initially formed widened at some point between the levels C and D forming a funnel. All the tracers located at level E come out next with the same residence time between them, this indicates that the flow channel continued widening until it intersected the walls at some point between levels D and E, allowing the tracers from level E to discharge in a mass flow – like pattern. This is confirmed by the residence time of the tracers at levels F and G, which follow a first in first out discharge as it was explained above. After all the tracers located at the upper levels have been discharged, the remaining tracers come out following a first in last out pattern with the last tracers to exit being those located near the walls at the deepest level B. This map clearly illustrates a mixed flow pattern.

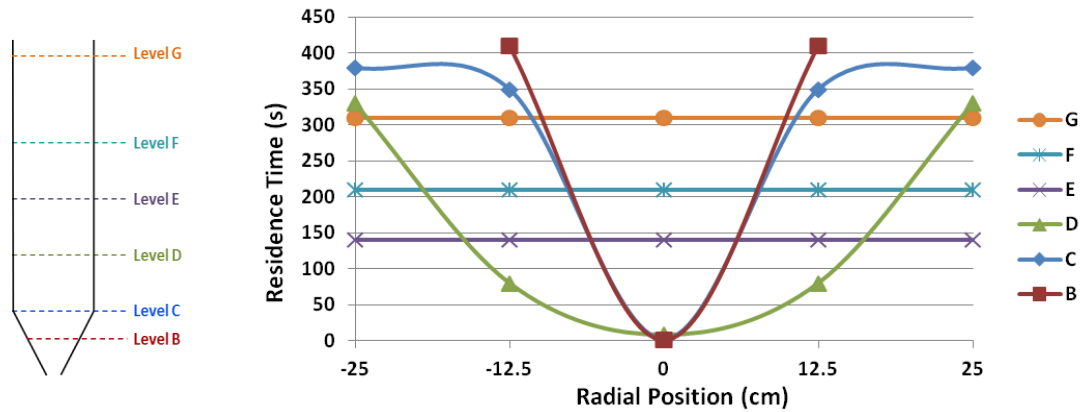
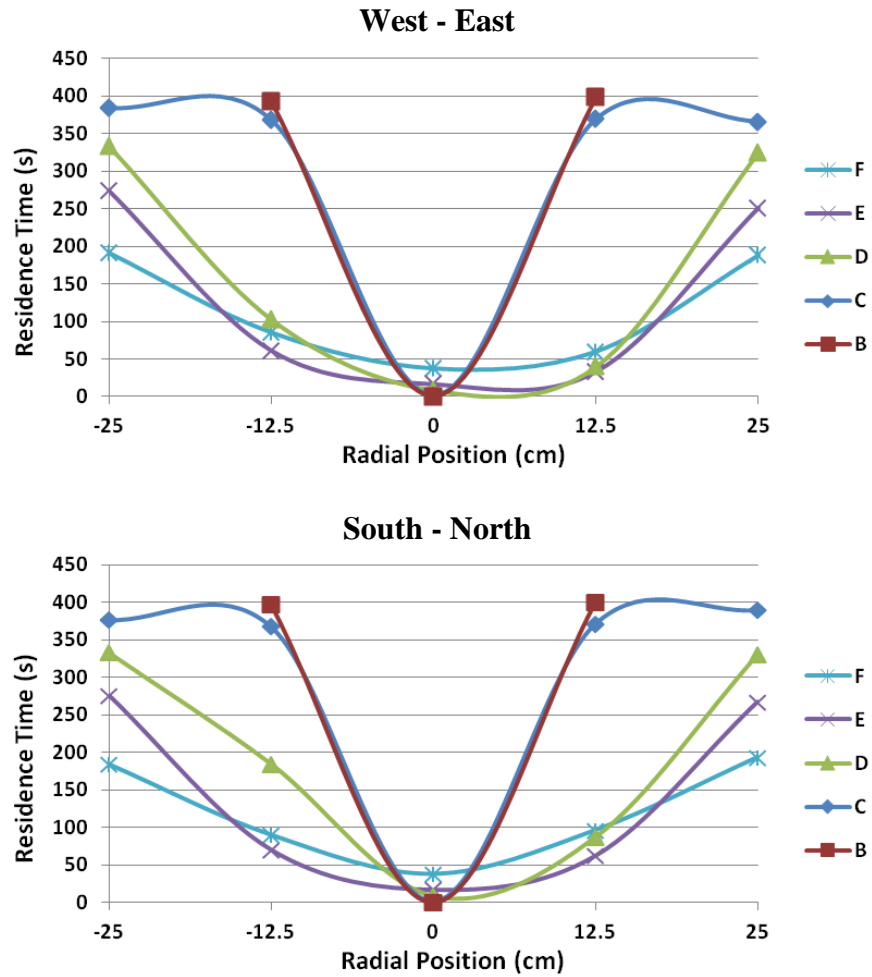
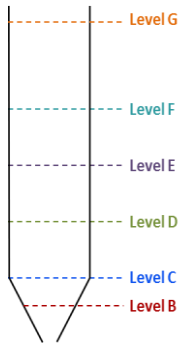


**Figure 4.21** Typical Mixed Flow Pattern

#### 4.4.2 Silo Allowed to Drain After Filling

Figure 4.22 presents the measured residence time of the tracers relative to their position, for the silo discharging without any insert fitted. Each plot represents a perpendicular plane where the tracers were placed. The first evident aspect from this process is the fact that all the tracers placed along the symmetry axis of the bin were the first to be discharged. As explained before, this indicates that a central flow channel developed immediately after the discharge started. The next tracers to come out were all the ones placed half way between the axis and the wall of the bin, except for those located at the transition. From this, it can be inferred that after the column of material placed directly above the outlet of the bin has been discharged, the channel widens above the transition (between levels C and D) and the material below the transition remains static. Then, the tracers placed at the wall began to come out starting from the ones in the upper most level and subsequently the ones placed deeper in the bin. The last tracers to be discharged were those placed at the transition of the silo and near the wall inside the converging section. This clearly describes a first in last out discharge, which, in addition to the central flow channel, are distinctive characteristics of the core flow discharge pattern. If the plots from Figure 4.22 are compared to the map from Figure 4.20 it is evident the development of core flow and the main difference between these maps is given by the width of the discharge channel.

Figure 4.22b shows the surface profiles that were observed from the top of the silo during discharge. The shape of the profiles observed agrees with the results obtained with the tracers, as a central channel was observed immediately after the start of discharge. The material was observed to roll from the top of the solids bed and go through the central channel, this behaviour was noticed during the entire discharge.



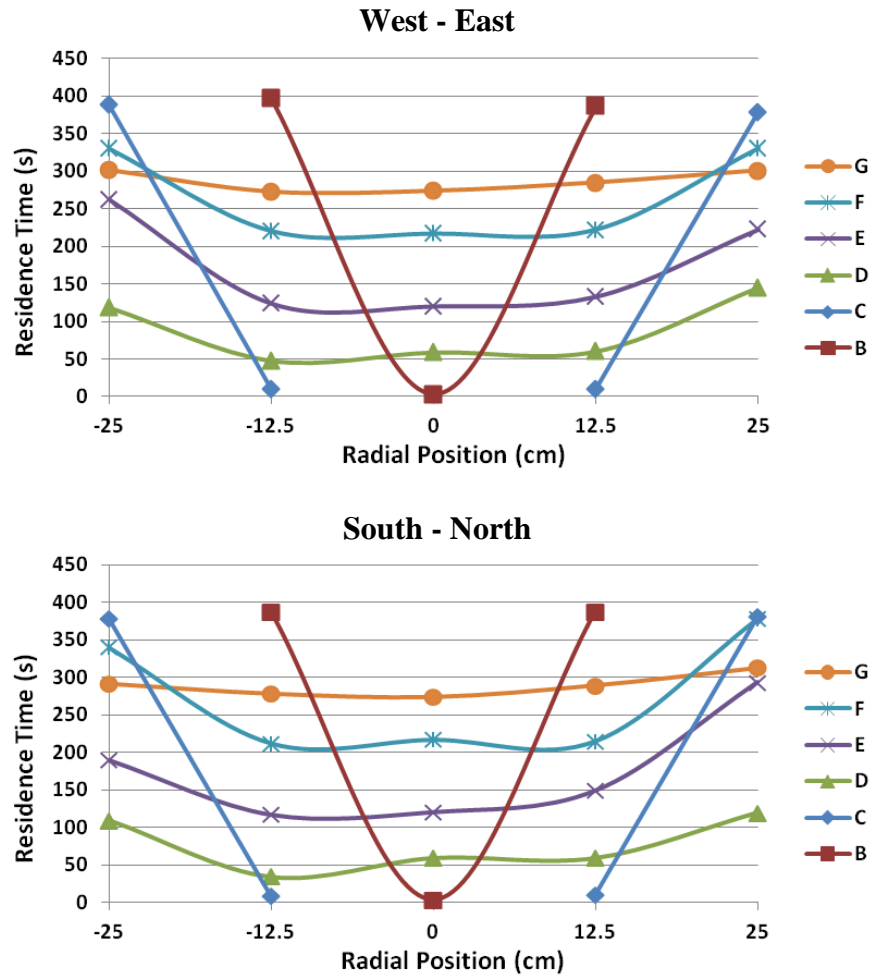
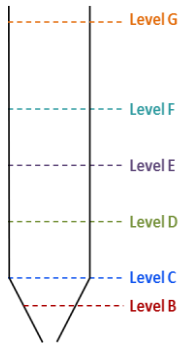
a. Tracers Residence Time

b. Surface Profile

Figure 4.22 No Insert - Results

The effect that installing Johanson's insert has on the discharge behaviour, is evident in Figure 4.23a. The tracers placed along the axis are not the ones to come out first. Instead, it can be seen that above the transition, all the tracers positioned at a specific level have similar residence times and those placed deeper in the bin discharge first. This indicates a first in first out discharge, a characteristic of the mass flow pattern. However, the behaviour below the transition is quite different, the last tracers to come out are those at the wall of the transition and the converging section, showing that the material in that zone remained stagnant, therefore mass flow was not obtained. The lower part of the bin discharged in core flow pattern, while the upper part discharged in a mass flow like pattern, this combination as it was explained before, is typical of a mixed flow pattern. In this case the initial channel was wide enough to include the tracers located at the intermediate radial position of the deepest level B. Then it continued widening until intersecting the walls at some point above the transition between levels C and D. From that point upwards the material slipped at the wall and discharged following a localised mass flow pattern.

An interesting detail that contradicts the statement above can be observed in Figure 4.23a. The tracers placed at the wall of level F came out after those of the level G. The explanation to this can be found with the help of Figure 4.23b. When the discharge started, the top surface of the material came down level and moving at the wall, suggesting that mass flow had been achieved. However, when the top surface was near the middle point of the vertical section, a central channel started forming. At that point, the material at the wall continued moving but at a lower speed until no further movement was observed and core flow was fully developed. With this, it can be inferred that the material stopped moving before the tracers of level F were discharged, and then the material at the top started rolling down the central channel allowing the tracers at the wall of level G to be discharged first.



a. Tracers Residence Time

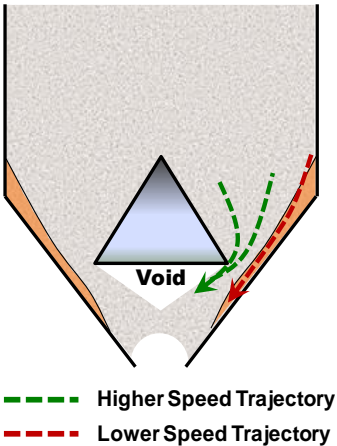
b. Surface Profile

Figure 4.23 Johanson's Insert - Results

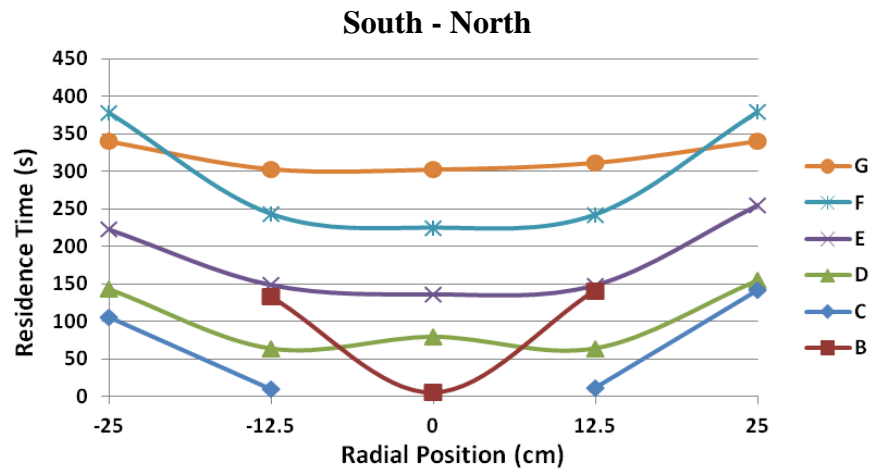
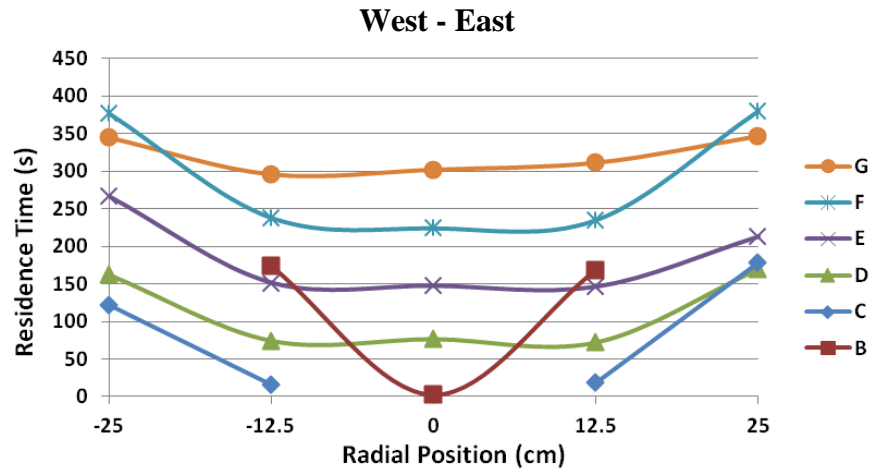
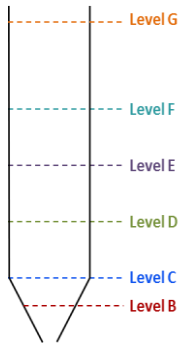
A further change to the discharge pattern is produced when the modified insert is installed, as shown in Figure 4.25a. The upper levels of tracers have similar discharge behaviour to the process using the smaller insert. However, the tracers placed at the wall of the transition and converging section were not the last to be discharged, instead, they came out at the early stages of the test, providing evidence that there were no stagnant zones of material in the bin, and therefore it can be said that mass flow was achieved. This statement is valid only for a limited period of time during the test, because it was observed (see Figure 4.25b) that the material descended with a levelled top surface for around three-quarters of the length of the vertical section. At that point, the central channel started forming and then the material stopped moving at the wall. This explains the difference between the wall tracers of levels F and G (as it was explained for the smaller insert). Although the surface profiles and the behaviour of the tracers in the upper part of the bin are very similar for both inserts, it can be inferred that the mechanism differs considerably. In the case of Johanson's insert, the material near the wall of the converging section never moved creating a barrier that hindered the discharge of the material above. With the modified insert, the material at the wall in the converging section moved, as shown by the residence time of the tracers, therefore the impeding barrier was not present at the early stages of the test. However, when the inventory of material became low, the vertical force, that helps the material move at the wall also reduced, allowing the formation of the stagnant zone. This is a clear indication that the head of material plays an important role in the performance of inverted cones when the  $z/D$  ratio is small (typically  $< 3$ ).

From the results presented in Figure 4.25a (as it was explained above) it can be deduced that for a part of the discharge all the contents of the silo were in motion, which leads to the conclusion that mass flow was achieved in the silo. However, when comparing Figure 4.25a to the residence time map for an ideal mass flow (presented in Figure 4.19), it is clear that the pattern obtained with the modified insert was relatively far from the ideal pattern which is illustrated by the difference in residence time between the tracers placed at the same level. In particular, it can be seen that the tracers placed at the wall of the converging section (level B) have a higher residence time than those placed at the wall on levels C and D. The key to the difference in residence time lies on the shapes of the insert and hopper walls, and the void space created

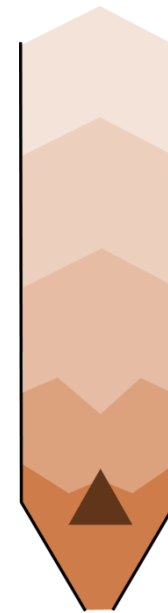
below the insert. The wall of the inverted cone has a convex shape which facilitates the movement of material by relieving stress in the angular direction. This is one of the main reasons that enable inverted cones to be used as flow promoting devices. By contrast, the hopper wall has a convex shape which compresses the material in the angular direction interfering with the movement of material. In addition to this, when the material passes through the annular gap between the insert and the silo wall, it finds in the empty space below the insert a region of low stress into which it is easier to move and then continue to the outlet. The combination of these two mechanisms produces a velocity gradient inside the hopper, with a high speed region flowing in the vicinity of the insert and a low speed region flowing in the vicinity of the hopper walls (see Figure 4.24).



*Figure 4.24 Speed Zones in the Vicinity of the Insert*



a. Tracers Residence Time



b. Surface Profile

Figure 4.25 Modified Insert - Results

#### **4.4.3 Silo with additional material fed during discharge**

The flow behaviour of the silo, when a 0.5 tonne big bag is utilised to maintain a constant head of material in the silo until the big bag empties and completely drains down, is shown in Figure 4.26, Figure 4.27 and Figure 4.28. The process without inserts illustrated in Figure 4.26 does not differ much from the process analysed above. However, the differences in the residence time of the tracers placed near the walls and those closer to the centre of the bin are more exaggerated than before. This is due to the fresh material fed into the bin from the big bag flowing straight down the central flow channel and therefore being discharged before the material near the wall, confirming the first in last out discharge.

Unlike the process without the insert, when Johanson's insert is fitted there is a substantial change in the discharge behaviour with respect to the same process previously analysed. As seen in Figure 4.27, the markers placed at the wall of the converging section are not the last ones to come out, and there are small differences in the residence times of tracers placed at a common level in the silo. From this it can be inferred that mass flow was achieved during the discharge. The fact that mass flow was not achieved in the process without additional material fed, but it was achieved when the head of powder was kept constant, suggests that in the former process the magnitude of the stresses was not enough to make the area of influence of the insert reach the walls of the hopper. Instead, the stress characteristic passing through the apex of the insert would intersect the stress characteristic passing through the base, at some point before reaching the walls of the hopper, producing a widening of the discharge channel but no achieving mass flow.

In general, it can be deduced that further improvement was achieved when fitting the modified insert. Although mass flow had already been obtained for the process with a variable head of powder, here the difference between the residence times of tracers at a specific level was reduced further, getting closer to the concept of ideal mass flow, where that difference is non-existent. In general terms, the performance of the bin is more consistent and homogeneous when the large insert is fitted. It can be observed in Figure 4.27 and Figure 4.28 that the behaviour of the tracers located at

level B is similar to the process without additional material (using the modified insert), this was expected due to velocity difference between the region near the insert and the region near the wall of the hopper as it was explained previously.

In section 4.2 the author formulated a hypothesis regarding the effectiveness of Johanson's method for the design of an inverted cone insert, when the stresses around it become a strong function of the head of material (typically silos with  $z/D < 3$ ). The author postulated that the calculation of the position of the inverted cone apex in Johanson's method should include a safety factor, this would ensure that the area influenced by the insert could reach the walls of the hopper as the inventory of material reduced during discharge. The hypothesis was supported by the experiments undertaken with the bench scale model, where it was observed that the use of the insert designed with the safety factor produced more consistent improvement than the insert designed following Johanson's method.

The performance enhancement achieved using the modified insert is yet more evident from the results obtained during the commissioning of the semi-industrial test rig. When the head of material was kept constant at  $z/D$  ratio equal to 3 Johanson's insert produced mass flow in the silo, which could be deduced from the fact that the tracers located at the walls of the hopper were not the last to be discharged and by the analysis of the other tracer residence times (as explained above). Even though this result supported the validity of Johanson's design method, it was also found that the modified insert could produce better results. This is demonstrated by the reduction on the residence time difference between tracers placed at a determined depth in the silo, which makes the discharge pattern closer to ideal mass flow. However, the difference in performance between the two inserts was emphasised by the results obtained when the head of material was allowed to reduce from the start of the discharge. In that case, Johanson's insert did not produce mass flow in the silo and just widened the discharge channel enough to produce a mixed flow pattern, which confirms that the performance of the insert is strongly affected by the stress field and therefore by the head of material. By contrast, the modified insert did produce mass flow during the discharge of the silo, validating the use of a safety factor for the size and position of the insert as suggested by the modified design method presented by the author.

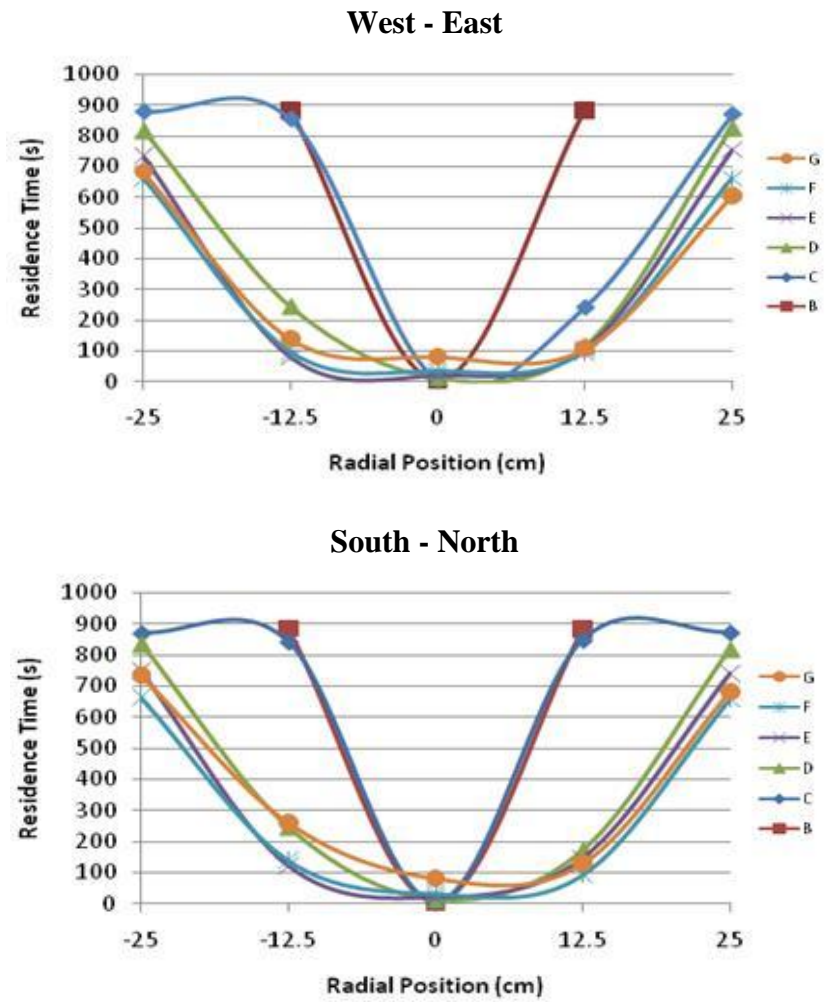
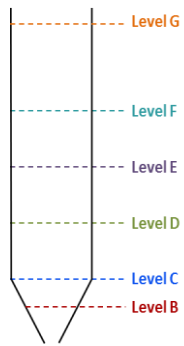


Figure 4.26 No Insert - Results

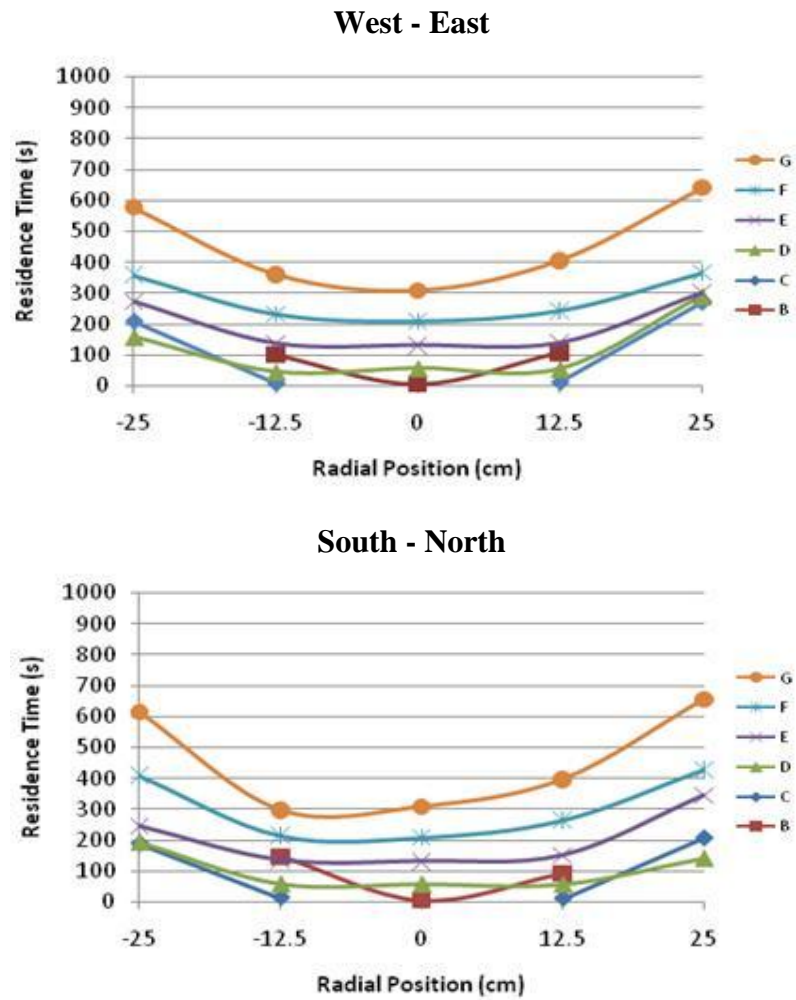
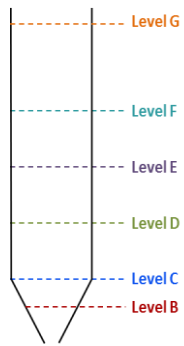


Figure 4.27 Johanson's Insert - Results

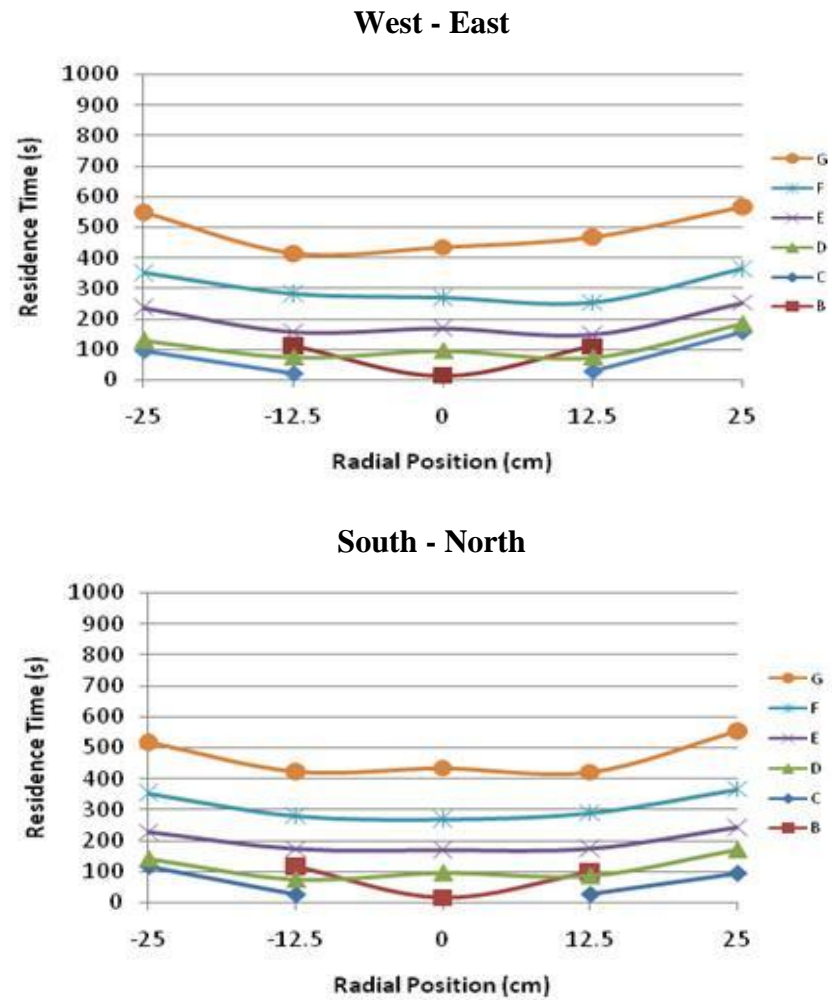
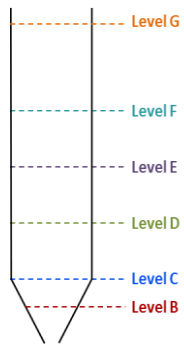
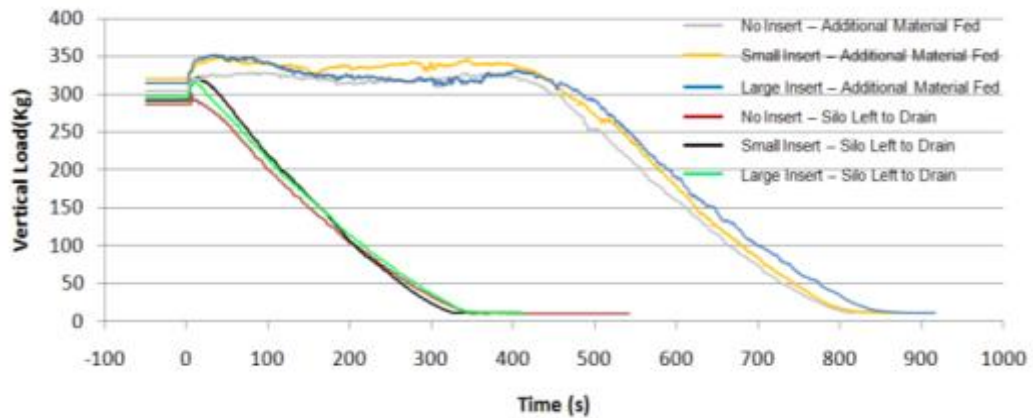


Figure 4.28 Modified Insert - Results

#### 4.4.4 Vertical Load Acting on the Cylindrical Section of the Bin



*Figure 4.29 Comparison of Vertical Loads on the Cylindrical Section of the Rig*

The magnitudes of the loads measured on the cylindrical section of the bin, both with and without inserts, are presented in Figure 4.29 as a function of the discharge time. The value before time zero represents the vertical load acting on the walls at the end of the filling process. It is noticeable that an incremental change in the load occurs at the start of the discharge process, and what happens after depends on the head of material and flow pattern developed.

For the process where the silo was left to drain, the load decreases rapidly as the head of material decreases, but, when additional material was fed, the load remains approximately constant at the incremented value as long as the head of material does not decrease. In the data collected, a decrement of the load is observed after some time even while material was still being fed. This was due to a slight reduction in the height of the top surface in the silo resulting from the big-bag hopper elongating as it emptied.

The vertical force measured on the cylindrical section of the silo is the result of the friction between the bulk solid and the wall material. When the materials is charged into the silo the particles accommodate relatively loosely reaching a determined bulk density and transferring part of the weight of the bulk to the walls of the silo, the transferred load due the friction is shown Figure 4.29 before the discharge started at

time equal to zero. When the discharge starts, the motion of particles at the wall causes mobilisation of friction increasing the drag force. When the maximum drag force is reached, the frictional forces are fully mobilized and the system is deemed to have reached steady state flow. The maximum value of shear stress obtained after reaching steady state flow, together with the steady state flow value of the stress normal to the walls represent a point of the wall yield locus and can be used to calculate the kinematic angle of wall friction. However, the values of both stresses – shear stress and normal stress – are a function of the depth of material at each point inside the bin and the vertical load recorded is a measure of the average shear stress acting on the whole inside area of the vertical cylindrical section. Therefore, to calculate the average angle of wall friction, the shear stress needs to be averaged over the internal wall area, or along the depth of the cylindrical section as the radius is constant. The mathematical deduction for this purpose was presented in section 4.1 obtaining Equation (4-7), which is written below once more.

$$F_{Load\ Cells} = \frac{\pi\rho g D^2 z}{4} + \frac{\pi\rho g D^3}{16\mu K_j} e^{-4\mu K_j \frac{z}{D}} - \frac{\pi\rho g D^3}{16\mu K_j} \quad (4-7)$$

The measured load from the experiments can be multiplied by the gravitational acceleration  $g$ , then the coefficient of friction and therefore wall friction angle can be obtained. However, as it can be seen from Equation (4-7) the selection of the value for the horizontal to vertical stress ratio ( $K_j$ ) can affect the value of the coefficient of friction. In section 2.6 it was explained how Rankine's equation (Equation (2-42)) could be used to calculate the value of  $K_j$ .

$$K_j = \frac{1 - \sin\delta}{1 + \sin\delta} \quad (2-42)$$

However, the use of Equation (2-42) produces very low values of  $K_j$  yielding high values of vertical stress and underestimating the values of stress normal to the silo walls. The use of this equation is more suited for the calculation of the stresses near the axis of the vertical section where the direction of the major principal stress is almost vertical, in fact this equation could only be valid at the axis where the vertical and horizontal stresses are principal stresses. This equation was used in the case of

calculating the loads on the inserts because they are normally positioned in the centre of the bin and also because this equation would produce the worst case scenario in terms of insert loads, encouraging a more robust design for the structural support.

As it was mentioned above, the values of stresses normal to the silo walls obtained with Equation (2-42) are generally very low compared to experimental measurements which could result in unsafe design of silo structures. Other equations have been derived for the calculation of  $K_j$  which produce better predictions of lateral stresses in particular Equation (4-9) which was proposed by Kezdi and is commonly used for this purpose [Schulze, 2008<sub>1</sub>].

$$K_j = 1 - \sin\delta \quad (4-9)$$

Another approach for the value of  $K_j$  is simply to use  $K_j = 0.4$  which is recommended for rough estimates with most materials [Schulze, 2008<sub>1</sub>]. Taking this into account, the values of wall friction angle ( $\phi$ ) have been calculated from the traction loads measured experimentally. For comparison reasons, the results from the calculation are presented in Table 4-2 using each of the methods explained above for the estimation of the value of  $K_j$ .

**Table 4-2**      **Calculated Wall friction Angle**

	$\phi$ (Deg)			
	From Shear Tests	Equation (2-42) $K_j = 0.23$	Equation (4-9) $K_j = 0.37$	$K_j = 0.4$
<b>Johanson's Insert</b>	29	41	28.4	26.5
<b>Modified Insert</b>	29	40.1	27.6	25.8

The results from Table 4-2 clearly demonstrate the importance of selecting the appropriate value of the horizontal to vertical stress ratio ( $K_j$ ) for calculation related to stresses at near the walls of the silo. In this case, if the inappropriate method for the computation of  $K_j$  is chosen (Equation (2-42)), the resulting angle of wall friction needs to have a very high value to compensate the low horizontal stresses calculated.

In fact, the angle of friction obtained using this method is larger than the angle of internal friction of the test material ( $\phi > 40^\circ$ ,  $\delta = 39^\circ$ ), this would mean that the material would not be able to slide at the wall of the silo, shearing internally instead and producing core flow. This contradicts the visual evidence from the tests where the material was observed to slide along the vertical section of the silo and a funnel was not seem to form (a least during the earlier parts of the each test).

By contrast, when Equation (4-9) was used to calculate the value of  $K_j$ , the results obtained for  $\phi$  were very close to the value found from the shear cell measurements, with 2% difference when using Johanson's insert and 4.8% difference when using the modified insert. The value of  $K_j = 0.37$  obtained with Equation (4-9) was also very close to the general recommended value of  $K_j = 0.4$ , but still it produced closer agreement to the shear test results, with the latter producing 8.6% and 11% differences for each insert respectively. The close agreement between the calculated values and the shear cell measurements indicates that the configuration of the test rig could be suitable for the measurement of wall friction. However, these results need to be treated with care as the model used for the calculations makes assumptions which are not faithful representation of the real flow phenomenon. For example, in the model the bulk density is assumed to be constant, however it is a known fact that bulk density is a function of the stresses acting on the solids which means that its value would change with the powder bed depth. In this particular case, the assumption of constant bulk density is not far from the reality because the sand used as test material is fairly incompressible. However, if a more compressible material was to be used, the changes in density could produce a larger deviation from shear cell results. Something very similar occurs with the angle of wall friction itself, which is also a function of the consolidation stress, but again in this case, the measured values obtained from the shear cell were fairly constant across the stresses tested.

An additional factor that could compromise the validity of the model used is modification of the stress distribution in the lower part of the cylindrical section due to the presence of the insert. The model assumes that the magnitude of the stress normal to the walls, as a function of the powder bed depth, follows a distribution typical of mass flow systems and similar to the line shown in Figure 4.30a, where the

stress increases with depth approaching an asymptotic value (similar to the explanation presented in section 2.6 for vertical stress). However, if the apex of the inverted cone protrudes into the cylindrical section, it reduces the area available for the material to flow and the material is therefore compressed horizontally. The horizontal compression of the powder creates a discontinuity at the level of the insert apex, where a maximum value of the normal stress is reached (as it can be seen in Figure 4.30b) [Chou, 2006]. Therefore, the stress distribution in the bottom part of the cylindrical section does not follow the function assumed in the model which introduces an error in the calculations. The magnitude of this error is expected to be larger when using the modified insert because the apex of the inverted cone is located higher in the silo, increasing the extension of the area where the stress distribution differs from the model.

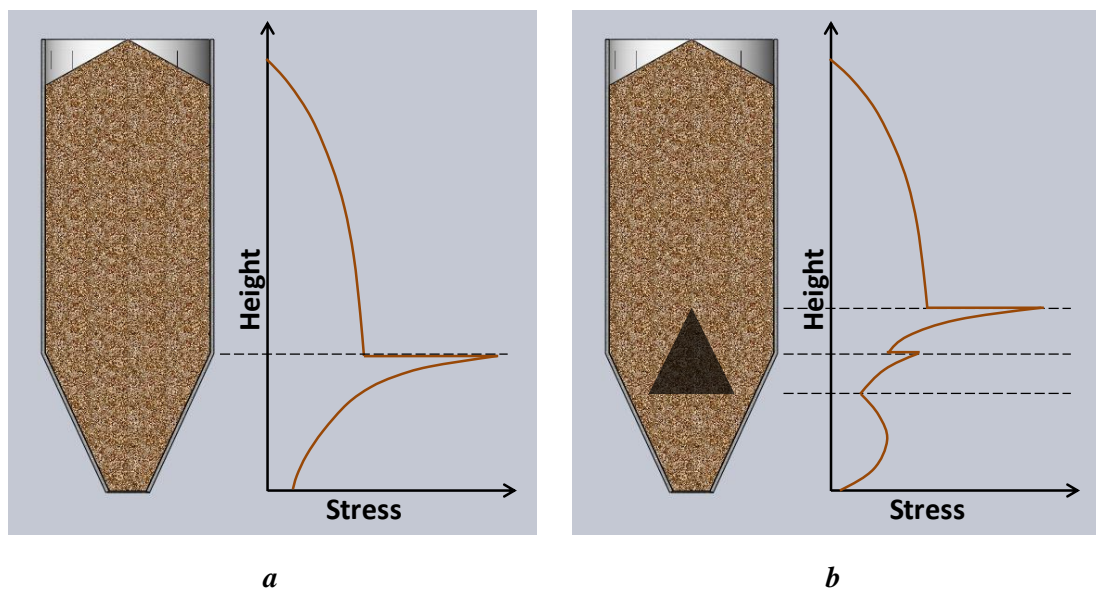


**Figure 4.30** *Normal Stress Distribution in the Vertical Section of a Silo with and without an Inverted Cone Insert*

#### 4.4.5 Vertical Load Acting on the Inserts

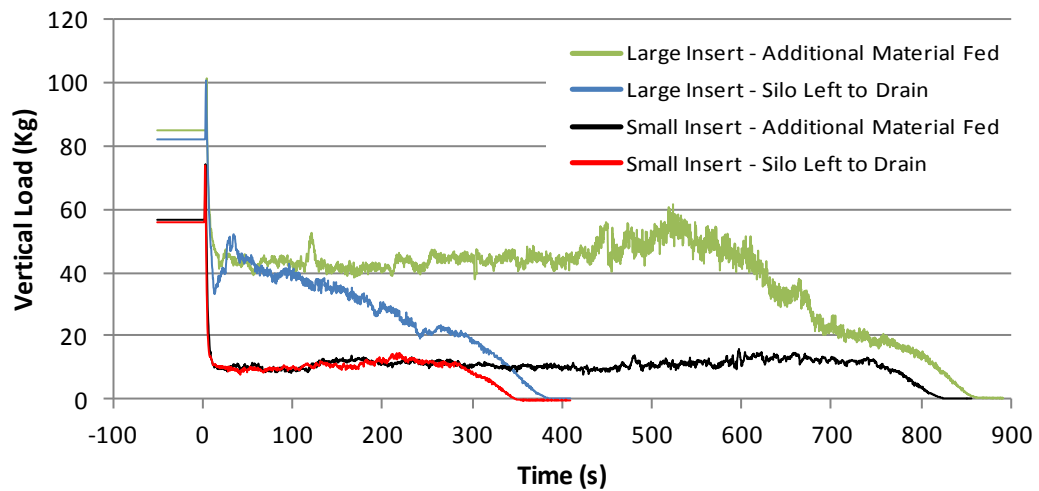


*Figure 4.31 Comparison of Vertical Loads on the Inserts*

The magnitudes of the vertical loads exerted on the inserts during discharge are presented in Figure 4.31. Time zero represents the start of the discharge and the values of the loads shown for times before zero represent the loads exerted at the end of the filling process. When the discharge of material starts, the load increases reaching a maximum value and then decreases until it reaches a constant value, as the flow approaches steady state. These changes in magnitude are the consequence of the changes in direction of the major consolidating stresses in the vicinity of the insert as it was explained in section 3.3. Although the main interest from the measurements for this project is the value of the load peak, it is also interesting to visualise the difference in magnitude between the load at the end of the filling process and the load when steady state is reached.

At the end of the filling process, it is clear from Figure 4.31 that the loads exerted on the modified insert are higher than those exerted on Johanson's insert. This is expected due to larger size of the modified insert which has a larger effective area supporting the bed of material. In fact, the modified insert has an area approximately 56% larger than Johanson's insert and the loads acting on the modified insert are 50-55% higher than those acting on Johanson's insert. However, after the discharge has started and steady state has been reached, the difference between the loads acting on

the modified insert and those acting on Johanson's insert no longer keep the same proportion. As it can be seen in Figure 4.31, the loads acting on Johanson's insert during steady state are much lower than those acting on the modified insert, which could be the effect of the following factors. First, the modified insert protrudes further into the cylindrical section than Johanson's insert. In the cylindrical section, the vertical stresses are higher than in the converging section which would increase the difference between the stresses acting on both inserts. However, it is the author's believe that the main contributor to the large difference in steady state loads, lies in the flowing channel of material around the inserts. The lower values of stress acting on Johanson's insert suggest that the diameter of the flow channel produced by that insert is smaller than the one produced by the modified insert which would also reduce the magnitude of the vertical stresses. In addition to this, if the channel in the vicinity of Johanson's insert was narrower this implies that the channel did not reach the walls of the silo. In that case, the flow channel generated would have an outer boundary in contact with zones of stagnant material adjacent to the silo walls and the coefficient of friction at that boundary would be considerably higher (almost twice in this case) compared to a channel with boundary at the silo walls.

As it was mentioned above, for the objectives of this project the most important value of vertical loads acting on the inserts is the peak load, which is key to ensure structural stability of the system. A theoretical approach proposed by Johanson for the calculation of the peak load was presented in section 2.6. This method was first evaluated with the results obtained in the previous chapter, where the experimental results did not compare favourably with the predictions made by the method. The modification undertaken on the test rig guarantee that the characteristics of the tests presented in this section offer a better platform to evaluate Johanson's method.

Table 4-3 presents the average peak loads measured for both inserts as well as the predictions obtained following Johanson's method (equation (2-44)) and also applying Johanson's recommendations to the Janssen - Rankine equation (equation (2-43)). In both cases the diameter of the acting bed of powder was assumed to be the diameter of the silo, the boundary friction was assumed to be represented by the angle of wall friction and the area that multiplies the stress to calculate the load was

obtained using the diameter of the insert, due to the highly free flowing characteristics of the material.

$$\sigma_z = \frac{\rho g D (1 + \sin \delta)}{4 \tan \varphi (1 - \sin \delta)} \quad (4-10)$$

$$\sigma_z = \frac{\rho g D (1 + \sin \delta)}{4 \sin \delta \cdot \sin \left( \sin^{-1} \left[ \frac{\sin \varphi}{\sin \delta} \right] - \varphi \right)} \quad (4-11)$$

**Table 4-3** *Measured and Calculated Loads Exerted on the Inserts*

<b>Insert</b>	<b>Johanson's Insert</b>		<b>Modified Insert</b>	
<b>Calculation Method</b>	Johanson Equation (2-44)	Janssen - Rankine Equation (2-43)	Johanson Equation (2-44)	Janssen - Rankine Equation (2-43)
<b>Average Calculated Load (Kg)</b>	60	66	94	103
<b>Average Measured Load (Kg)</b>	71		100	

As it can be seen from Table 4-3 the predictions obtained for this system are in much closer agreement with the experimental values than those obtained in the previous chapter. Even though the predictions obtained using Johanson's equation still underestimate the value of the peak, the method gives a starting point for the calculation of that load and when the recommendations (for diameter, frictions, etc.) are applied with the Janssen - Rankine equation the agreement of the predictions is further improved. Nevertheless, as the main interest for the knowledge of the peak load is for structural purposes the highest prediction should always be favoured (Janssen - Rankine produces slightly higher values) and then an additional safety factor should be applied to calculate the minimum support needed for the inserts.

## 4.5 Summary

The test work and results discussed in the previous chapter showed that the test rig used did not provide the appropriate tools for the study of static inserts and their effectiveness as flow promotion devices. The main shortcomings observed were the geometry of the silo, which did not allow the powder to achieve steady state condition during discharge; the absence of a system for the identification of the flow pattern developed during discharge; the unsuitability of the mechanism used for the measurement of stresses acting on the static inserts and the instability of the support used to position the inserts inside the silo.

This chapter presents the modifications undertaken on the test rig in order to overcome the deficiencies observed in past test programmes. To achieve this, the geometry of the silo was modified to increase the height to diameter ratio to a  $z/D$  value of 3 which would increase the consistency of stress conditions around the insert area. For the identification of the flow pattern, a tracking system was designed and built allowing the mapping of the movement of material inside the bin. The support of the insert was changed increasing the stability of the system and allowing the attachment of a heavy duty load cell with short couplings, which minimized the interference of side forces with the measurements of the forces acting on the inserts. The inserts evaluated consisted of two inverted cones made in polished mild steel. One of the inserts was designed following a method proposed by Jerry Johanson in 1965. The second insert was designed with a modification to Johanson's method, trying to improve some areas of the design where the author thought the original method lacked robustness.

The modification proposed was based on the high dependency of Johanson's method on the values of stress around the insert being close to the asymptotic values, which means deep beds of powder above the insert ( $z/D > 3$ ). The author hypothesised that the effectiveness of the insert would decrease when silos would not have the adequate height to diameter ratios, which is a very common feature in industrial silos. In order to evaluate the proposed modifications to the method a bench scale silo was designed and built and multiple inserts were tested varying their size and position in the silo. From the results, a modified design method was proposed

producing a slightly larger insert than that of Johanson's, keeping the base at the same height in the silo, therefore locating the apex slightly higher in the bin.

To evaluate the performance of Johanson's insert and the modified insert, two types of test were undertaken. In the first set of tests, the silo was filled and then allowed to drain completely without an insert, the procedure was repeated installing each inverted cone. The second type of tests consisted in filling the silo and then feeding additional material during discharge, to maintain a constant depth of material during testing. These tests were also undertaken with each insert and without any of them.

The results showed that when the silo was left to drain, the insert designed with Johanson's method widened the discharge channel until it touched the walls of the silo, making the material in the top of the bin flow in a mass flow-like pattern. However, the material near the walls in the lower part of the silo remained stagnant and discharged last, suggesting the development of a mixed flow pattern during discharge. On the other hand, the insert designed with the modified method produced mass flow in the entire silo for a period of time during discharge, and then, once the head of material in the bin reduced, it produced an effect similar to that of Johanson's insert. When additional material was fed during discharge, both inserts produced mass flow, however, the insert designed with the modified method achieved a more even distribution of velocities across the bin. In both cases the results validate the modified method proposed by the author, which improves the performance in comparison with the original insert. This is more evident with the lower heads of powder in the bin which validates the hypothesis formulated by the author. The measured vertical loads acting on the inserts were found to be in closer agreement with the predictions made by the theoretical methods, compared to the results obtained in the previous chapter. The theoretical method could be used as a starting point for the estimation of the maximum load in silos with  $z/D=3$  or higher, particularly using the Janssen-Rankine equation, which produces slightly higher predictions of loads. In any case, it is recommended that additional safety factors are applied to the results because as it was found during the test, the predictions can underestimate the value of the maximum load.

## **CHAPTER FIVE: INSERT CONFIGURATION TO OPTIMIZE DISCHARGE FROM SILOS: A STUDY AT BENCH AND SEMI-INDUSTRIAL SCALES**

---

The use of a bench scale test rig for the evaluation of inverted cone inserts was presented in the previous chapter. This proved to be an economic yet powerful tool for the development and evaluation of flow promoting inserts. The present chapter builds on the success obtained with the bench scale rig and evaluates the performance of other types of static inserts. Based on that approach, the design of a novel flow promoting insert is presented, as well as a proposed method for the design of double cone inserts. The performance of these inserts is compared to inverted cones, first at bench scale and then using the semi-industrial scale test rig.

### **5.1 Bench Scale Test Rig Modification**

The design and construction of a bench scale test rig for the development of static inserts was described in Chapter 4. The test rig comprised a Perspex cylindrical section 120 mm in diameter and 500 mm tall, interfaced to a conical converging section made of polypropylene with 30 degrees half angle and 20 mm outlet, as shown in Figure 5.1. The maximum capacity of the model silo was 6 litres with a maximum height to diameter ratio  $z/D > 4$ .

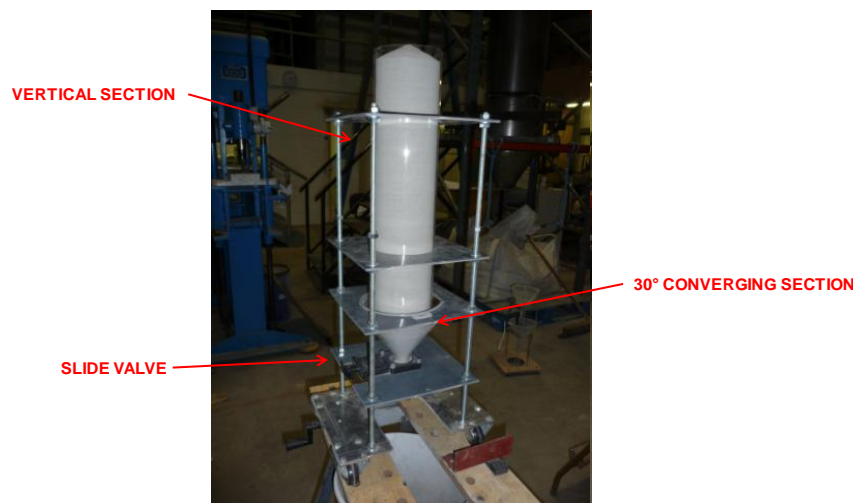


**Figure 5.1** *Bench Scale Model for Insert Development*

Using this setup, it was possible to observe the impact that inverted cones had on the flow pattern during discharge, converting a core flow bin to a mass flow bin or a mixed flow bin in some cases. By observing the behaviour of the solids during discharge through the clear walls of the model, it was possible to compare the performance of different inverted cones with subtle design variations. These results were later backed up when the scale up of the system was done running tests with the semi-industrial test rig, also described in Chapter 4. However, the differences in performance were not always easy to discern and the comparison technique could be considered subjective. For this reason, it was decided to equip the test rig with additional means of quantitative identification of the flow pattern.

The first modification consisted of an impact plate mounted on load cells and located underneath the outlet of the hopper (see Figure 5.2). By measuring the impact force, exerted on the plate by the solids stream during discharge, it would be possible to detect instantaneous changes in the flow rate, which in turn could highlight characteristics associated to certain discharge patterns. For example, bins where a core flow pattern is developed are prone to exhibit bulk density changes at different stages of the discharge. This is due to multiple mechanisms such as; particle size segregation, also, the different residence times across the bin (characteristic of first in last out discharge) don't allow the same de-aeration and particle packing across the different positions inside the silo. As a result, it would be expected that when core flow is developed, the force exerted on an impact plate would be less uniform than that obtained from a silo discharging in a mass flow pattern.

The second modification to help improve the flow pattern identification was the inclusion of a container mounted on load cells and located underneath the model silo outlet to measure the actual mass discharge rate during the test. The differences in average discharge rate between tests could also offer valuable information to infer the behaviour of the solids inside the bin during discharge.

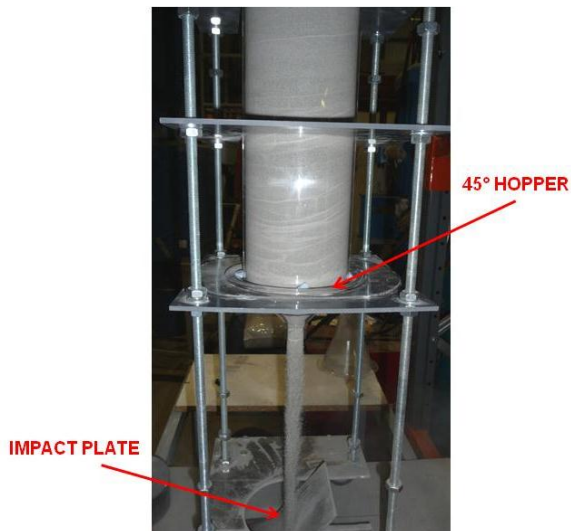


**Figure 5.2** *Additional Converging Section and Impact Plate*



**Figure 5.3** *Vertical Sections Employed (Smooth and Roughened Perspex Tubes)*

As mentioned in the previous chapter, the test rig was built as a modular structure so the main components could be altered to offer different silo geometry configurations. Taking this into account a second converging section with a 45° half angle and a 20 mm outlet was used as alternative hopper (see Figure 5.2). The shallower converging angle would pose a more challenging scenario for the inserts to transform a flow pattern from core flow to mass flow. In addition to this, the 45° convergence value was chosen because it is one of the most common hopper half angles used in industrial applications (along with 30° half angle). The 45° model hopper was made of glass which gave the possibility of observing the behaviour of the material in contact with the wall during discharge, which is a key feature needed in this rig for the identification of the flow pattern. However, the smoothness and hardness of the glass would provide a surface with very low frictional properties against the layer of powder in contact with it, opposing little resistance for particles to flow at the walls of the silo. Even though this situation would be highly desirable in industrial applications, it would not be representative of the vast majority of industrial processes. In order to obtain a better representation of processes at a larger scale, the internal walls of the hopper were lined with thin translucent sheets of polypropylene which provided a surface finish that was less smooth than the glass. For similar reasons, a second Perspex cylindrical section was also used, having its internal walls slightly roughened to increase the frictional properties (see Figure 5.3).

## **5.2 Initial Steps in Insert Development**

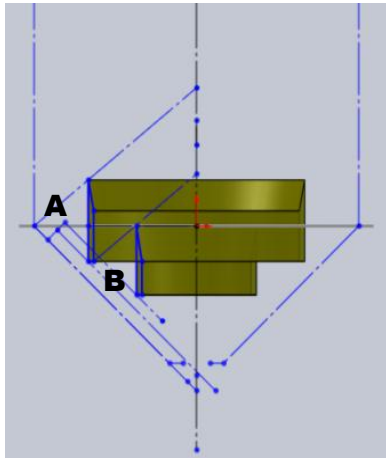
So far the work presented has included the study of inverted cone inserts as flow promotion devices and to some extent the use of circular flat plates for the same purpose. With the help of the bench scale model, the author decided to pursue an understanding of the way different insert geometries influence the behaviour of the flow of solids in an otherwise core flow bin.

### **5.2.1 Concentric Cylinders**

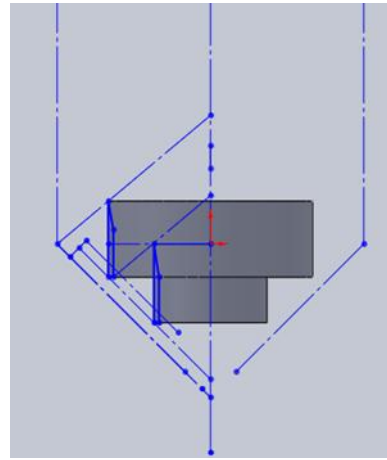
To try to understand how the conditions of the powder near the wall could be modified to produce flow, a fairly simple device was designed and built. To start with, the idea was to see whether a vertical wall placed near the transition of the hopper could influence flow at the wall. Therefore, the first feature of the insert was specified as a cylinder to be positioned near the transition of the bin. However, if placing a cylinder was successful and the powder in the region A started moving (see Figure 5.4a), it would be necessary to try to influence the wall closer to the outlet of the hopper as well, to avoid the formation of stagnant zones downstream which could impede the further movement of material from the influenced region. For this reason, a second cylinder (concentric with the first) was added to complete the general design of the insert, as shown in Figure 5.4.

A feature that was considered to be very important during the initial design was the gap between the hopper wall and the inner cylinder (insert). If the gap between the inner cylinder and the wall was the same as that between the outer cylinder and the wall, then the area available for flow would reduce due to the convergence of the wall (natural occurrence in a hopper). However, for the insert to be successful, the material in region B would also need to flow through the same area at the same time, increasing the compressive stresses and hindering the flow of material. For this reason, it was decided to increment the gap near the edge of the inner cylinder as shown in Figure 5.4a. In order to test the above theory, it was decided to also test an

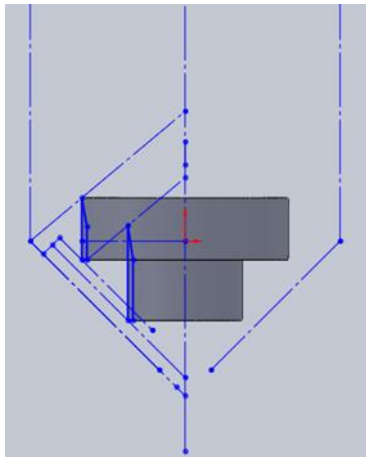
insert with a constant gap (Figure 5.4b) and an insert with a decreasing gap as the extreme case (Figure 5.4c). An example of the inserts tested is shown in Figure 5.4d.



*a. Concentric Cylinders with Increasing Gap*



*b. Concentric Cylinders with Constant Gap*



*c. Concentric Cylinders with Decreasing Gap*



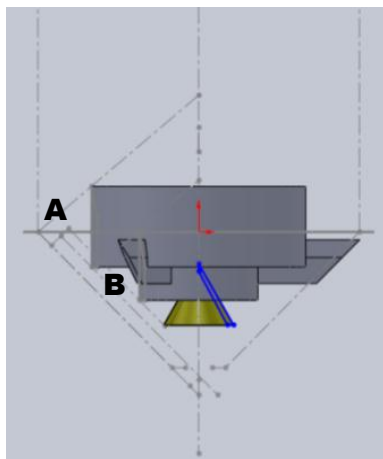
*d. Concentric Cylinders Insert*

**Figure 5.4** *Concentric Cylinders Inserts*

A series of tests were undertaken using olivine sand and following the procedure explained in section 4.2, for each of the inserts. However, in every case a central channel rapidly formed producing a funnel on the surface of the powder bed and the bin discharged in core flow. Movement of material in the region between the wall and the insert edges was not observed at any time, at least while there was material available to cascade through the central channel.

### 5.2.2 Concentric Cylinders with Inverted Cone

In order to prevent the formation of the central channel, an inverted cone was added to the design of the concentric cylinders (see Figure 5.5). The cone added was just slightly larger in diameter than the outlet of the hopper and it was placed inside the inner cylinder. With this set up it was expected that any preferential draw would be prevented by the cone. The inverted cone was added to each of the concentric cylinder inserts from the previous section.



*a. Design Example*



*b. Insert Example*

**Figure 5.5** *Concentric Cylinders Inserts with Inverted Cone*

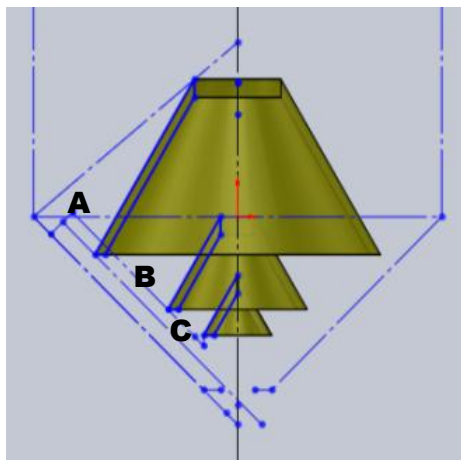
During the tests a channel, wider than in the previous tests, was formed from the moment the discharge started, but no movement was observed at the walls of the bin.

### 5.2.3 Concentric Truncated Cones with Inverted Cone

The next step of the process consisted in replacing the cylinders by truncated cones. It was thought that having an inclined surface, instead of a vertical one, would provide additional support to the material. This would help modifying the stress field to a greater extent in the regions where it was more difficult for the powder to move, facilitating flow. With this type of insert, multiple modifications and configurations were studied. As with the previous inserts, the gap between the edges of the truncated cones and the wall of the bin was progressively increased towards the

outlet (Figure 5.6a and b), progressively decreased (Figure 5.6c and d), and kept constant (Figure 5.6e and f).

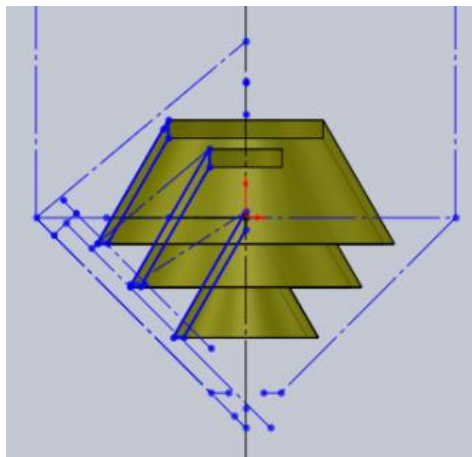
The influence of the size of the inverted cone was also studied with its base ranging from a diameter equal to the outlet diameter (Figure 5.6a and b), to double the size of the outlet diameter (Figure 5.6c and d). The last parameter studied was the height of the truncated cones, as it would modify the size of the top aperture of each cone affecting the amount of material redirected through each of the regions A, B or C.



*a.*



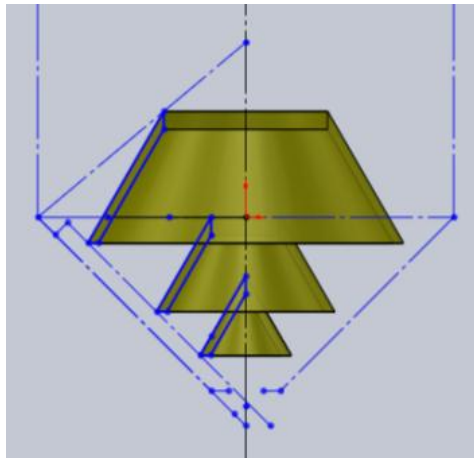
*b.*



*c.*



*d.*



*e.*



*f.*

**Figure 5.6** *Truncated Cones Inserts*

A total of eight inserts were studied incorporating different combinations of the parameters described above. However, none of them achieved mass flow in the model silo, even though, in some cases the channel width expanded considerably but still without movement of the material at the wall.

### **5.3 Open Double Cones – The Proposal of a Novel Type of Static Insert**

After all the failed attempts described above to produce an insert that was capable of changing the flow pattern, what became pretty clear was how simple and powerful inverted cones were when used as static inserts. However, inverted cones are not by any means perfect and there are problems commonly associated with their use such as preferential discharge through one side of the silo, possible rat-hole formation underneath the insert, low efficiency in silos with low vertical sections, among others. Nonetheless, the author decided to pursue the design of a new type of static insert using features from inverted cones and applying lessons learnt from the test work undertaken with the inserts described in section 5.2. A fact that became evident from the test work undertaken with the truncated cones and concentric cylinder inserts was that in order to prevent the formation of a preferential draw channel, the path directly above the hopper outlet needs to be restricted somehow. When there was no restriction above the outlet (e.g. truncated cones) a narrow preferential draw channel formed right at the start of the discharge, whereas when a small inverted

cone was added to the insert the discharge channel expanded considerably, improving slightly the flow pattern.

Taking this into account the author decided to employ a different method to restrict the flow above the outlet. Instead of placing a physical barrier (like an inverted cone) to deviate the flow of material, the restriction would be provided by slowing down the velocity of the solids in that region using an internal hopper, in other words a cone in cone insert, as those presented in sections 2.4 and 2.5. Then, looking to improve the influence from the insert near the wall of the silo, a truncated cone section (A in Figure 5.7a) would be added to the top of the internal hopper section (B in Figure 5.7a), this would provide support to the material near the wall modifying further the stress conditions in that area, hopefully facilitating flow. The insert would be completed by joining the lower edge of the truncated cone section to the outlet of the internal hopper, as shown by wall C in Figure 5.7b.

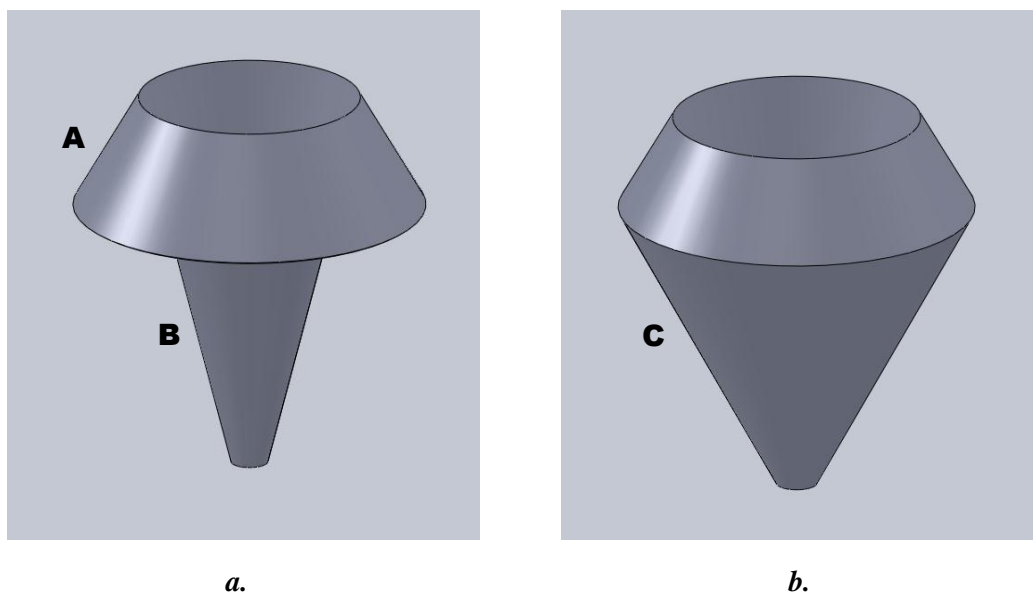


*Figure 5.7 Open Double Cone Concept*

Even though the concept of the insert was pretty clear, its morphology presented the author with multiple challenges before proposing a design method. Before getting to that point, many aspects needed to be defined such as: overall size, positioning in the hopper, angles of each of the component walls, size of the insert inlet and size of the insert outlet. It was decided to start with the design of the internal hopper where the only clear aspect was that it needed to support mass flow in its interior, avoiding the

development of stagnant regions of material. Although the design of a internal mass flow hopper would be fairly straightforward following Jenike's method, additional features also had to be defined as before, i.e. positioning in the silo, outlet size and inlet size. Therefore it was decided to make use of the existing design methods for cone in cone inserts proposed by Johanson and by Enstad et al, which were explained in section 2.5.

### **5.3.1 Evaluation of Cone in Cone Inserts**

To decide which design method would be used for the internal hopper of the insert, two inserts were designed applying the procedures recommended by Enstad and Johanson as explained in section 2.5. The main differences between the two methods are the position of the insert within the silo hopper and relationship between the size of the insert outlet and the size of the hopper outlet. Figure 5.8 illustrates the application of both design methods to the bench scale silo using the 30° half angle hopper.

The critical half angle for mass flow was calculated both for the insert walls and the silo walls. For the insert, the maximum angle from the vertical to support mass flow was determined as 18° whereas the maximum angle for the hopper walls was 20° (it needs to be remembered that the hopper and inserts were made of different materials). From this it was decided that both inserts would have a half angle of 15° from the vertical, which would support mass flow in the interior of the inserts and also complies with the criterion for the angle between the insert wall and the hopper wall. As it can be seen in Figure 5.8 both methods require the angle between the insert wall and the hopper wall to be less than the critical angle for mass flow, which is fulfilled when using the 30° half angle hopper.

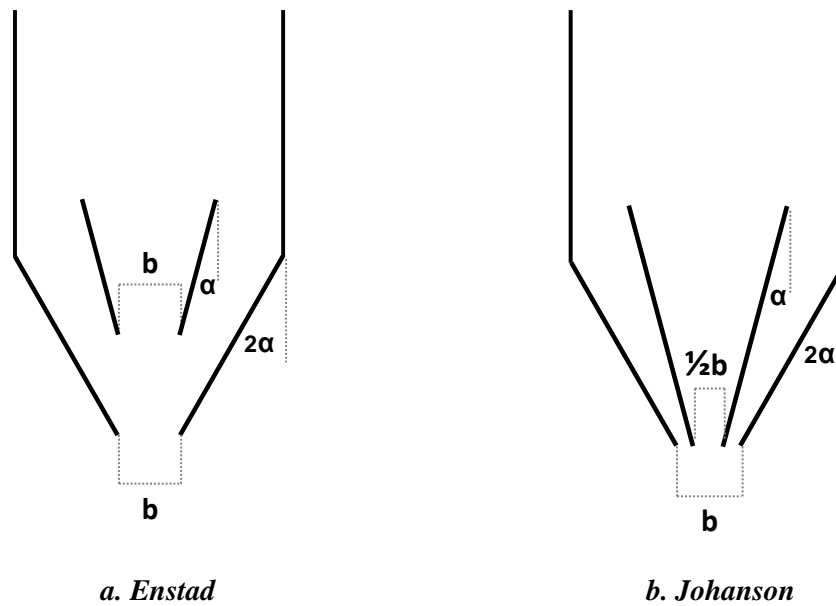


**Figure 5.8** *Cone in Cone Design for the Bench Scale Silo*

In the case of Enstad’s method, the outlet of the insert was the same as the outlet of the hopper and the insert was positioned at a height where the area of the insert outlet was equal to 1/10 of the cross sectional area of the hopper. The design of the insert was completed by extending the walls of the insert past the transition of the bin until the diameter of the insert inlet was equal to half the diameter of the vertical section of the silo. This was done according to a recommendation made by Dr Gisle Enstad [Enstad, 2008], where he advised the insert to be extended past the transition of the bin, but the concise point to extend to was not clarified. Please note that this piece of work was undertaken before the author found a second recommendation advising on the size of the insert inlet. That recommendation is included in [Wójcik, 2008], which advises the insert outlet to have an area equal to 50% of the cross sectional area of the vertical section.

When applying the method proposed by Johanson, the outlet of the insert was reduced to half the diameter of the hopper and the insert was positioned with its outlet on the same plane as the hopper outlet. As the design procedure deduced from Johanson’s does not make reference to the position or size of the insert inlet (as mentioned in section 2.5), it was decided to extend the insert to the same upper position of Enstad’s insert, which produced an insert with an inlet diameter close to

60% of the diameter of the vertical section of the silo. As shown in Figure 5.9, by comparison this method produced much taller insert with a smaller diameter outlet.

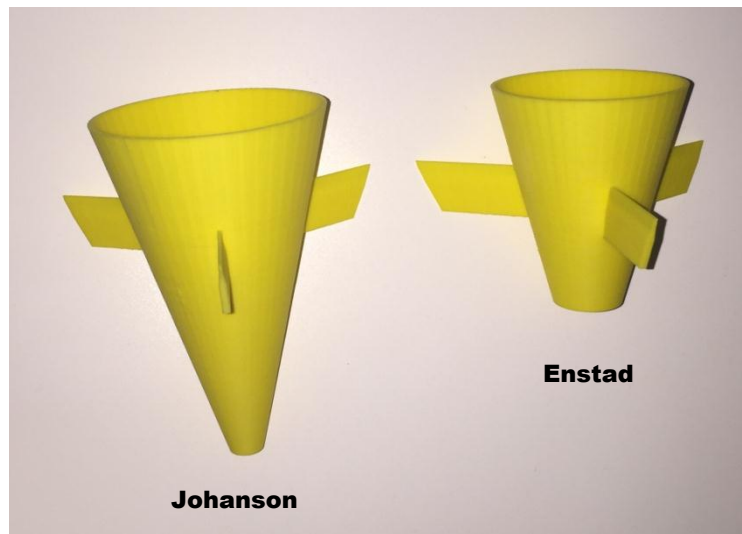


*Figure 5.9 Cone in Cone Inserts Tested*

Both inserts were then evaluated using the bench scale silo. When the insert designed with Enstad's method was installed and the silo was allowed to discharge, the upper surface of the material remained constant as the solids were observed to slip at the wall in a short section at the top of the silo. However, in the rest of the silo the material in contact with the wall remained static. This indicates that the insert widened the flow channel until it reached the wall in the upper part of the bin, producing a mixed flow pattern. Shortly after the start of the discharge, the movement at the wall stopped and the upper surface began to change forming a central funnel (as shown in Figure 5.10a). The upper material cascaded into the central channel while the regions near the wall remained stagnant. This behaviour continued until the top of the insert was exposed, where it could be seen how most of the material flowed through the inside of the insert, although some material was also observed flowing along the external wall of the insert. Once all the material directly above the insert had been discharged, the movement of material between the insert and the silo walls was more evident and always flowing faster near the walls of the insert. Throughout the multiple repetitions, the channel widening did not always reach the walls of the silo. In some cases, the upper surface of the powder bed was observed to form a central funnel straight after the discharge started, without any

movement of material at the wall being detected (see Figure 5.10b). After this, the discharge continued in the same fashion as the tests described above.

It is the opinion of the author that by having the outlet of the insert the same size of the outlet of the silo, a channel forms between the two outlets restricting the draw of material from the sides, favouring the movement of material through the cone insert. This would be similar to the way a dynamic tube works as it was explained in section 2.4. However, as the flow of material from the hopper was unrestricted, it is possible that the outlet of the hopper could support a higher flow rate of material than the outlet of the insert, if mass flow developed inside the insert. This could explain the additional material that was observed discharging simultaneously around the external wall of the insert.

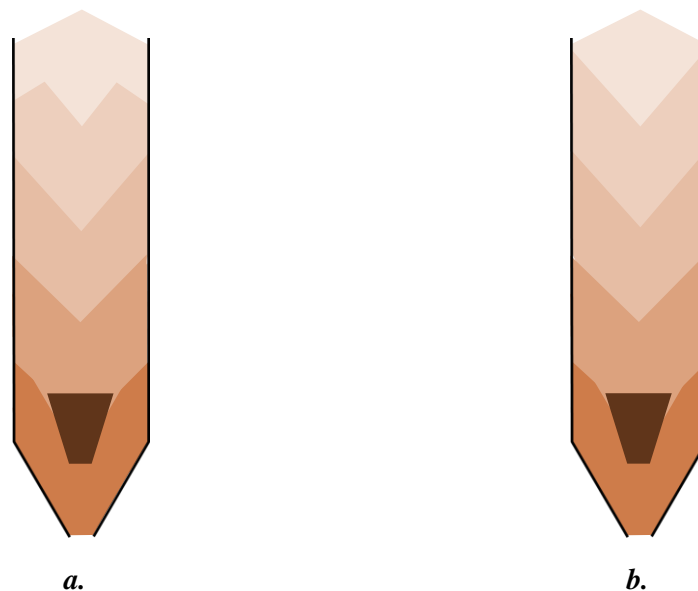


**Figure 5.10** *Observed Discharge Patterns with Enstad's Insert*

The discharge behaviour of the solids changed dramatically when the insert designed using Johanson's method was installed. As illustrated in Figure 5.11 the upper surface of the powder bed retained its shape during discharge until the top level was approaching the region near the top of the insert. This is the first indication that mass flow was achieved in the silo. However, the most conclusive evidence of mass flow was the fact that material was observed to move along the walls of the silo both in the vertical and convergent sections during discharge. When the upper level of material was close to the region where the insert was located, the shape of the

powder bed surface began to change forming a steeper pile. This was caused by material flowing faster in the outer regions of the bin. Shortly after this, the powder in contact with the wall of the converging hopper seemed to stop moving (including material above the transition of the bin), nonetheless, the overall flow of material was faster through the annulus formed between the insert and the hopper wall than inside the cone insert, with the highest velocity observed near the external wall of the insert. As a result the level of solids outside the insert went down faster than inside and after all the material around the insert had been discharged, there was still powder flowing from the insert.

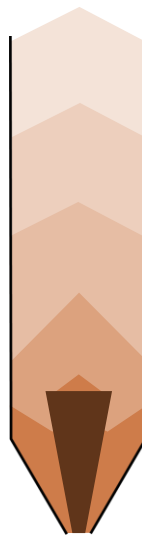


**Figure 5.11** *Observed Discharge Pattern with Johanson's Insert*

The difference in performance between the two inserts was obvious from the results obtained through the test work presented above. Johanson's insert produced a higher level of influence over the contents of the silo, changing the flow pattern from core flow to mass flow. In the case of Enstad's insert, the discharge pattern was modified from core flow to mixed flow, although the results were not always consistent. From this, it is evident that the method proposed by Johanson produced a more effective flow promoting insert, therefore the author decided to use that method as a guide for the design of the inside section of the open double cone insert.

### 5.3.2 Open Double Cone Insert: First Generation

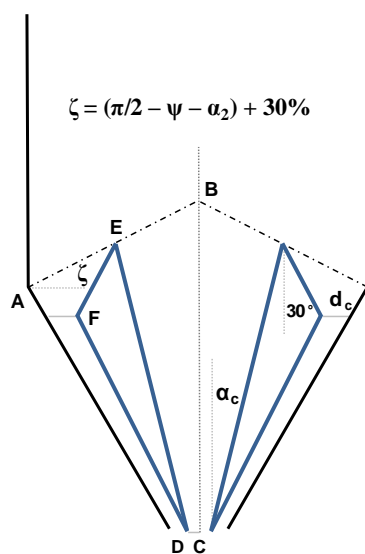
By using Johanson's method for the design the internal hopper of the inserts, outlet size and position of the insert is fixed, as well as the half angle of the convergent section. However, the extension of the insert or its inlet size still need to be defined as the design method is not explicit in that matter. For this reason and for the fact that the internal hopper would join a truncated cone at the top, it was decided to use the modified method for the design of inverted cones (presented in sections 4.1 and 4.2) to help fix the upper position and shape of the insert. The insert would be completed by extending the truncated cone downwards, until the gap between its edge and the silo wall equals the critical arching dimension of the powder.

The following procedure and Figure 5.12 illustrate the design technique for the novel open double cone insert.

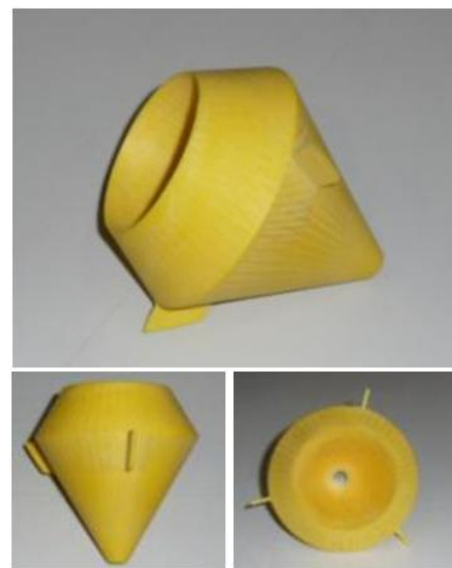
- a. Select  $30^\circ$  as the half angle ( $\alpha_2$ ) of the insert.
- b. Obtain the values of the effective angle of internal friction ( $\delta$ ) of the bulk solid and the wall friction angle ( $\phi$ ) between the bulk solid and the material of the hopper wall. These properties can be obtained through the use of a powder shear test.
- c. Calculate the arching diameter ( $d_c$ ) and critical half angle ( $\alpha_c$ ) for mass flow using Jenike's standard silo design technique for conical hoppers [Arnold, 1979].
- d. Obtain the value for the angle  $\psi$  from Figure 2.25.
- e. Make a scale drawing of the existing silo.
- f. Check the outlet of the bin is at least twice the critical arching diameter of the material, if not, the outlet will need to be enlarged.

- g. Draw a line from the transition of the silo at an angle  $(\pi/2 - \psi - \alpha_2) + 30\%$  from the horizontal until it intersects the central axis of the hopper (line AB in Figure 5.12).
- h. From the centre of the bin outlet, draw the horizontal line CD of length equal to half the critical arching diameter for conical hoppers.
- i. Draw the line DE. Starting from D, draw a line at an angle from the vertical smaller or equal to the critical half angle for conical hoppers, until it intersects the line AB.
- j. Draw the line EF. Starting from E, draw a line at  $30^\circ$  from the vertical until the horizontal gap between the line and the wall of the hopper, equals the arching dimension for conical hoppers.
- k. Draw the line FD. The cross section of the insert will be given by the triangle DEF.

Figure 5.12b shows an open double cone made to work with the  $30^\circ$  half angle model hopper.



a.



b.

**Figure 5.12** *First Generation Open Double Cone Design Procedure*

There are a couple of points worth elaborating on from the above procedure. First it can be noticed that to obtain the intersection point between the internal mass flow hopper and the surrounding truncated cone, a 30% increment has been made on the angle recommended by Johanson's method. From the experimental work presented in section 4.2 for inverted cones with the bench model, the 30% increment produced the best results in terms of discharge consistency, although the results were not massively different from the insert designed using a 20% increment (which was later used for the scale up to the semi-industrial test rig). For the first attempt to design the open double cone insert, it was decided to take a conservative approach to obtain the maximum influence from the insert on the converging section of the bin. For this reason, the 30% increment was chosen even if that could produce a larger insert than was necessary. The second aspect where also a conservative approach was taken was the gap between the edge of the insert and the silo wall. By choosing the size of the gap as the critical arching dimension for mass flow, the edge of the insert is as close to the wall as it is safe to avoid flow issues but the size of the insert is consequently enlarged. This tight gap also minimizes the angle between the external wall of the insert and the silo wall, which in turn reduces the compressive stresses of the flowing material facilitating flow.

One of the disadvantages of this type of inserts; is that the outlet of the bin has to be larger than the arching dimension of the material (twice, as proposed in the design method). However, hypothetically it would be the same even if the hopper was very shallow (i.e.  $45^\circ$ ). This becomes an advantage when compared with cone in cone inserts, as two or three of them have to be used for these types of hoppers and therefore the outlet of the bin would have to be three or four times the arching dimension.

Due to the conservative approach explained above, an additional disadvantage of the use of this type of insert is the amount of space it takes up inside the bin, reducing the total capacity. This becomes more evident when the converging section of the silo is shallower, as can be seen with the insert designed for the  $45^\circ$  half angle model hopper in Figure 5.13. In this case, the volume displaced by the insert is approximately 80% of the volume of the converging section of the silo but the

amount of volume taken up by the insert is a function of the silo geometry, frictional properties of the materials of construction, surface finish and flow characteristics of the material.

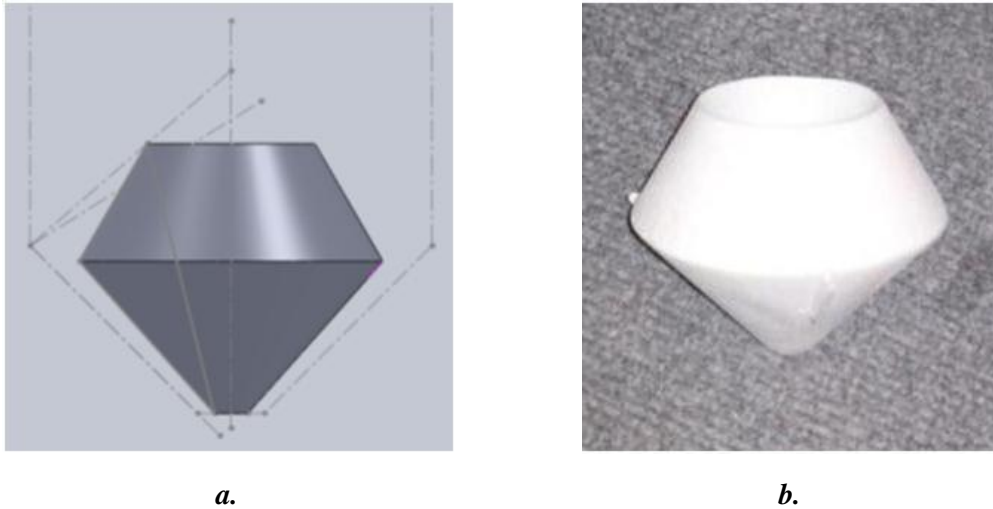


**Figure 5.13** *Open Double Cone for 45° Model Hopper*

The inserts were tested for both model hoppers with 30° and 45° convergences respectively and the results were very similar in both cases. After the discharge started, movement of the material in contact with the wall was observed both in the vertical section and in the converging hopper. The upper surface of the material descended without changing its profile and sliding at the wall all the way to the surface of the insert (as illustrated in Figure 5.14). The material moving around the insert seemed to move faster than the powder in the internal hopper of the insert, but the difference was not as noticeable as with the cone in cone insert where the profile of the upper surface changed to a steep pile due to the differences in velocity. Also, while with the cone in cone insert the powder was observed to stop moving at the wall when the inventory in the silo was low, this was not observed with the open double cone where the material continue to move at the wall even when the level had reached the surface of the insert. At the end of the discharge a small amount of material was still discharging from the internal hopper after all the material on the external side of the insert had discharged. The discharge behaviour was very similar between the 30° and 45° hoppers, the main difference was that the discharge rate in the annulus between the hopper wall and the outer circumference of the insert appeared to be slightly higher for the 30° hopper.

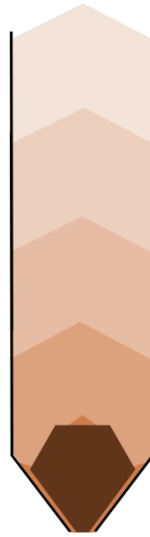


*Figure 5.14 Observed Discharge Pattern*

### **5.3.3 Open Double Cone Insert: Second Generation**

The original design method was created with the idea of achieving mass flow at any cost. The insert was designed to be as large as possible and to get as close as possible to the walls of the bin without causing cohesive arching over the annular gap. Taking this into account, the second generation of the insert targets areas where the original insert could have been oversized and produces a smaller insert, which could reduce manufacturing costs, running costs (as the reduction of the storage capacity of the silo would be smaller) and would facilitate its installation. The features targeted by the design method to achieve the reduction in size are the safety factor for the top of the insert and the gap between the silo walls and the external wall of the insert. The procedure below explains the steps for the design of the second generation insert including the changes to the original method.

- a. Select  $30^\circ$  as the half angle ( $\alpha_2$ ) of the insert.
- b. Obtain the values of the effective angle of internal friction ( $\delta$ ) of the bulk solid and the wall friction angle ( $\varphi$ ) between the bulk solid and the material of the hopper wall. These properties can be obtained through the use of a powder shear test.

- c. Calculate the arching diameter ( $d_c$ ) and critical half angle ( $\alpha_c$ ) for mass flow using Jenike's standard silo design technique for conical hoppers [Arnold, 1979].
- d. Obtain the value for the angle  $\psi$  from Figure 2.25.
- e. Make a scale drawing of the existing silo.
- f. Check the outlet of the bin is at least twice the critical arching diameter of the material, if not, the outlet will need to be enlarged to this value.
- g. Draw a line from the transition of the silo at an angle  $(\pi/2 - \psi - \alpha_c) + 20\%$  from the horizontal until it intersects the central axis of the hopper (line AB in Figure 5.12).
- h. From the centre of the bin outlet, draw the horizontal line CD of length equal to half the critical arching diameter for conical hoppers.
- i. Draw the line DE. Starting from D, draw a line at an angle from the vertical smaller or equal to the critical half angle for conical hoppers, until it intersects the line AB.
- j. Draw the line EF. Starting from E, draw a line at  $30^\circ$  from the vertical until it intersects the transition of the bin.
- k. Draw the line FD. The cross section of the insert will be given by the triangle DEF.

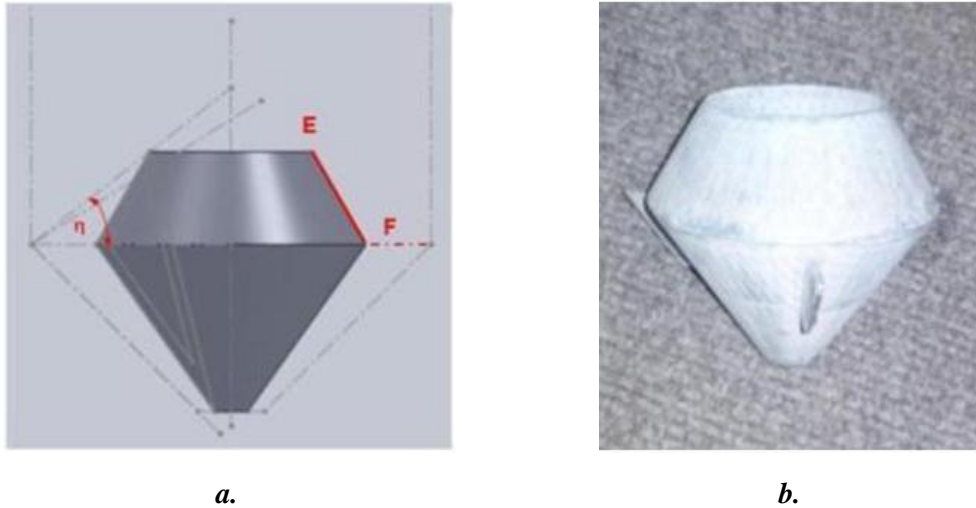


**Figure 5.15** *Second Generation Open Double Cone for 45° Model Hopper*

In the previous section it was discussed that for the particular system of the bench scale model, the volume of the insert was equivalent to 80% of the volume of the converging section of the silo. This was a result of the conservative design approach. By undertaking the modifications proposed in the second generation method, the new insert for the same system (shown in Figure 5.15) displaces only 55% of the volume of the hopper.

The first modification to the original method reduces the safety factor of the angle  $\zeta$  from 30% to 20%, this makes the insert slightly shorter than its predecessor which in turn reduces the diameter of the inlet of the internal mass flow hopper. This is important because by reducing the inlet size, the proportion of material flowing within the insert with respect to the material flowing around it also reduces. The second modification changes the length of the truncated cone section of the insert which, increases the annular gap between the external insert wall and the silo wall. The increment of that gap changes the angle of inclination of the lower external wall of the insert, increasing the angle of convergence between the silo wall and the lower external wall of the insert.

The second generation inserts were tested using the 30° and 45° model hoppers, and the results were very similar to those obtained with the first generation inserts. The material in contact with wall was observed to slip on the cylindrical walls as well as on the walls of the conical hoppers, indicating that the inserts changed the flow

pattern from core flow to mass flow. With respect to the upper surface profile (as shown in Figure 5.16), the results again replicate the behaviour observed with the previous generation, where there was no change in the profile until the upper surface was in the proximity of the top of the insert. After the top of the insert was exposed the material again seemed to move faster around the insert than inside it. However, compared to the first generation, the difference in velocities seemed to be less and the amount of material to be discharged last from the inside of the insert was also smaller.



*Figure 5.16 Observed Discharge Pattern*

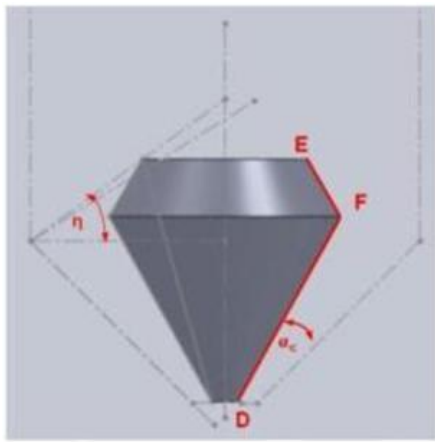
#### **5.3.4 Open Double Cone Insert: Third Generation**

With the third generation, a further reduction in the size of the insert was sought, and further modifications of the original method were made to achieve this. As with the second generation, the first point to tackle was the safety margin for the angle  $\zeta$ . In the original method, the angle  $\zeta$  was increased by 30%, in the second generation the increment was brought down to 20% and for the third generation, an increase of just 10% is proposed. As previously discussed this reduction also decreases the size of the insert inlet which theoretically modifies the ratio between the material flowing around the insert and inside it.

So far, the shape of the lower external part of the insert has been just a consequence of fixing the internal and upper external parts, and the position of the point F has been relative to the geometry of the bin and fixed in a rather arbitrary way. For the third generation, the external shape of the insert is governed by the lower converging wall rather than the truncated cone as is the case for the other two generations. This is done by fixing the angle of the external insert wall in such a manner that the resulting convergence between the silo wall and the insert is capable of sustaining mass flow. The detailed procedure for the design of the third generation of open double cone inserts is described below.

- a. Select  $30^\circ$  as the half angle ( $\alpha_2$ ) of the insert.
- b. Obtain the values of the effective angle of internal friction ( $\delta$ ) of the bulk solid and the wall friction angle ( $\phi$ ) between the bulk solid and the material of the hopper wall. These properties can be obtained through the use of a powder shear test.
- c. Calculate the arching diameter ( $d_c$ ) and critical half angle ( $\alpha_c$ ) for mass flow using Jenike's standard silo design technique for conical hoppers [Arnold, 1979].
- d. Obtain the value for the angle  $\psi$  from Figure 2.25.
- e. Make a scale drawing of the existing silo.
- f. Check the outlet of the bin is at least twice the critical arching diameter of the material, if not, the outlet will need to be enlarged to this value.
- g. Draw a line from the transition of the silo at an angle  $(\pi/2 - \psi - \alpha_2) + 10\%$  from the horizontal until it intersects the central axis of the hopper.
- h. From the centre of the bin outlet, draw the horizontal line CD of length equal to half the critical arching diameter for conical hoppers.

- i. Draw the line DE. Starting from D, draw a line at an angle from the vertical smaller or equal to the critical half angle for conical hoppers, until it intersects the line AB.
- j. Draw a line starting from point E, at  $30^\circ$  from the vertical. Simultaneously, draw a line from point D to form an angle with the wall of the hopper, equal or smaller than the critical half angle for mass flow. The place where these two lines intersect locates point F.
- k. The cross section of the insert will be given by the triangle DEF.



a.



b.

**Figure 5.17** *Third Generation Open Double Cone for 45° Model Hopper*

For the silo model system with the  $45^\circ$  hopper, it had previously been established that a first generation insert would occupy a volume equivalent to 80% of the volume of the converging hopper. The modifications applied for the second generation reduced the size to a volume equivalent to 55% of the hopper and in the case of the third generation, the volume displaced by the insert (shown in Figure 5.17) was only 25% of the hopper volume. This improvement is important particularly for systems where the impact on the capacity of the silo needs to be minimised.

For the practical evaluation of the insert, it needs to be noted that only the insert for the  $45^\circ$  hopper was built. This was due to the fact that the critical half angle for mass flow was more than half the half angle of the hopper, which means that if the

procedure was to be followed a cone in cone insert would be produced instead. As with the previous generations, the insert also caused movement of the material at the walls in the silo achieving mass flow and the surface profile also remained unchanged until the proximity to the insert as shown in Figure 5.18. However, once the insert was exposed there was no velocity difference between the material flowing externally and internally with respect to the insert.



*Figure 5.18 Observed Discharge Pattern*

### **Disclaimer**

After all the development and experimental work on open double cone inserts had been completed and the author was compiling the information on static inserts for the literature review of this thesis, the mention of an insert with a similar profile was found in [Hartl, 2008]. There, an insert with the label of open double cone is shown as part of a group described as non-displacing inserts (see Figure 5.19) but there is no further comment about that particular insert and the original reference is not explicit either. However, the fact that the insert is described as non-displacing it means that it is made of just an external shell that could be completely filled with material and that would not have an internal mass flow hopper, like the insert described in this thesis. This is confirmed by the arrows indicating the direction of flow inside the insert, which diverge from the inlet of the insert indicating that the only internal wall is the same shell that forms the external shape of the insert. Another difference with the insert proposed in this thesis is the position of the insert in the hopper; the insert in

Figure 5.19 is shown high in the silo with the outlet of the insert at a different level than the outlet of the silo. The insert proposed in this thesis has the outlet on the same plane as the outlet of the silo.

After contacting J. Hartl to find information about the original document describing the insert, *Silo-Handbuch* by P. Martens and H. Franken [Martens, 1988] was identified as the original reference. However, in that book only a sketch similar to the figure in Hartl's work (Figure 5.19) was found. It presents the insert as part of a group described as non-displacing inserts, without any additional information as in Hartl's work. The only difference is that in Marten's book the insert is referred to as double cone while Hartl refers to it as open double cone.

The author declares that the development of the insert presented in this thesis and the name given to it (open double cone) have no relation with either of the two references discussed above.

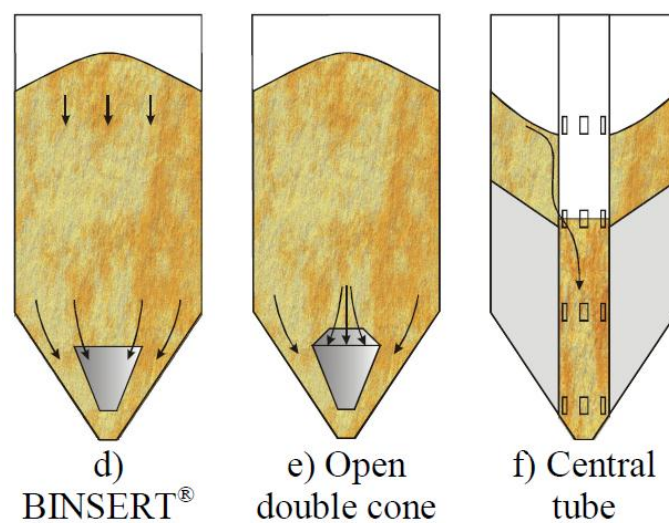


*Figure 5.19 Non-Displacing Inserts [Hartl, 2008]*

#### 5.4 Double Cone Inserts

In the same way the open double cone was designed to overcome some of the problems associated with the use of inverted cones, the use of double cones was studied as an alternative in cases where limited benefits could be expected from an

open double cone or an inverted cone. Highly cohesive materials (i.e. high moisture granular coal) present good examples where inverted cones or open double cones might not be the best retrofit option. This type of material is commonly prone to forming rat-holes when discharging from core flow bins, which would constitute a major problem if an inverted cone was installed, as the formation of a rat-hole underneath the insert could cause the blockage of the bin. The problem of using open double cones with highly cohesive material lies in the size of the bin outlet that would have to be used. The minimum outlet size that needs to be used with this type of material is in most cases large, and the requirement for an outlet double the minimum size could be impractical because the discharge rate could be extremely high, or the cost of the feeding equipment could become excessive.

The main advantage of a double cone when compared to an open double cone is that it does not require the silo to have an outlet larger than the critical arching of the material. However, depending on the relative size between the both inserts, the double cone could displace a larger volume in the hopper reducing its capacity due to its solid profile. When compared to an inverted cone, the double cone eliminates the void area under the insert which is one of the reasons for the velocity gradient between the insert and the silo wall as explained in Chapter 4. In addition to this, providing that the diameter of double cone insert is larger than the minimum dimension to prevent rat-holing, a rat-hole should not form in the silo, while with inverted cones a rat-hole developing under the insert is a risk that needs to be considered.

In order to study the performance of double cone inserts, the author decided to propose two design procedures based on the combination of the main features of the methods presented for the design of open double cones and inverted cones. Both design procedures are introduced in the following sections.

#### **5.4.1 Double Cone Inserts: First Generation**

The first generation takes advantage of the modified design method for inverted cones presented in section 4.2. An inverted cone is produced by following that

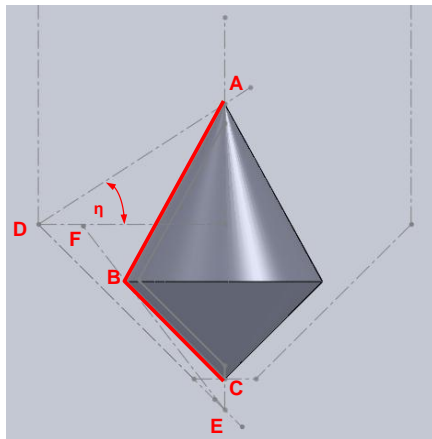
method and then the insert is completed by building the second cone between the edge of the upper cone and the centre of the outlet of the silo. The complete procedure for the design of the insert is presented below.

- a. Select  $30^\circ$  as the half angle ( $\alpha_2$ ) of the insert.
- b. Obtain the values of the effective angle of internal friction ( $\delta$ ) of the bulk solid and the wall friction angle ( $\phi$ ) between the bulk solid and the material of the hopper wall. These properties can be obtained through the use of a powder shear test.
- c. Once the flow properties are known, the values for the critical W/R ratio and angle  $\psi$  can be obtained from Figure 2.24 and Figure 2.25 respectively.
- d. Make a scale drawing of the existing silo.
- e. Draw a line from the transition of the silo at an angle  $(\pi/2 - \psi - \alpha_2) + 20\%$  from the horizontal until it intersects the central axis of the hopper (see Figure 5.20), line DA). This intersection (point A) represents the apex of the upper cone.
- f. Draw a line from the apex of the hopper at angle  $\eta$  from the vertical, such as:

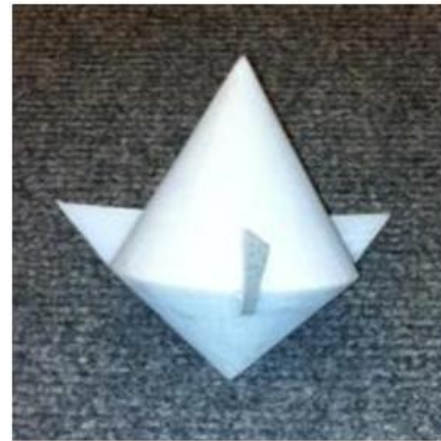
$$\tan\eta = \frac{\tan\alpha_1}{1 + W/R} \quad (5-1)$$

This line represents the critical ratio W/R (see Figure 2.26, line EF).

- g. Draw a line from the apex of the inverted cone at an angle  $\alpha_2$  from the vertical, until it intersects the critical W/R line (see Figure 5.20, line AB). The intersection point (point B) represents the transition from the upper to the lower cone of the insert.
- h. Draw a line from B to the centre of the outlet of the bin (point C). Point C locates the apex of the lower cone.



a.



b.

**Figure 5.20** *First Generation Double Cone for 45° Model Hopper*

As mentioned before, one of the main issues of inverted cones and the first generation in particular is the volume occupied by the insert as it can be seen in Figure 5.20. For this particular case, the insert displaces a volume equivalent to 50% of the volume of the conical hopper.

A feature worth analysis from the first generation double cone insert is the angle formed between the wall of the hopper and the wall of the lower cone of the insert. As it can be observed from the procedure, this angle is not specified and instead is a consequence of the relationship between the outlet of the silo and the gap of the inverted cone and the wall of the silo. The interesting aspect of this feature is that depending on the silo geometry and material characteristics that angle could be positive (converging towards the outlet), zero (width of the annulus remains constant) or negative (diverging towards the outlet). Therefore, it is important to understand that the resulting angle will have an impact on the performance of the insert as the behaviour of the material in the lower part of the hopper could vary considerably. If the angle diverges in the direction of the outlet, the material will have less constraint towards the axis of the bin facilitating flow in that region, as a result, the velocity of the material near the wall of the insert will be higher than the velocity of the material near the wall of the hopper. This is a similar phenomenon to that which occurs with inverted cones. However, if the angle converges in the direction of the outlet the difference in velocities should be reduced and the behaviour of the material should be closer to that flowing in a true mass flow hopper.

Two first generation double cone inserts were tested with the 30° and 45° model hoppers respectively. In both cases the material was observed to move at the walls of the bin, indicating that mass flow was achieved. After the discharge started, the upper surface of the powder bed descended without changing its profile until it was close to the upper apex of the insert. At that point, a funnel started forming creating a zone of high velocity in the centre of the bin (as shown in Figure 5.21) but the material at the wall continued to move. The funnel then changed shape into an annulus as the material flowed around the insert until all material was discharged.

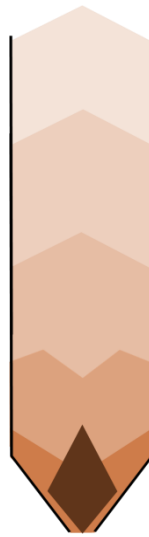
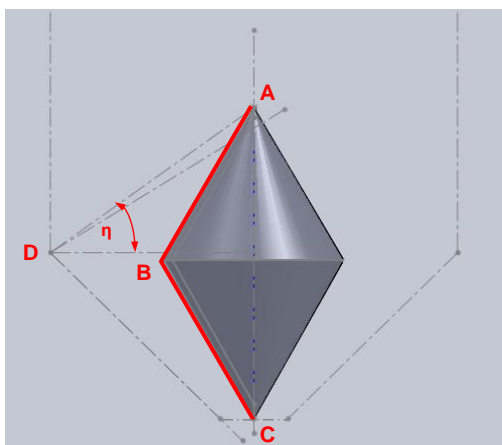


*Figure 5.21 Observed Discharge Pattern*

#### **5.4.2 Double Cone Inserts: Second Generation**

As discussed in the previous section, the shape of the lower cone of the insert was just the consequence of joining the edge of the upper inverted cone with a point at the centre of the outlet of bin. Therefore the influence of the lower cone on the flow pattern would not be targeted by design and instead it would depend on the geometry of the silo and characteristics of the material. For the second generation of double cones, a method that designed the lower cone of the insert was sought to ensure a convergence towards the outlet to minimize the velocity gradients across the bin. For this purpose, the lower cone is designed keeping the angle with the wall of the silo smaller than critical half angle for mass flow, in a similar way to open double cone and cone in cone inserts. The design procedure for the second generation of double cones is presented below.

- a. Select  $30^\circ$  as the half angle ( $\alpha_2$ ) of the insert.
- b. Obtain the values of the effective angle of internal friction ( $\delta$ ) of the bulk solid and the wall friction angle ( $\phi$ ) between the bulk solid and the material of the hopper wall. These properties can be obtained through the use of a powder shear test.
- c. Obtain the value for the angle  $\psi$  from Figure 2.25.
- d. Make a scale drawing of the existing silo.
- e. Draw a line from the transition of the silo at an angle  $(\pi/2 - \psi - \alpha_2) + 20\%$  from the horizontal until it intersects the central axis of the hopper (see Figure 5.22), line DA). This intersection (point A) represents the apex of the upper cone.
- f. Draw a line from the apex of the inverted cone (point A) at an angle  $\alpha_2$  from the vertical. Simultaneously, draw a line from point C (located at the centre of the hopper outlet) to form an angle, with the wall of the hopper, smaller than the critical half angle for mass flow. The place where these two lines intersect locates point B.



a.



b.

**Figure 5.22** *Second Generation Double Cone for 45° Model Hopper*

As it can be seen in step f, the angle between the wall of the silo and the wall of the lower cone should be less than the critical half angle for mass flow and not equal to it. In the case of the open double cone, that angle was allowed to be equal to the critical half angle because the insert and the hopper converge towards the same apex and this means the radial stress theory could be applied. In the case of the double cone, the apex of the insert and the apex of the bin do not coincide and strictly speaking the solutions to the radial stress field should not be applied. In any case the author has assumed that the critical half angle calculated from Jenike's method could still be applied by applying a safety factor to reduce the maximum value of the angle to be used. It is worth remembering that it is common practice when designing mass flow hoppers to apply a safety factor to the calculated critical half angle reducing it by 3°, therefore it is suggested that a further reduction of the same order is made for the angle between the insert and the hopper.

By targeting the design of the shape of the two cones that make up the insert, both the velocity gradients created and the volume occupied by the insert are reduced with respect to the first generation. For the particular case of the 45° model hopper, the size of the insert was reduced to a volume equivalent to 33% of the volume of the hopper. For the practical tests, inserts were evaluated for both model hoppers with results very similar to those obtained for the first generation. Mass flow was achieved during discharge as indicated by the material moving at the walls of the bin and by the shape of the powder bed surface which descended unchanged until it started approaching the region close to the apex of the insert (as shown in Figure 5.23).

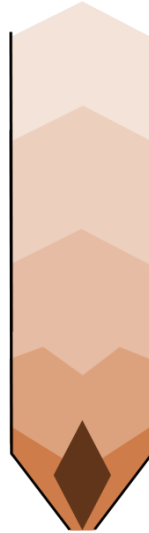


*Figure 5.23 Observed Discharge Pattern*

### **5.5 Performance Comparison at Bench Scale**

From the sections above it is clear that all the inserts tested changed the pattern in the model silo achieving mass flow, even though the conclusions have been drawn just from the visual observations of the discharge behaviour of the material. The material has been seen moving at the walls of the silo and the upper surface of the material has been observed to descend uniformly, which are typical characteristics of mass flow behaviour. In some cases, there has been some indication of differences between the performances of some of the inserts, for example when comparing the three generations of open double cones. There it was observed that the third generation did not have much material still discharging through the insert when all the material around it had been discharged, on the other hand, with the first generation the amount of powder still discharging from the insert at the end was considerably more. All these observations provide important data for the evaluation of the inserts but make any comparison rather subjective and subtle differences are likely to be missed. For this reason, the test rig was equipped with an impact plate to detect instantaneous variations on flow rate and also with gain in weight system to quantify the discharge rate from the model.

The data below presents the results obtained when the 45° model hopper was used, for tests carried out without any insert, with a modified inverted cone, with an open

double cone from each generation and with a double cone from each generation. Figure 5.24a to Figure 5.30a present the gain in weight of the receiving vessel during the tests and Figure 5.24b to Figure 5.30b show the signal from the impact plate illustrating the stability of the discharge rate.

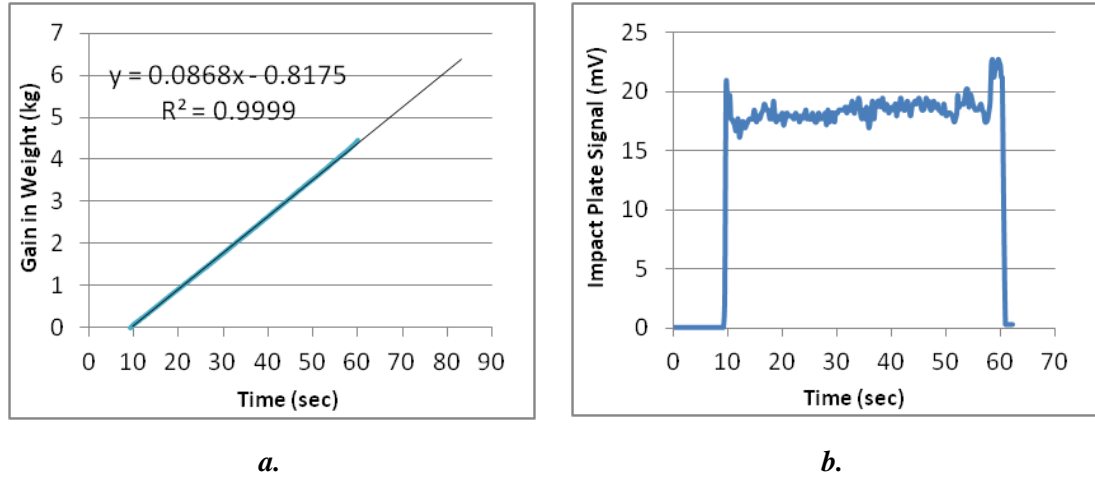


**Figure 5.24** *No Insert Results*

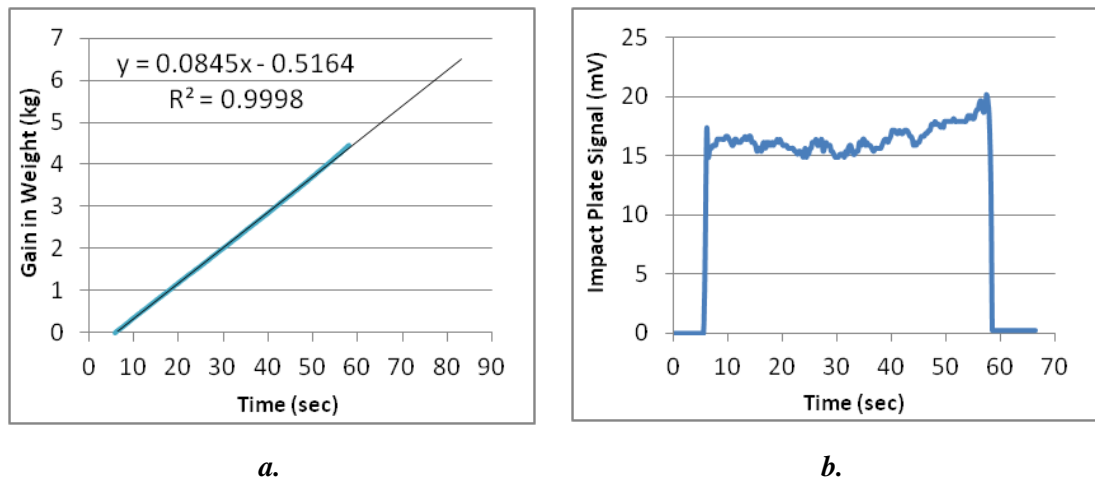
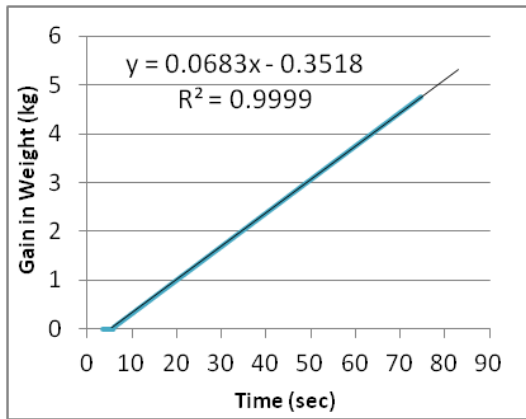
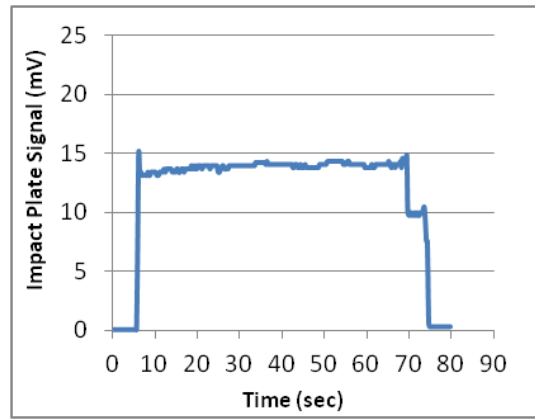


**Figure 5.25** *Modified Inverted Cone Results*

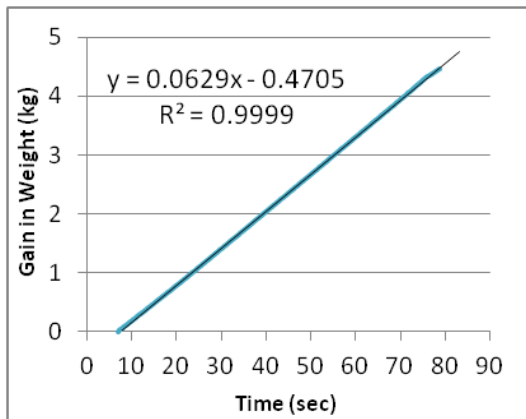


a.

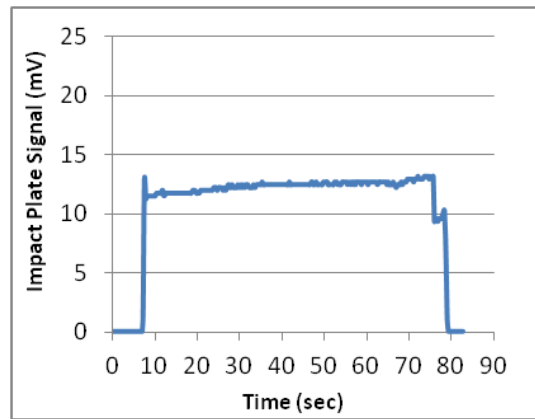


b.

**Figure 5.26** *Open Double Cone First Generation Results*

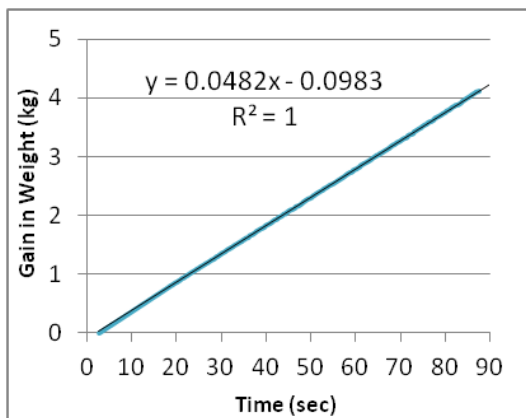


a.

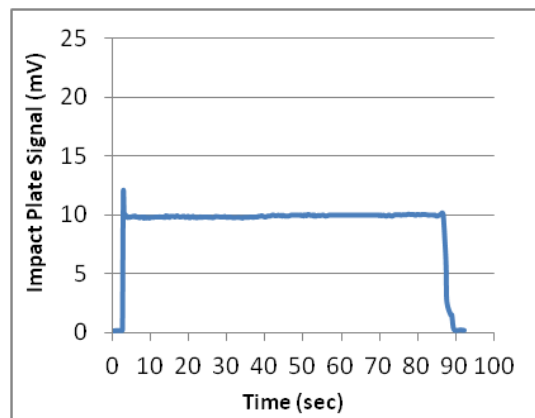


b.

**Figure 5.27** *Open Double Cone Second Generation Results*

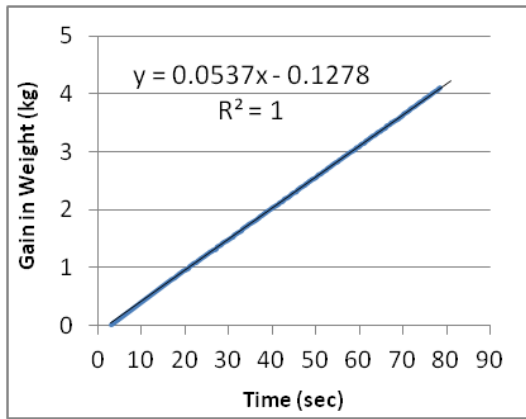


a.

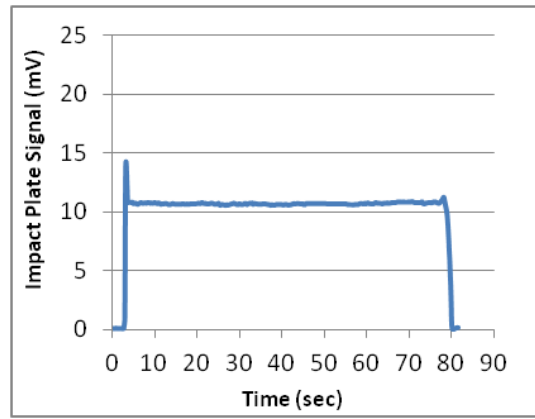


b.

**Figure 5.28** *Open Double Cone Third Generation Results*

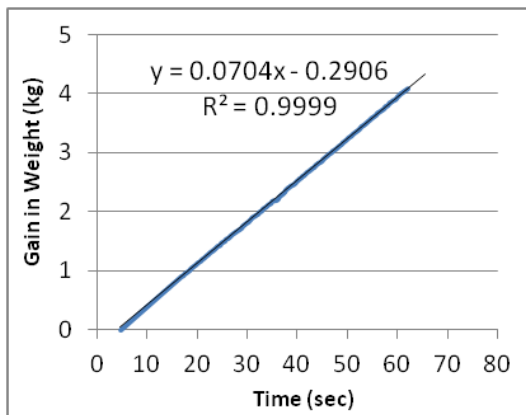


a.

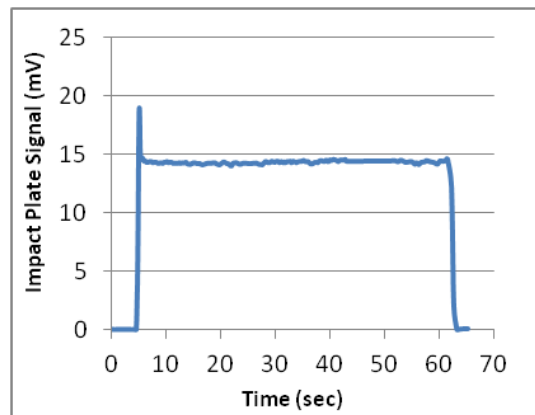


b.

**Figure 5.29 Double Cone First Generation Results**



a.



b.

**Figure 5.30 Double Cone Second Generation Results**

A linear regression has been applied to the data from Figure 5.24a to Figure 5.30a and the resulting equations are shown within each figure. From the slopes of the fitted lines, the average discharge rate in each case can be inferred and the results are presented in Table 5-1.

**Table 5-1 Average Discharge Rate from the Silo with and without Insert**

	No Insert	Inverted Cone	Open Double Cone 1 <sup>st</sup> Gen.	Open Double Cone 2 <sup>nd</sup> Gen.	Open Double Cone 3 <sup>rd</sup> Gen.	Double Cone 1 <sup>st</sup> Gen.	Double Cone 2 <sup>nd</sup> Gen.
Average Flow Rate (g/s)	86.8	84.5	68.3	62.9	48.2	53.7	70.4

Generally speaking, when comparing the flow rate from two silos with similar characteristics (particularly outlet size) and handling the same powder but where one of them discharges in core flow and the other in mass flow, it is expected that a higher flow rate would be obtained from the silo where core flow was developed. The main cause of this difference is that in a mass flow silo, the failure point where the powder bed expands to produce flow is very close to the outlet and the material does not have much space to accelerate before being discharged. By contrast, in a core flow silo, the failure point occurs within the flow channel relatively far from the outlet, allowing the particles to accelerate and reach higher velocities. The faster movement of the particles then translates into higher discharge rates.

For the reasons mentioned above it is not surprising that the highest flow rate was obtained when there was no insert fitted with the silo discharging in core flow. By contrast, when mass flow was achieved by fitting an insert, the discharged rates were up to 45% lower; in the case of the open double cone third generation. An interesting finding is that even though the hopper fitted with an inverted cone was observed to develop mass flow, its discharge rate value is very close to that of the hopper without inserts. The reason for this is that when the inverted cone is fitted the powder above it moves following a mass flow pattern and the failure of the material and expansion of the bed occurs in the annulus around the insert. The area of the annulus at the base of the insert is larger overall than the outlet of the silo but the flow rate is ultimately limited by the outlet of the silo. With the other types of inserts, the granular material moves as a compacted bed until a point near the outlet of the hopper where the failure occurs. At this point, the particles start separating from each other and accelerating towards the outlet. The acceleration, and therefore the speed of the particles, is controlled by the amount of air that permeates and fills the empty gaps in the bed, ultimately limiting the discharge rate.

The comparison of the instantaneous discharge rate plots also show similarities between the core flow hopper and the hopper with the inverted cone. These similarities also set them apart from the behaviour of the silo with the other inserts, suggesting two distinctive discharge mechanisms as it can be seen in Figure 5.31. Both discharge rates without an insert and with the inverted cone are fairly erratic and noisy, whereas the signal obtained using an open double cone and a double cone

depict a very steady instantaneous discharge rate. That difference could also suggest that under the inverted cone the pattern is then reverted to core flow, as that is the area where the flow rate is ultimately controlled.

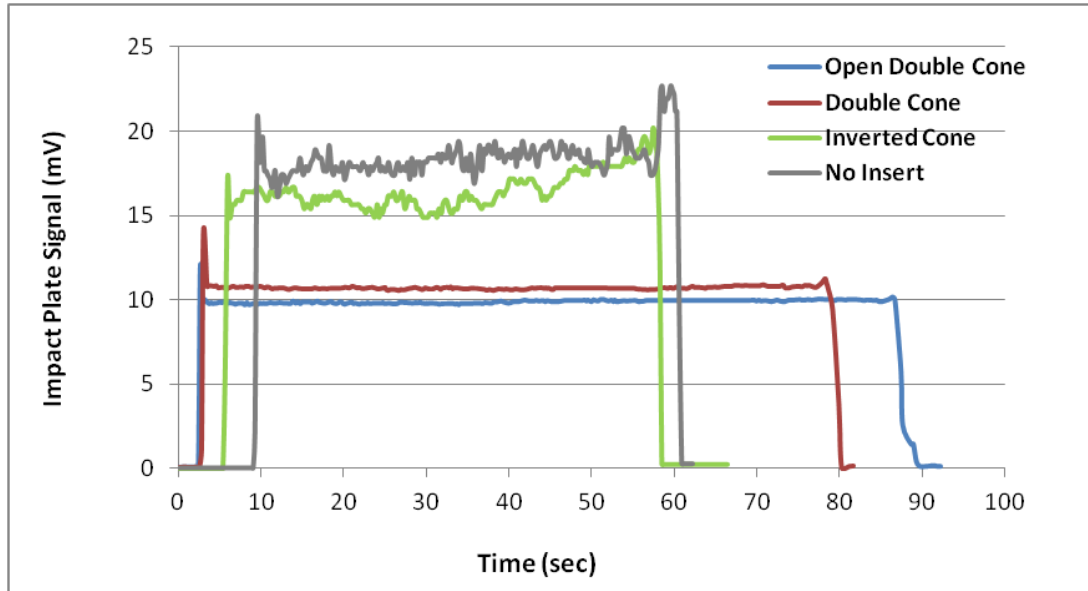


**Figure 5.31 Comparison Between the Types of Inserts**

Figure 5.32 presents a comparison of the impact plate signal from the three generations of open double cones. This figure coupled with the average flow rate data from Table 5-1, will help quantify the differences in performance between the three generations of inserts. The first aspect that suggests a difference in performance between the inserts is the average discharge rate obtained with each of them. From Table 5-1 it can be seen that the discharge rates were 68.3 g/s, 62.9 g/s and 48.2 g/s for the first, second and third generations respectively. Also, in Figure 5.32 it can be seen that the overall discharge time decreased from the first to the second generation and then from the second to the third (similar amounts of material were used during the tests). The main difference between the inserts was the design of the external wall which produced flow regions with different profiles between the insert and the silo walls. In any silo, the most critical section which will have a direct impact on flow pattern and flow rate, lies in the convergence that reduces the area perpendicular to flow from the vertical section to the outlet of the hopper. When comparing the shape of the three inserts (Figure 5.33) it can be seen that the first generation has the largest inverted cone section which also gets very close to the wall of the silo, which is

important because most of the convergence of the flow channel, is achieved by this section. While in a conical hopper the walls represent a restriction to flow as they converge in two directions, the inverted cone section of the insert promotes flow by diverging in one direction as it converges in the other. This relieves some of the stress acting on the particles facilitating flow. In the region below the inverted cone section, the convergence continues but at a more gradual rate with a very small angle between the silo and the insert.

For the second generation, the extension of the inverted cone section is reduced therefore reducing the converging region where part of the minor principal stress is relieved. As a result, more of the convergence needs to be achieved by the lower section of the insert with higher compressing stresses than in the same region of the first generation. The resulting combination of a smaller inverted cone section with a larger converging angle between the silo walls and the lower part of the insert, impose a higher restriction to flow reducing the flow rate. This effect continues with the insert of the third generation where there is a further reduction of the inverted cone section, therefore increasing the angle of convergence in the lower region between the insert and the silo walls. As most of the convergence of the flow channel is achieved without stress relief, this insert produced the lowest values of discharge rate. Another aspect linked to the explanation given above, is the consistency of the instantaneous discharge rate. As it can be seen from Figure 5.32 the difference between the signals is not only the magnitude but also the stability, with the insert from the third generation producing the most consistent signal from the impact plate. The larger converging angle towards the outlet keeps the particles together with larger stresses allowing less expansion of the bed and producing a point of failure closer to the outlet, maintaining more uniform stress conditions to the point of release.

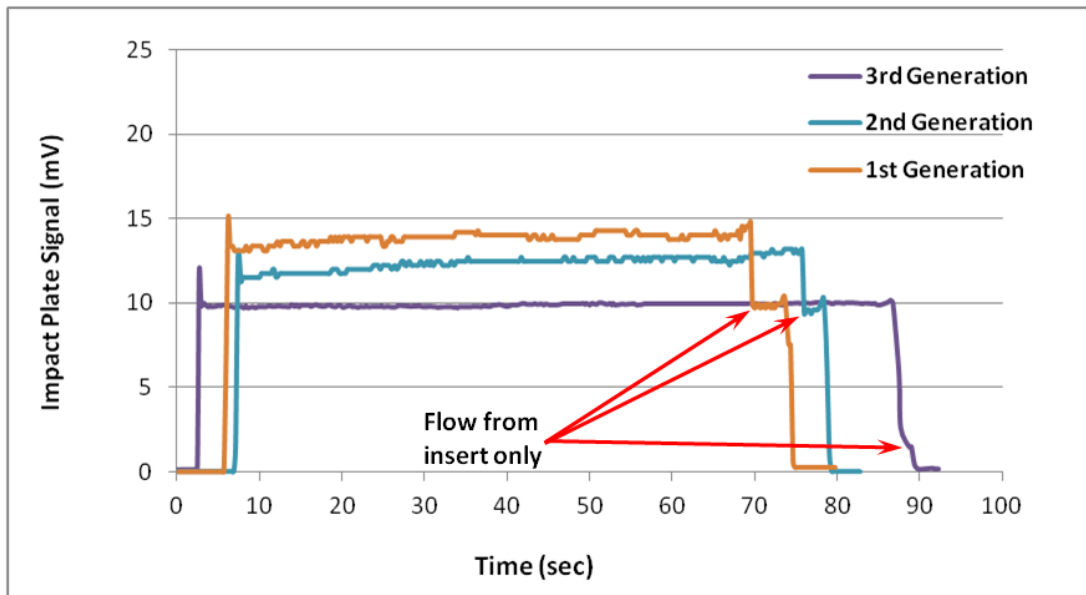


**Figure 5.32** Comparison Between Open Double Cone Generations

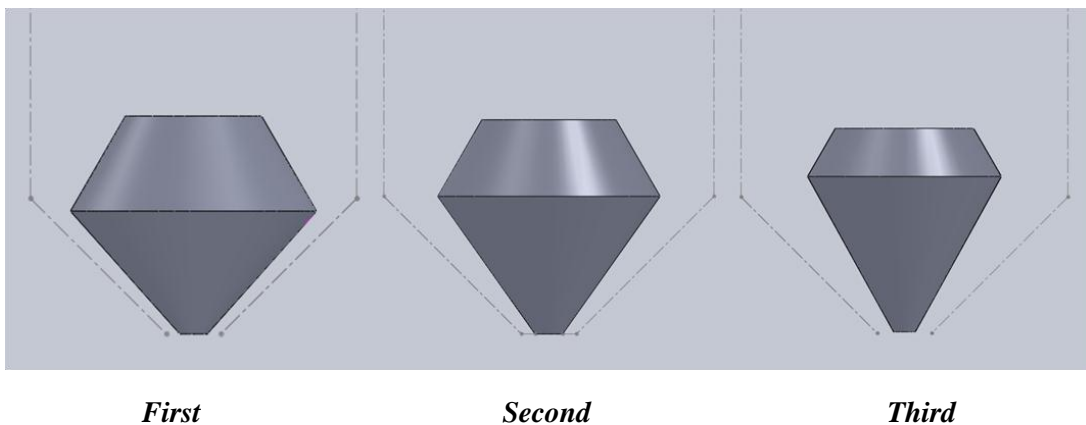


**Figure 5.33** Open Double Cone Generations

A difference observed during the tests was the amount of material still discharging from the inside of the insert when the surrounding material had all been discharged from the silo. That amount was largest for the first generation insert and almost non-existent for the third generation, with the second generation somewhere in between, this is corroborated by the data from the impact plate as shown in Figure 5.32, where for the first and second generations significant step change in the output signal is observed towards the end of the discharge. At that point the annulus between the insert and the silo wall was empty and the material was only being discharged from the internal hopper of the insert. It can be seen that the duration of the signal at the

lower value lasts longer for the first generation insert than for the second, suggesting that there was more material left in the hopper of the first generation insert. In the case of the third generation, a very small change can be seen at the end of discharge that indicates a very small amount of material still discharging from the insert, but as observed during the tests both regions finished discharging almost at the same time.

Taking into account all the results obtained, the third generation of open double cones offer the best solution as a flow promoting insert because it produced mass flow effectively, occupied the least amount of volume inside the hopper, produced the most consistent discharge rate and seemed to produce the most uniform velocity distribution across the different flow regions of the silo.

During the discharge tests with double cone inserts, both generations were observed to produce very similar results with no noticeable differences in the behaviour of the material in the silo. However, the signal obtained from the impact plate and the average discharge rates obtained from the gain in weight system show a significant difference. As with the results obtained for the open double cone inserts, it was expected that the second generation double cone would produce a lower discharge rate than the first generation insert. However, as it can be seen from Figure 5.34 and Table 5-1 the results are completely the opposite with the second generation insert producing a discharge rate considerably higher than the first generation. It is difficult to try to explain this difference without contradicting the analysis made for the open double inserts. However, the low flow rate obtained with the first generation double cone could be explained based on the small area available for flow at the edge of the inverted cone section. As it can be seen in Figure 5.35, the inverted cone section of the first generation double cone gets very close to the wall of the hopper and compared to the first generation open double cone, that gap is of a similar dimension. However, the edge of the double cone is significantly lower in the hopper which means that the area of the annulus formed between the insert and the silo is considerably smaller than in the case of the open double cone. In addition to this, with the double cone all of the material of the silo needs to flow through that gap whereas with the open double cone just part of the contents of the silo flow through the reduced area as the rest of the material flows through the internal hopper of the insert. In the end it is possible that the flow rate through the region around the open

double cone and the double cone could be fairly similar in magnitude but in the case of the open double cone the additional stream from the interior of the insert would increase the overall flow rate.

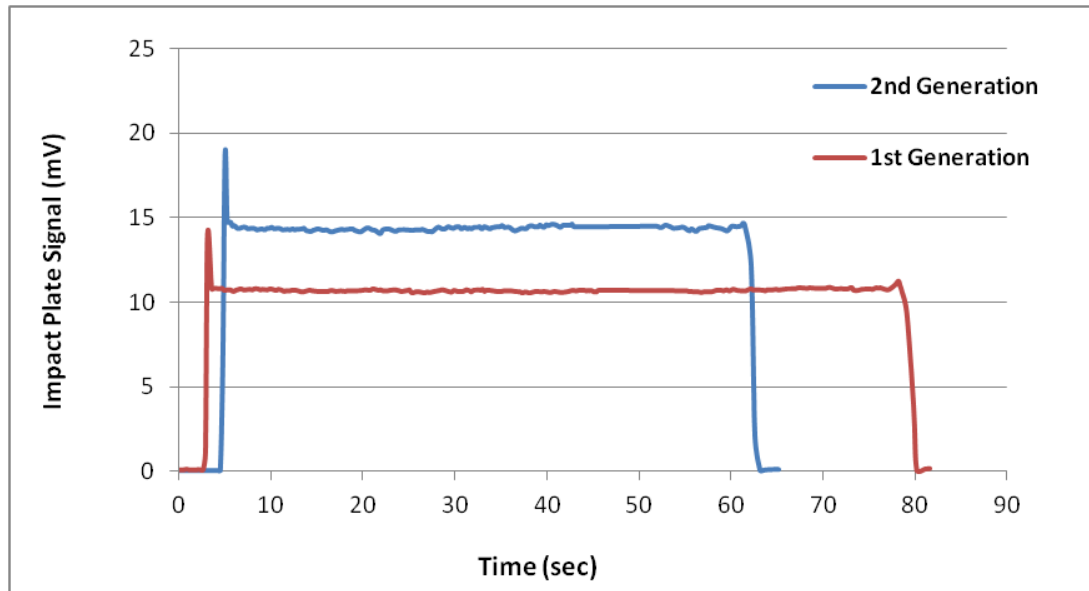
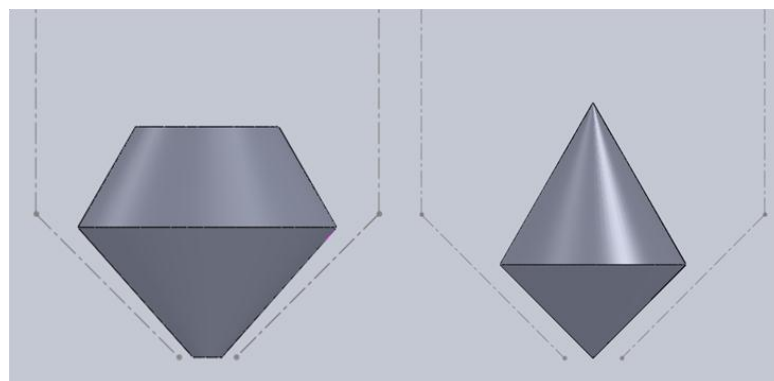


**Figure 5.34 Comparison Between Double Cone Generations**



**First Generation Open Double Cone**

**First Generation Double Cone**

**Figure 5.35 Insert Shape Comparison**

Before finishing this section it is worth having a look at a common characteristic found in all the plots of the impact plate signal presented above. At the start of the discharge, the signal shows a peak indicating a maximum value of the instantaneous discharge rate. This is explained from the fact that before the discharge has started the direction of the major principal stress is predominantly vertical and the material

above the outlet rests on the plate of the slide valve. When the valve is open, the material above has little restriction to flow and falls out of the hopper, this causes the change of direction of the major principal stress lines which become predominantly horizontal restricting movement and limiting the flow rate. The initial peak is therefore a measurement of the first amount of material coming from the silo before the change of direction of the stresses. It is worth noting that not in every repetition of the tests a clear peak was obtained in the data, this however is believed to be a consequence of the maximum sampling rate of the data acquisition instrumentation. The maximum sampling rate was of the order of 5 samples per second and in most of the plots the peak consisted of only one data point, which suggests that information from the peak is likely to have been missed like in the case where the data showed no initial peak. Therefore, even the in plots where a peak is shown it might not be true representation of the maximum instantaneous flow rate as the maximum signal acquired and the actual maximum value could have been different.

## 5.6 Performance Evaluation of Inserts at Semi-Industrial Scale

### 5.6.1 Test Material

To evaluate the performance of the inserts developed it was decided to use a test material with slightly more cohesive flow characteristics than the sand used in Chapter 4. A detergent powder was chosen as test material based on its flow properties which were measured using a Brookfield Powder Flow Tester. With the flow-ability results obtained from the measurements, the calculations for the design of a conical mass flow silo were undertaken and the results are presented in Table 5-2.

*Table 5-2 Flow Properties of the Detergent Powder Used as Test Material*

Wall Friction Angle for Stainless Steel (Deg)	Internal Friction Angle (Deg)	Bulk Density (kg/m <sup>3</sup> )	Critical Conical Half Angle for Mass Flow (Deg)	Critical Conical Arching Dimension (mm)
27	55	710	15	45

### 5.6.2 Test Rig

To test the inserts at a larger scale, the 0.4 m<sup>3</sup> test rig described in Chapter 4 was used (see Figure 5.36). As mentioned before, the test rig offered the possibility of inferring the discharge pattern developed in the silo by plotting the residence time of numbered markers placed in known positions across the powder bed. The only modification made to the test rig described in Chapter 4 was the size of the outlet which needed to be increased from 50 mm to 100 mm, to be able to accommodate an open double cone insert avoiding the possibility of the formation of a stable cohesive arch.



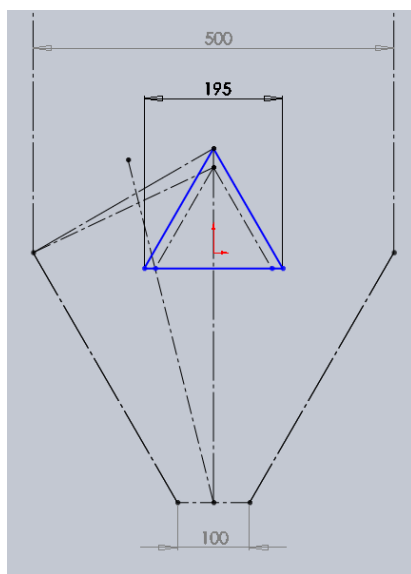
*Figure 5.36 Semi-Industrial Test Rig*

### 5.6.3 Inserts

To undertake the test programme three different inserts were used; one inverted cone, one open double cone and one double cone. Please note that even though evaluating a prototype for each of the generations of open double cones and double cones would have been ideal, the cost of construction would have significantly exceeded the remaining budget allocated to the project.

### 5.6.3.1 Inverted Cone

For the design of the inverted cone it was decided to use the modified method that has been proposed in this project and that was explained in Chapter 4. Figure 5.37a shows the design sketch for the insert following the steps of the modified method, with dimensions in millimetres. As it can be seen in Figure 5.37a the resulting insert would need to be 195 mm in diameter. However, as one of the inserts evaluated in Chapter 4 was 200 mm in diameter (insert shown in Figure 5.37b), it was decided to use that insert for the tests with the detergent powder.



a.



b.

**Figure 5.37** *Inverted Cone Design and Prototype*

### 5.6.3.2 Open Double Cone

As mentioned before, it would have been ideal to test a prototype from each generation of the open double cone, but due to financial reasons only one could be made. From the tests undertaken with the bench scale model, it was clear that the most promising insert was produced following the method for the third generation. That insert occupied the least volume in the hopper but more importantly produced the most consistent discharge rate and seemed to minimize the velocity gradients across the silo. However, because the half angle of the material to obtain mass flow was  $15^\circ$  and the half angle of the conical silo was  $30^\circ$ , if the third generation

procedure was to be followed then a cone in cone insert would be produced instead. For this reason it was decided to design the insert following the second generation procedure which showed the second best performance during the test and also occupies less volume inside the hopper compared with an insert from the first generation. Figure 5.38a shows the design of the insert obtained following the second generation procedure with dimensions in millimetres, please note that the half angle of the internal hopper of the insert was chosen as  $13^\circ$  even though  $15^\circ$  could have been used according to Table 5-2. This reduction of the half angle was made to try to reduce the difference in velocity observed at bench scale between the material flowing through the insert and the material flowing around it. Figure 5.38b shows a photograph of the insert built for the tests.

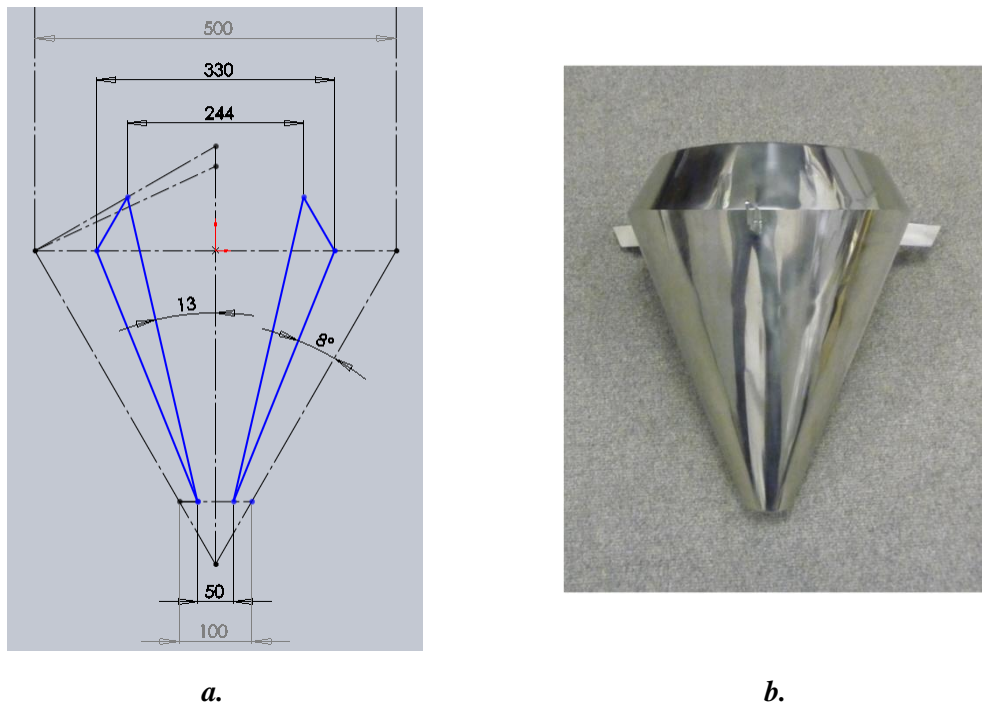


**Figure 5.38** *Open Double Cone Design and Prototype*

### 5.6.3.3 Double Cone

The results of the practical tests with double cones using the bench scale test rig showed that both generations of inserts successfully changed the flow pattern from core flow to mass flow. Visually, there were no noticeable differences between the two generations and in both cases the output signal from the impact plate was very

consistent, illustrating a very stable instantaneous flow rate. The only differences detected were the magnitude of the impact plate signal and the overall discharge rate, which showed the first generation insert to produce a lower flow rate. The trade-off however, was the size of the insert which would reduce considerably the holding capacity of the silo. The second generation would therefore be more practical for industrial applications mainly due to its smaller size which would also reduce fabrication costs and would simplify installation. Based on this and the good performance obtained from the tests it was decided to carry out the scale up of the insert using the design procedure of the second generation of double cones. Figure 5.39a shows the insert design obtained including dimensions in millimetres. Please note that a  $13^\circ$  angle was specified between the wall of the hopper and the lower cone of the insert. This angle is  $2^\circ$  smaller than the recommended angle for mass flow, which was recommended in the procedure to compensate the fact that the insert and the hopper do not share the same apex. Figure 5.39b shows a photograph of the insert built for the tests.

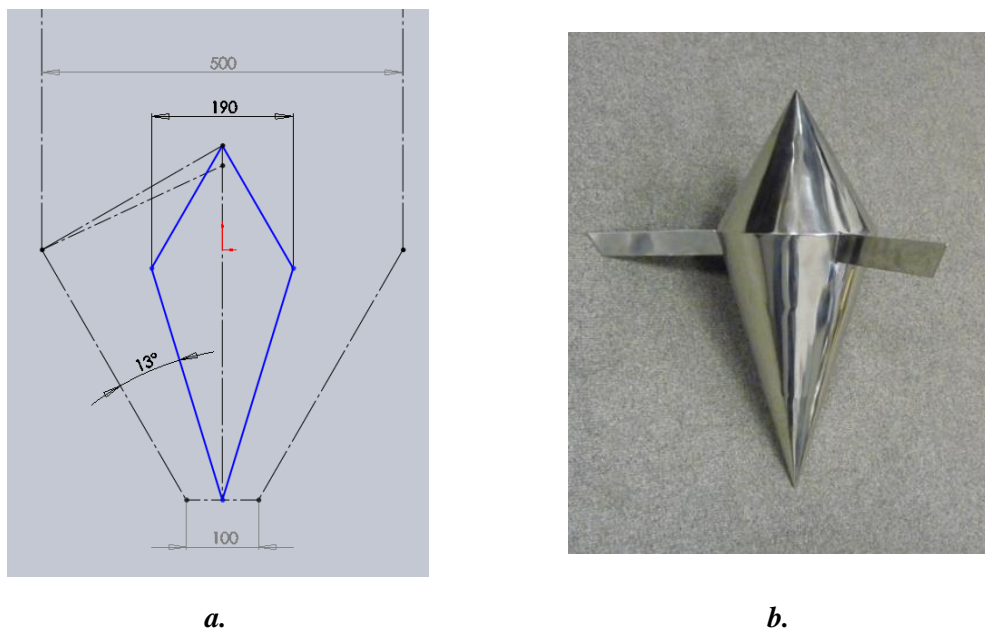


**Figure 5.39** Double Cone Design and Prototype

#### 5.6.4 Test Method

For the experimental tests, the silo was filled with approximately 300 kg of detergent powder and individually numbered markers were positioned within the powder bed following the

template shown in Figure 5.40 and Figure 5.41 (for further explanation of this procedure please refer to section 4.3). When the inverted cone and the double cone were fitted, the apex of the insert protruded past level C, in those cases the central marker for that level was placed just above the apex of the inserts. The silo was then allowed to discharge and the residence time of each marker was recorded. A total of five repetitions were undertaken for each type of insert and also for the silo without an insert fitted.

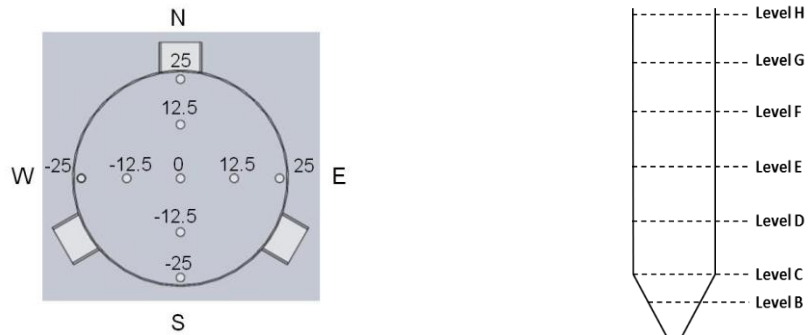
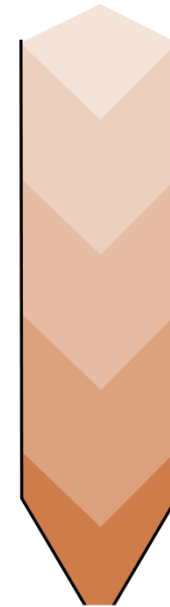
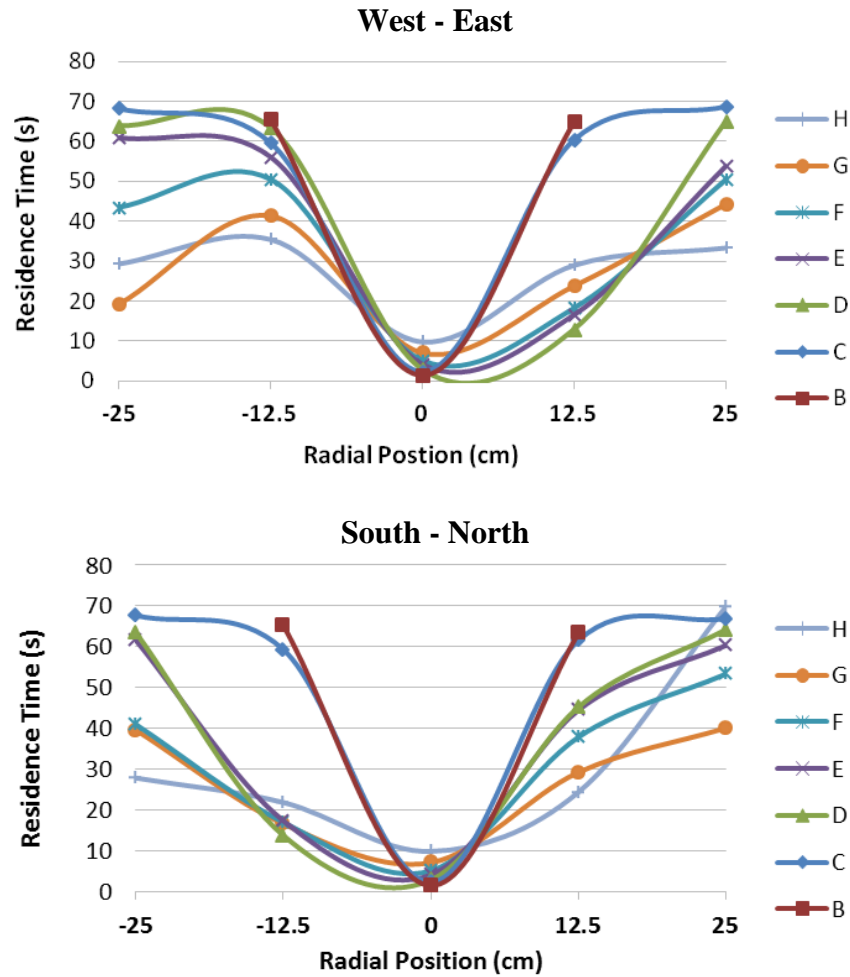
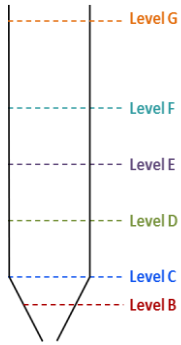


**Figure 5.40** *Horizontal Tracer Location*    **Figure 5.41** *Vertical Tracer Location*

### 5.6.5 Results and Discussion

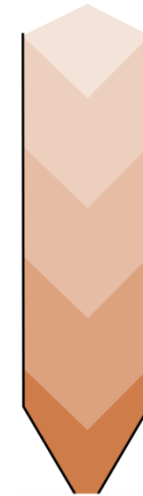
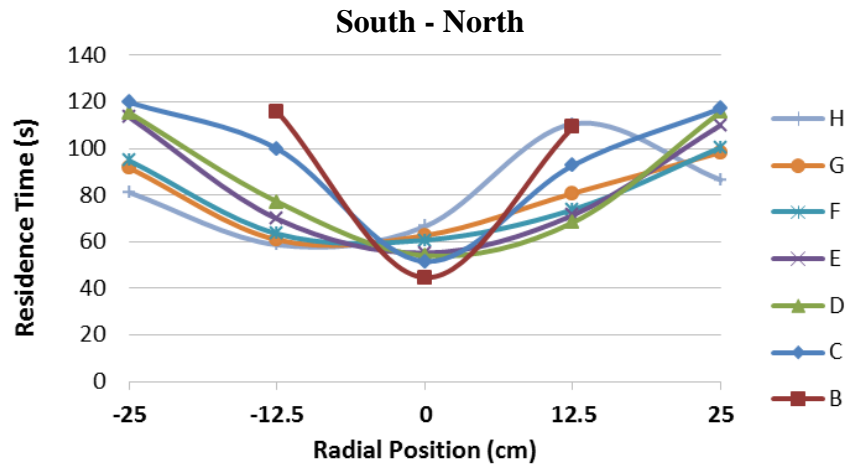
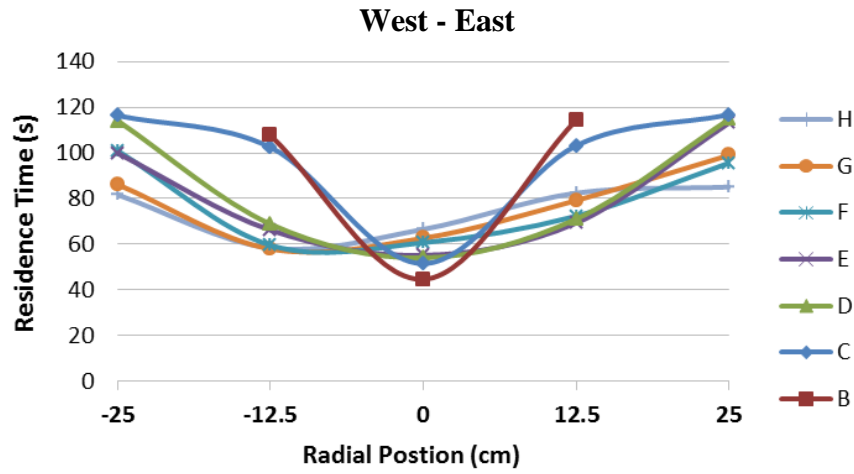
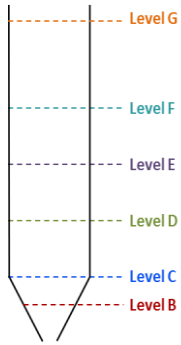
The results obtained from the experimental test are presented in Figure 5.42 to Figure 5.46. The results include the residence times of the markers plotted in lines grouping markers placed at the same vertical level. The figures also include the profile of the upper surface of the powder bed as the inventory of material in the silo diminished during discharge.



a. Tracers Residence Time

b. Surface Profile

Figure 5.42 No Insert - Results



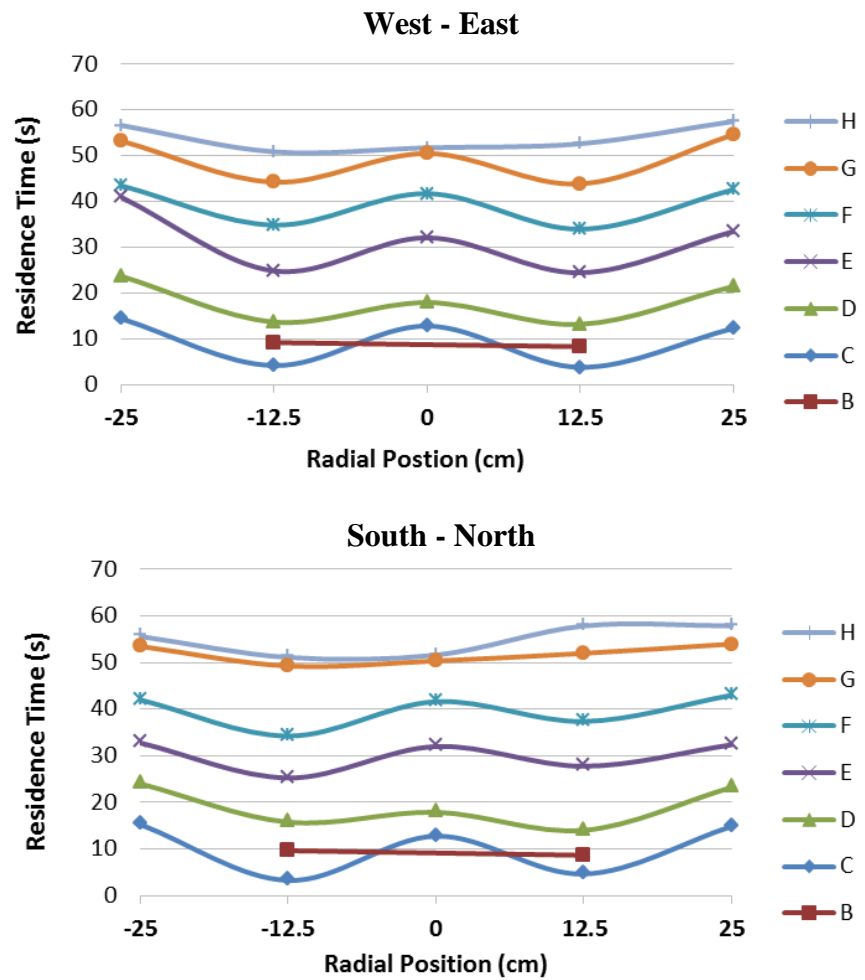
a. Tracers Residence Time

Figure 5.43 No Insert – Results Showing Cohesive Arching

b. Surface Profile

Figure 5.42 illustrates the results obtained from one of the tests when there was no insert fitted in the silo. Interpreting the residence times of the markers it can be seen that most of the material discharged through a channel formed on the central - southeast region of the silo. This can be inferred from the fact that all the markers placed along the axis of the silo had a fairly short residence time with similar results for the markers placed in the intermediate positions of the south and east sides of the silo. It also can be observed how the material near the walls and in the north – west region of the silo cascaded from the top into the discharge channel while the material at the bottom remained stagnant. This is illustrated by the low residence time of the markers located high in the powder bed compared to those located deeper in the silo, which discharged later following a direct relationship between depth and residence time. Finally it can be observed that the last markers to be discharged were those located adjacent to the walls on the transition of the silo and in the converging hopper, showing that the material in those regions remained stagnant until all the rest of the contents had been discharged. Looking at the upper surface during discharge the formation of a slightly off centre funnel was observed straight after the start of flow, with the material near the walls cascading into the neck of the funnel and material slipping along the walls of the silo was never observed.

The analysis above clearly illustrates the development of a core flow pattern during discharge which is characterised by stagnant zones of material and the formation of a flow channel that allowed the discharge of material preferentially from the top of the silo. The core flow behaviour was expected from the flowability measurements of the material which showed that the silo was not steep enough to support mass flow. In all the repetitions the development of core flow was evident, although the form and location of the preferential channel was different almost in every case, which illustrates the inconsistency expected from this type of pattern. However, there was a peculiarity observed in two of the test which is illustrated in Figure 5.43. In these tests, a stable arch formed when the outlet of the silo was opened and there was no flow of material; that is the reason why in Figure 5.43 the residence time of the tracers is much higher than in Figure 5.42. In fact it can be seen that none of the tracers came out of the silo for over 40 seconds after the outlet was open and during that time the arch had to be manually broken to allow the flow of material.



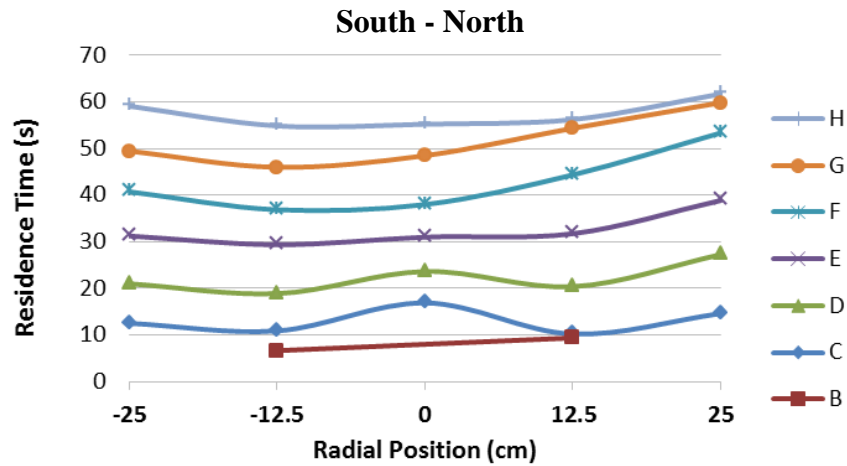
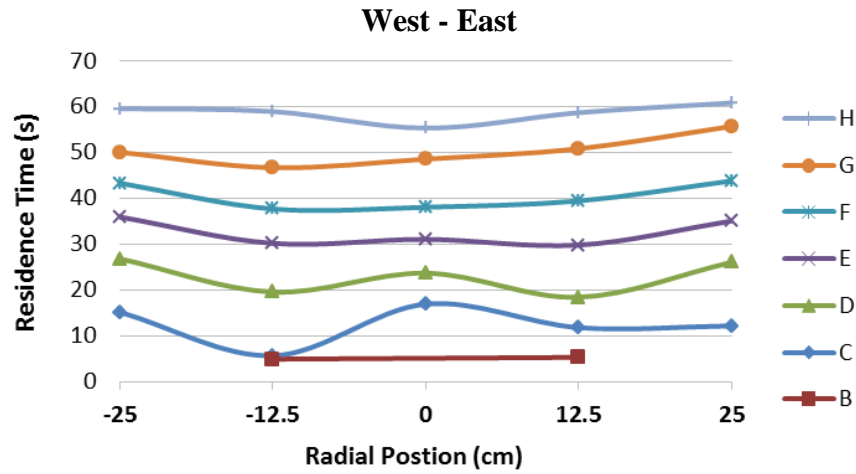
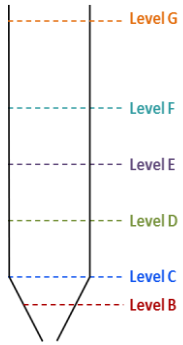
a. Tracers Residence Time

b. Surface Profile

Figure 5.44 Inverted Cone Insert – Results

Figure 5.44 shows the results obtained when the inverted cone insert was fitted in the silo. The inverted cone successfully changed the flow pattern from core flow to mass flow, this can be inferred from the fact that the markers located near the walls and deep in the silo were not the last ones to be discharged. In addition to this and apart from level B, it can be seen that the contents of the silo discharged in a first in first out pattern, developing an inverse relationship between depth and residence time. The only level for which that was not exactly the case was level B which contained the tracers positioned adjacent to the walls of the conical hopper. These tracers came out slightly after the markers placed directly above in the intermediate position of level C. This is consistent with the results obtained with the modified insert in Chapter 4 and supports the theory that even though all the material between the insert and the hopper was in motion, the velocity of the material near the walls of the hopper is lower than the velocity of the material near the walls of the insert. It is also worth noting that the difference in residence time between markers placed at the same level is small, although the velocity of the inserts in the intermediate positions was slightly higher than those near the wall and those along the axis of the silo. This can be explained by the annulus formed between the insert and the hopper that would facilitate the flow of material in that region of the silo.

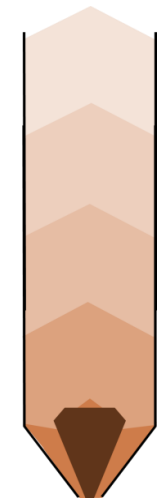
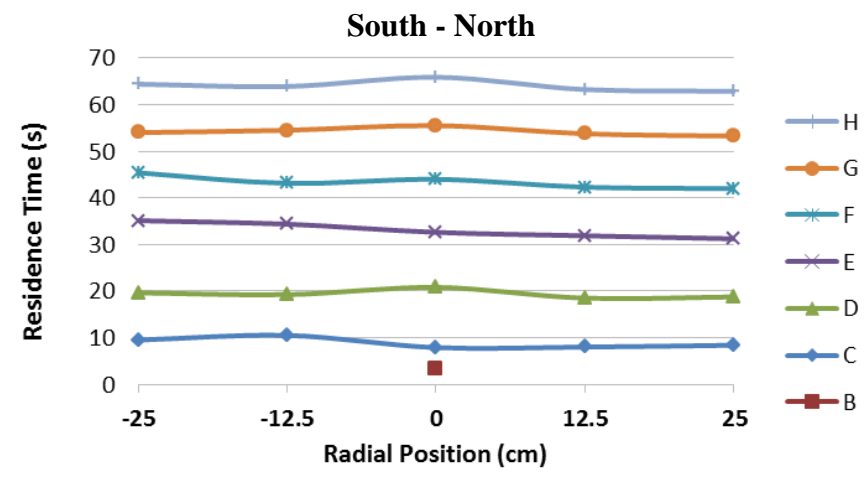
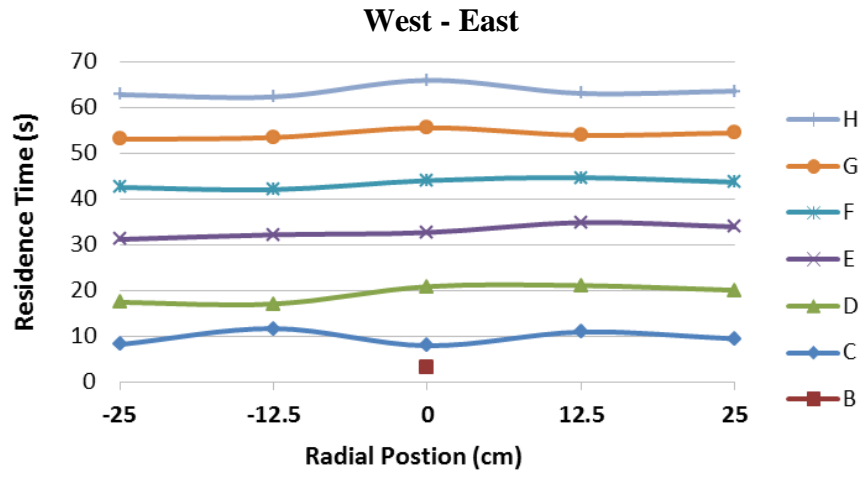
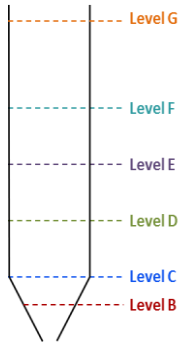
The results obtained when fitting the double cone insert are presented in Figure 5.45. There it can be seen that mass flow was achieved during discharge with residence time profiles fairly similar to those obtained with the inverted cone. The main difference between the performances of these two inserts is that with the double cone the markers placed adjacent to the walls of the conical hopper (level B) were discharged before than the markers located on level C. This indicates that the double cone insert reduced the velocity differences across the annular gap between the silo and the insert improving the uniformity of motion in the converging hopper. These results also support the hypothesis formulated by the author in Chapter 4 that the difference in velocity across the annular gap is not only a consequence of the diverging wall of the inverted cone compared to the converging wall of the hopper, but also it is a consequence of the void space under the inverted cone which provides a region of low stress where it is easier flow the powder to flow towards. That region of low stress is eliminated by the addition of the lower cone in the double cone insert.



a. Tracers Residence Time

b. Surface Profile

Figure 5.45 Double Cone – Results



a. Tracers Residence Time

b. Surface Profile

Figure 5.46 Open Double Cone – Results

Figure 5.46 presents the results obtained when the open double cone was fitted in the silo. As with the analysis made for the other tests, it is clear from the residence time profiles that mass flow was achieved during discharge. In fact, the open double cone produced the performance closest to an ideal mass flow pattern with very small differences between the residence times of markers placed at the same level. During the tests undertaken with the bench scale model, the prototype of the second generation of open double cone showed a velocity difference between the material flowing through the interior of the insert and the material flowing through the annulus between the hopper and the insert. In order to avoid that issue, the internal hopper of the prototype used with the semi-industrial rig was made slightly steeper than the recommended angle for mass flow. The results of the tests show that the modification was successful (at least for this particular system) and the velocity differences were minimized. This can be inferred mainly from the residence times of levels B and C. In the case of level C the only tracer flowing through the interior of the insert was the one located on the axis of the hopper, whereas all the other tracers flowed through the external annulus. This is a fact because the level C markers placed near the wall and at the intermediate position were located outside and lower than the inlet of the insert, with the intermediate markers located adjacent to the wall of the inverted cone section of the insert. Taking this into account and looking at the residence time of the tracers on level C it can be seen that the difference is negligible demonstrating the uniformity of velocities. As it can be seen in Figure 5.46 level B consisted only of one tracer, the reason for that is that due to the shape and size of the insert it was not possible to reach the other locations to position the rest of the markers. In any case, the fact that the residence time of this marker (flowing through the interior of the insert) is lower than all the markers from level C, also supports the conclusion of negligible differences in velocity of material flowing in and around the insert.

Another result to highlight was that cohesive arching was not observed in any of the tests undertaken with an insert fitted in the silo. Arching was not anticipated to form with the double cone or the open double cone because mass flow was expected to develop in the lower part of the silo and the silo and insert outlets were larger than the minimum arching dimension of the material. However, after the results observed for the silo without an insert, there was a concern that an arch could form when the

inverted cone was installed, because the region under the insert does not necessarily discharge in mass flow and would not necessarily benefit from the reduced critical outlet dimension that this flow pattern affords relative to core. In any case, a cohesive arch did not develop and the silo discharged without any issues, which could be explained by the insert acting as a barrier and reducing the consolidating stresses from the weight of the powder bed acting on the particles near the outlet of the silo.

## **5.7 Summary**

This chapter presented the process for the development of design procedures for open double cone and double cone inserts. Open double cones are a novel type of insert that was designed to try and influence the whole area of the converging section of a silo. The development process was based on the success obtained with the study of inverted cone inserts at bench scale presented in Chapter 4. The first step consisted of the design and practical evaluation at bench scale of a variety of static inserts, including cylinders, truncated cones and combinations of those shapes with inverted inserts. All these inserts however, failed to produce mass flow with some expanding the flow channel more than others, but with the presence of stagnant regions of material in every case. In any case that work was not in vain, as it helped the author understand further the way the different shapes affected the powder bed in the silo. With this experience and the work carried out with inverted cones the author proposed a novel type of insert called open double cone which comprises three sections: an internal conical hopper, an upper external inverted cone section and a lower external conical section. For this insert three design methods were evaluated, each producing an insert of a different size. The practical tests showed that all the three inserts successfully changed the flow pattern in the silo from core flow to mass flow and also produced very stable discharge rates.

Continuing with the bench scale approach, the author also proposed two design methods for double cone inserts with the resulting inserts differing mainly in size. When these inserts were evaluated experimentally, they also generated mass flow in the model hopper and produced very consistent discharge rates. Then based on the

results obtained at bench scale, three inserts were built to be evaluated in the semi-industrial test rig. The inserts consisted of an inverted cone designed following the modified method proposed by the author in Chapter 4, an open double cone following the second generation method (middle size insert) and a double cone following the second generation method (smaller insert). The results from the test showed that all inserts changed the flow pattern from core flow to mass flow, with the open double cone producing the most uniform velocity distribution across the silo.

## CHAPTER SIX: INDUSTRIAL APPLICATIONS

---

This chapter presents three cases where insert technology is used to improve the performance of bulk solids discharge equipment. The first case consists of a granular coal silo exhibiting flow and material quality inconsistencies, the second case involves a pneumatic conveying system where the feed silo has been reported to be prone to rat-holing and the third case includes the design of a drum tipper to be used under restricted headroom conditions.

### 6.1 Granular Coal Silo with Multiple Outlets

In the previous chapters, the use of static inserts for the promotion of flow in conical hoppers with a single outlet has been presented. However, a common source of problems in plants handling granular materials is silos with multiple outlets that are used independently. Devising a procedure for using inserts to correct core flow issues in multiple outlet bins is an extremely complex problem, due to the number of variables involved: the geometry of the silo, the number of outlets, the outlet size, shape and position, the type of feeder interfaced. If all the outlets are operated simultaneously, the general rules for inserts should still apply. However, if outlets are to be operated singularly (independently), the process of expanding the flow channel becomes significantly more difficult with each case becoming potentially unique. In this section, the problems occurring in a 650 tonnes granular coal silo featuring multiple outlets are analysed, and a solution based on insert technology is proposed.

#### 6.1.1 Description of the Process

The main two uses of coal in the steelmaking industry are the production of metallurgical coke and the direct injection of granular coal into blast furnaces. In a blast furnace, coke is used as fuel for the smelting process and also as an agent to reduce the iron ores to metallic iron. In order to reduce the amounts of coke needed for the smelting process, granular coal is also injected into blast furnaces as a

secondary fuel and reducing agent, decreasing the operating costs of the process. The rate of coal injection is critical to achieve the adequate process conditions and bath chemistry within the furnace.

In a UK steelmaking plant, a coal injection process with injection rate instabilities has been identified, where the discharge performance of a storage silo is believed to be the main cause of the process variability. For the injection of coal to the blast furnace, raw coal is milled, dried and pneumatically transferred to a storage silo using nitrogen. The coal is then discharged by gravity into blow tanks and injected into the blast furnace using dense phase pneumatic conveying. A previous study reported that depending on the level of inventory in the main storage silo, variations of the characteristics of the coal discharged could be found, particularly referring to changes in particle size distribution. The changes in particle size were believed to cause inconsistent bulk density of the material producing variability in the fill weight of the blow tanks and in the injection rate of coal into the furnace. As a result of this, the inventory in the silo is not allowed to fall below 75%, point beyond which the inconsistent characteristics of the coal cause unacceptable deviation of the process control variables. This effectively reduces the working capacity of the storage silo to 25% of its total capacity

The silo has a cylindrical vertical section of 18 m height and 6.5 m diameter, a 20° half angle conical hopper with a 2.7 m diameter outlet, which is transitioned to a wedge hopper with a 0.4 m by 3.5 m slot. Four circular outlets 0.4 m in diameter are equally spaced along the slot, with each of them discharging into an individual blow tank except for one which is permanently blocked (see Figure 6.1). In order to improve the discharge, the silo is equipped with an agitator along the bottom slot with a paddle rotating above each of the outlets.

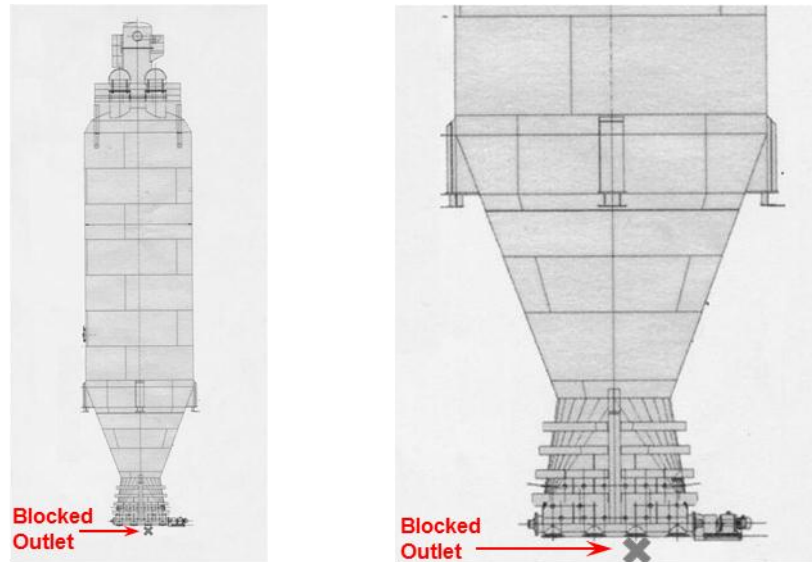


**Figure 6.1** Granular Coal Silo

### 6.1.2 Product Quality Study

In order to determine if the characteristics of the coal discharged depended on the inventory level in the silo, multiple samples were taken from the silo starting from full and letting it discharge until a 70% fill level was reached. Sampling at lower inventory levels was not possible due to the injection instability that is known to be produced. A total of 9 samples were taken at each of the following fill levels: 100%, 90%, 80% and 70% and the particle size analysis was undertaken using sieves between 56 and 850 microns. The results of the particle size measurements are presented in Figure 6.2.

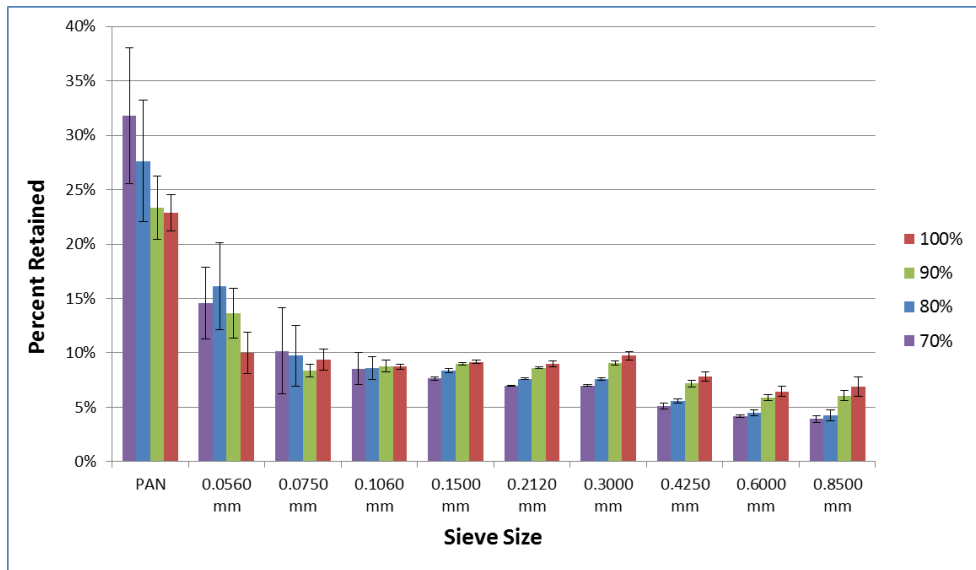


**Figure 6.2** Particle Size Distribution of Discharged Coal

The results presented in Figure 6.2 show that a trend exists for the variation of particle size distribution with the inventory level of material in the silo. There it can be seen how the fraction of fines increased as the inventory level reduced whereas the fraction of coarse particles decreased with the falling level of material. In order to evaluate the impact this variation in particle size distribution could produce on the injection process, the bulk density of the samples taken at the different levels was measured using a Brookfield Powder Flow Tester and the results are presented in Figure 6.3.

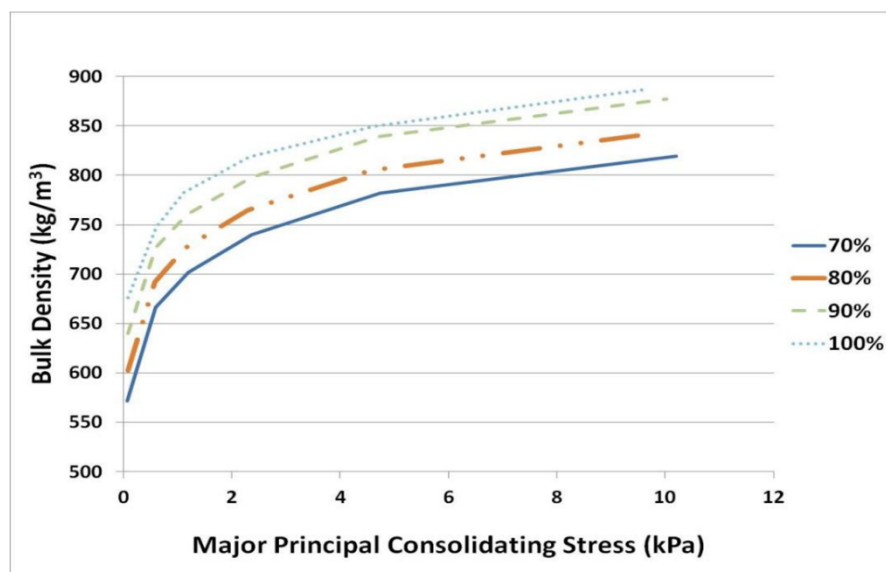


**Figure 6.3** Bulk Density of Discharged Coal

Figure 6.3 clearly shows the variation in bulk density according to filling level with the discharged bulk material becoming less dense as the inventory in the silo decreases. This is therefore the main reason for the instabilities observed in the plant where the injection rate is controlled using volumetric feeders which depend on a consistent bulk density to achieve a stable mass flow rate. However, from the data it can be seen that differences in bulk density up to 20% can be expected between the material being discharged from the silo 100% full and the material discharged from the silo filled to 70% of its capacity. These differences in particle size and bulk density are likely to be caused by segregation in the silo as well as differences in settling time of the material prior to discharge, particularly as the coal was observed to be highly air retentive. The combination of these two factors and its consequences is commonly more evident in silos discharging in a core flow pattern. By comparison, mass flow silos by definition feature a high degree of remixing which minimizes segregation and the longer settling times allowing more consistent bulk density in the product. Therefore it was determined that in order to minimize the bulk density variations the silo needed to discharge in mass flow whereas the multiple outlets and the mode of operation most likely caused the silo to develop a core flow pattern.

### **6.1.3 Proposed Feeding Interface Solutions**

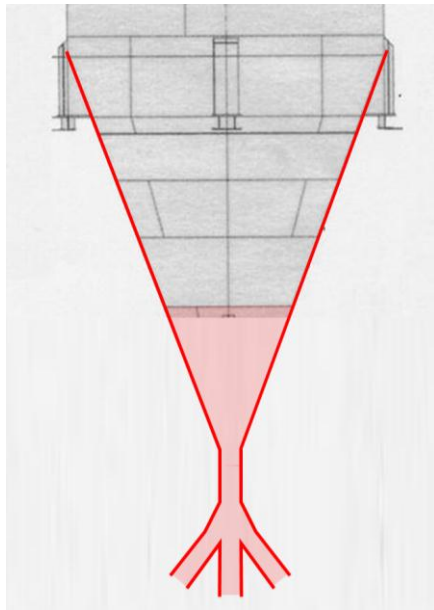
According to flow the property measurements undertaken with the samples collected, the geometry of the silo should be capable of achieving mass flow, if material was drawn over the entire length of the slot. However, because coal is discharged from a single outlet at a time, mass flow is not possible and a discharge channel is expected to form above the outlet that is operated. To avoid this problem, the author proposed four solutions where by modifying the feeding interface of the silo an even draw of material could be achieved, obtaining a mass flow pattern during discharge.

The first proposed solution consisted in replacing the circular to slot transition of the silo with an extension of the conical hopper. It would extend to an outlet of similar dimensions (or slightly larger) to each of the chutes diverting the material to the each

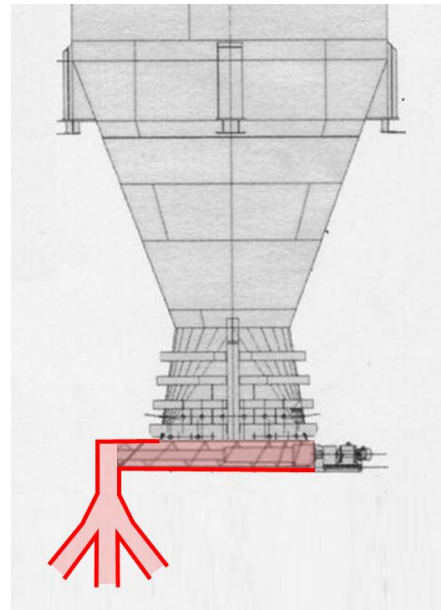
of the blow tanks (0.4 m). Under the hopper outlet a stand pipe with a length of 0.6-0.8m would be added at the end of which the three diverting chutes could be connected (as shown in Figure 6.4a). The stand pipe would allow the expansion of the flow channel created when only one of the blow tanks is being filled, in this way the whole area of the hopper outlet is activated and an even draw of material is produced.

In the second solution the current shape of the silo is kept and a screw feeder is interfaced to the discharge slot (see Figure 6.4b). Provided that the screw is designed with an increasing transport capacity, an even draw of material should be achieved producing mass flow in the silo. The screw feeder would then discharge into a chute where each of the three branches could be connected. The third solution is based on the same principle as the second but a bidirectional screw is used instead, this allows a central discharge facilitating the routing of the discharge chutes towards the blow tanks (see Figure 6.4c). For this solution however, a tent needs to be installed above the central outlet to avoid a preferential draw of material from the centre of the hopper.

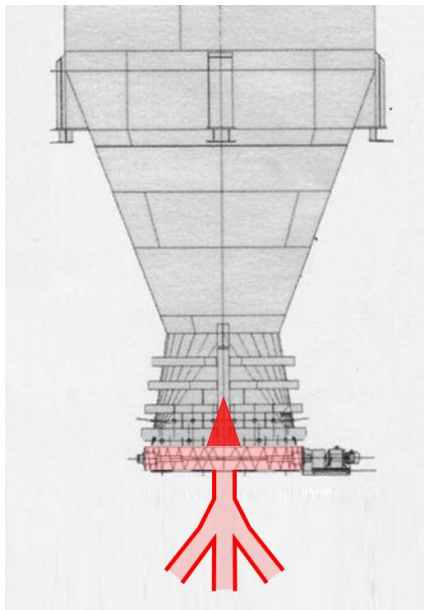
The last solution proposed consisted in removing the circular to slot transition of the silo and installing a plough feeder directly under the conical hopper as shown in Figure 6.4d. The feeder would produce a central discharge to which the three branches could be connected. A plough feeder consists of one (or more) rotating arms that draw material radially from the circular section and can produce an even discharge from a silo. The feeder would decouple the discharge stream from the contents of the silo, ensuring the behaviour of the material in the blow tank chutes does not affect the discharge pattern in the silo.



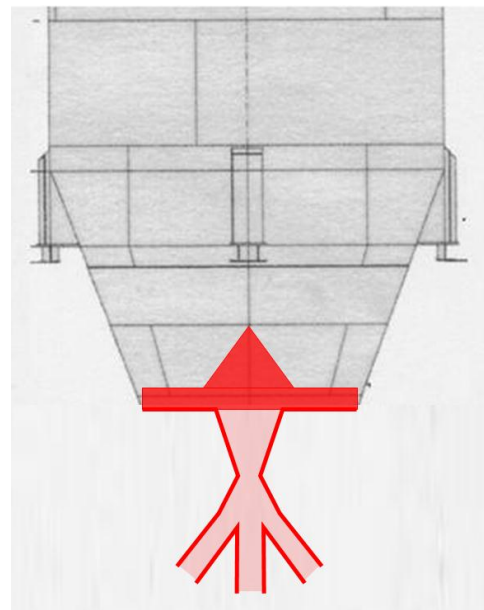
*a. Extended Conical Hopper*



*b. Screw Feeder*



*c. Bidirectional Screw Feeder*



*d. Plough Feeder*

**Figure 6.4 Feeding Interface Solutions**

Any of the modifications described above would be capable of transforming the discharge pattern in the silo from core flow to mass flow. However, each would also create some challenges for their implementation. The main issue with solutions a, b, and c was that the headroom available between the silo and the blow tanks was not enough to extend the transfer chutes to connect them to a common point. Therefore, either the silo would need to be raised or the blow tanks had to be repositioned,

which meant high installation costs and possible excessive down time for the plant. Solution d was considered more viable because it did not need the silo or blow tanks to be moved, but high capital costs and long downtime also hindered the feasibility of its installation.

Taking this into account, it was decided to explore the possibility of applying insert technology to modify the discharge pattern in the silo.

#### **6.1.4 Study at Bench-Scale**

##### **6.1.4.1 Bench-Scale Model Fabrication**

In order to study the discharge behaviour of the silo and to evaluate possible modifications that could improve its performance, it was decided to build a bench-scale model of the silo. The support structure and the cylindrical segments of the rig described in Chapters 4 and 5 were used, but the converging part of the silo had to be rebuilt. An important characteristic of the model is that it should be transparent, as visual inspection would be the only way to determine the discharge pattern. This reduced the range of materials that could be used and complicated the fabrication process. Several techniques were considered to make the model, and finally it was decided that vacuum forming would be the easiest and most accurate. The problem was that the silo had divergent sections making it impossible to build the model in one piece, as the mould could not be taken out. For this reason a plastic mould of half of the model was made using a rapid prototyping machine, then using a CR Clarke thermoforming centre 911 and 2 mm extruded acrylic sheets, the clear halves of the model were made (see Figure 6.5).

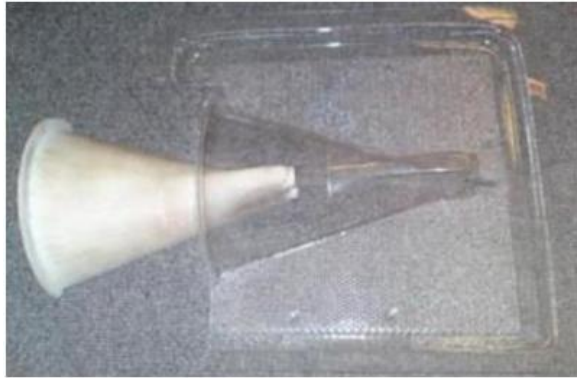


**Figure 6.5** *Vacuum Formed Model and Mould*

#### **6.1.4.2 Half Silo Test Rig**

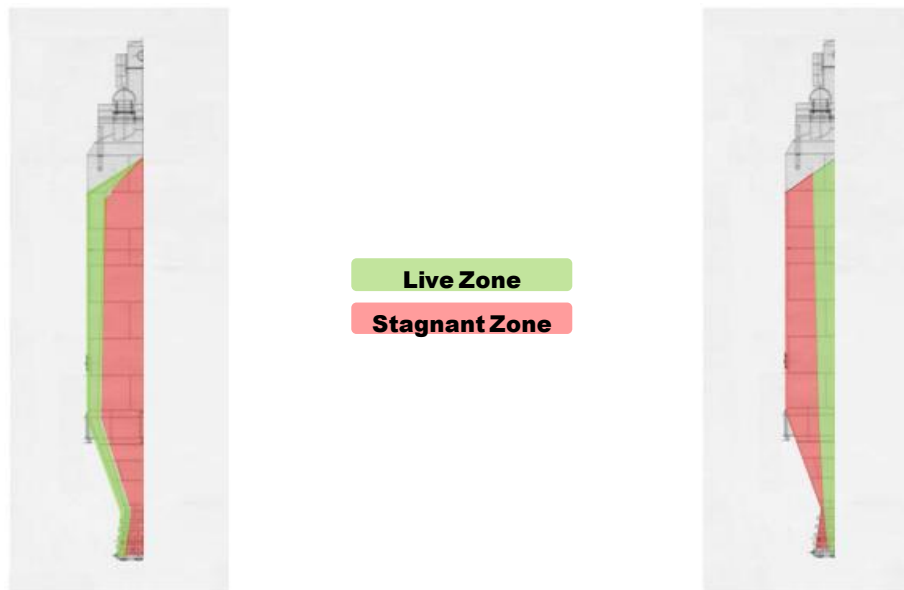
The first trials with the model were carried out in a test rig comprising a 140 mm diameter Perspex half tube attached to a Perspex sheet. One of the half models fabricated was fitted onto the rig as shown in Figure 6.6.



**Figure 6.6** *Half Silo Test Rig*

The rig was filled with olivine sand and allowed to discharge through one outlet at a time. The coal from the real silo could not be used at this scale because the minimum outlet size to prevent arching was too large compared to what could be achieved with the model. When the outlet used was the one furthest from the centre, a lateral channel was formed from the moment the discharge started. When the central outlet was used, the silo discharged through a central channel (see Figure 6.7). These observations confirmed that core flow was occurring in the silo and

helped to explain the problems that have been found with the handleability of the material on plant.



*a. Discharge Through Lateral Outlet*

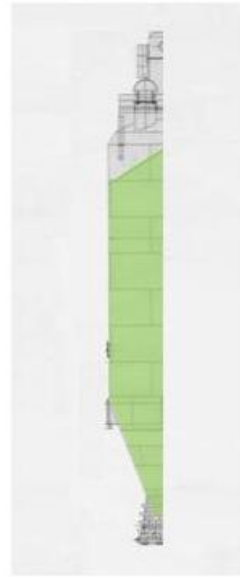
*b. Discharge Through Central Outlet*

**Figure 6.7** *Half Silo Discharge Results*

In order to stop the material discharging through the side of the hopper when using the lateral outlet, the flow of material had to be restricted to favour a more central draw. For this purpose the conical section was extended downwards, as shown in Figure 6.8. With this modification, the model silo discharged in mass flow until the surface of the material was near the silo transition from cylindrical to conical. This result was achieved when using either outlet, therefore this was the chosen configuration to carry out tests with the complete model.



*a. Extension of the Conical Section*



*b. Discharge Through Either Outlet*

*Figure 6.8 Half Silo Modification*

### 6.1.4.3 Complete Silo Test Rig

The test rig described in Chapters 4 and 5 was modified to carry out the test work. The 45° glass hopper was replaced with the model shown in Figure 6.9.



*Figure 6.9 Test Rig Set Up*

The rig was filled with olivine sand and allowed to discharge through one outlet at a time, as the silo was symmetric with respect to a central plane. It was not necessary to discharge through all the outlets, but just through two of them. The results resembled what was observed with the half silo rig, as a lateral and a central channel were formed when using the lateral and the central outlet respectively. Then, the cone extension was tried, but in this case there was not much improvement and channels were still appearing during the discharge.

However, there was a substantial difference between the half and the complete silo rigs. The flat sheet, to which the half tube was attached, acted as an extra wall reducing the resistance to flow. The friction between two layers of powder is higher than the friction between a layer of powder and the surface of the wall.

To achieve the same result in the complete rig, a flat plate should be installed in the centre of the silo and along the full height of it. However, this would not be adequate at large scale because only one side of the silo would discharge creating enormous side loads endangering the stability of the silo. Instead, it was decided to install a flat plate that extended up to the transition of the silo (see Figure 6.10). This point was chosen because it is where the cross section area stops changing, and therefore it is the lowest point where the maximum discharge channel width could be achieved with the central plate.



*Figure 6.10 Flat Plate*

The installation of the flat plate had a very positive impact in the discharge behaviour of the hopper, a short section at the top of the silo was observed to slide at the wall and then discharge through a channel notably wider than before. However, it was observed that at the outlet of the conical extension, the material was moving a lot faster near the cone than near the flat plate where it was almost stagnant.

In order to achieve further improvement, it was decided to vary two parameters and study the effect on the discharge pattern. The first parameter was the length of the conical extension, which involved a variation of the size of its outlet, and the second one was the shape of that outlet. The idea of changing the shape of the conical extension outlet was considered to promote flow near the flat plate and restrict flow near the cone.

Three types of outlets and several extension lengths were tried, as the symmetry of the silo allowed two different configurations to be tested within the same set up. Figure 6.11a shows the first type of outlet shape, which was discussed above. It has a semi-circular shape with the edge at an even level, and Figure 6.11a also shows how two different extension lengths could be tested. Figure 6.11b shows the second type of outlet that was tried. It allowed the powder to discharge with less restriction near the flat plate. This produced a lengthening of the section at the top of the silo where the material slid at the wall and went down levelled. Although, the improvement obtained with the change of outlet shape was evident, the powder was still discharging more slowly near the central plate. For that reason, it was decided to modify the shape of the outlet to promote further flow of the material near the flat plate. Figure 6.11c shows the third type of outlet, which allowed the material near the flat plate to start discharging at a higher point. With this, the length of the mass flow section at the top of the silo was increased further.



*a.*

*b.*

*c.*

**Figure 6.11** *Shapes and Lengths of the Conical Extensions*

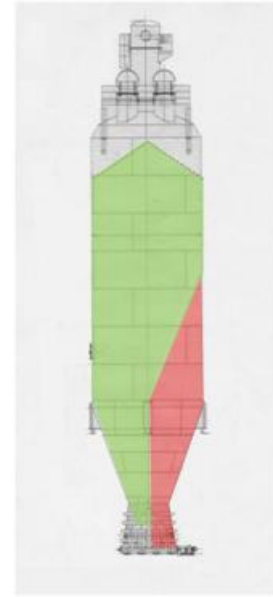
The optimal length of the conical extension was found to be where the vertical projection of its lower edge coincided with the outer edge of the central outlet. Figure 6.12 shows the results when the shape and length of the extension were optimized. It can be seen that in both cases the material in the top part of the silo moved in a mass flow like pattern. However, the stagnant region was larger when the silo was discharged through the lateral outlet due to material building up on top of the central outlet and hindering the flow along the central plate. In the case of discharge through the lateral outlet, the height of the stagnant zone in the cylindrical section was approximately 1.5 times the diameter of the silo. In the case of the central outlet, it was around 1.2 times the diameter of the silo.



*a. Optimal Length of the Conical Section*



*b. Discharge Through Lateral Outlet*



*c. Discharge Through Central Outlet*

**Figure 6.12 Optimal Conical Section Results**

The next step was to try to reduce the size of the stagnant zone in the silo. Two aspects had to be addressed: the build-up of material in the centre of the hopper that impeded the smooth flow of material, and the material retained by the central plate on one side of the silo. For this purpose a slightly different approach was made, the central plate was removed and instead a triangular tent was installed at the lowest part of the original conical section of the silo. The tent together with the cone extension formed a flow splitter known as trouser legs. When the lateral outlet was used, the tent acted as a shield protecting the flowing material sliding against the static material that sat on top of the closed central outlet. As a result the restriction to flow was reduced improving the discharge in the central part of the silo. However, the new approach presented a problem, the valleys formed in the joints of the cone extensions and the triangular tent caused an additional hindrance to the flow of material. To overcome this, the valleys were eliminated by tapering the sides of the tent and reducing the width of the cone extension, this created gaps in the trouser legs allowing the material to expand and slide at the walls of the silo (see Figure 6.13).

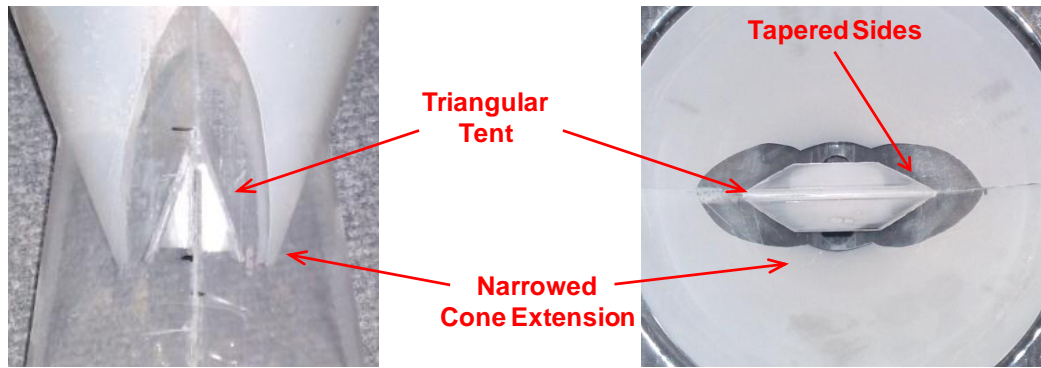
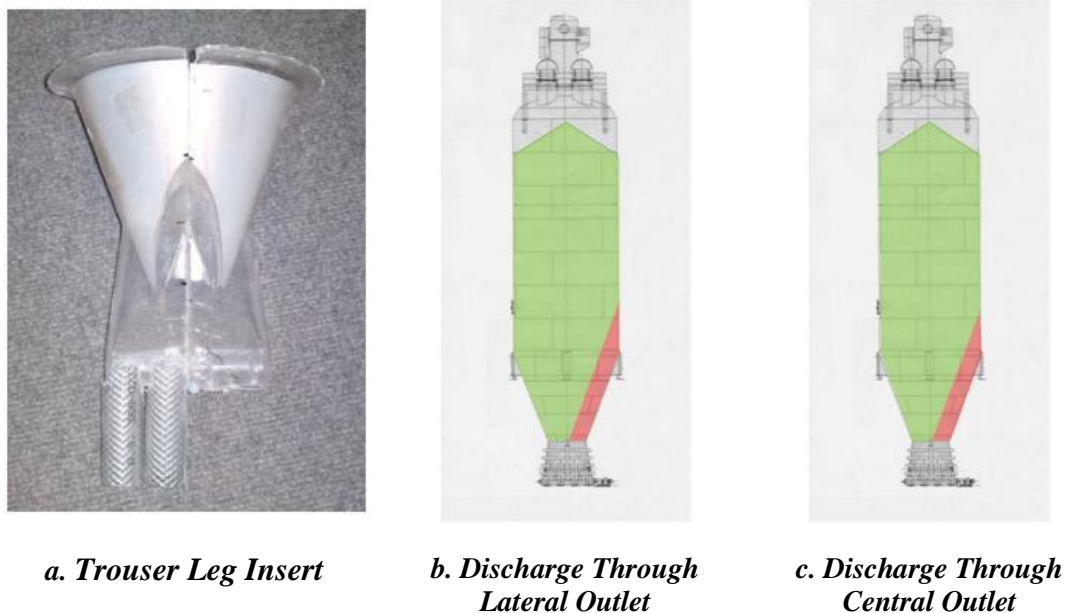


**Figure 6.13** *Open Trouser Leg Insert*

Figure 6.14 shows that, when the trouser leg insert was installed, the percentage of live material increased considerably, the height of the stagnant zone in the vertical section was reduced to 0.6 times the diameter of the silo using the lateral outlet, and to 0.4 times with the central outlet. With most of the material in the silo flowing in a pattern close to mass flow, the consistency of the properties of the discharged material should increase and therefore a reduction of the problems should be observed in the plant.



**a. Trouser Leg Insert**

**b. Discharge Through Lateral Outlet**

**c. Discharge Through Central Outlet**

**Figure 6.14** *Trouser Leg Insert Results*

### 6.1.5 Insert Validation at 1:10 Scale

Following the positive results obtained with the bench scale model it was decided to build a larger test rig where the proposed insert could be tested with the coal used in the industrial silo. This sections presents the test rig built for that purpose as well as the results from the test programme undertaken.

#### 6.1.5.1 Test Rig Description

For the design of the test rig it was decided to maximize its size to try to simulate as close as possible the behaviour of the full size silo. The overall size of the model was limited by the headroom available in the laboratory and the height of the equipment used for loading. Taking this into account the test rig was designed to be a 1:10 model of the industrial silo. The model silo was made of stainless steel (with a 2B internal finish) which was consistent with that used in the industrial silo. As shown in Figure 6.15, the model consisted of a vertical section 1800 mm tall and 650 mm in diameter, a conical hopper section converging from 650 mm to 270 mm at a 20° half angle from the vertical, a transition converting the 270 mm circular outlet to a 350 mm by 40 mm slot with 20° converging half angle and finally a feeding interface transforming the discharge slot into four 40 mm outlets. All the sections were joined using flanges which would also allow the installation and removal of the insert during the trials.

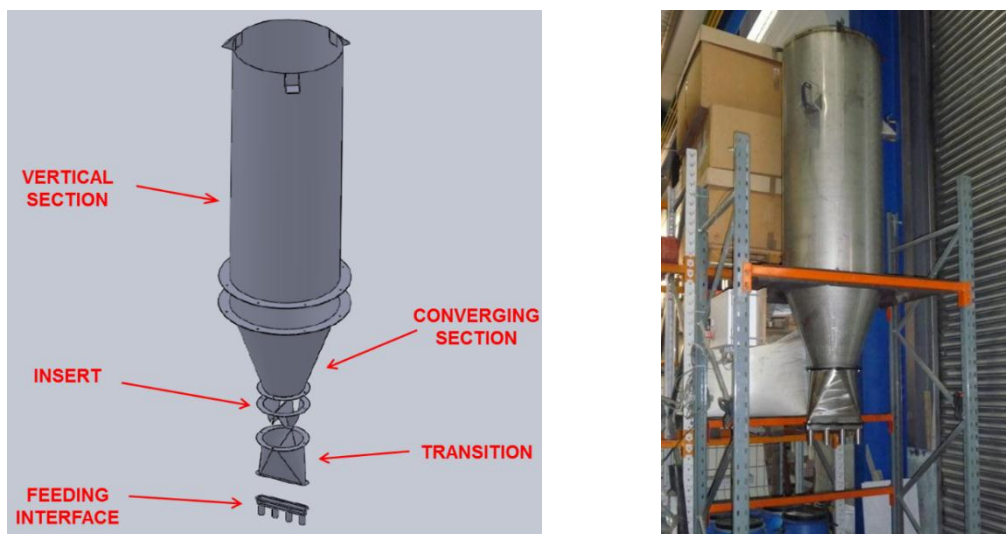


*Figure 6.15 1:10 Model Silo*

The insert, as shown in Figure 6.16, was built following the results obtained from the work undertaken with the bench scale silo. It consisted of a central V tent and two lateral extensions of the conical hopper forming two open trouser leg channels.

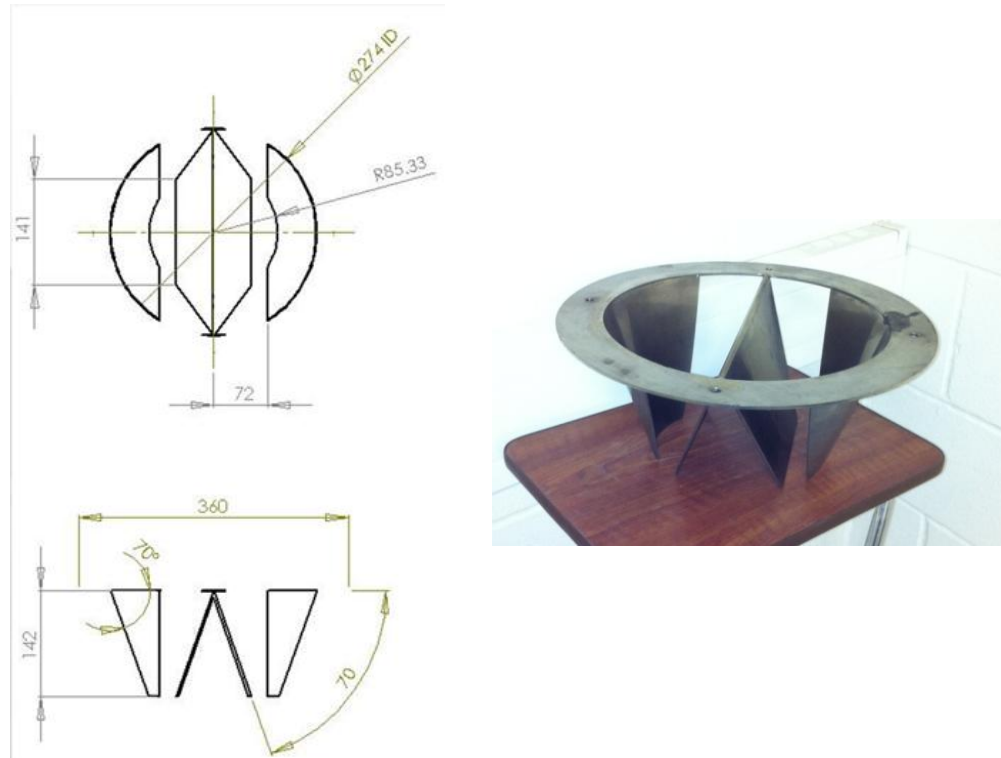


**Figure 6.16** 1:10 Insert

### 6.1.5.2 Test Material

To undertake the test programme with the 1:10 scale model it was intended to use a sample of coal obtained from the industrial silo. However, flow characterisation of the material showed that the critical arching dimension of the material was in the order of 100 mm whereas the outlets of the model silo were only 40 mm. For this reason, if the coal for the industrial silo was to be used for the tests, it needed to be modified to avoid arching in the model silo. For this purpose, a sample of the coal was sieved using a 63 micron sieve and the material retained was characterised to obtain its critical arching dimension. This procedure was then repeated using 90, 125, 180, 250, 355 and 500 micron sieves, with the results presented in Figure 6.17. As mentioned before, the arching dimension for samples of material with the full size distribution was 100 mm. When the fraction of particles passing the 63 micron mesh

was removed the critical arching dimension reduced to 60 mm, which was not enough to produce reliable flow in the silo. By removing the fines passing a 90 micron sieve, the arching dimension reduced to just under 40 mm while removing the material passing through the 125 micron sieve the arching dimension reduced to 35 mm. The results therefore suggested that in order to avoid discharge problems in the model silo the test material should be screened to remove the size fractions below at least 90 microns. As a precautionary measure, a 125 micron mesh was used instead and 1500 kg of coal were sieved producing around 800 kg of oversize material to be used in the tests.

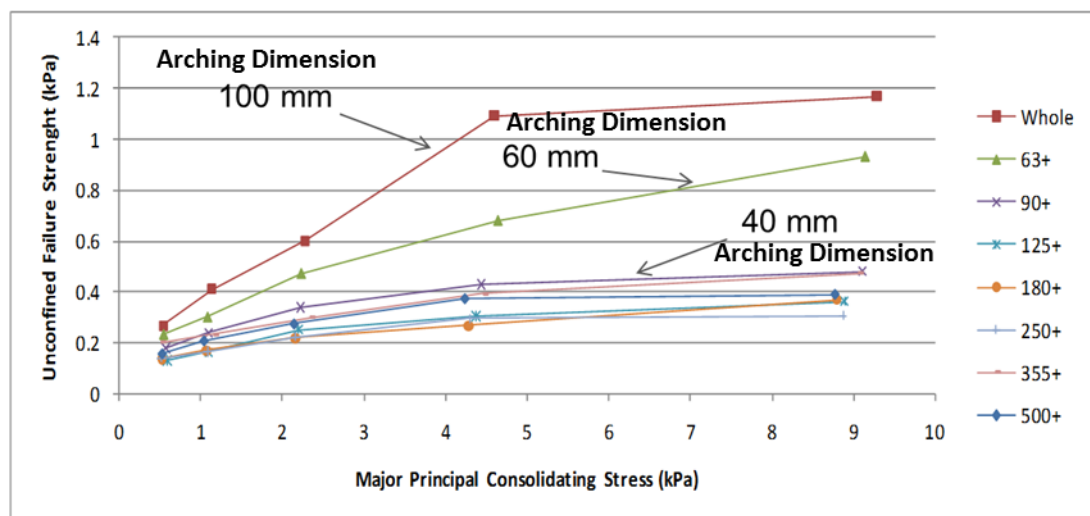


**Figure 6.17** Coal Characterisation

### 6.1.5.3 Test Procedure

The main purpose of the test work was to determine the flow pattern developed during discharge with and without the proposed insert. In order to achieve this, the model silo was equipped with the pattern identification system described in section 4.1, where numbered tracers are positioned at known locations in the silo and the residence time is measured for each of them. The tracers were located on 7 levels at different depths as shown in Figure 6.18 and on each level 9 tracers were positioned following the template shown in Figure 6.19, except for level B where only 5 tracers were positioned due to the reduced area.

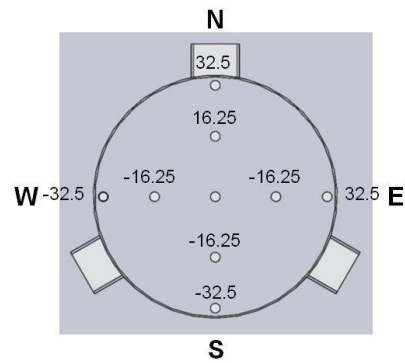
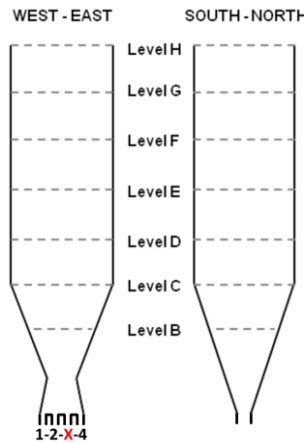


**Figure 6.18 Vertical Tracer Location    Figure 6.19 Horizontal Tracer Location**

To start the test the tracer positioning tool was placed in position, the silo was filled with the sieved coal and the first set of tracers dropped to the respective level. Then, the tracer positioning tool was raised to each subsequent level and the rest of the tracers dropped to their respective positions as shown in Figure 6.20. To start the discharge one (or more) outlets were opened and the silo was allowed to drain. During the discharge, the tracers were screened out of the stream using the mesh shown in Figure 6.20 which also directs them towards the collection hose where a micro switch recorded the time for each marker. As shown in Figure 6.18, outlet 3 was kept closed at all times replicating the setup of the industrial silo, tests were carried out discharging through outlet 4 only, outlet 2 only, outlets 1 and 2, outlets 1 and 4, outlets 2 and 4, and finally outlets 1, 2 and 4, trying to replicate any possible combinations in the real plant.



**Figure 6.20** *Tracer Positioning Tool*

#### **6.1.5.4 Results and Discussion**

The residence time maps for each of the outlet combinations with and without an insert are presented from Figure 6.21 to Figure 6.32. Please note that due to the symmetry of the silo, discharge through outlet 1 only was not undertaken as it should provide similar results to outlet 4 only, with the expected difference of the residence time map being a mirror image on the plane west – east.

Figure 6.21 presents the results obtained when there was no insert fitted and the silo was allowed to discharge only through outlet 4. The residence of the tracers located in the South-North plane clearly show the development of a central channel shortly after the start of the discharge with most of the tracers placed along the axis of the silo coming out first. The residence times of the tracers located near to the walls of the silo are also clear indicators of the development of a core flow pattern during discharge with those located higher in the silo coming out before those in the deeper levels. In general, on the plane South-North not much variation is expected side to side as the silo is symmetric on that plane. This however, is not necessarily true for the plane West-East where the symmetry would depend on the outlets that are open, in fact the only possible combination where true symmetry would be produced is when the silo discharges through outlets 1 and 4 simultaneously. For that reason the

analysis of the residence times on the plane West-East would be the main focus of attention. On that plane it is clear the asymmetry caused by the single outlet which created a lateral discharge channel on the east side of the silo (same side of the open outlet) as it was expected. The material on the west side remained static until most of the material from the east side had been discharged. This behaviour confirms the hypothesis of core flow developing in the silo due to the mechanism of extraction of material.

Figure 6.22 presents the results when the silo is allowed to discharge through outlet 4 after the insert has been fitted. From the results it is evident that by fitting the insert, the flow pattern in the silo is drastically modified. The Plane South-North suggests that mass flow was achieved during discharge. The flow of material followed a first in first out pattern and the velocity differences between tracers are very small. On the West-East plane the results are slightly more complex but also confirm that mass flow was achieved in the silo. The velocity differences across the plane however, show that the material located on the east side of the silo moved at a higher velocity than the material on the west side. However, the important point is that the material on the west side was not static during discharge and was just moving at a lower velocity, which can be deduced from the tracers near the wall which discharge in a first in first out fashion, and came out when material from the east side was still being discharged. The exception was perhaps the tracers of the two upper most levels which came out together at the end of discharge which suggests that towards the end movement along the wall on that side of the silo might have stopped. In any case, the improvement made by the insert is evident changing the flow pattern in the silo from core flow to mass flow.

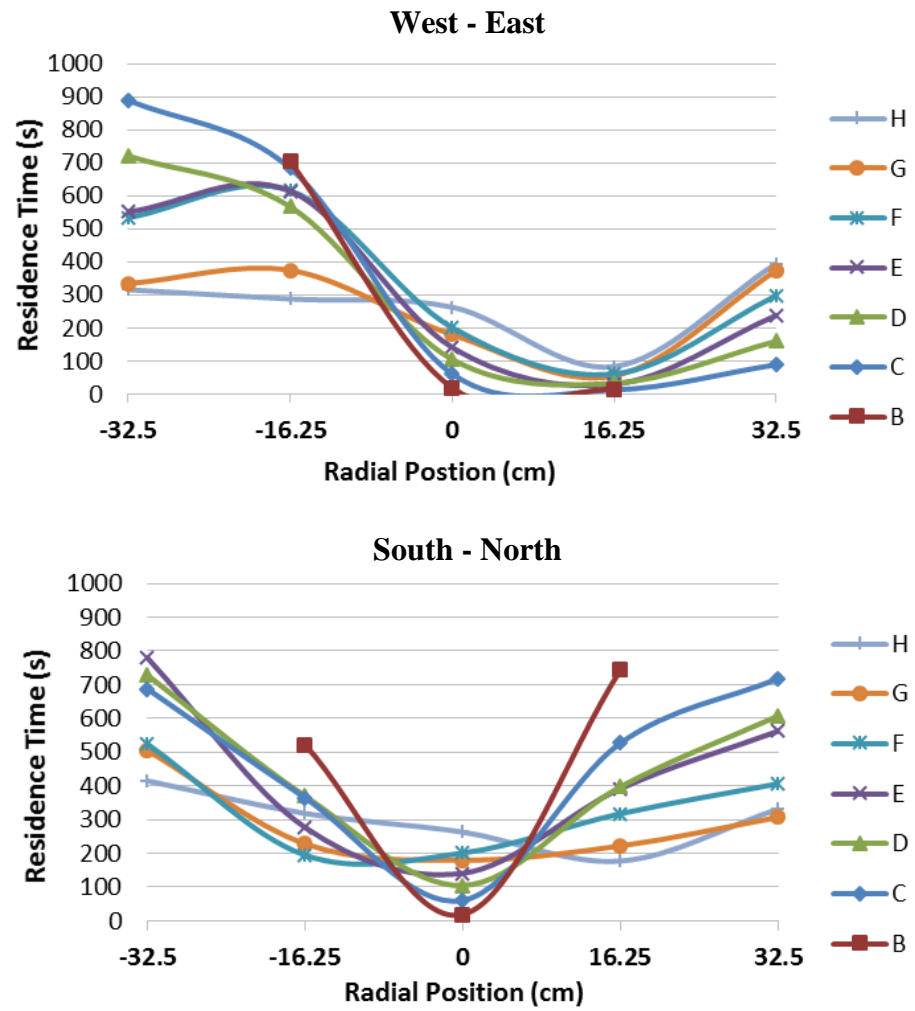
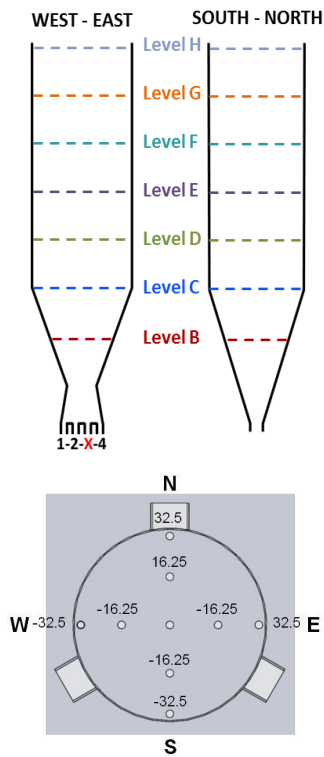


Figure 6.21 Outlet 4 - No Insert

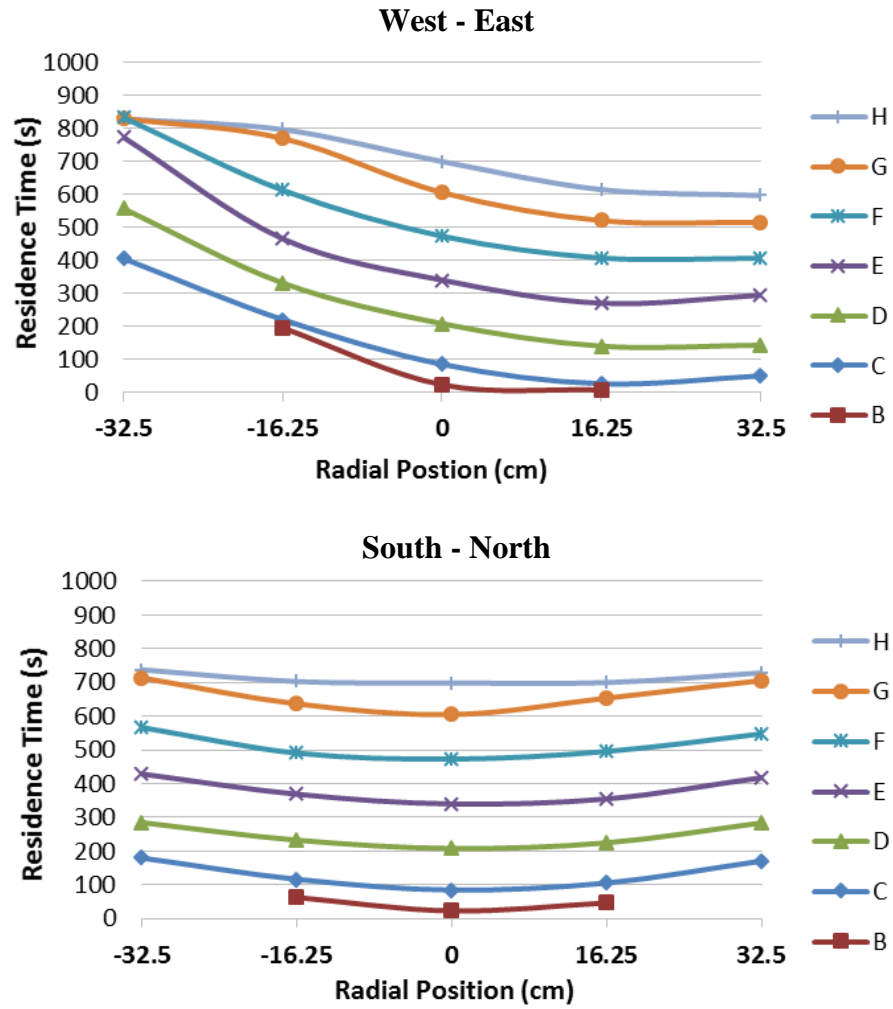
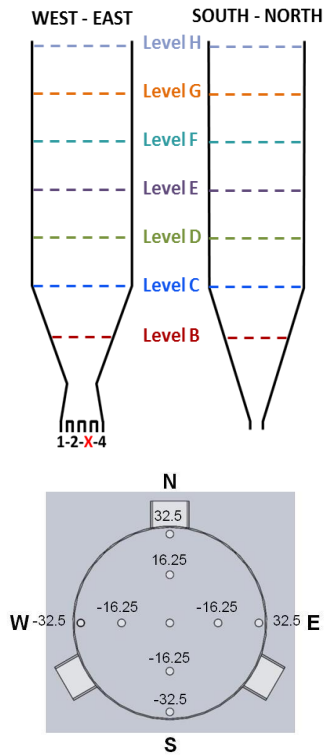


Figure 6.22 Outlet 4 - With Insert

The results presented in Figure 6.21 and Figure 6.22 illustrated the flow patterns obtained when one of the lateral outlets was used. Figure 6.23 and Figure 6.24 present the results for the case when one of the central outlets is open, although it needs to be remembered that outlet 3 in the industrial silo is permanently blocked. The results from the silo discharging without the insert (Figure 6.23) are similar to those obtained when discharging through the lateral outlet. On the plane South-North, the formation of the central channel can clearly be seen, but in this case the channel is wider than with the lateral outlet. This can be deduced from the order in which the tracers in the intermediate position came out. When discharging through a lateral outlet (4) the tracers in the intermediate position discharged in an inverse order suggesting first in last out in that region whereas in this case (through outlet 2), the tracers in those positions followed a first in first out pattern indicating that the discharge channel was wider at least on that plane. In the case of the plane West-East, the results are also fairly similar confirming the development of a core flow pattern. The channel formed drew material preferentially from the side of the open outlet as expected. However, in the case of the discharge through outlet 2, the flow channel is located slightly more centrally than with outlet 4 which can be observed from fastest set of tracers to come out, central position for outlet 2 and intermediate position for outlet 4.

When the inlet was installed the improvement obtained is again evident from the results shown in Figure 6.24. Most of the contents of the silo discharged in a mass flow like pattern with only very small differences in velocity between tracers placed at the same level. A peculiarity however can be seen from the West-East plane with the tracers located next to the wall on the east side of the silo. All the tracers in that region were the last to be discharged from the silo, indicating that the material in that zone remained static until the end of the discharge. Nonetheless the insert proved again to be an effective method to modify the flow pattern in the silo, even if the achievement of mass flow was not always possible.

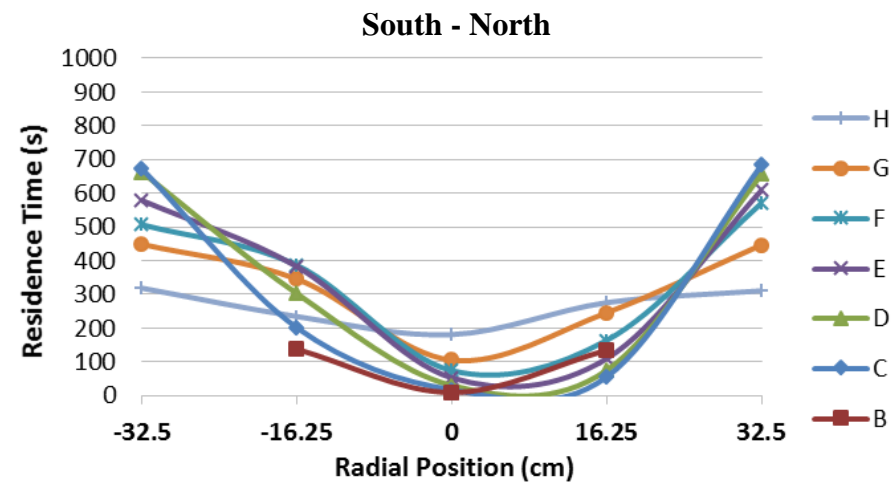
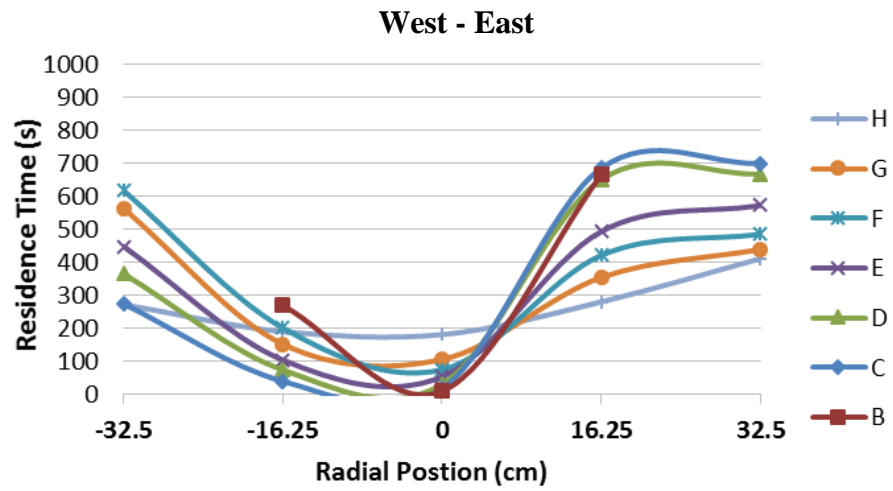
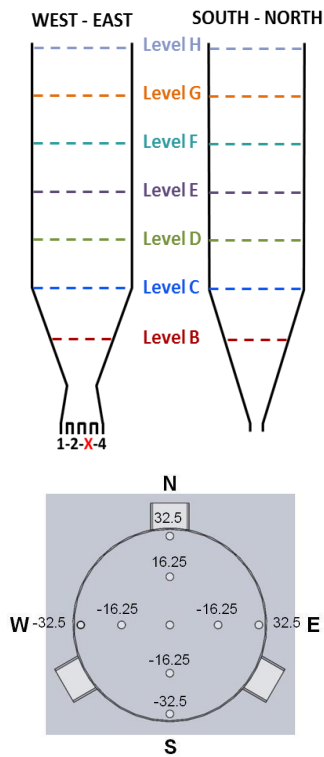


Figure 6.23 Outlet 2 - No Insert

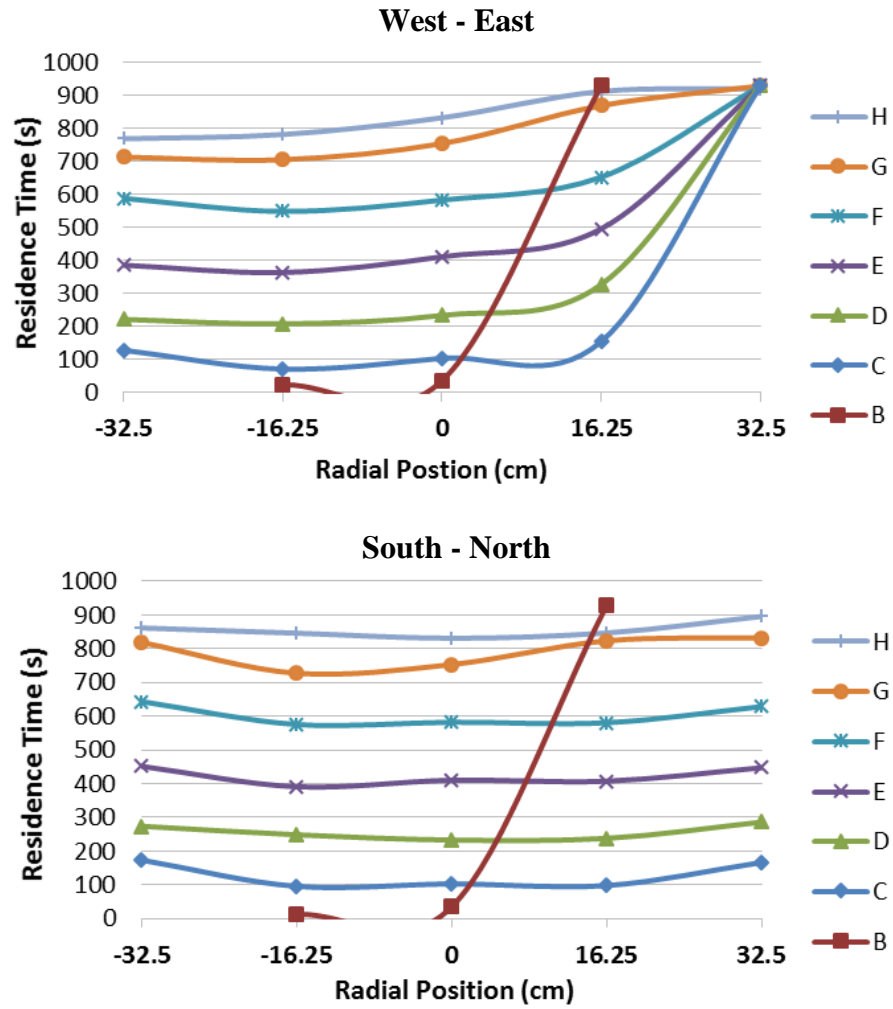
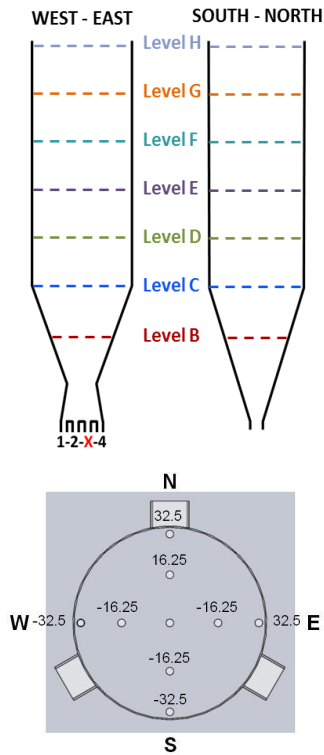


Figure 6.24 Outlet 2 - With Insert

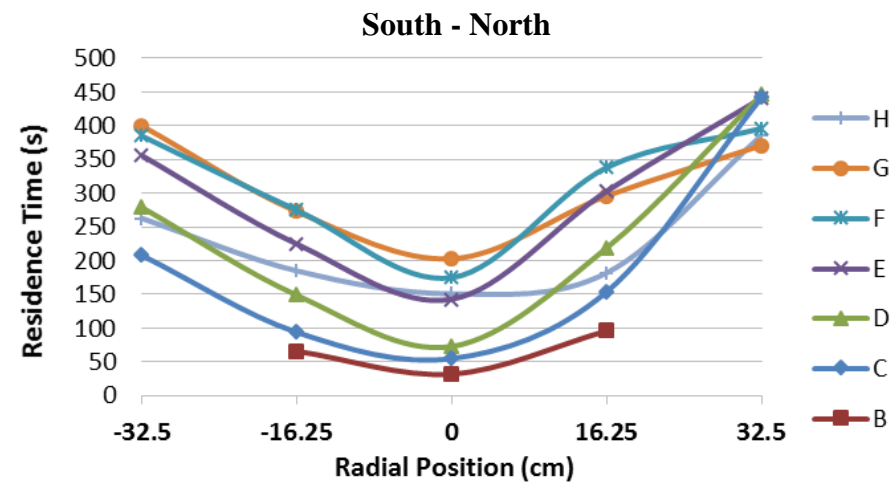
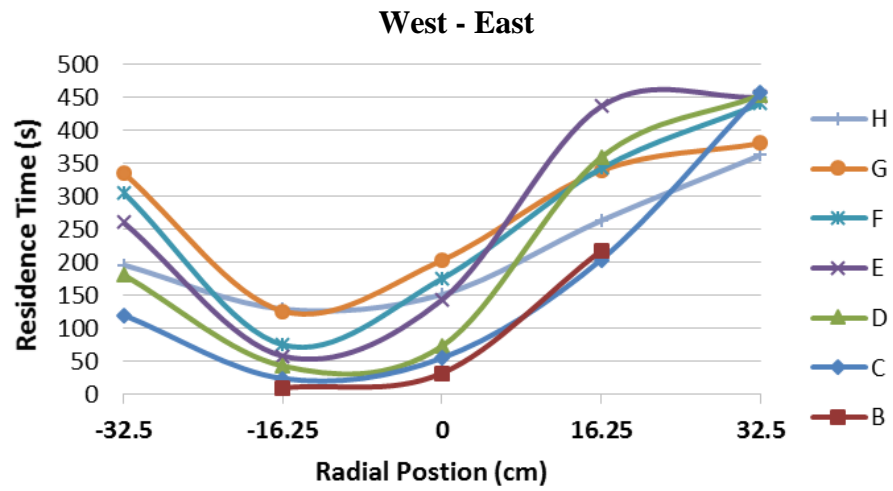
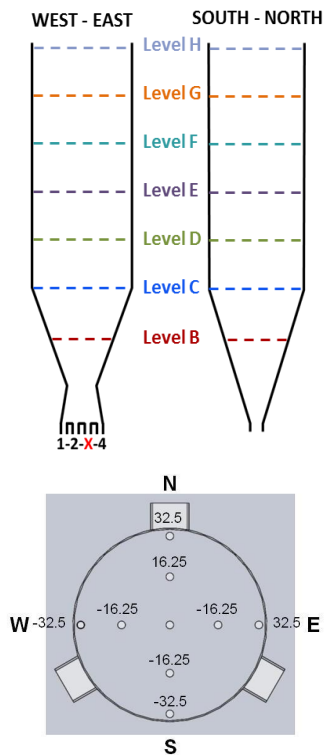


Figure 6.25 Outlets 1 and 2 - No Insert

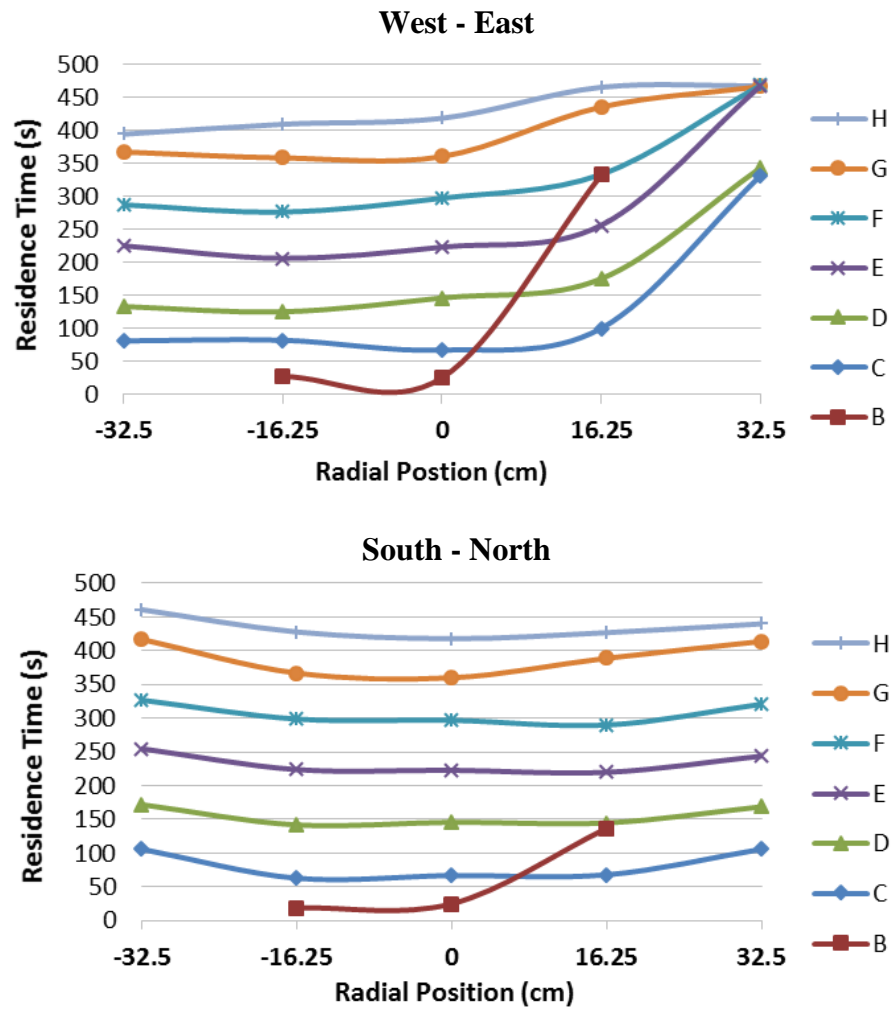
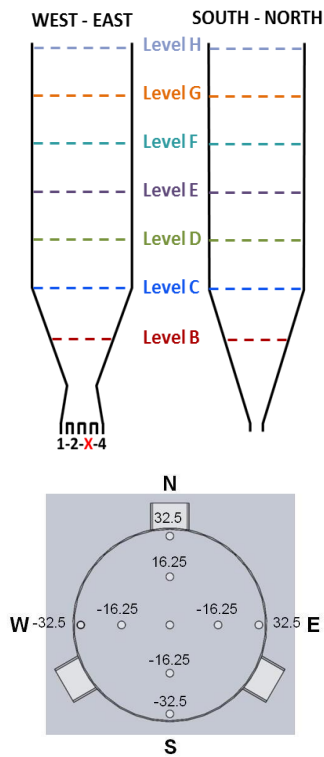


Figure 6.26 Outlets 1 and 2 - With Insert

The results analysed above are the most relevant regarding the operation of the industrial silo, because during normal operation only one outlet is operated at a time. However, it is also possible that more than one outlet could be operated simultaneously and for that reason tests were also carried out discharging through different outlet combinations.

Figure 6.25 presents the results obtained when discharging through outlets 1 and 2 when there was no insert installed. With these two outlets open the discharge from the silo was expected to still be unbalanced because both outlets are on the west side of the West-East plane. On the South-North plane the results showed that a slight improvement was obtained by discharging through two outlets instead of one, most of the tracers followed a first in first out discharge, except those placed near the wall of the north side. However, the velocity differences across the plane were significant with the material along the centre of the silo moving considerably faster than the material near the walls. The plane West-East shows a more marked difference between the behaviour of the tracers across the silo, with the formation of a preferential channel on the west side and material remaining stagnant on the east side. Overall, the discharge behaviour was very similar to the silo discharging just through outlet 2 but with a wider preferential channel.

The results obtained by fitting the insert and discharging through outlets 1 and 2 (Figure 6.26) show that a very similar performance was achieved to the tests discharging through outlet 4. Mass flow was achieved for most of the discharge with fairly small velocity differences across the silo, except for the material near the wall of the east side where movement was significantly slower. Towards the latter part of the discharge, the material near the wall on the east side stopped moving altogether which can be observed from the residence time of the last tracers to come out from the silo.

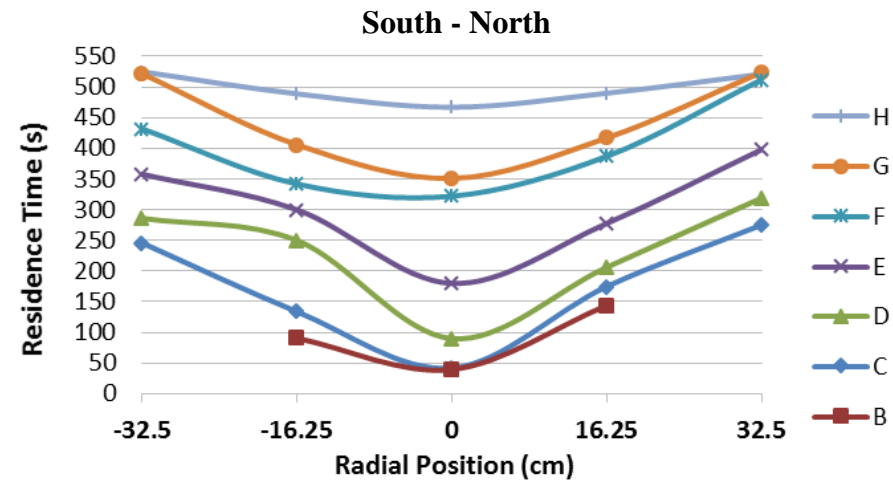
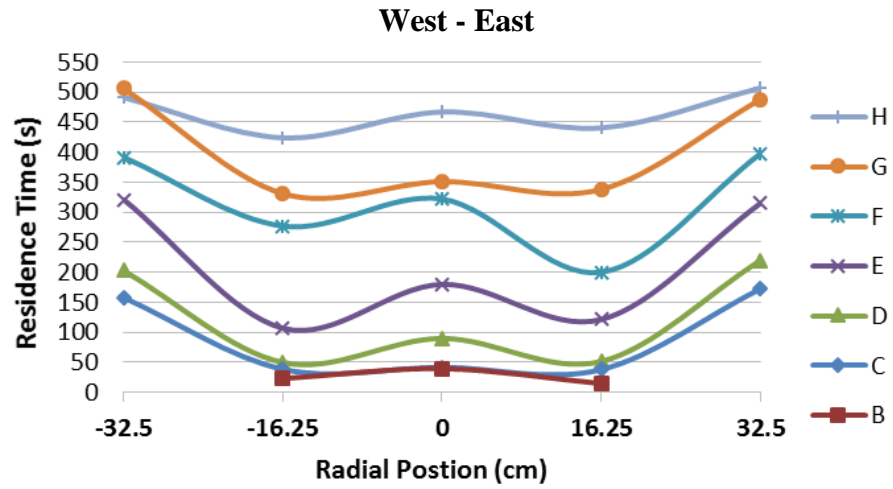
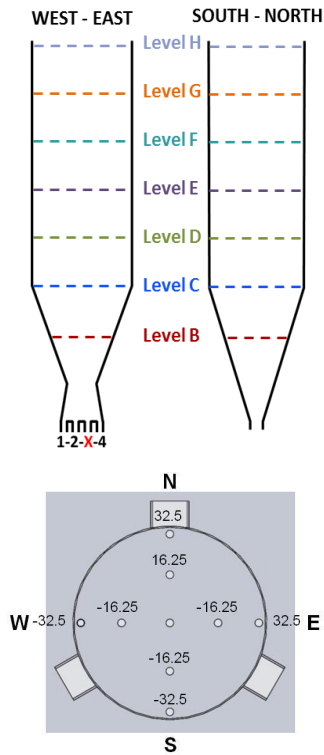


Figure 6.27 Outlets 1 and 4 - No Insert

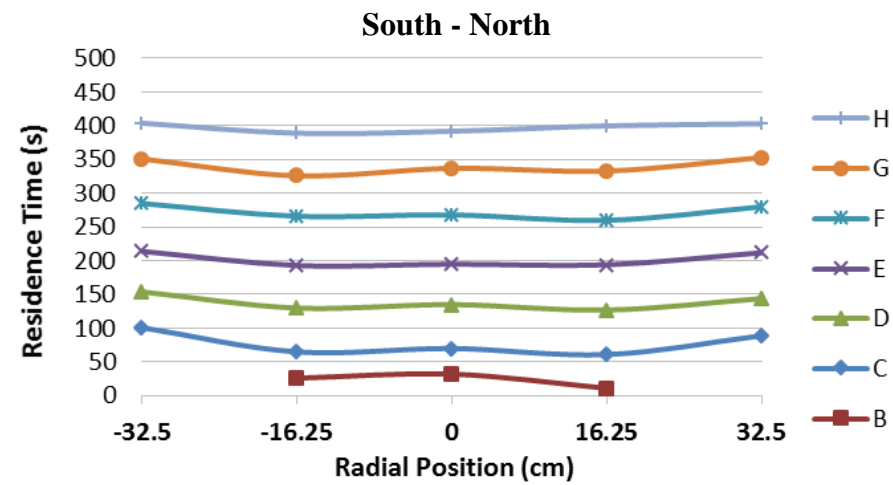
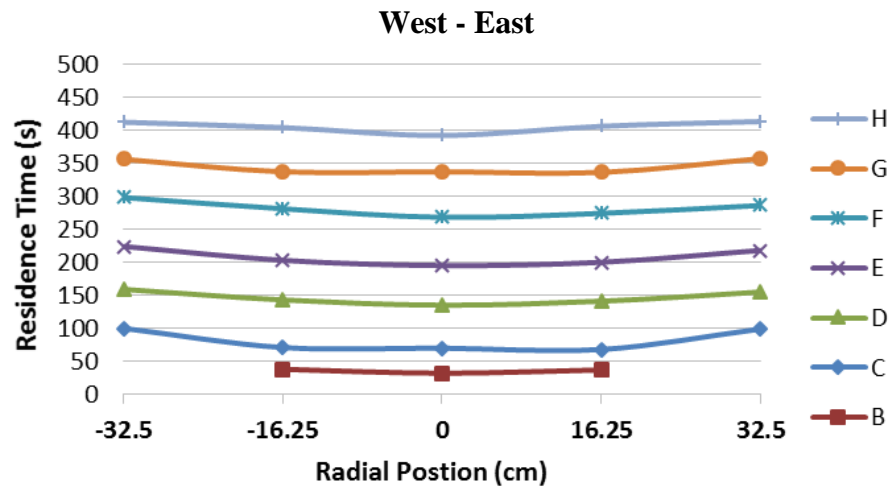
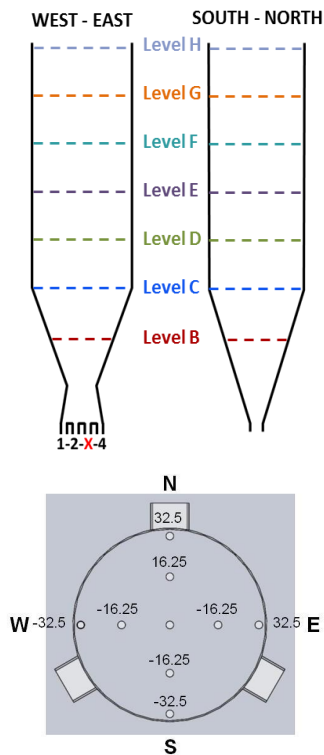


Figure 6.28 Outlets 1 and 4 - With Insert

The following set of tests were undertaken discharging through outlets 1 and 4 without an insert in the silo and the results are presented in Figure 6.27. By having one open outlet on each side of the silo a completely different pattern is obtained during discharge. From both planes it can be observed that mass flow was achieved in the silo with all tracers following a first in first out pattern. However, the velocity differences across the silo are considerably high on both planes with the material in the intermediate position of the plane West-East moving fastest of all, with the slowest being the material near the wall on both planes. By opening outlets on both sides the flow channels produced intersect allowing the contents of the silo to discharge in a more uniform manner. The installation of the insert improved further the discharge pattern in the silo as shown in Figure 6.28. The pattern obtained closely approximates an ideal mass flow, where the velocity profiles across the silo are completely flat. In this case, the residence times measured on tracers placed at the same level showed very small differences producing almost flat profiles.

Very similar results are also obtained when the silo is discharged through outlets 2 and 4, one on each side on the silo and when the silo was allowed to discharge through all the three outlets. During the discharge without an insert, mass flow was achieved but with considerable velocity differences as shown in Figure 6.29 and Figure 6.31, whereas an almost ideal mass flow pattern was achieved when the insert was installed as shown in Figure 6.30 and Figure 6.32, with residence time profiles almost flat.

Overall, the installation of the insert proved to be an effective solution to improve the discharge performance of the silo. This was most evident when the silo discharged through only one outlet which is the case that best represents the actual mode of operation of the industrial silo. The design of an insert for the full scale silo has been provided to the sponsoring company and its construction and installation is to be decided internally. It is worth remembering that the tests were undertaken after removing the fines from the test coal to avoid flow stoppages in the test silo. The material including the fines is more cohesive and it is likely that the width of channels formed internally might be less than with the screened material. In any case it is expected that the insert once installed in the full scale silo will improve the consistency of the bulk density of the coal discharged.

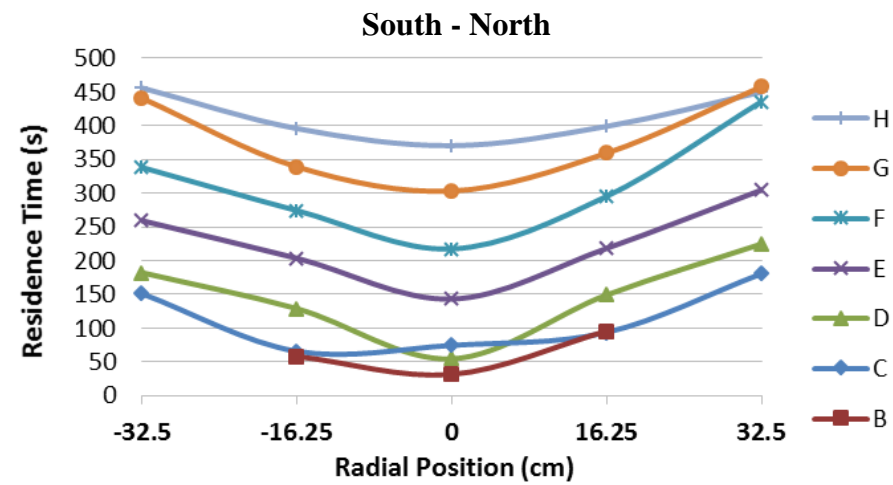
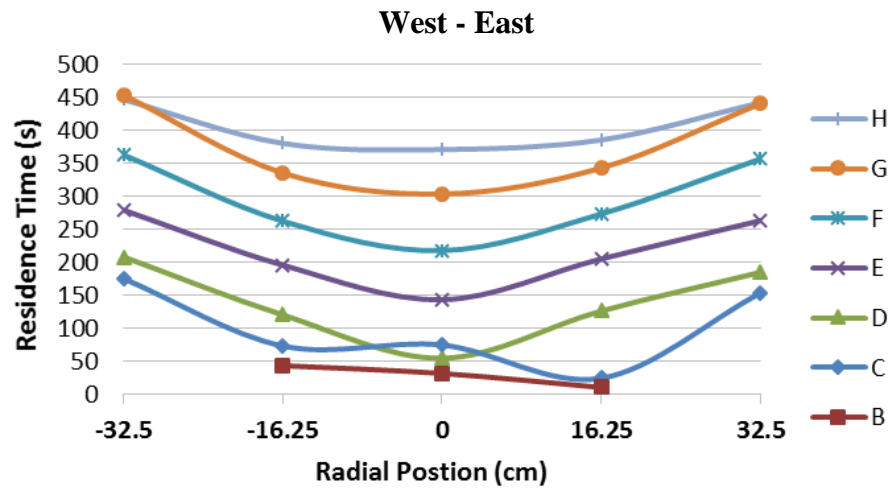
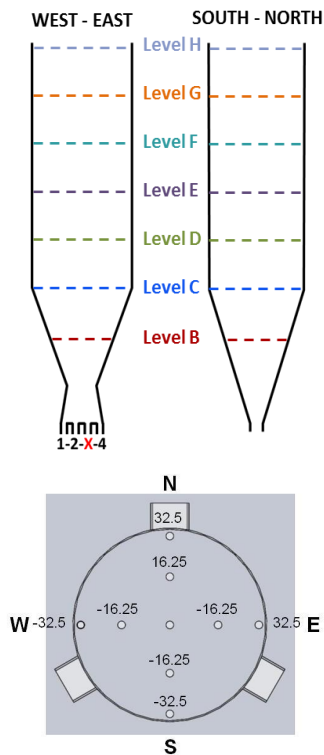


Figure 6.29 Outlets 2 and 4 - No Insert

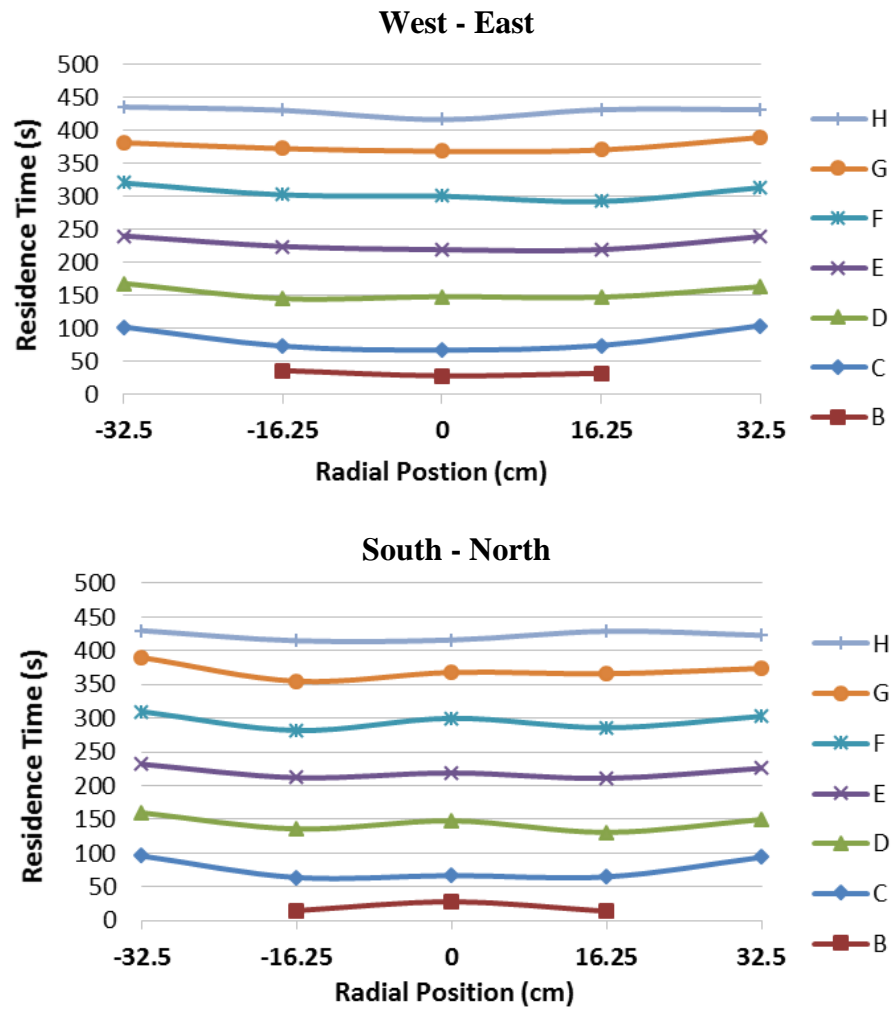
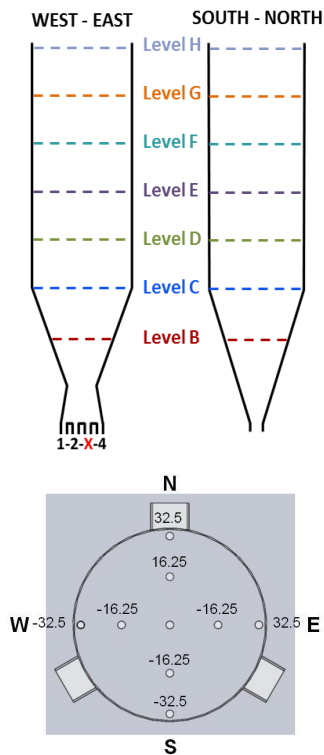


Figure 6.30 Outlets 2 and 4 - With Insert

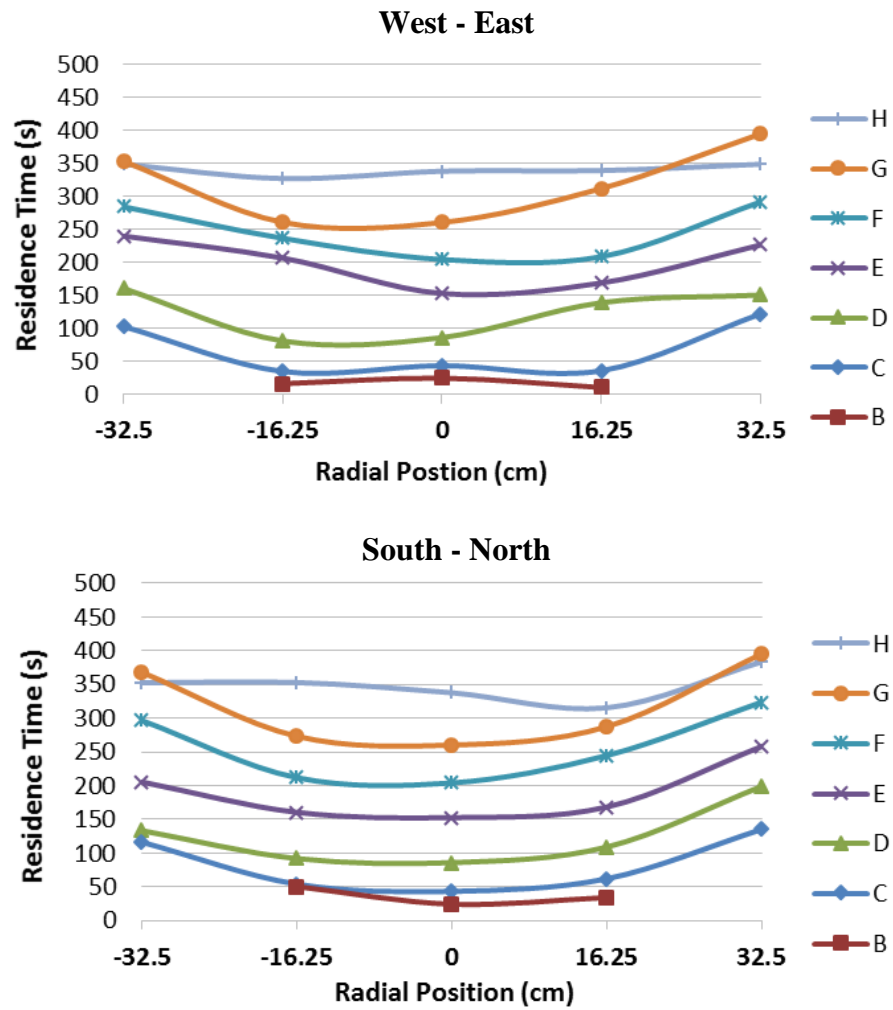
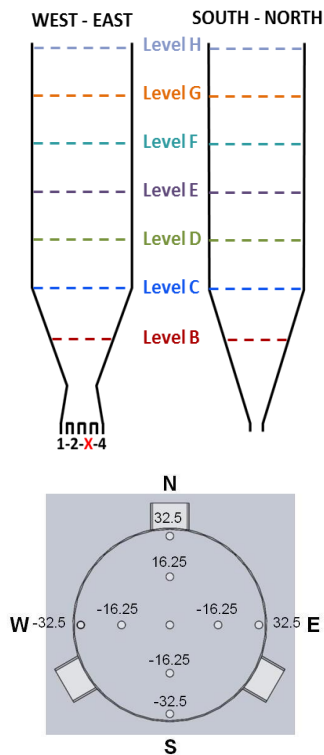


Figure 6.31 Outlets 1, 2 and 4 - No Insert

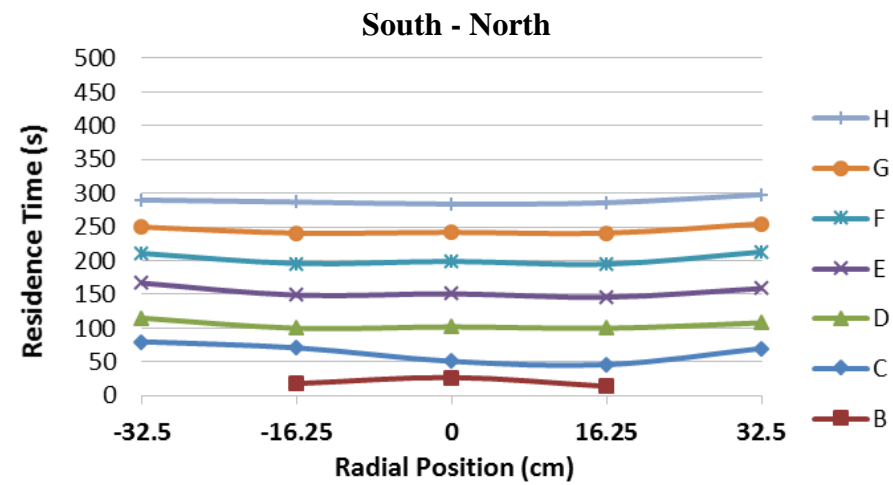
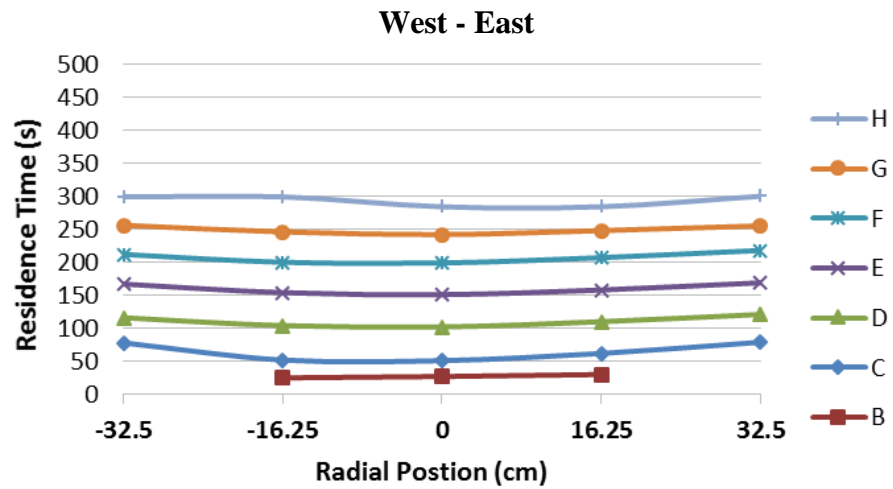
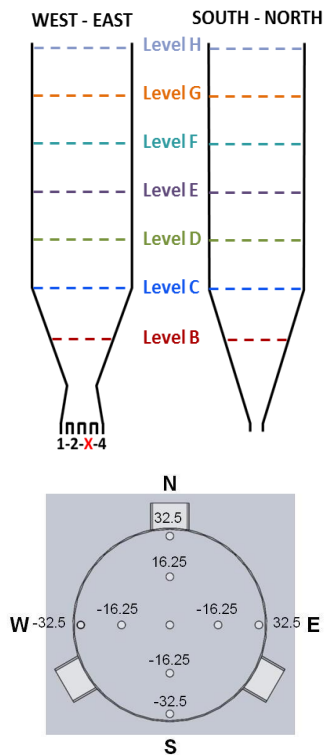


Figure 6.32 Outlets 1, 2 and 4 - With Insert

## 6.2 Rat-Holing in Conical Hopper

### 6.2.1 Description of the Process

The demand of precious metals to the world market is supplied through two main industrial processes, mining and waste material recovery. In a precious metals recovery process from waste, the materials are first milled and sampled to determine their value, smelted to obtain a rich metal alloy and then hydro-chemically refined to separate each precious metal. As part of a UK precious metal refining process, a ceramic material containing precious metals is stored in a silo and transferred to the top of the smelting furnace via vacuum conveying where is then fed by gravity.

The silo has been reported to develop rat-holes during discharge (as shown in Figure 6.33) affecting the feeding of the furnace and extending the duration of the smelting process, therefore reducing productivity. The silo has a capacity of 3000 kg of material but it is not normally allowed to empty below 1000 kg otherwise the rat-holing problems are increased, this reduces the effective capacity of the silo which increases the frequency of non-added value tasks as the silo needs to be manually filled more often. When a rat-hole develops in the silo, the operators have to manually disturb the bed of powder by poking the material with a steel bar from the top of the silo, creating unnecessary health and safety risks.



*Figure 6.33 Rat-Hole Observed in the Storage Silo*

The silo (as shown in Figure 6.34) is made of mild steel and has a cylindrical vertical section of 1000 mm height and 1360 mm diameter, with a 30° half angle conical hopper converging to a 90 mm diameter outlet, which is interfaced to the pneumatic conveying system using a feeding elbow. At the top of the vertical section a 50 mm grid is welded to stop tramp material getting into the silo, which is filled using bulk bags.

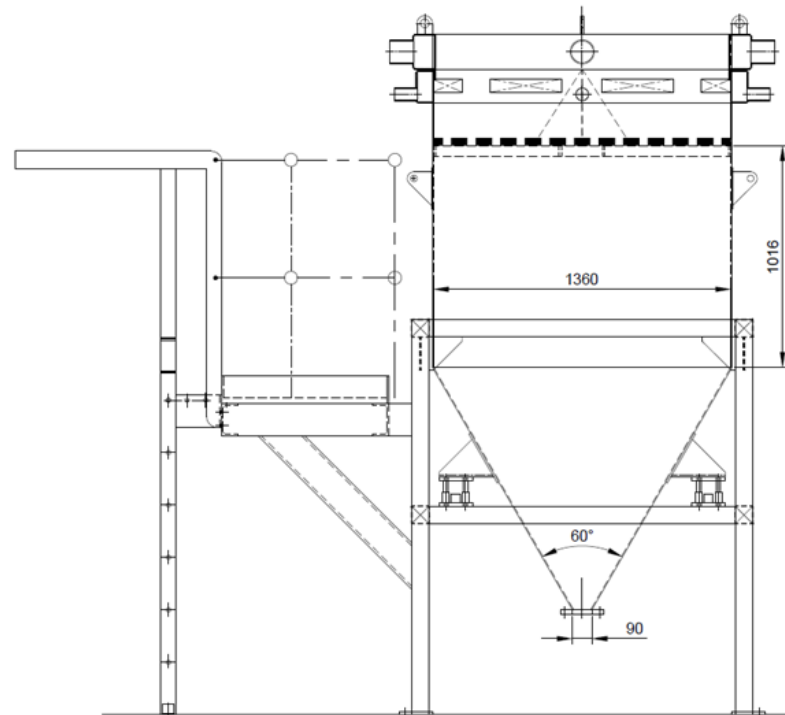


**Figure 6.34** Storage Silo for Precious Metals Refining

### 6.2.2 Insert Design

The material stored in the silo is highly abrasive due to its ceramic composition and the angular morphology resulting from the milling process. This fact, combined with the desire to empty the silo on a regular basis, suggest that achieving mass flow would not be necessary, all that is needed is to provide a reliable discharge of material into the pneumatic conveying line. For this reason, it was decided to employ insert technology to expand the flow channel in the silo beyond the rat-holing dimension of the material in order to achieve reliable core flow. The flow properties of the material were measured using a Brookfield Powder Flow Tester and the rat-hole dimension of the material for the silo described above was determined following

Jenike's procedure for reliable core flow silo design [Schulze, 2008<sub>1</sub>, Arnold, 1979], the silo design for mass flow was also carried out as it was needed for the design of the insert and the results are presented in Table 6-1.

**Table 6-1** *Silo Design Results for the Ceramic Material Containing Precious Metals*

<b>Critical Rat-Hole Dimension (mm)</b>	<b>Critical Conical Half Angle for Mass Flow (Deg)</b>	<b>Critical Conical Arching Dimension (mm)</b>
300	10	80

From the inserts studied along this research project, double cones offer the most benefits for situations where rat-holing is an issue. For this particular application it was decided to install a double cone designed adapting the procedure from the second generation presented in section 5.4. The procedure requires that the angle formed between the lower cone of the insert and the silo walls to be less than the conical half angle for mass flow, which was calculated as 10 as shown in Table 6-1. For this reason it was decided to design the insert so the angle formed with the silo walls was 5°, resulting in a lower cone with half angle of 25° (50° inclusive as shown in Figure 6.35). The lower cone would need to be extended until a diameter larger than the critical rat-holing dimension was reached, therefore it was decided to extend it to a diameter of 400 mm to give some safety margin over the 300 mm critical rat-holing dimension calculated for the material. The design of the insert was completed by forming the upper cone at a 30° half angle from the 400 mm diameter edge of the lower cone.

For the installation of the insert it was considered whether to gain access from the top but it would have meant to cut the welded tramp material screen and the work under confined space entrance permits. However, it was decided that it was more convenient to cut a section at the bottom of the hopper and weld flanges to both parts as shown in Figure 6.35, the insert was then supported on the conical piece removed by welding three vertical support plates separated 120° from each other. Once the insert was firmly supported in place, the two conical sections were bolted back together.

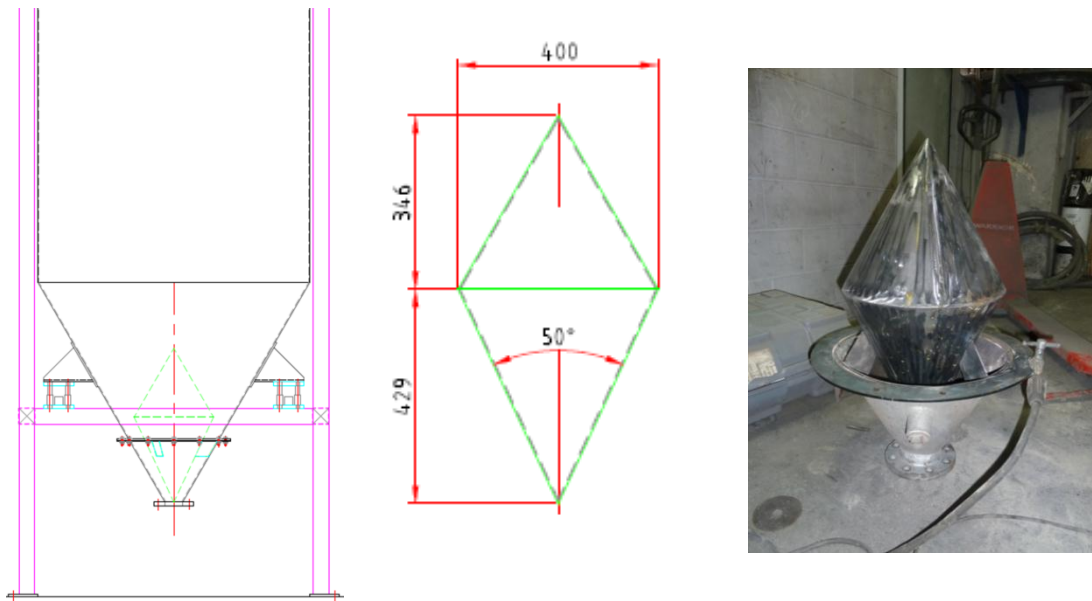


**Figure 6.35** *Insert Design*

After the installation of the insert the immediate impact on the discharge behaviour of the silo was evident. The silo could be emptied without operator intervention and the pneumatic conveying system had a constant provision of feed. As a result, the risk to injuries to operators was reduced, the productivity was increased by reducing charge times and the silo had to be replenished less often adhering to the lean initiatives of the company. After approximately three months of successful performance from the system, another two silos were also retrofitted with the double cone insert to alleviate the rat-holing problems reported.

### **6.2.3 Problems Encountered with the Performance of the Inserts**

#### **6.2.3.1 Incorrect Insert support**

Shortly after the two additional silos were fitted with the inverted cones, one of them was reported to develop multiple rat-holes, affecting the productivity of the process and requiring manual intervention from the operators to force the material to flow. After inspection, it was noticed that material was held on three places around the insert separated at approximately 120° (Figure 6.36 shows material retained at two places around the insert).



**Figure 6.36** *Material Held Around the Insert*

It was decided to remove the lower hopper section in order to investigate further the cause of the material holdups. After removing the section where the insert was mounted, the cause of the problem was evident. The double cone had not been installed as instructed with vertical supports perpendicular to the direction of flow. Instead, the support plates had been welded at angle creating sharp valleys with the walls of the insert and the walls of the silo where the material would get stuck as shown in Figure 6.37. The shape of the support plates also provided an inclined surface offering support to the powder therefore restricting flow. As a result of this, the plates created zones of stagnant material which allowed the powder to consolidate and form stable rat-holes. One of the support plates had also bended slightly altering the original position of the insert and creating uneven stress distribution worsening the conditions for flow.



**Figure 6.37** *Insert Supports Restrict Flow*

To solve the problem, the support plates were removed and replaced using vertical supports perpendicular to the direction of flow and with a knife edge on the upper surface as shown in Figure 6.38. After the insert supports were repaired, the double cone was fitted back into the silo and flow irregularities have not been reported since then with the silo being able to be fully emptied without operator intervention.



**Figure 6.38** *Insert Supports Perpendicular to Flow*

### 6.2.3.2 Chemical Attack to Insert Surface

After approximately six months from the moment the first double cone insert was fitted, rat-holing issues were reported in that first silo. Inspection from the top of the silo showed that material was flowing through a preferential channel on one side of the hopper, which then developed into a rat-hole when the inventory level in the silo decreased. It was then decided to remove the hopper section where the insert was supported, but after the connection to the pneumatic conveying line was disassembled, the first problem was observed. The outlet of the hopper and the feeding elbow from the pneumatic conveying line had been joined using a very poorly made gasket, which protruded into the flow channel partially blocking the flow path of the material as shown in Figure 6.39a. In that figure, which was taken looking up through the outlet of the silo, it also can be seen an amount of material firmly lodged between the insert and the hopper wall, stopping a flow on that side of the silo. After removing the insert and clearing the powder blockage, it became evident that both the insert and the hopper walls were seriously corroded (as shown in Figure 6.39b) producing a very rough surface which would be detrimental for flow, providing support for the powder bed. Further investigation uncovered that a couple of lots of material had been fed to the silo with very high moisture content, as a result of rain water ingress due to faulty storage containers. The water dissolved some components of the feed powder increasing its corrosivity, resulting in chemical attack to the insert and hopper walls.



*a.*

*b.*

**Figure 6.39 Corroded Insert**

To solve the problem and avoid a similar scenario in the future, it was decided to replace the insert and the lower section of the hopper with another set made with stainless steel. By changing the wall material to stainless steel and providing a better surface finish (2B), the wall friction was reduced which increased the critical angle for mass flow from  $10^\circ$  to  $15^\circ$ . This allowed the use of a larger angle between the lower cone of the insert and the hopper walls, which was increased from  $5^\circ$  to  $10^\circ$  degrees as shown in Figure 6.40. This also created a wider annulus between the insert and the hopper wall, reducing the possibility of material arching between the two surfaces. At the time this thesis was completed, the insert and hopper section were under construction.

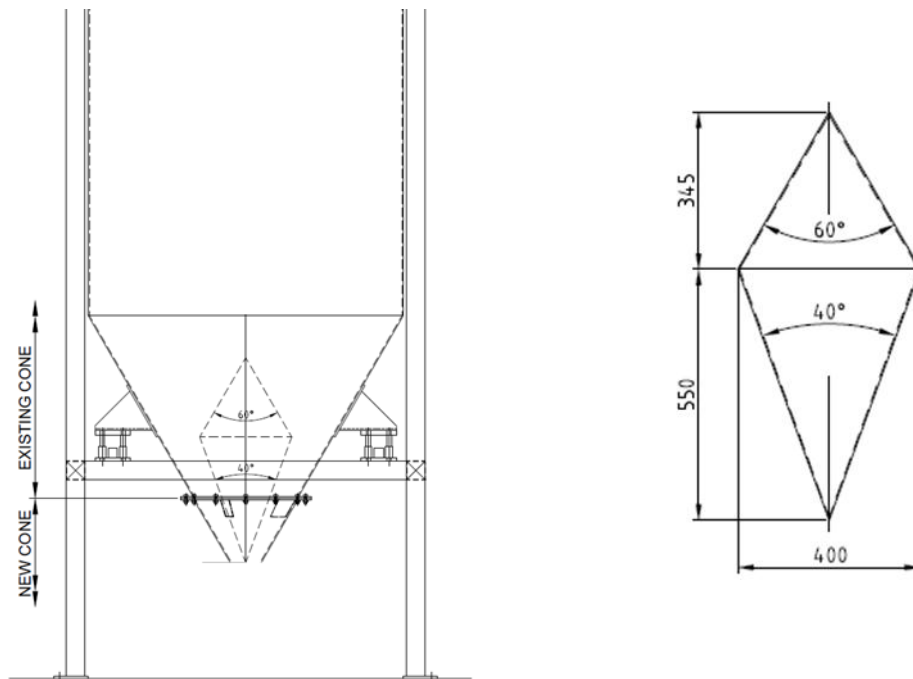


**Figure 6.40** *Stainless Steel Modification*

### 6.3 Low Headroom Drum Tipper

#### 6.3.1 Description of the Process

As mentioned in the previous section, the first step in the industrial process for the recovery of precious metals from waste material is the evaluation of their content of recoverable metals. This determines the worth of the materials and also defines the

appropriate refining process route. Materials to be evaluated are received in different physical forms such as powders, pastes, slurries, whole or broken pieces (anything from 1 mm to 500+ mm) and job sizes can vary from a few grams to several tens of tonnes. For the materials to be evaluated they first need to be converted to fairly dry and fairly fine powders, this could involve processes like drying, crushing and milling depending on their original form. Then, depending of the weight of the jobs, material characteristics and expected precious metal contents, different sampling methods (not discussed for confidentiality reasons) might be selected to produce a representative sample for the final metal content assaying.

As part of this process, the author has designed and built a cascade system for the mechanical sampling of material stored in drums (typically 45 gal drums). Although due to confidentiality reasons the sampling rig cannot be described in this thesis, an exception has been made on one of its components which incorporates a direct application of the main research subject of this project.

### **6.3.2 Drum Tipper and Insert Design**

One of the most complex aspects of the design of the sampling rig was the feeding system. The author faced several challenges due to the strict requirements of the process and the location of the rig, these included very limited headroom, high containment, minimum segregation, constant flow rates, minimal material retention, ease of cleaning after each job, ability to discharge through two stations and ability to handle a vast number of different materials.

The first step taken was to characterise the materials to be handled, which in itself presented the author with a big challenge. Due to the waste nature of most of the materials processed each job could be considered as unique, this meant that in order to produce a robust design each material had to be individually tested which would have made the design task impossible. Instead, over 30 samples were obtained from the types of material that from experience were considered difficult to handle. Then, each sample was characterised using a Brookfield Powder Flow Tester and a silo design was produced for each of them. In order to produce a robust system for

reliable flow the discharge equipment needed to be capable of avoiding flow stoppages (cohesive arching and rat-holing) and ideally produce a mass flow discharge pattern. From the silo design undertaken for the test samples, the largest critical arching dimension calculated was in the order of 190 mm whereas the steepest conical half angle to achieve mass flow was in the order of 8°.

The top of the sampling rig consisted of two discharge stations of which one used a rotary valve and the other a vibratory feeder. The overall height available between the discharge stations and the existing overhead crane was in the order of 2200 mm. Transport equipment such as screw elevators, bucket elevators, belt elevators and pneumatic conveying systems were discarded mainly due to material retention and ease of cleaning as it needs to be remembered that in this type of industry a few grams of material left in the equipment can have a big financial impact. Also, it was likely that two sets of equipment would have been needed, one for each discharge station increasing considerably the capital costs involved. Instead, it was decided that a drum tipper would be used, which could be transported to either discharge station with the help of the overhead crane. However, the design of a drum tipper was not straightforward either due to the height restrictions of the system.

The drum tipper had to provide means of interfacing the drum to the feeders in the discharge stations. In order to avoid flow unreliability issues a hopper interfaced to these two type of feeders needs to have a circular or square outlet which meant that a conical, pyramidal or double plane flow hopper had to be used. However, due to the steep geometry needed to support mass flow (i.e. 8° for a conical hopper) a simple convergence between the drum and the feeders would have not been achievable within the available height. Therefore it was decided to apply insert technology to try to obtain a discharge pattern as close as possible to mass flow within the headroom available. The solution was based on a drum tipping frame used for other processes within the company which was redesigned to improve discharge performance. The main components of the drum tipper are: a support frame which can be handled either by a forklift truck or by a crane, a conical hopper with a double cone insert and a pneumatic slide valve. When a drum needs to be charged, it is placed onto the rollers at the base of the support frame and secured in place with a side chain (see Figure 6.41). Then using compressed air, an airbag under the rollers is inflated lifting

the drum and locking it against the discharge cone providing a tight seal. After ensuring that the slide valve is closed, the frame is rotated 180° using a forklift truck with rotating forks. The drum tipper is then lifted using the overhead crane onto the required discharge station where it can be unloaded after opening the slide valve.

It is important to discuss some design features of the tipper besides the double cone insert. As it can be seen from Figure 6.41 the outlet of the discharge cone is 200 mm which ensures cohesive arching is avoided according the material characterisation and silo design undertaken for the multiple feed samples. Also, as one of the discharge stations uses a rotary valve, a stand pipe had to be added at the end of the discharge cone to ensure the whole of the discharge outlet is activated avoiding the formation of stagnant zones of material in the cone and drum. It is a known fact that rotary valves create preferential flow channels as the rotor pockets are filled before they complete their travel over the entire outlet of a silo as shown in Figure 6.42a. A stand pipe can solve this issue by allowing the expansion of the flow channel before it reaches the outlet minimizing the amount of stagnant material, as shown in Figure 6.42b.

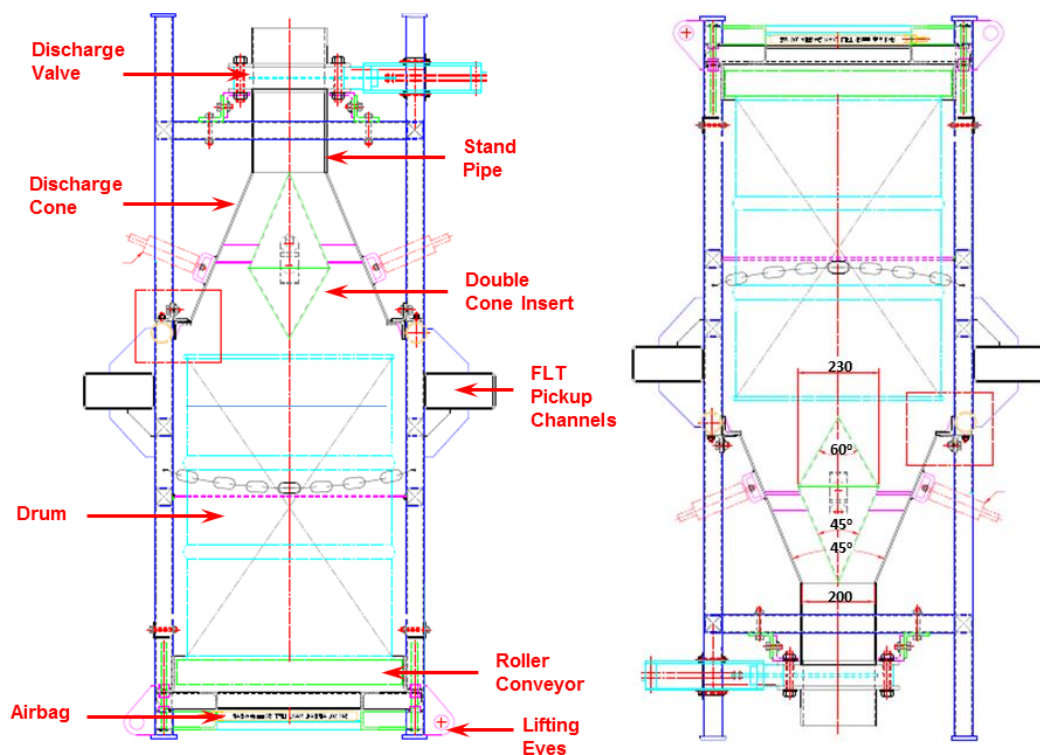


**Figure 6.41** Drum Tipper with Double Cone Insert

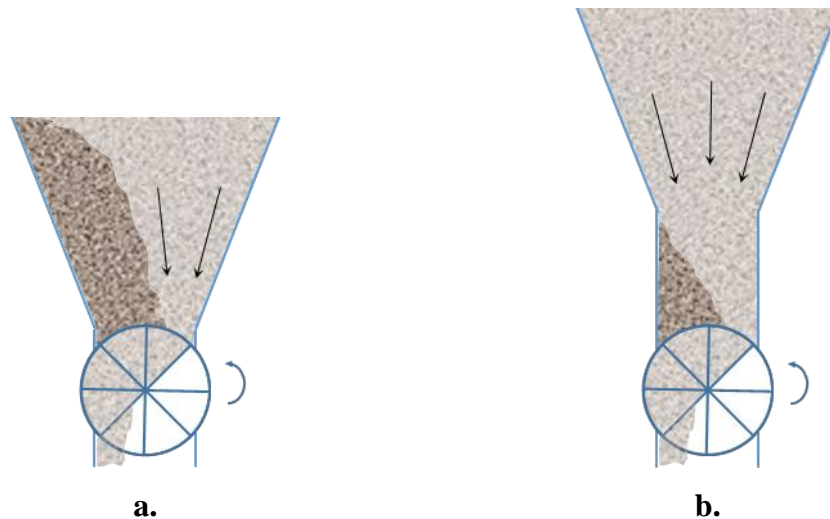


**Figure 6.42** Use of Stand Pipes Above Rotary Valves

The discharge cone was designed as steep as the remaining headroom allowed, resulting in a half angle of  $22.5^\circ$  from the vertical which was clearly not steep enough to support mass flow. Then, looking to improve the performance of discharge a double cone insert was added adapting the procedure from the second generation presented in section 5.4. Please note that according to the procedure the upper part of the insert should be designed to protrude beyond the transition from the cylindrical to the conical section. However, in this case that was not possible due to the small clearance between the drum and the discharge cone because if the insert protruded as recommended by the procedure, the apex would impede the locating of the drum under the cone. This imposed an upper limit for the apex of the insert which was kept at the same height as the edge of the discharging cone. For the lower cone the angle between the insert was kept at  $0^\circ$  to maximize the diameter of the insert, which could have been smaller than the outlet of the discharge cone if an angle  $> 0^\circ$  would have been used. This should be avoided because if the insert is smaller than the outlet, some of the material will have an unrestricted path towards the outlet potentially creating preferential draw channels. It is likely that reduction in size of the insert will reduce its effectiveness to minimize the velocity gradients during discharge. Nonetheless, it is still expected that that the insert will improve the uniformity of the discharge, reduce segregation and minimize the consolidation of the material near the outlet, particularly the moment the tipper is rotated and the contents of the drum fall into the discharge cone.

At the time this thesis was completed, the sampling rig (including the drum tipper) had been completely installed and commissioning was due to be started.

#### **6.4 Summary**

This chapter presented three industrial processes where insert technology could be used to improve the discharge performance of handling equipment. The first case study comprised a 650 tonne silo storing granular coal, which had been reported to exhibit an unreliable flow rate and changes in the bulk density of the coal. The silo featured four outlets one of which was permanently blocked and the others were operated independently. To study the discharge behaviour of the silo, a 3 litre bench scale model was built. As expected, the silo was found to develop a narrow discharge channel above the open outlet, this type of core flow behaviour was thought to be the cause of the problems experienced on plant. The type of geometry of the silo did not allow the use of one of the inserts described in previous chapters and a new approach had to be taken. Several alternatives were tested and the one that gave the best results was developed further. The solution proposed consisted of using inserts to make the coal flow channel develop from a point independent of which outlet is being discharged to minimize the effect of having only one outlet open. For this purpose an internal trouser leg was installed. With the insert in place the flow channel was expanded until it touched the walls of the silo allowing most of the material in the cylindrical section of the silo to discharge in a mass flow-like pattern. In order to validate the results at a larger level, a 1:10 scale model of the silo and insert was built. The model was commissioned using a sample of coal from the industrial silo to which the fines were removed to avoid flow stoppages. The results showed that the insert effectively changed the flow pattern in the silo from core flow to either mass flow or expanded flow, which should solve the problems experienced in the industrial plant.

The second case study consisted of a conical silo feeding a pneumatic conveying system which had been reported to present rat-holing, affecting the productivity of the plant. To avoid the formation of a rat-hole, a double cone insert was designed and installed. The impact was immediate solving the rat-holing issues and based on that

similar inserts were installed in another two silos. One of the additional inserts was mistakenly installed with supports that interfered with the flow of material and ultimately worsened the rat-holing problem. To solve this issue the supports were replaced, eliminating the flow problems observed. Another issue was experienced with the first insert installed, after it became corroded by the material that had unexpectedly been contaminated with water. This produced very rough surfaces which promoted arching of the material between the insert and the hopper. To solve this problem it was decided to replace the original mild steel insert with one made of stainless steel.

The third case study consisted in the design of a drum tipper capable of handling a large number of different materials, under very restricted headroom conditions and minimizing segregation of the material handled. The silo design undertaken for multiple samples of the materials to be handled, showed that it was not possible to use a hopper designed for mass flow within the headroom available. For this reason it was decided to use a double cone insert as part of the design in order to produce a flow pattern as close to mass flow as possible.

## CHAPTER SEVEN: CONCLUSIONS

---

### Early Test Rig Development

- The maximum load exerted on an insert is applied immediately after the silo starts discharging. When a silo is filled the direction of the major principal consolidating stress is mainly vertical near the axis of the silo where the insert is likely to be located. When the outlet of the bin opens and the discharge starts, the material moves downwards through a reducing transversal area forming a transitory arch which collapses to produce flow. As a result, the material is compacted in the horizontal direction and dilated in vertical direction changing the direction of the major consolidating stress which becomes almost horizontal. This effect propagates upwards as the material starts moving until it reaches the vicinity of the insert where the material around the insert forms an arch. This arch is supported on the edge of the insert and part of the load acting on the arch gets transferred to the insert reaching the maximum value of load exerted.
- Although for slender silos the maximum vertical stress is regarded as independent of the head of material, when the height of the vertical section of the silo is not much bigger than its diameter (less than three times), the vertical stress becomes a strong function of the head of powder. In general, it could be concluded that, for this type of silo, the lower an insert is placed in the hopper the higher the force exerted on it. However, if the insert is lowered beyond a certain point, the walls of the convergent hopper support some of the material around the insert and the exerted force decreases, as it is shown by the results obtained from the tests using a hopper with a vertical section length equal to half its diameter.
- If an insert placed deep in a silo is to be supported from the top of the silo the side loads acting on the insert will need to be taken into account. If the support provided is not stiff enough to withstand the bending moment

produced by the sides forces exerted on the insert, the location and effectiveness of the insert would be compromised. A lateral displacement of the insert will result in off centre discharge through the silo.

### **Study of Inverted Cones as Flow Promotion Inserts**

- The developed discharge pattern tracer system accurately mapped the behaviour of the solids discharging from the silos. It not only differentiated core flow, mass flow and expanded flow patterns but also identified velocity profiles across the bin. The system therefore provided a quantitative method for the evaluation and comparison of the performance of the inserts.
- An important finding, made from the tracer system data, showed that the particles passing through the annular gap between the insert and the hopper move at different speeds. The particles passing near the wall of the insert move faster than those near the walls of the hopper, which is a consequence of two mechanisms. Firstly, the wall of the inverted cone has a convex shape which facilitates the movement of material by relieving stress in the angular direction. By contrast, the hopper wall has a convex shape which compresses the material in the angular direction hindering the movement of material. Then, when the material passes through the annular gap, it finds a void space below the insert (a region of low stress) into which, it is easier to move and then continue to the outlet.
- The comparison made in a 0.4m<sup>3</sup> Laboratory scale test rig between two inverted cone inserts, one designed using a the method developed by Johanson and the other one using a modification of that method proposed in this project, showed that the modified insert was more effective at achieving mass flow in silos previously discharging in core flow. When the head of material in the silo was higher than three times the diameter of the bin, both inserts successfully converted the discharge pattern in the bin from core flow to mass flow. However, the modified insert produced a more uniform

velocity profile across the silo. The advantages of the modified insert were more significant when the head of material in the silo dropped under three times the diameter of the bin. In this case the insert designed using Johanson's method did not produce mass flow, instead it widened the discharge channel until it touched the walls of the silo obtaining an expanded flow pattern. By comparison, the modified insert successfully produced mass flow under the same test conditions. The key difference between both inserts was not only the larger size of the insert but also and probably more importantly, the higher location of its apex. This allowed changes in the stress field around the insert without compromising its performance.

- The results obtained with Johanson's insert show the effect the head of material has on the size of the region influenced by the insert, this region lies between two lines starting from the apex and the base of the insert respectively. When the head of material is large, both influencing lines touch the wall of the silo before they intersect each other, therefore the material near the wall is influenced and movement occurs. When the head of material reduces, the trajectory of the lines change intersecting each other before reaching the wall. In this case only the material in the region comprised by the intersecting lines move and the material near the wall of the silo remains stagnant.
- Both the laboratory scale rig and the bench scale rig provided evidence that hoppers operating in core flow are more prone to exhibit a preferential draw down one side, than those operating in mass flow. The results also suggested that the discharge behaviour of core flow hoppers is more sensitive to filling conditions, and consolidation. For example in core flow silos where the filling stream is not central, the consolidating stresses will be different on the side where the material enters the silo and the opposite side where the material just slides from the pile formed. In this case it is likely that the discharge channel could be off centre favouring the discharge of the material under lower consolidating stress.

## Study of Insert Configuration to Optimize Discharge Performance

- The method developed for the design of a novel open double cone insert was conceived to try to overcome the problems commonly associated with the use of inverted cones; such as preferential discharge down one side of the silo, possible rat-hole formation underneath the insert and low efficiency in silos with low height vertical sections. The profile of the insert was designed to influence the whole area inside the converging section of the bin, as opposed to inverted cones which only influence a small area of that section. The results obtained in the bench scale model showed that the open double cone not only produced mass flow in the 45° half angle hopper, but this pattern was maintained until very low values of the head of material. Additionally, the tendency to draw material down one side of the silo was almost non-existent. However, the open double cones presented two main disadvantages. Firstly the size of the insert, which could take up to 80% of the volume of the converging section of the silo, would affect the storage capacity of the bin. However, by modifying the design method, it was possible to reduce the size of the insert to only 25% of the volume of the converging section of the silo without any apparent loss in performance. Secondly, the minimum size of the silo outlet necessary for the installation of the insert has to be at least twice the value of the minimum arching dimension of the powder. With highly cohesive material this could be a limiting aspect because, in some cases, the outlet would need to be so big that the interfacing equipment could become too expensive, or would deliver material at a rate far in excess of that required.
- The design method for double cones was conceived when trying to present an alternative for improving the discharge of cohesive powders. These types of material are prone to form rat-holes when discharging from core flow bins, which would constitute a major problem if an inverted cone was installed, as the formation of a rat-hole underneath the insert could cause the blockage of the bin and using an open double cone could result in the need for additional investment in the downstream process. The main advantage of double cones is that they eliminate the possibility of rat-holing without increasing the

minimum size of the silo outlet, making downstream equipment more economic and the process more controllable. The experimental results showed that the double cones used changed the pattern from core flow to mass flow effectively. However, they also have a slight tendency to exhibit lateral discharge (observed mainly on the bench scale model) and reduced performance at low levels of head of material. Nevertheless, the lateral discharge tendency and reduction in performance with double cones were less noticeable than with the use of inverted cones at similar conditions.

- The superior performance of the open double cone insert was also validated at semi-industrial scale where that insert successfully achieved mass flow and produced the most uniform velocity profiles across the silo. The double cone and inverted cone inserts also achieved mass flow, with the double cone producing smaller velocity differences than the inverted cone.
- In addition to the visual results, the inserts were also evaluated comparing the average discharge rate of the silo and the variation in the instantaneous discharge rate. In general, mass flow silos discharge at a lower rate than core flow silos. This is due to material in mass flow silos discharging more compactly and with less air penetration that delays the expansion of the particles. The results showed that open double cones and double cones produced the lowest flow rates as well as the least variation in the instantaneous discharge rate. The results obtained from the inverted cone were in fact very similar to the silo discharging without fitted inserts, which is explained by the fact that the material fails at the annulus around the insert allowing higher interaction between air and the particles. Then, due to the void space under the insert the particles have more space to accelerate and reach a higher speed before getting to the outlet. Therefore the hopper section underneath the inserts behaves in a similar way to a core flow hopper. A comparison of the performance of the inserts evaluated is shown in the table below.

### *Insert Performance Comparison*

	No Insert	Inverted Cone Inserts	Double Cone Inserts	Open Double Cone
<b>Effectiveness to Achieve Mass Flow in Silos with Shallow Hopper Half Angles</b>	N/A	7	9	10
<b>Effectiveness to Achieve Mass Flow Under Low Values of Head of Material</b>	N/A	6	7	9
<b>Consistency of Discharge Rate</b>	3	4	10	10
<b>Central/Symmetric Discharge Rather than Eccentric Discharge</b>	3	7	8	10
The scale 1-10 is a qualitative scale where 10 represents the best performance				

### **Industrial Applications**

- The case study of a 650 tonne conical to plane silo with multiple outlets shows an excellent example of a hopper that was designed to operate in mass flow, but the actual operation occurs in core flow producing flow reliability problems due to inappropriate feeder interfacing. The silo is cylindrical with a conical converging section which is transitioned into a wedge hopper and is used for storing granular coal. Four circular outlets were equally spaced along the slotted bottom of the wedge hopper, but one was permanently blocked. According to flow property measurements, the geometry of the vessel should be capable of achieving mass flow, if material was drawn over the entire length of the slot, instead the silo is operated by discharging from one outlet at a time and it has been reported to exhibit an unreliable flow rate and changes in the bulk density of the coal. When the operation of the silo was replicated by means of a bench scale model and a 1:10 scale model, a flow channel was observed to appear above the outlet that was opened. This confirmed that a core flow pattern developed in the silo due to inappropriate interfacing.
- The complexity of the silo geometry was unsuited to any of the inserts previously studied. Nevertheless, the understanding of insert technology provided the basis for the design of a non-conventional type of insert to try to modify the discharge pattern in the silo. The open trouser leg insert,

designed and evaluated at bench scale and 1:10 scale, changed the flow pattern in the silo from core flow to expanded flow. This would allow an even draw of material in the majority of the silo, which would allow the powder a longer settling time in the silo, so that discharged material could have more uniform flow properties.

- The practicality of the design procedures proposed in this project was demonstrated in an industrial application to eliminate rat-holing in conical silos. Double cone inserts proved to be a powerful tool to expand the flow channel in a core flow hopper beyond the critical rat-hole dimension of the material. For that particular application mass flow was avoided due to the highly abrasive characteristics of the material and a smaller insert (than optimal for mass flow) was used instead just to widen the discharge channel.
- The mechanical installation of an inserts in a silo also plays a very important role in the performance of the system. As it was found with the installation of one of the double cones, if the mounting arms that support the insert are not installed perpendicular to the surfaces of the insert with the minimum area restricting flow, the powder would also be supported by these arms. This will create zones of static material which could promote arching and rat-holing as was experienced in the process studied.
- Chemical compatibility of the materials of construction of the inserts are key on the long term performance of the insert. If the insert is chemically attacked, the frictional properties of its surface will change most likely reducing the effectiveness of the device. The chemical degradation of the surface could provide support for the bulk solids increasing the possibility of the formation of arches and rat-holes as it was experienced with one of the double cone inserts installed.

## Original Contributions to Knowledge

The aim of the research project was to develop an understanding for the use of inserts to improve the performance from silos and from that understanding, issue practical guidelines for the design and positioning of the inserts. Chapter 2 of this thesis presented a comprehensive review of the techniques used to design flow promoting inserts. From that review it became clear that apart from inverted cones for tall silos, there were not clear guidelines available for the design of inserts to solve flow unreliability in hoppers and silos

This thesis provide the practical tools for the design of static inserts to change the flow pattern in silos from core flow to mass flow; or to expanded flow where convenient. The change in flow pattern would minimize or eliminate most of the problems associated to core flow such as segregation, rat-holing, degradation of time dependent materials, bulk density variability, flooding and flushing.

The only complete technique found in the literature was developed by J. Johanson for the design of inverted cones. The experimental work from this thesis showed that the method produced good results in tall silos with high material inventory levels ( $z/D > 3$ ). However, the effectiveness of that method was compromised when the vertical section of the silo was short with respect to its diameter or when the inventory levels in the silo fell. This thesis proposes a modification of the original method which improves the performance of the inverted cone inserts for the conditions explained above. The test results demonstrated that the modified insert could produce mass flow in silos where the original insert was no longer effective. This is important because a large proportion of silos used in industry do not provide the optimal conditions for the original insert to perform effectively.

Even though inverted cones can be regarded as effective flow promotion devices, they are not ideal for every process, like silos with very shallow convergences or systems prone to rat-holing. They also can cause other issues that might need to be avoided such as off centre discharge. In order to produce a more robust

solution for these types of systems, the author has developed a new type of static insert known as open double cone. This type of insert proved to provide the most consistent results in terms of changing the flow pattern and producing uniform discharge. One of the main advantages of this insert is that achieving mass flow was independent of the head of material in the silo, improving further the results obtained with the modified inverted cones. It was also shown that an almost ideal first in first out discharge could be achieved with the use of this insert, obtaining very small velocity differences across the silo.

The main drawback of the open double cone is that the outlet of the silo needs to be at least twice the critical arching dimension of the material, which can be problematic particularly for highly cohesive materials. As an alternative for these cases, the author also presents guidelines for the design of double cone inserts, which have the advantage (over open double cones) that the outlet of the silo needs to be only equal to the critical arching dimension of the material. These inserts also have the advantage (over inverted cones) that they can be effective solving flow issues in systems prone to the formation of rat-holes. The test results also showed that double cones produce better results than inverted cones achieving mass flow and producing more uniform discharge.

The general understanding of the use of inserts was also demonstrated through the development of a flow promoting device for an industrial silo with multiple outlets. For that case, the complex geometry of the system did not allow for one of the inserts mentioned above to be used as a solution. However, by applying the knowledge developed throughout this project, an effective solution was developed.

## CHAPTER EIGHT: RECOMMENDATIONS FOR FURTHER WORK

---

The results obtained from the bench-scale model are an important step forward, towards the application of insert technology for the improvement of discharge reliability and consistency from industrial silos. Although the guidelines for the design and positioning of the flow-promoting inserts have been provided in this project, it is imperative to evaluate the robustness of the methods proposed on an industrial scale. The first step towards that objective was already done in Chapter 5 with the insert prototypes that were tested in the semi-industrial test rig. However, it is recommended that the design techniques proposed in this thesis are tested using materials with a wide variety of flow properties. This should include highly cohesive materials which will need to be tested at larger scales in order to avoid the risk of causing blockages due to cohesive arching. Also it would be ideal to evaluate the inserts with different silo geometries, more specifically hoppers with different half angles (and wall surfaces with different frictional properties) to determine the working limits of each type of insert and the optimum solution for a given process configuration.

The second research programme that could be derived from this project should focus on the application of insert technology for the improvement of discharge from silos with multiple outlets. The work carried out in this project barely scraped the surface of the problem because the number of variables involved in the performance of this type of silos, makes each case practically unique. Nevertheless, the results obtained proved that inserts are a valid alternative for changing the flow pattern of granular material discharging from silos with multiples outlets. For this research, exploration of two different approaches is recommended: the use of inserts to achieve mass flow in silos with multiple outlets and the use of inserts to overcome rat-holing in silos with multiple outlets.

## NOMENCLATURE

---

D:	Diameter
$d_c$ :	Critical arching dimension for conical mass flow hoppers
$D_{in}$ :	Diameter of the insert
$D_{silo}$ :	Diameter of the silo
$F_{LoadCells}$ :	Traction force measured by the load cells
g:	Gravitational constant
$K_j$ :	Ratio between principal stresses
R:	Insert radius
u:	Velocity component in x direction
v:	Velocity component in y direction
W:	Annulus width between insert and hopper walls
$W_c$ :	Critical arching dimension for plane flow mass flow hoppers
z:	Head of powder
$\alpha$ :	Half angle
$\alpha_2$ :	Half angle of inverted cone inserts
$\alpha_2$ :	Hopper half angle
$\alpha_c$ :	Critical conical half angle for mass flow
$\delta$ :	Effective angle of internal friction
$\theta_r$ :	Angle of repose
M:	Coefficient of friction
$\rho$ :	Powder bulk density
$\sigma$ :	Mean stress
$\sigma_1$ :	Major principal stress
$\sigma_2$ :	Minor principal stress
$\sigma_r$ :	Normal stress on the plane perpendicular to the radial direction in a spherical coordinate system
$\sigma_z$ :	Vertical stress
$\sigma_\theta$ :	Normal stress on the plane perpendicular to the $\theta$ -direction in a spherical coordinate system
$\sigma_\phi$ :	Normal stress on the plane perpendicular to the $\phi$ -direction in a spherical coordinate system

- $\tau_{rzw}$ : Shear stress at the wall in a cylindrical silo
- $\tau_{r\theta}$ : Shear stress on the plane perpendicular to the radial direction acting in the  $\theta$ -direction in a cylindrical coordinate system
- $\tau_{r\phi}$ : Shear stress on the plane perpendicular to the radial direction acting in the  $\phi$ -direction in a cylindrical coordinate system
- $\tau_{\theta\phi}$ : Shear stress on the plane perpendicular to the  $\theta$ -direction acting in the  $\phi$ -direction in a cylindrical coordinate system
- $\varphi$ : Effective angle of wall friction
- $\omega$ : Angle between x-axis and direction of major principal stress

## GLOSSARY

---

Angle of internal friction:	Angle between the normal stress axis and the tangent to the steady flow Mohr circle
Angle of wall friction:	Angle between the normal stress axis and a line from the origin to a point on the wall yield locus
Bin:	Storage container for bulk solids
Cohesive arching:	Formation of a stable arch across a flow channel as a result of the cohesive strength of the bulk solid
Cone in cone insert:	Type of insert in the shape of a conical hopper
Core flow:	Flow pattern where parts of the contents of a silo remain static during discharge
Critical arching dimension:	Minimum outlet dimension to avoid cohesive arching in a mass flow hopper
Critical half angle:	Maximum value of a hopper half angle in order to support mass flow
Critical rat-hole dimension:	Minimum outlet dimension to avoid rat-holing in a core flow hopper
Double cone insert:	Type of static insert formed by two cones with opposing apices
Elutriation:	Separation of particles due to interaction with a gas
Expanded flow:	Particular case of mixed flow where sections of the silo are designed to produce local mass flow behaviour
Flooding:	Fluid like behaviour of a bulk solid due to high retention of gas between the particles
Flow channel:	Region of moving material in a silo during discharge
Flow pattern:	Term used to describe the bulk movement of material in a silo during discharge
Flushing:	Fluid like behaviour of a bulk solid due to high retention of gas between the particles
Funnel flow:	See core flow
Hopper half angle:	Angle formed between the hopper walls and the vertical coordinate

Hopper:	Storage container for bulk solids, although in this thesis has been mainly used to refer to the converging section of the storage container
Ideal Coulomb material:	Cohesionless material that present a linear relationship between normal stress and shear stress
Insert:	Device installed inside a silo to modify the storage or discharge conditions of the bulk material
Internal mass flow:	Particular case of mixed flow pattern where the discharge channel naturally expands until it reaches the walls of the silo
Inverted cone insert:	Type of static insert with diverging walls
Major principal stress:	Largest principal stress acting on a bulk solid
Mass flow:	Flow pattern where the entire contents of a silo are in motion during discharge
Mechanical arching:	Formation of a stable arch across a flow channel due to interlocking of particles
Minor principal stress:	Principal stress perpendicular to the major principal stress
Mixed flow:	Particular case of core flow where parts of the contents of the silo discharge is a mass flow like pattern whereas the rest discharge following a core flow pattern
Modified insert:	Inverted cone insert designed following the modified design method proposed in this thesis
Open double cone insert:	Novel type of insert developed through this research project
Plane flow hopper:	Vee shaped hopper that converges in only one plane
Powder shear test:	Practical procedure to determine the stress conditions to produce failure in a bulk solid
Radial stress field:	Theory developed by A. Jenike for the flow of granular materials in silos
Rat-hole:	Stable pipe channel formed within bulk solids stored in core flow hoppers, with the material around the channel unable to be discharged

Segregation:	Separation of particles in a bulk solid typically by particle size or particle density
Silo:	Storage container for bulk solids
Switch stress:	Discontinuity of the normal stress created by a change of direction of the major principal stress lines
Tracers:	Individually marked spheres used to deduce the flow pattern in a silo

## REFERENCES

---

- Advantech, 2015<sub>1</sub> Advantech, ADAM-4016, [http://www2.advantech.com/products/GF-5VTD/ADAM-4016/mod\\_213B0997-05D1-43C5-9830-D43A0A4C9333.aspx](http://www2.advantech.com/products/GF-5VTD/ADAM-4016/mod_213B0997-05D1-43C5-9830-D43A0A4C9333.aspx), visited May 2015
- Advantech, 2015<sub>2</sub> Advantech, ADAMView, [http://www2.advantech.com/products/1-39JG4I/ADAMView/mod\\_328DB466-4B81-4652-B8AF-F5568F24A103.aspx](http://www2.advantech.com/products/1-39JG4I/ADAMView/mod_328DB466-4B81-4652-B8AF-F5568F24A103.aspx), visited May 2015
- Arnold, 1979 P. Arnold, A. McLean and A. Roberts. Bulk Solids: Storage, Flow and Handling, TUNRA Ltd, University of Newcastle, Australia, 1979.
- Arnold, 2001 P. Arnold, Some Observations on the Application of Static Flow Promotion Devices for Discharging Bulk Solids from Bins, Proceedings of 7<sup>th</sup> International Conference on Bulk Materials Storage, Handling and Transportation. 2001
- Bates, 1997 L. Bates, Mass Flow Generator, United States Patent 5,651,479; 1997
- Bates, 1998 L. Bates, Bulk Storage Hoppers, United States Patent 5,769,281; 1998
- Bates, 2001 L. Bates, Improving Flow from Hoppers Using Inserts and Novel Wall Profiles, Proceedings of 7<sup>th</sup> International Conference on Bulk Materials Storage, Handling and Transportation. 2001
- Bates, 2010 L. Bates, S. Dhodapkar and G. Klinzing, Using Inserts to Address Solids Flow Problems, Chemical Engineering, Vol. 117, No.7, 2010
- Bates, 2012 L. Bates. Regimes of Flow in Storage Hoppers, Bulk-online, 2012, visited April 19 2012
- Bauman, 2001 I. Bauman. Solid-Solid Mixing with Static Mixers, Chemical and Biochemical Engineering Quarterly, Vol. 15, No. 4, 2001
- Beckschulte, 2013 Beckschulte Verfahrenstechnik GmbH, Discharging aids with porous stainless steel, [http://www.bv-net.de/englisch/050\\_components/05230\\_stainless.htm](http://www.bv-net.de/englisch/050_components/05230_stainless.htm), visited 18 January 2013
- BinMaster, 2013 BinMaster Level Controls, AirBrator Aeration Pad, <http://www.feedandgrain.com/product/10001137/binmaster-level->

[controls-airbrator-aeration-pad](#), visited April 2013

- Bradley, 2000 M.S.A. Bradley et al. Effects of the Properties of Bulk Solids on the Relative Performance of Polyethylene and Stainless Steel Wall Lining Materials in Mass Flow Hoppers and Other Applications, Proceedings of the Institution of Mechanical Engineers, Part E: Journal of Process Mechanical Engineering, Vol. 214 no. 1, 2000
- Brown, 1971 G.N. Brown. Gravity Flow Solids Blending, United States Patent 3,583,681; 1971
- Chou, 2006 C. Chou and J. Chang, Theoretical Wall Stresses and Insert Loads in a Bin-Hopper with a Conical Insert Using the Differential Slice Method, Advanced Powder Technology, Volume 17, Issue 5, 2006
- Coleman, 2001 C.B. Coleman. Mass Flow Bulk Material Bin, United States Patent 6,328,183 B1; 2001
- Denis, 2006 M.P. Denis. Modeles Markoviens Pour le Melange des Poudres en Melangeur Statique, PhD Thesis, Institut National Polytechnique De Toulouse, 2006
- Dewitz, 1990 T.S. Dewitz et al. Compartmented Gas Injection Device, United States Patent 4,941,779; 1990
- Ding, 2002 S. Ding, Predictions of Loads on Walls and Insert in a Gravity Flow Silo Using ABAQUS, POSTEC Newsletter, No 20, 2002
- Ding, 2003 S. Ding, Parameter Investigation of the Effect of a Double-Cone Insert on Silo Discharge Mode, POSTEC Newsletter, No 21, 2003
- Ding, 2003 X. Ding and L. Zhao. Analysis, Comparison and Selection of Wearable Liner, Sulphur Phosphorus & Bulk Materials Handling Related Engineering, Vol. 6, 2003.
- Ding, 2004<sub>1</sub> S. Ding, An Experimental Study of Effect of a Double Cone Insert, POSTEC Newsletter, No 22, 2004
- Ding, 2004<sub>2</sub> S. Ding, Investigation of Flow and Pressure in Silos During Filling and Discharging in Presence of Inserts, PhD Thesis, The University of Edinburgh, 2004
- Ding, 2005 S. Ding, Effect of a Double Cone Insert on Silo Discharge, POSTEC Newsletter, No 23, 2005
- Ding, 2008 S. Ding, G. Enstad, M. Jecmenica, J. Ooi and J. Rotter, Prediction of Flow Mode During Silo Discharge and its Preliminary Verification, Proceedings of RELPOFLOW IV, 2008
- Dirkse, 1992 H.A. Dirkse et al. Aeration Tube Discharge Control Device, United States Patent 5,129,766; 1992

- Enstad, 1996 G. Enstad, Investigations of the Use of Inserts in Order to Obtain Mass Flow in Silos, POSTEC Newsletter, No 15, 1996
- Enstad, 1997 G. Enstad, Further Investigations of the Use of Inserts in Order to Obtain Mass Flow in Silos, POSTEC Newsletter, No 16, 1997
- Enstad, 1998 G. Enstad, Use of Inverted Cones and Double Cones as Inserts for Obtaining Mass Flow, POSTEC Newsletter, No 17, 1998
- Enstad, 2008 Personal Interview with Professor Gisle G. Enstad, Norway, August 2008
- Fisher, 1977 G.W. Fisher. System for Controlling Segregation within a Bin During Material Withdrawal, United States Patent 4,030,633; 1977
- Fisher, 1985 G.W. Fisher. Flow Control Insert for Hopper Bottom Bins. United States Patent 4,548,342; 1985
- Goldberg, 1991 E. Goldberg, S. Bernes and K. McAtee. TIVAR-88 provides reliable gravity discharge form coal storage silos: A case study. Bulk Solids Handling, Vol. 11 No.1, 1991
- Gyenis, 2002 J. Gyenis. Motionless Mixersin Bulk Solids Treatments – A Review, Kona Powder and Particle, No. 20, 2002
- Hartl, 2008 J. Hartl, J. Ooi and G. Enstad, An Experimental Study of Cone-in-Cone Insert Configurations in a Full-Scale Silo, Proceedings of RELPOFLOW IV, 2008
- Hartl, 2008 J. Hartl, A study of granular solids in silos with and without an insert, PhD Thesis, The University of Edinburgh, 2008
- Horne, 1978 R.M. Horne and R.M. Nedderman, Stress Distribution in Hoppers, Powder Technology, Vol. 19, 1978
- Jackson, 1989 M. Jackson. Apparatus for Dispensing Particulate Material. United States Patent 4,854,722; 1989
- Jenike, 1961 A. Jenike. Gravity Flow of Bulk Solids, University of Utah Engineering Experiment Station, Bulletin No. 108, 1961
- Jenike, 1964<sub>1</sub> A. Jenike. Storage and Flow of Solids, University of Utah Engineering Experiment Station, Bulletin No. 123, 1964
- Jenike, 1964<sub>2</sub> A. Jenike. Steady Gravity Flow of Frictional-Cohesive Solids in Converging Cannels, Journal of Applied Mechanics, Vol. 31, 1964
- Jenike, 2008<sub>1</sub> Jenike & Johanson Inc., Binsert Retrofit Solves Segregation Problems at Owens-Brockway Glass, [http://www.jenikeandjohanson.com/pages/education/cases/glass\\_batch\\_case/glass\\_batch.html](http://www.jenikeandjohanson.com/pages/education/cases/glass_batch_case/glass_batch.html), visited June 12 2008

- Jenike, 2008<sub>2</sub> Jenike & Johanson Inc., Binsert Systems Prevents Flow Problems at Chino Smelter Modernization Project, [http://jenike.net/pages/education/cases/pdf\\_docs/22jcase.pdf](http://jenike.net/pages/education/cases/pdf_docs/22jcase.pdf), visited June 12 2008
- Jenike, 2013<sub>1</sub> Jenike & Johanson Inc., Concentrate Bins Prevent Flow Problems at Chino Mines, <http://jenike.com/case-study/concentrate-bins-prevent-flow-problems-at-chino-mines-2/>, visited March 2013
- Jenike, 2013<sub>10</sub> Jenike & Johanson Inc., Innovative Hopper Design for Decaffeinating Coffee, <http://jenike.com/case-study/innovative-hopper-design-for-decaffeinating-coffee-beans/>, visited March 2013
- Jenike, 2013<sub>2</sub> Jenike & Johanson Inc., Overcoming Poor Flow and Segregation with Dolomite, <http://jenike.com/case-study/overcoming-poor-flow-and-segregation-with-dolomite/>, visited March 2013
- Jenike, 2013<sub>3</sub> Jenike & Johanson Inc., Quality Improved with Reduced Segregation at Libbey Glass, <http://jenike.com/case-study/quality-improved-with-reduced-batch-segregation-at-libbey-glass/>, visited March 2013
- Jenike, 2013<sub>4</sub> Jenike & Johanson Inc., Minimizing Direct Compression Content Uniformity Variations, <http://jenike.com/case-study/minimizing-direct-compression-content-uniformity-variations/>, visited March 2013
- Jenike, 2013<sub>5</sub> Jenike & Johanson Inc., Problems at Owens-Brockway: Retrofit Solves Glass Quality, <http://jenike.com/case-study/retrofit-solves-glass-quality-problems-at-owens-brockway/>, visited March 2013
- Jenike, 2013<sub>6</sub> Jenike & Johanson Inc., Preventing Stuffing Mix Segregation at Kraft Foods, <http://jenike.com/case-study/solving-stuffing-mix-segregation-at-kraft-foods/>, visited March 2013
- Jenike, 2013<sub>7</sub> Jenike & Johanson Inc., Fluidized Handling of Detergent Improves Production Capability, <http://jenike.com/case-study/fluidized-handling-of-detergent-ingredient-improves-production-capability/>, visited March 2013
- Jenike, 2013<sub>8</sub> Jenike & Johanson Inc., Coal Handling Problems Solved at Northern States Power, <http://jenike.com/case-study/solving-coal-handling-problems-at-northern-states-power/>, visited March 2013
- Jenike, 2013<sub>9</sub> Jenike & Johanson Inc., Alumina Powder Silo Retrofit Improves Product Quality, <http://jenike.com/case-study/alumina-powder-silo-retrofit-improves-product-quality/>, visited March 2013
- Johanson, 1964 J. Johanson, Stress and Velocity Fields in Gravity Flow of Bulk Solids, Journal of Applied Mechanics, Vol 31, Trans. ASME, Vol 86, Series E, 1964

- Johanson, 1965 J.R. Johanson, The Use of Flow-Corrective Inserts in Bins, J. Eng. Ind., Paper No. 65-MH-1, 1965
- Johanson, 1966 J.R. Johanson and W.K. Kleysteuber, Flow Corrective Inserts in Bins, Chemical Engineering Progress, Vol 62, No 11, 1966
- Johanson, 1968 J.R. Johanson, The Placement of Inserts to Correct Flow in Bins, Powder Technology, Vol. 1, 1968
- Johanson, 1981 J.R. Johanson, Blending Apparatus for Bulk Solids, United States Patent 4,286,883; 1981
- Johanson, 1982 J.R. Johanson, Controlling Flow Patterns in Bins by Use of an Insert, Bulk Solids Handling, Nol. 2, No. 3, 1982.
- Johanson, 1989 J.R. Johanson. Solids Blender with Cylindrical Inserts, United Sates Patent 4,795,266; 1989
- Johanson, 2006 K. Johanson. Prediction of Cone-in-cone Blender Efficiencies and Scale-up Parameters From Knowledge of Basic Material Properties, Powder Technology, Vol. 170 No. 3, 2006
- Karlsen, 1998 A. Karlsen, Use of Inserts for Controlling the Flow Pattern in Silos, Telemark College, Dep of Technology, Final Year Project, 1998
- Klonteig, 1997 J. Klonteig, Control of Flow Patterns in Silos by Means of Internal Structures Placed in the Hopper. Telemark College, Dep of Technology, Final Year Project, 1997
- Ledgett, 1970 L.A. Ledgett. Material Blending Silo, United States Patent 3,490,655; 1970
- LCM Systems, 2015 LCM Systems, BF2 Stainless Steel Low Range Dual Cantilever Beam Load Cell, <http://www.lcmsystems.com/res/BF2%20Stainless%20Steel%20Low%20Range%20Dual%20Cantilever%20Beam%20Load%20Cell.pdf>, visited May 2015
- Lucas, 1968 D.H. Lucas. Granular Flow Stimulating Devices, United States Patent 3,366,282; 1968
- Martens, 1988 P. Martens and H. Franken. Silo-Handbuch, Berlin, Ernst, 1988
- Matthews, 1961 M.A. Matthews. Blending Hopper, United States Patent 2,994,460; 1961
- Matuszek, 2008 D. Matuszek and M. Tukiendorf, Application of roof shaped and double cone inserts in mixing of granular elements in the flow process, International Agrophysics, Vol. 22, No. 2, 2008
- McCandliss, E.S. McCandliss. Concrete Mixer, United States Patent 1,224,656;

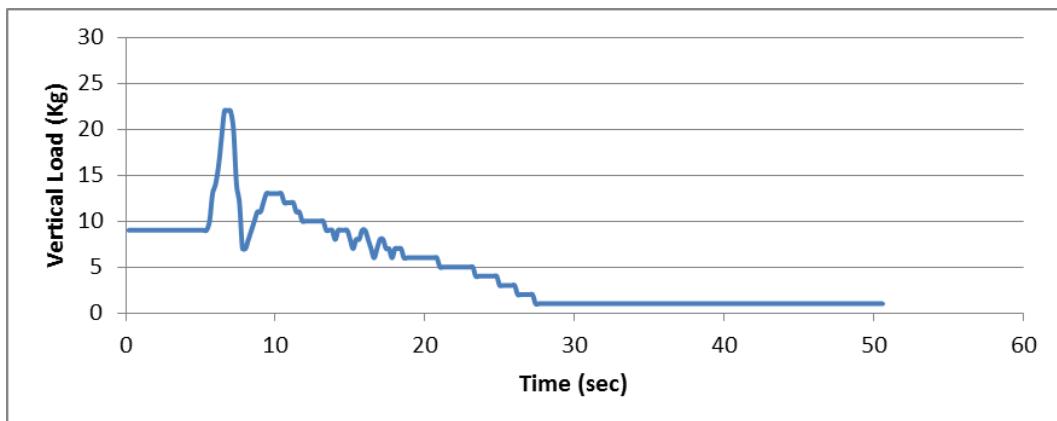
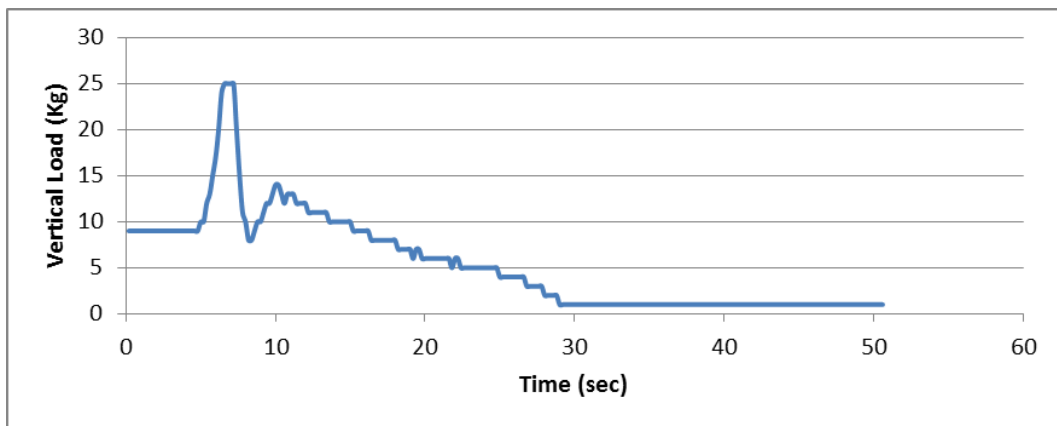
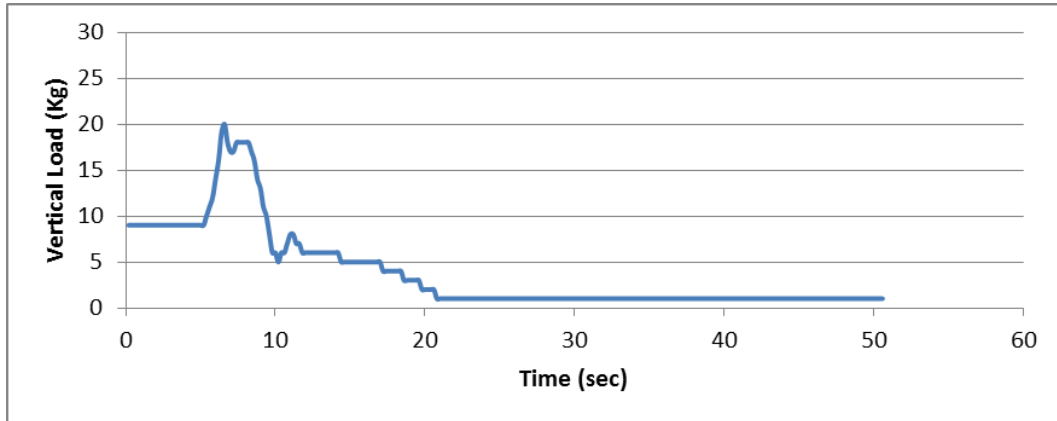


- Strusch, 1998 J. Strusch and J. Schwedes, Wall Stress Distributions in Silos with Inserts and Loads on Inserts, in: Silos: Fundamentals of Theory, Behaviour and Design, Brown and Nielsen (Eds), 1998
- Sudgen, 1980 M.B. Sugden. Effect of Initial Density on Flow Patterns in Circular Flat Bottomed Silos, Proceedings International Conference on Design of Silos for Strength and Flow, University of Lancaster, 1980
- Tedea, 2015 Tedea-Huntleigh, Aluminium High Capacity Single-Point Load Cell, <http://www.vishaypg.com/docs/12019/1260.pdf>, visited May 2015
- Tedea, 2015<sub>2</sub> Tedea-Huntleigh, 1004 Single-Point Load Cell, <http://docs-europe.electrocomponents.com/webdocs/010f/0900766b8010f46a.pdf>, visited May 2015
- Tuzun, 1985<sub>1</sub> U. Tuzun, R.M. Nedderman, Gravity Flow of Granular Material Round Obstacles I, Chemical Engineering Science, Vol 40, 1985
- Tuzun, 1985<sub>2</sub> U. Tuzun, R.M. Nedderman, Gravity Flow of Granular Material Round Obstacles II, Chemical Engineering Science, Vol 40, 1985
- Vaynshteyn, 2006 M. Vaynshteyn and P.M. Wegman, Bin Partitions to Improve Material Flow, United States Patent US 7,114,638 B2, 2006
- Watson, 1976 L.A. Watson. Discharge from Hoppers, United States Patent 3,940,037: 1976
- Williams, 1958 G.M. Williams, Flow Control Baffle for Granular Material, United States Patent 2,843,274; 1958
- Wójcik, 2007 M. Wójcik et al, Experimental Investigation of the Flow Pattern and Wall Pressure Distribution in a Silo with a Double-Cone Insert, Part. Part. Syst. Charact., Vol. 24, 2007
- Wójcik, 2012 M. Wójcik, J. Tejchman and G. G. Enstad, Confined granular flow in silos with inserts - Full-scale experiments. Powder Technology, Vol. 222, 2012
- Wójcik, 2008 M. Wójcik, Experimental and Theoretical Investigations of Flow Pattern and Wall Pressures in Silos with and without Inserts, PhD Thesis, Gdansk University of Technology, 2008
- Xiao, 2008 G. Xiao, D. Xu and S. Ding, Numerical Simulation Study upon Granular Materials Flow in Silos, Proceedings of RELPOFLOW IV, 2008

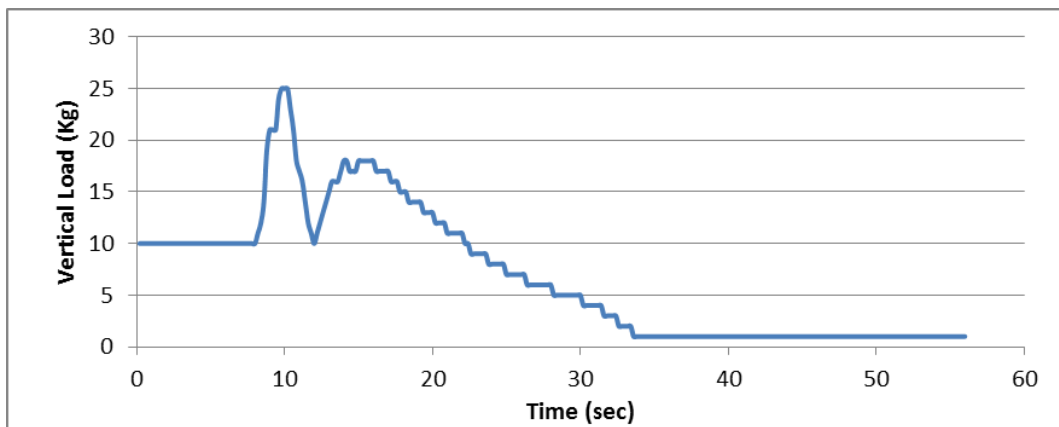
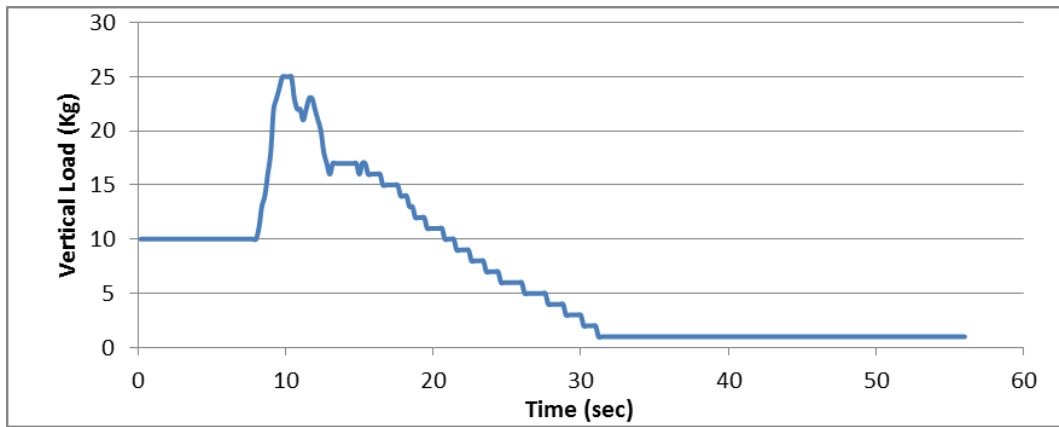
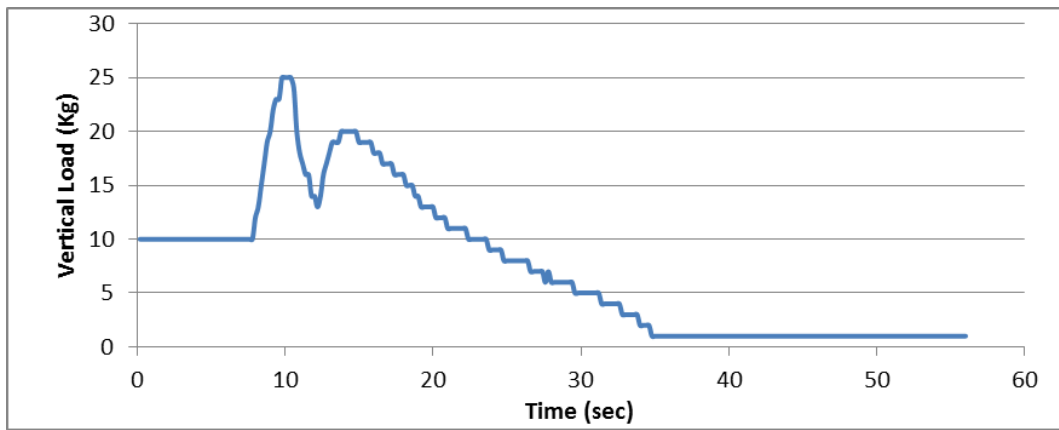
## APPENDIX A: Supporting Data for Chapter 3

---

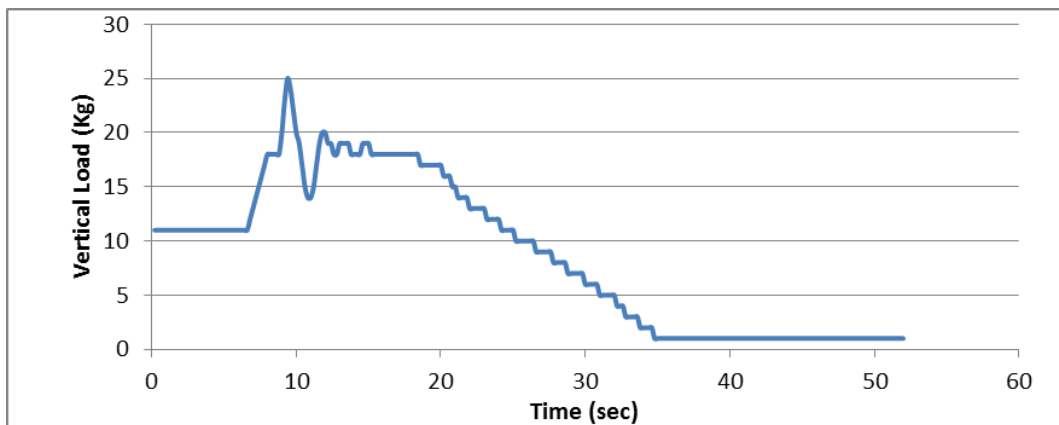
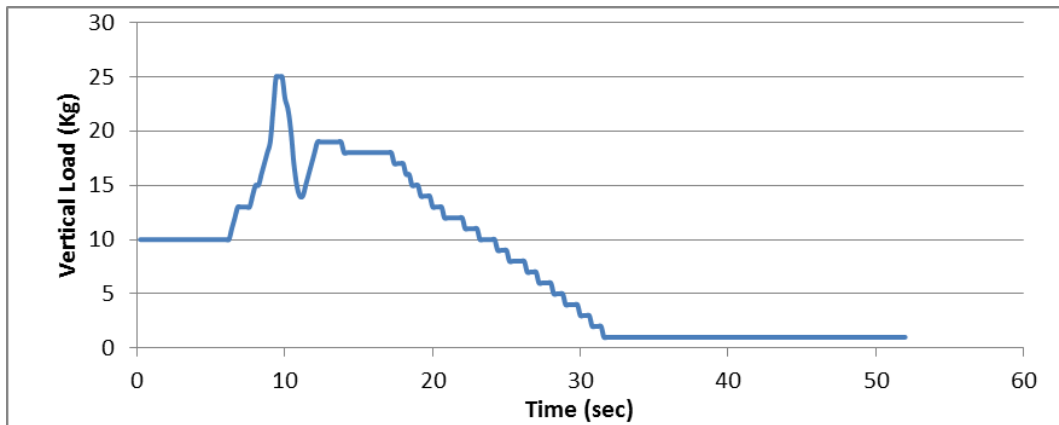
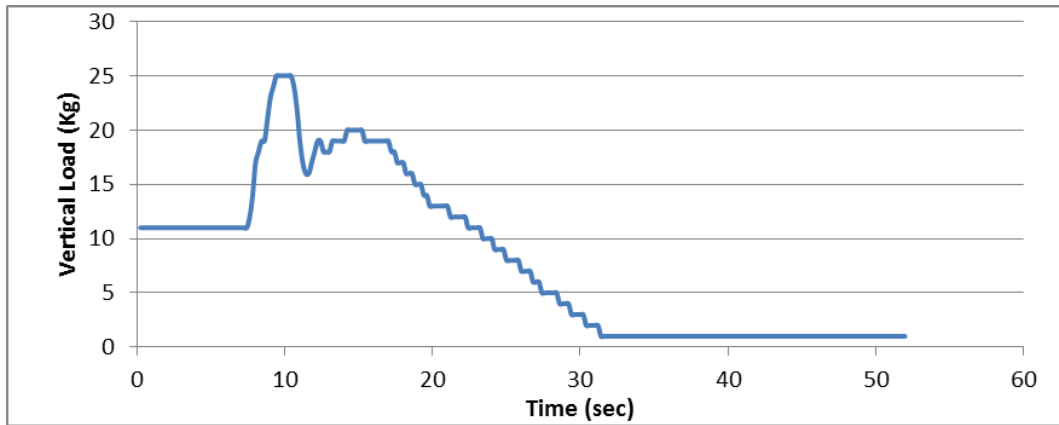
### Measurements of the Vertical Load Acting on the Large Insert Position A



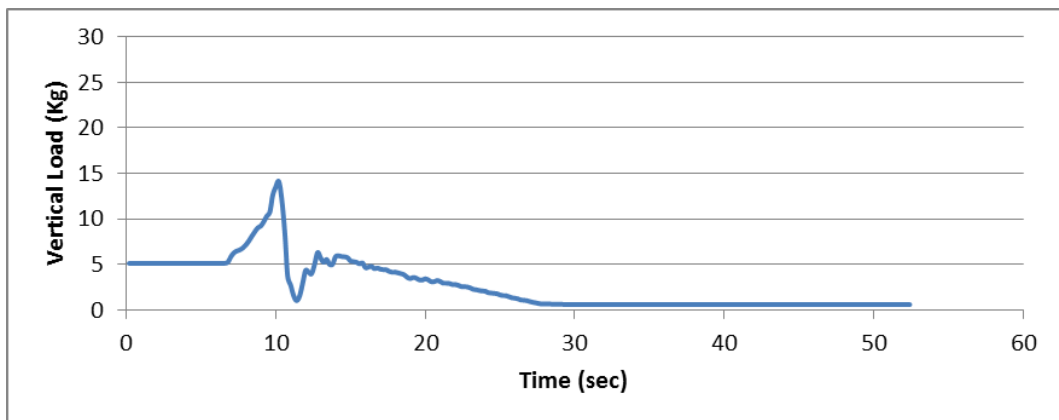
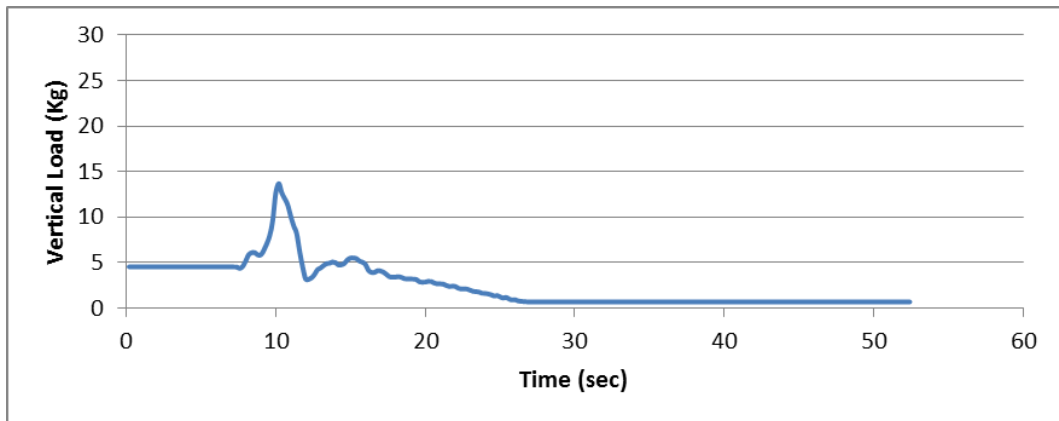
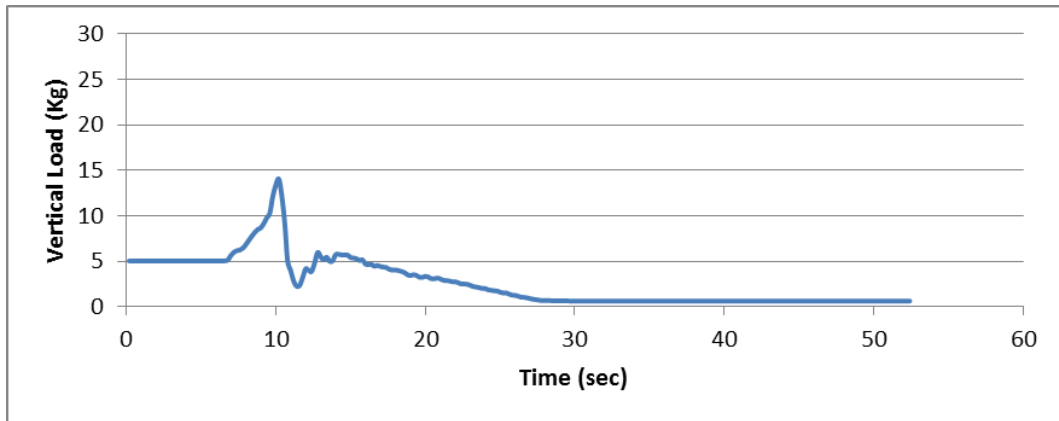
### Measurements of the Vertical Load Acting on the Large Insert Position B



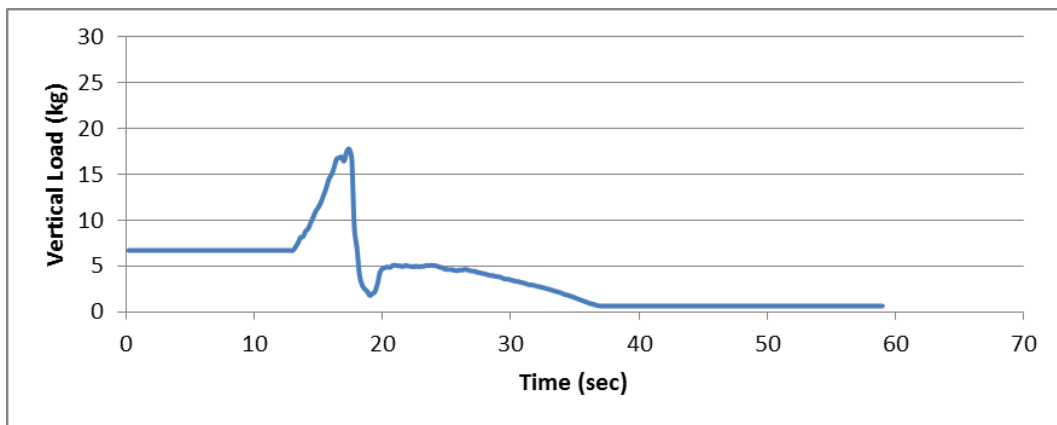
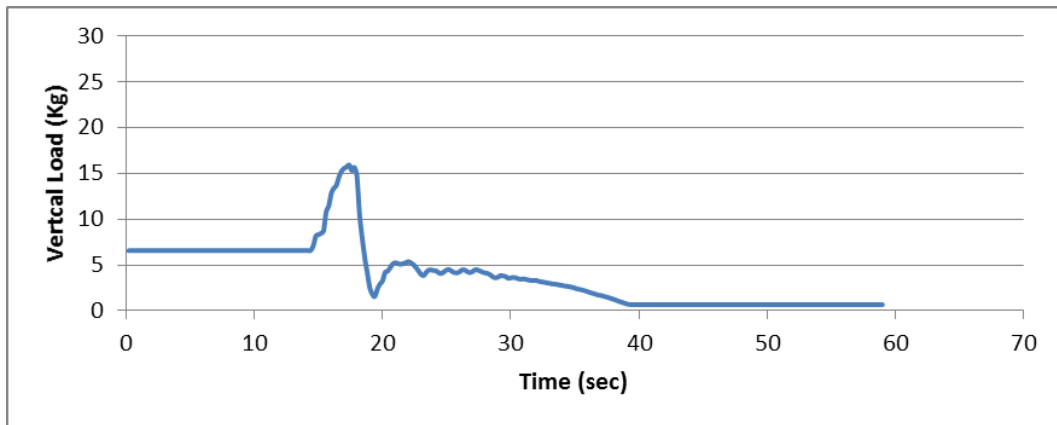
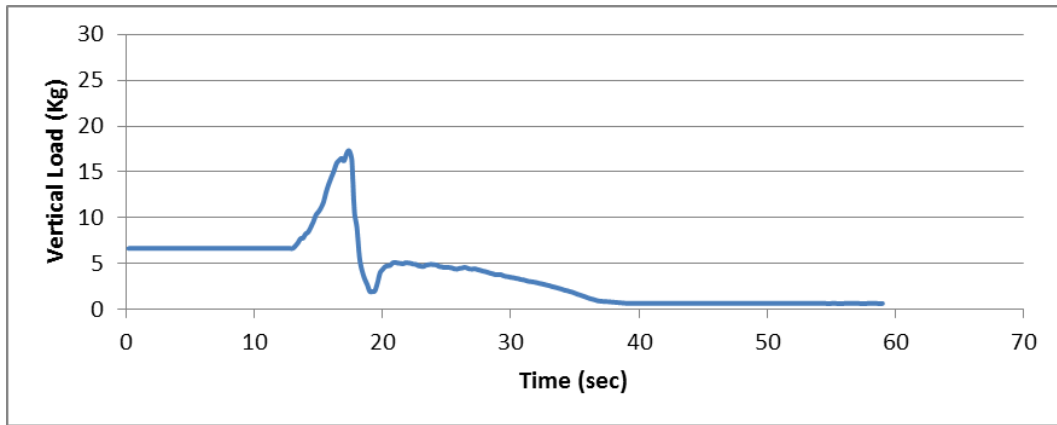
### Measurements of the Vertical Load Acting on the Large Insert Position C



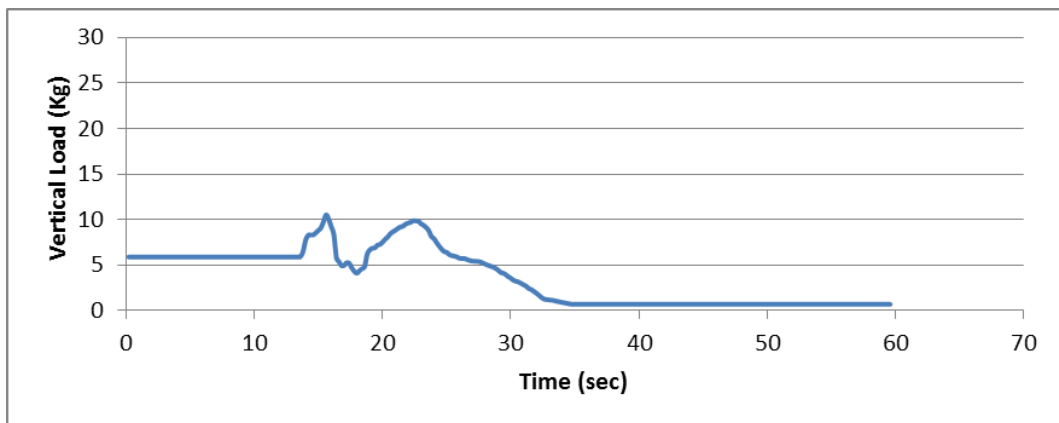
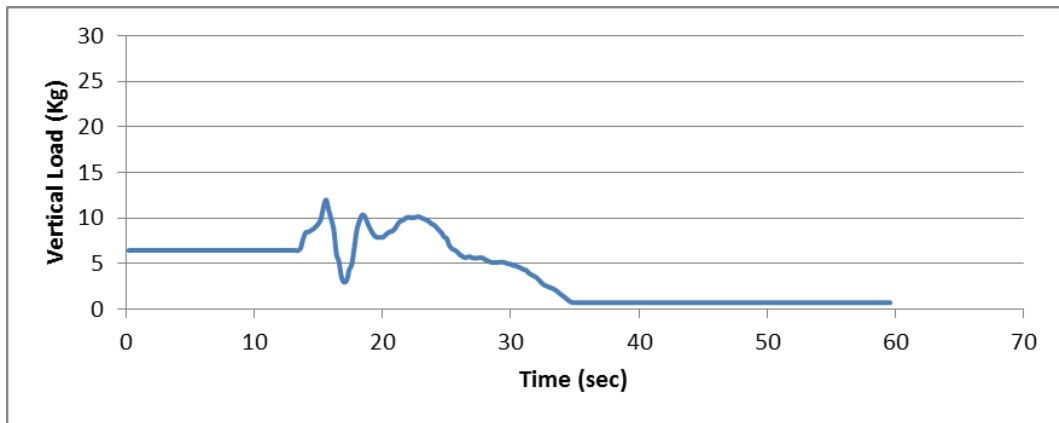
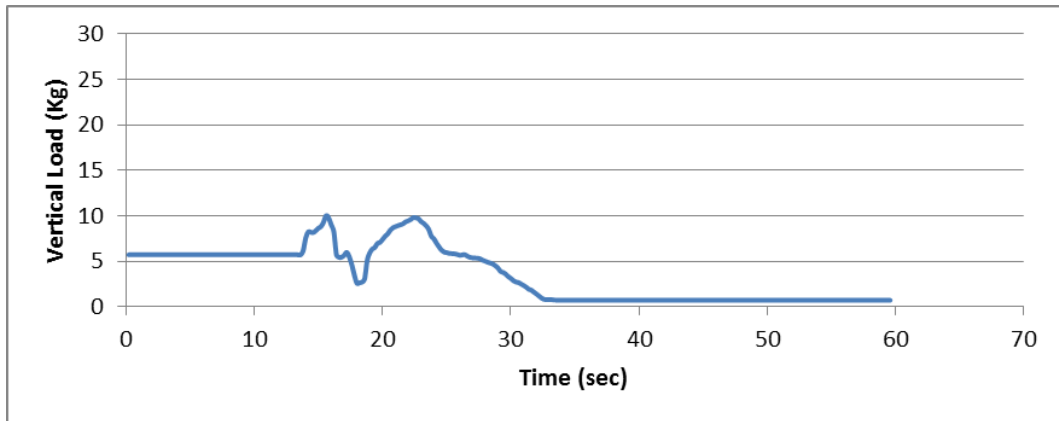
### Measurements of the Vertical Load Acting on the Small Insert Position A



## Measurements of the Vertical Load Acting on the Small Insert Position C



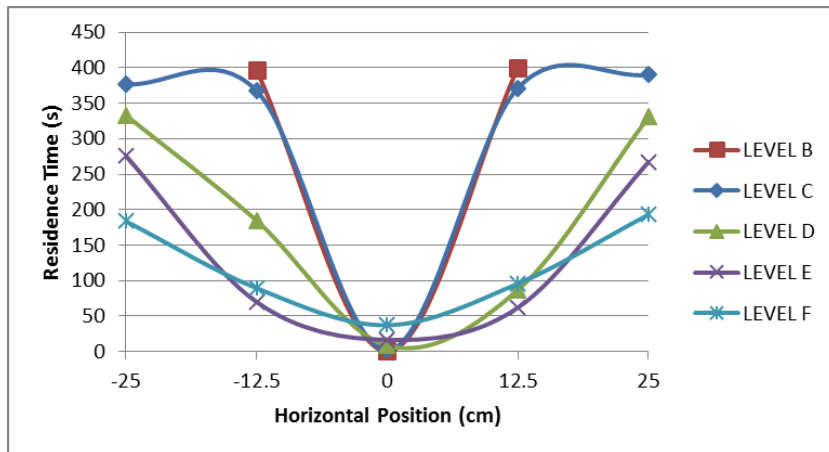
### Measurements of the Vertical Load Acting on the Small Insert Position C



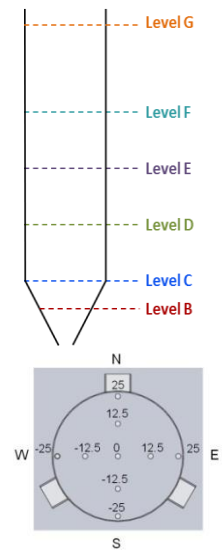
## APPENDIX B: Supporting Data for Chapter 4

### Variable Head of Powder - Flow Pattern Results (No Insert)

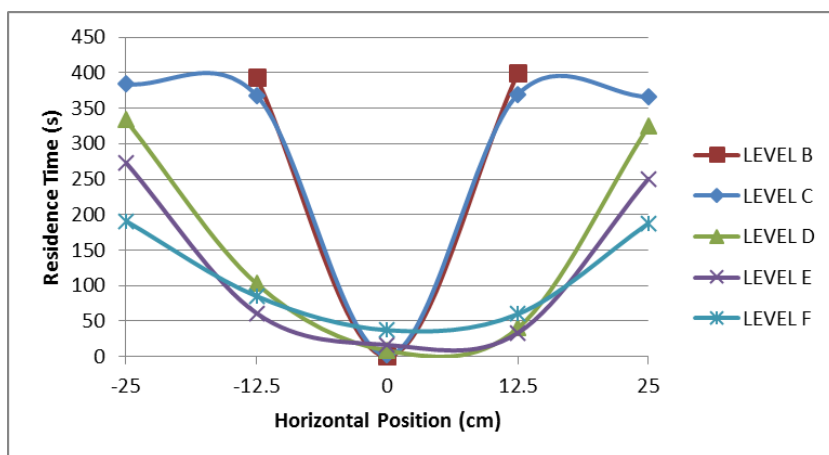
**South - North**



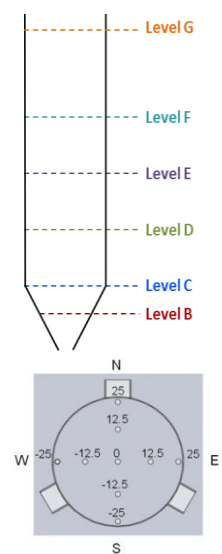
**TEST 1**



**West - East**

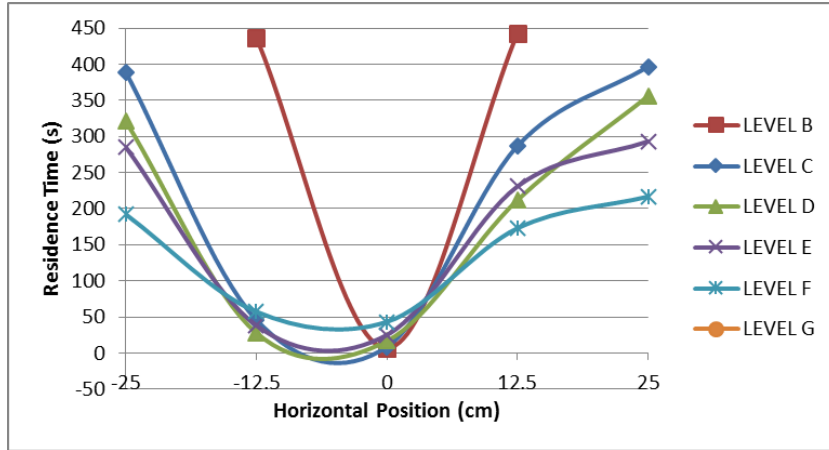


**TEST 1**

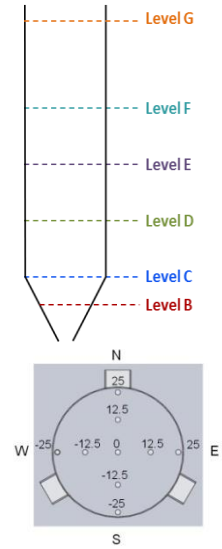


## Variable Head of Powder - Flow Pattern Results (No Insert)

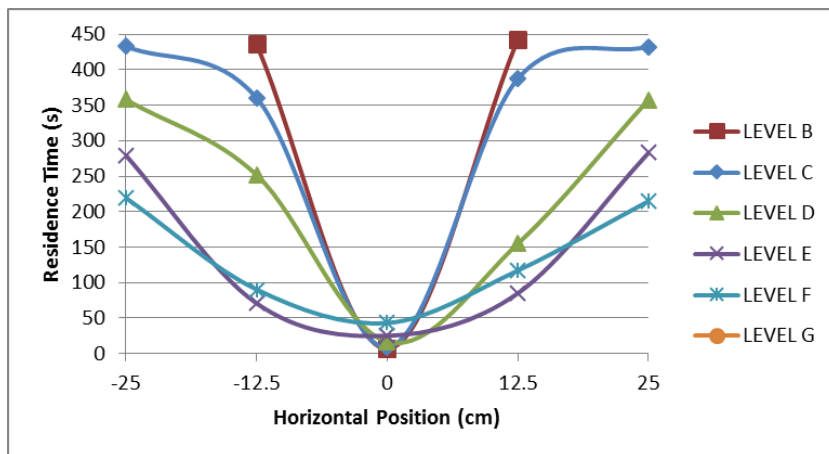
### South - North



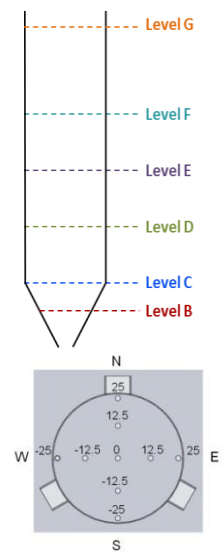
### TEST 2



### West - East

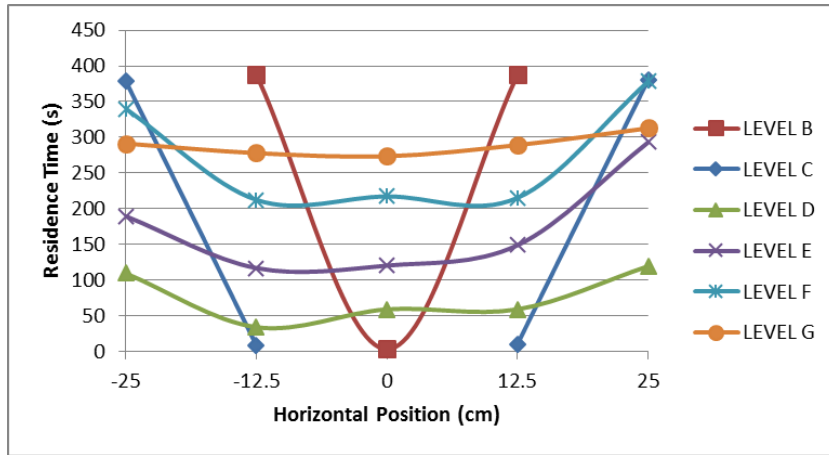


### TEST 2

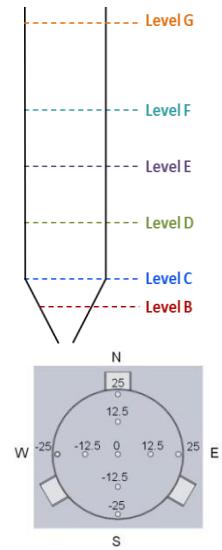


## Variable Head of Powder - Flow Pattern Results (Small Insert)

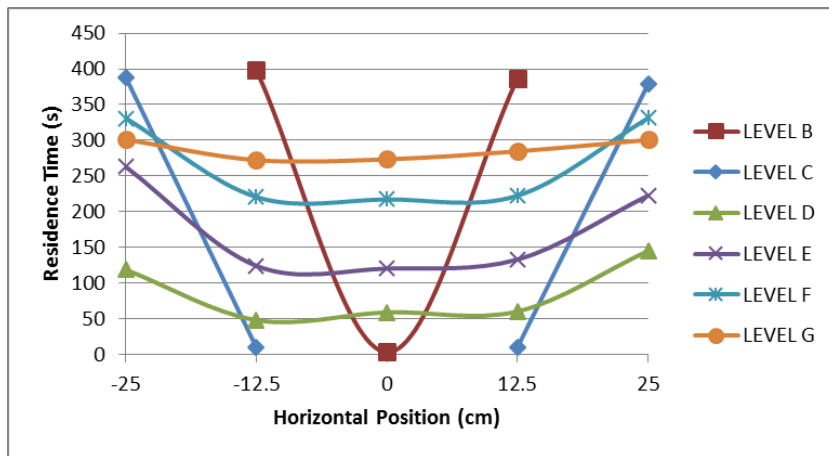
### South - North



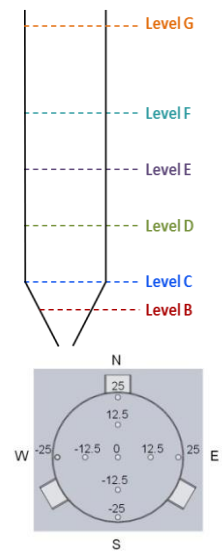
### TEST 1



### West - East

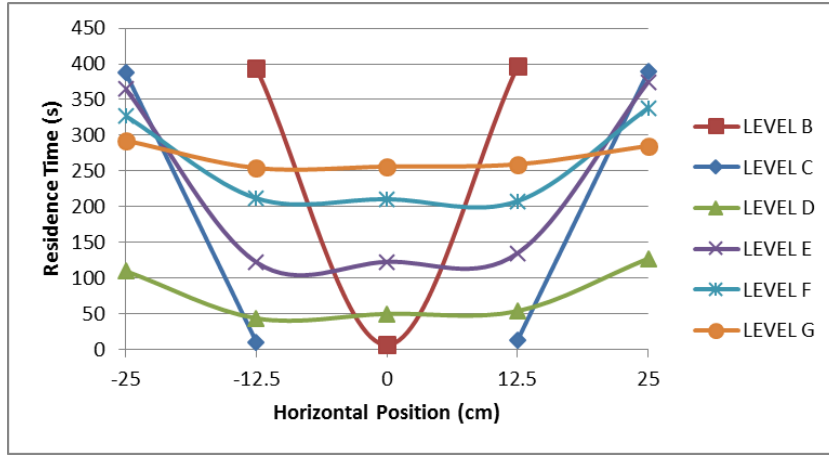


### TEST 1

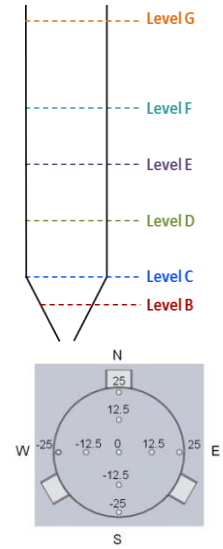


## Variable Head of Powder - Flow Pattern Results (Small Insert)

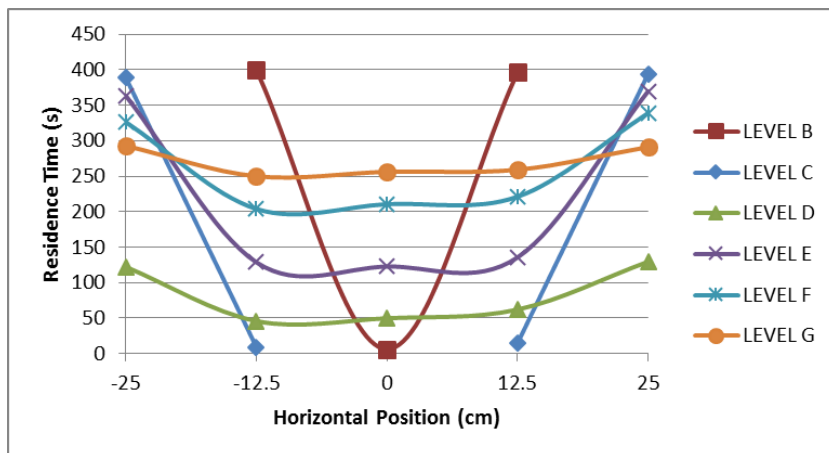
### South - North



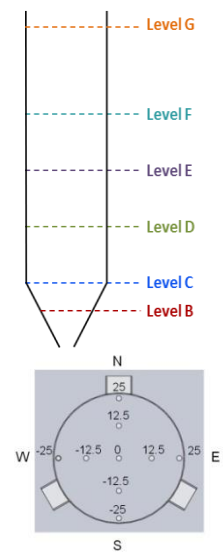
### TEST 2



### West - East

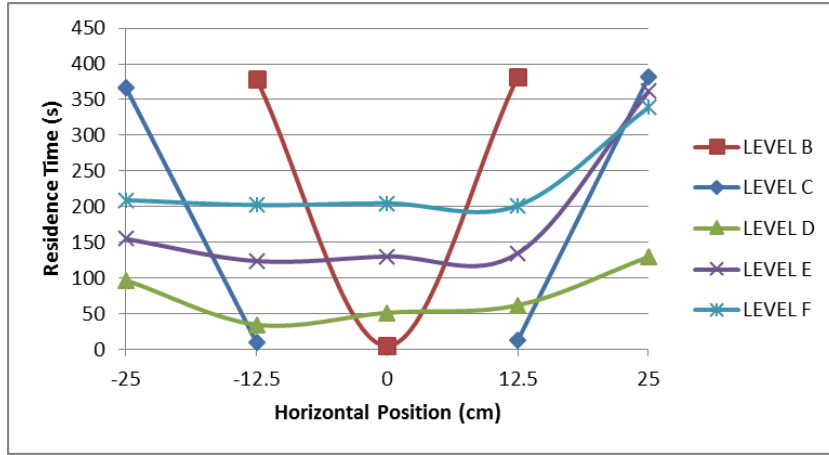


### TEST 2

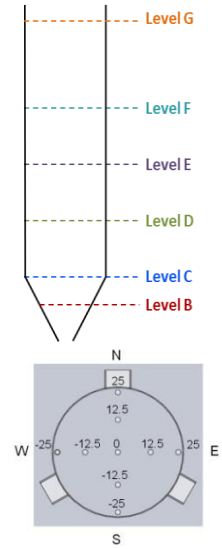


## Variable Head of Powder - Flow Pattern Results (Small Insert)

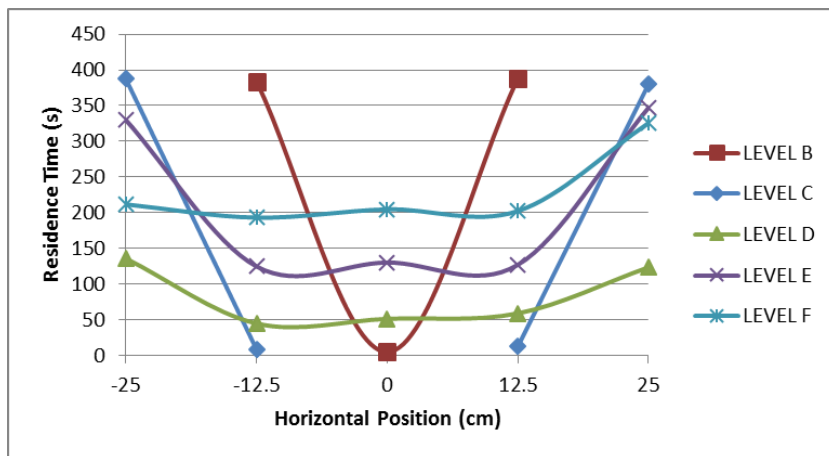
### South - North



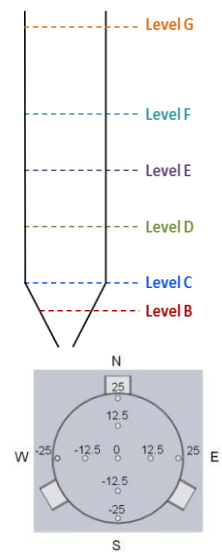
### TEST 3



### West - East

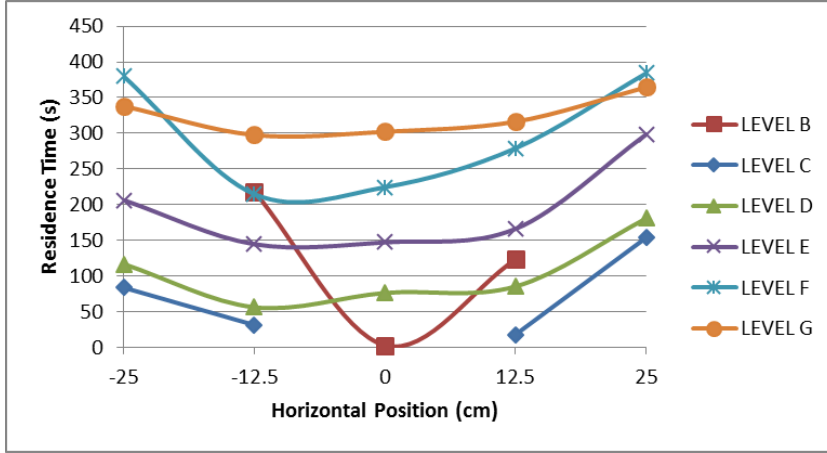


### TEST 3

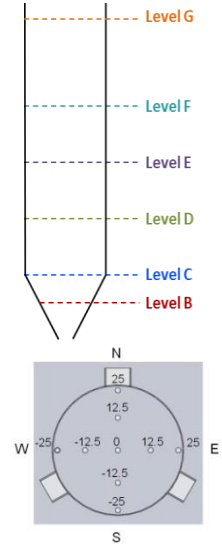


# Variable Head of Powder - Flow Pattern Results (Large Insert)

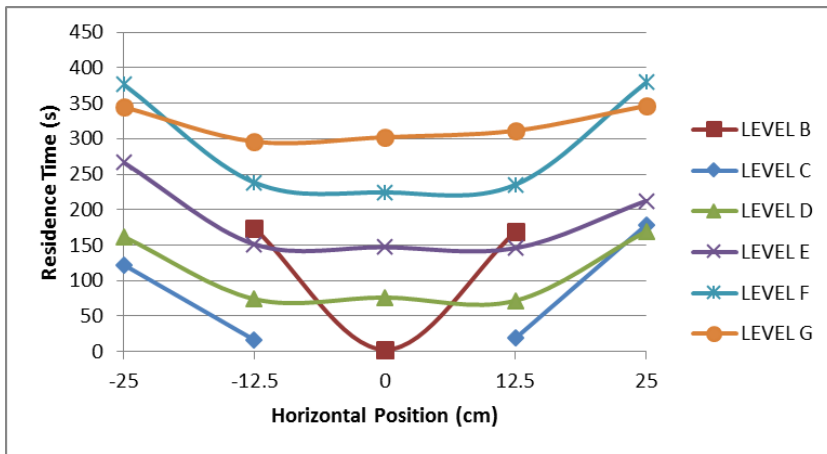
## South - North



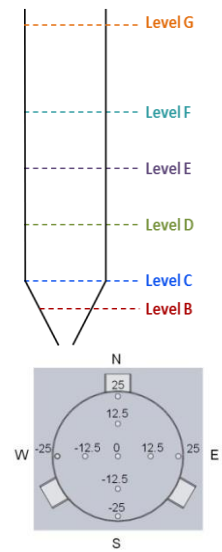
## TEST 1



## West - East

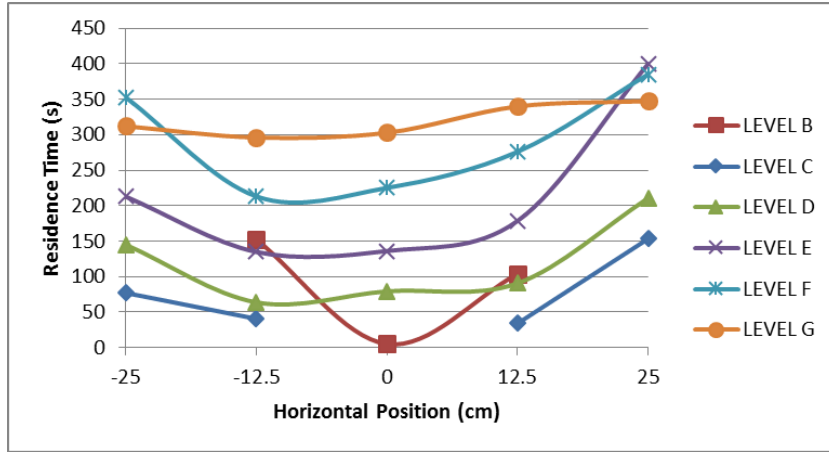


## TEST 1

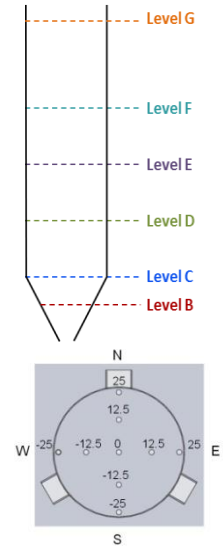


## Variable Head of Powder - Flow Pattern Results (Large Insert)

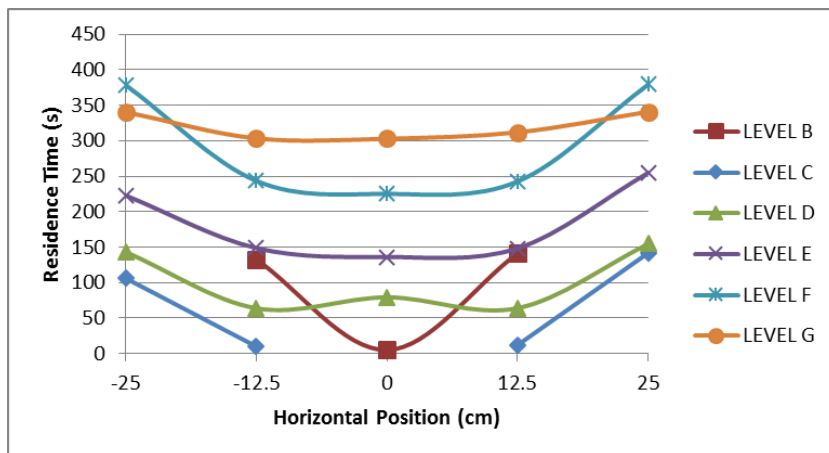
### South - North



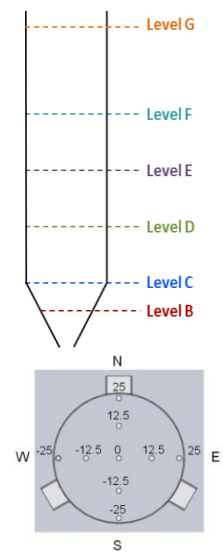
### TEST 2



### West - East

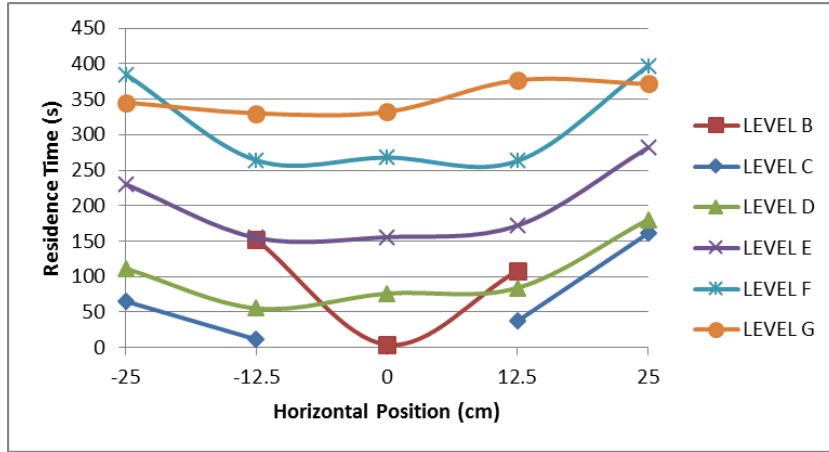


### TEST 2

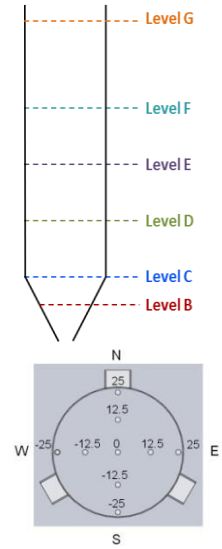


## Variable Head of Powder - Flow Pattern Results (Large Insert)

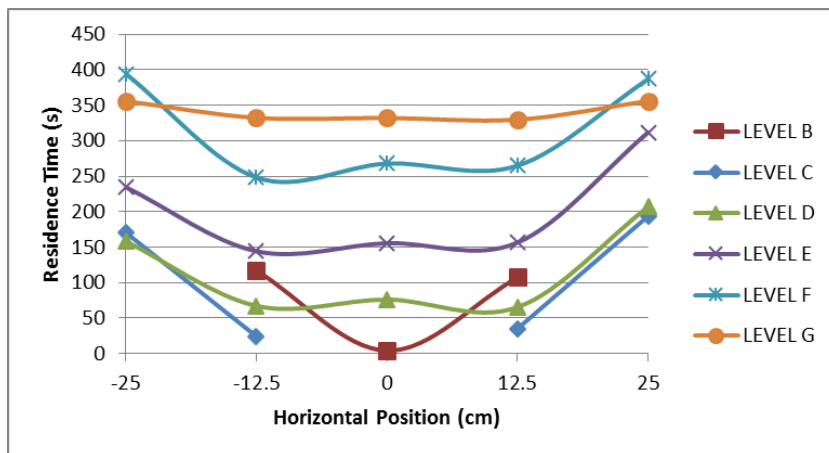
### South - North



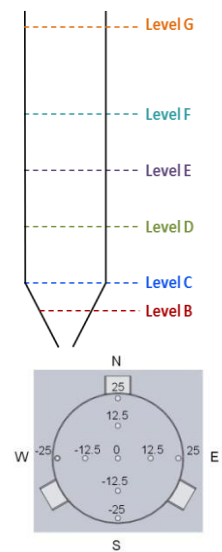
### TEST 3



### West - East

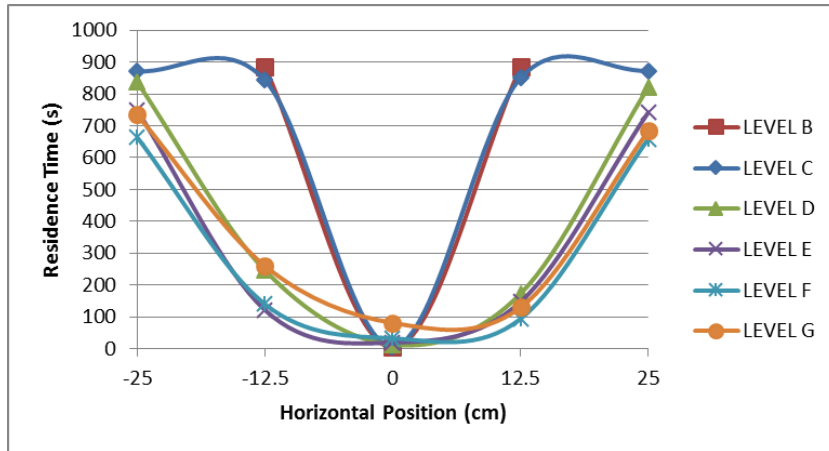


### TEST 3

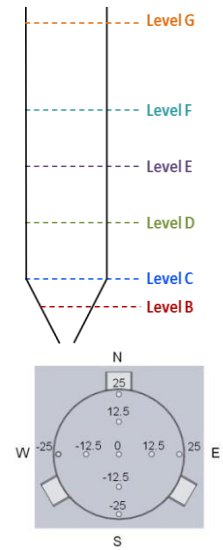


## Constant Head of Powder - Flow Pattern Results (No Insert)

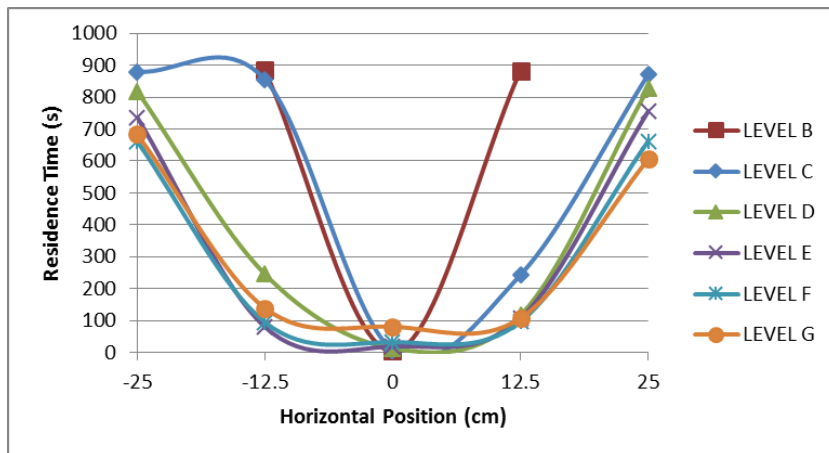
### South - North



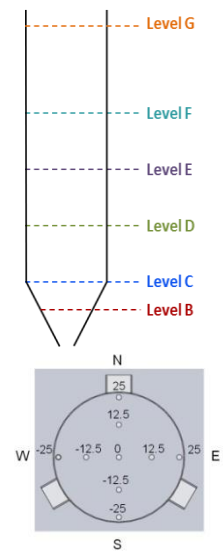
### TEST 1



### West - East

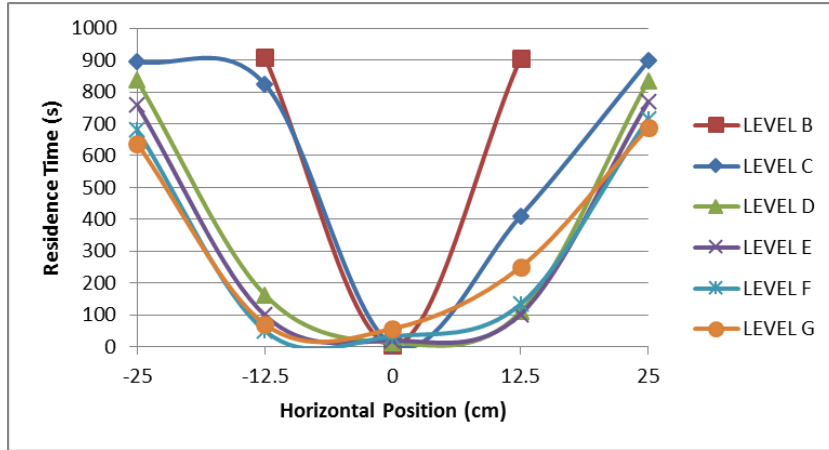


### TEST 1

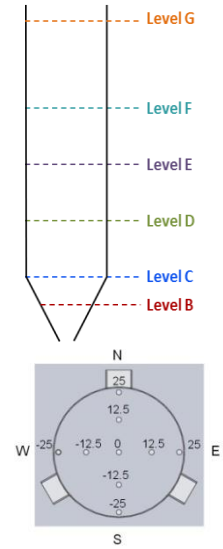


## Constant Head of Powder - Flow Pattern Results (No Insert)

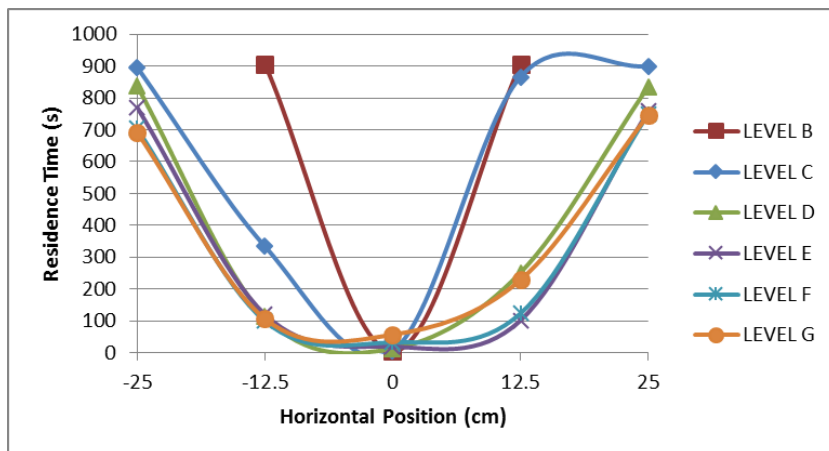
### South - North



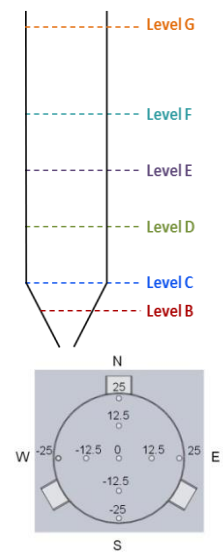
### TEST 2



### West - East

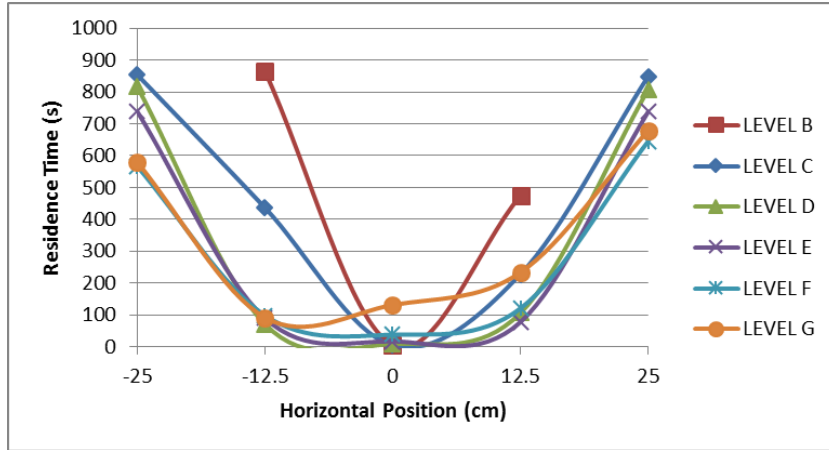


### TEST 2

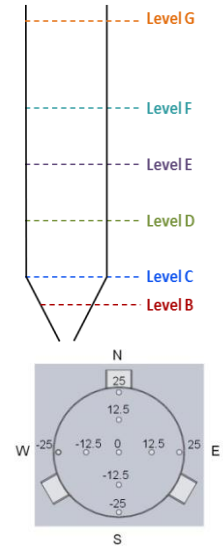


## Constant Head of Powder - Flow Pattern Results (No Insert)

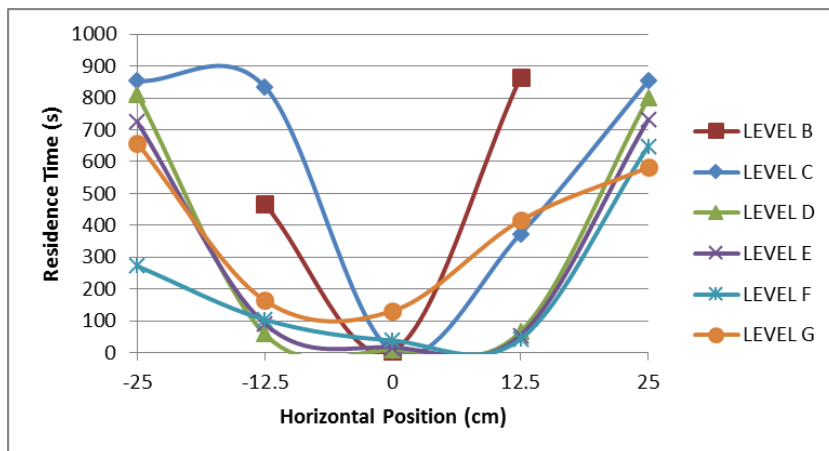
### South - North



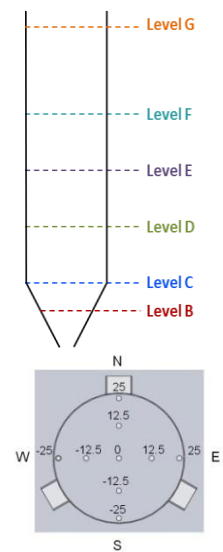
### TEST 3



### West - East

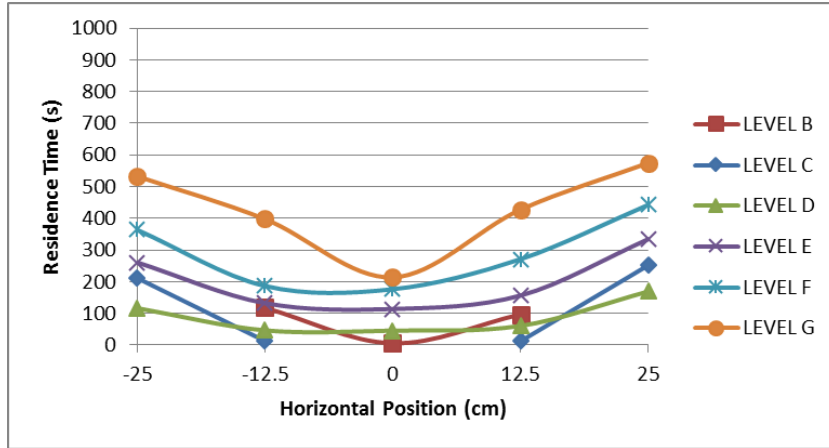


### TEST 3

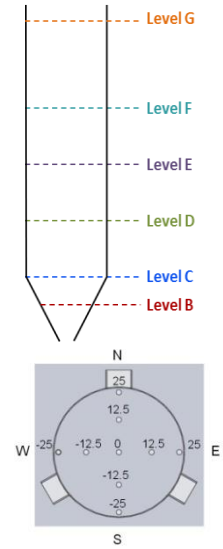


## Constant Head of Powder - Flow Pattern Results (Small Insert)

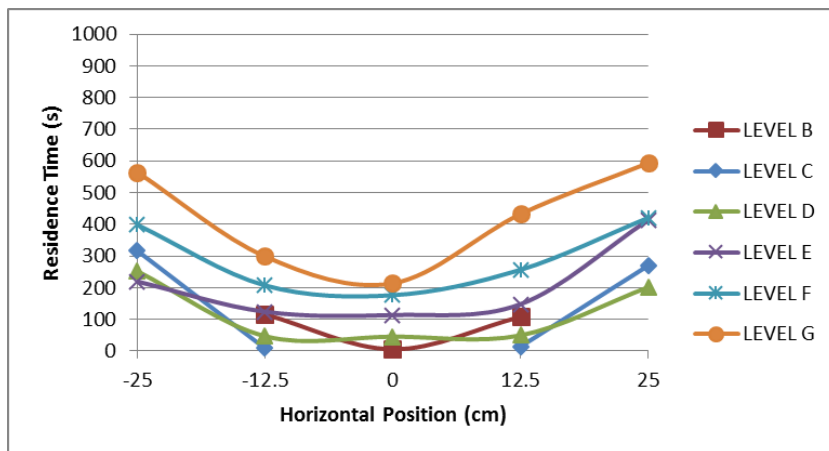
### South - North



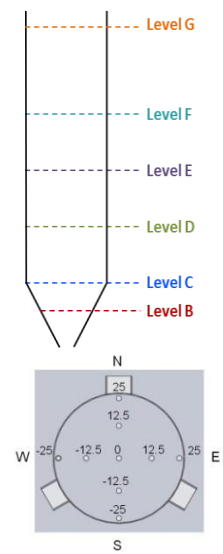
### TEST 1



### West - East

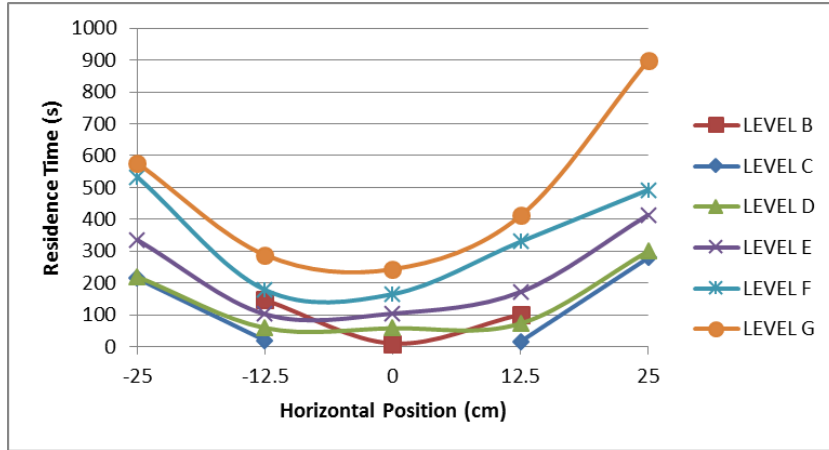


### TEST 1

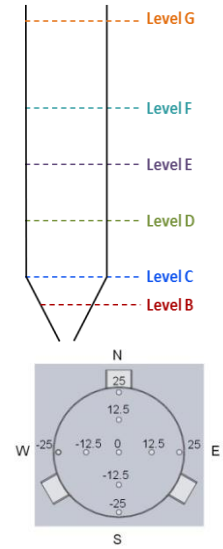


## Constant Head of Powder - Flow Pattern Results (Small Insert)

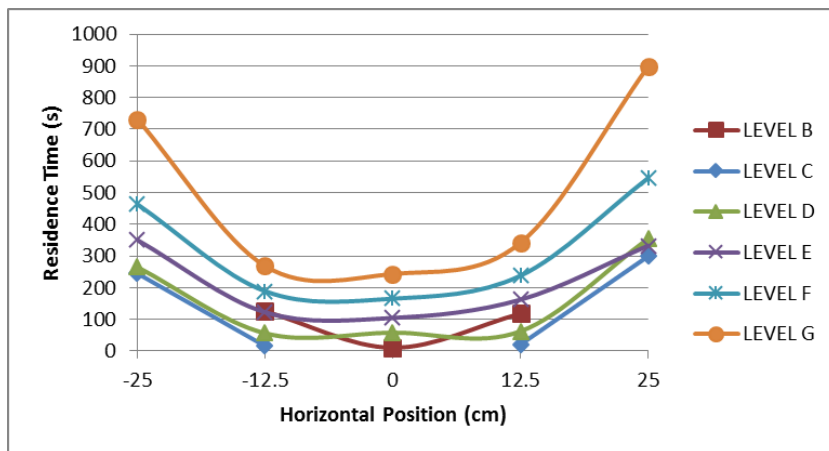
### South - North



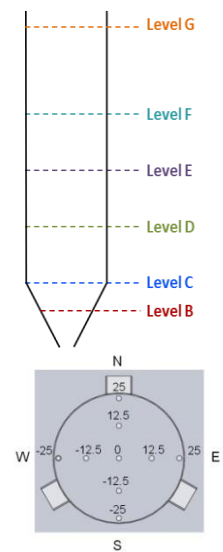
### TEST 2



### West - East

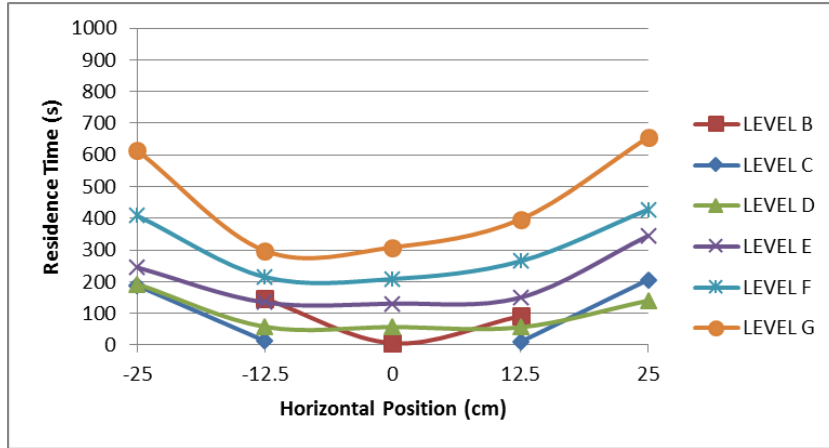


### TEST 2

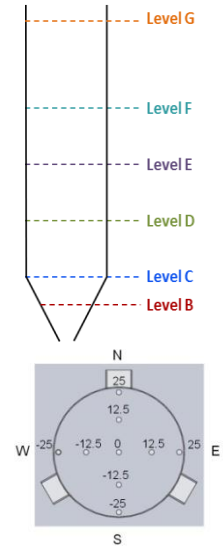


## Constant Head of Powder - Flow Pattern Results (Small Insert)

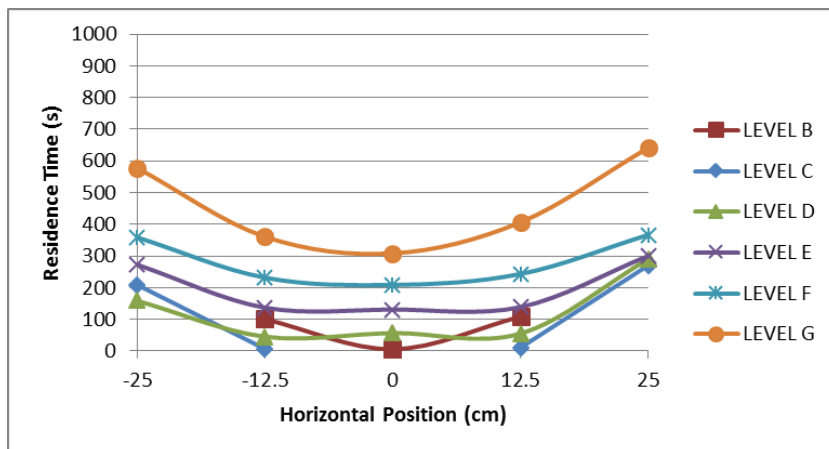
### South - North



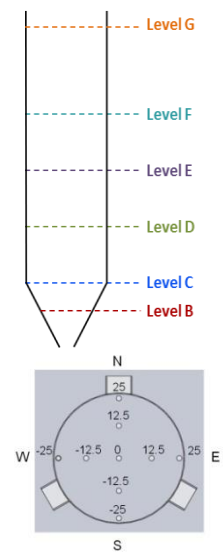
### TEST 3



### West - East

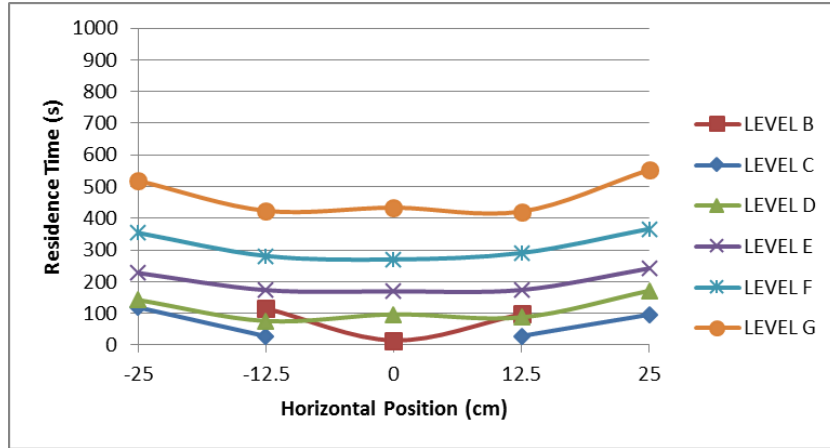


### TEST 3

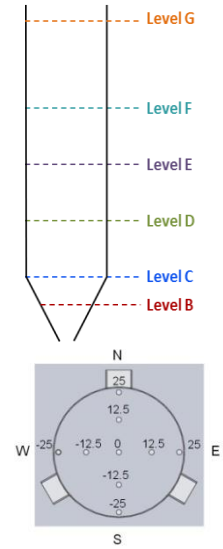


## Constant Head of Powder - Flow Pattern Results (Large Insert)

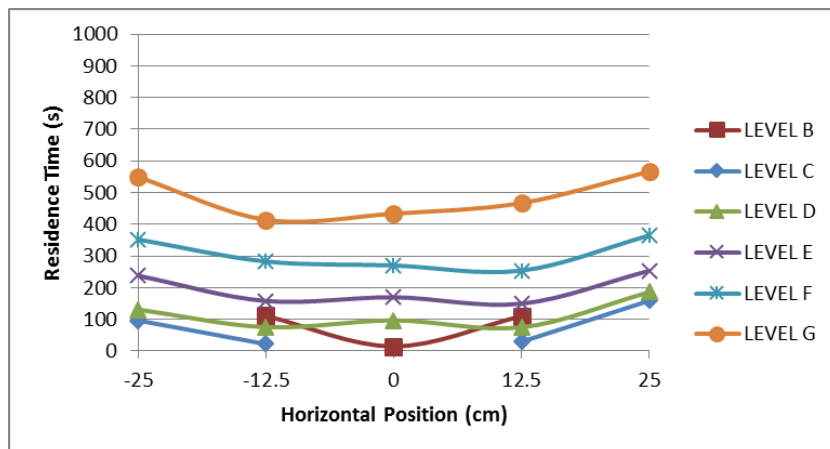
### South - North



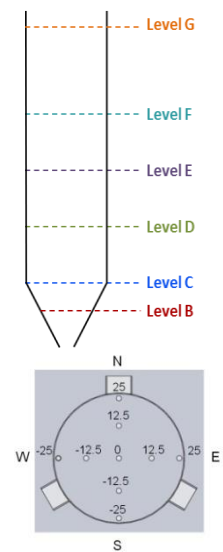
### TEST 1



### West - East

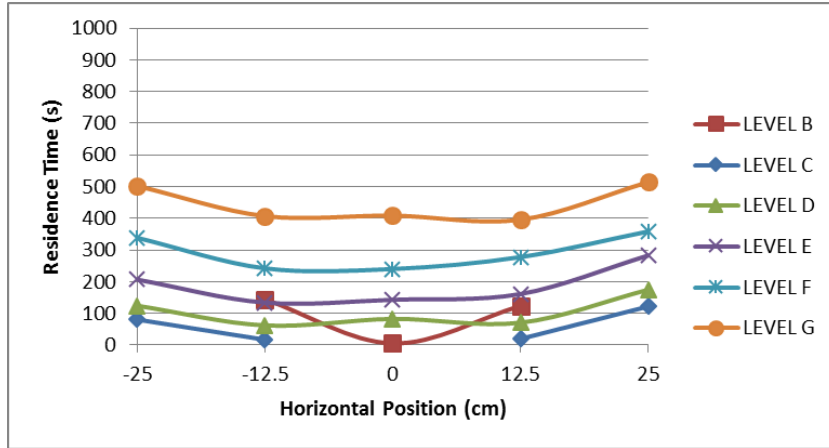


### TEST 1

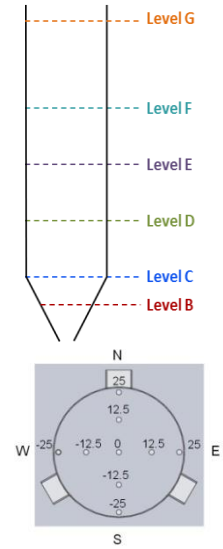


## Constant Head of Powder - Flow Pattern Results (Large Insert)

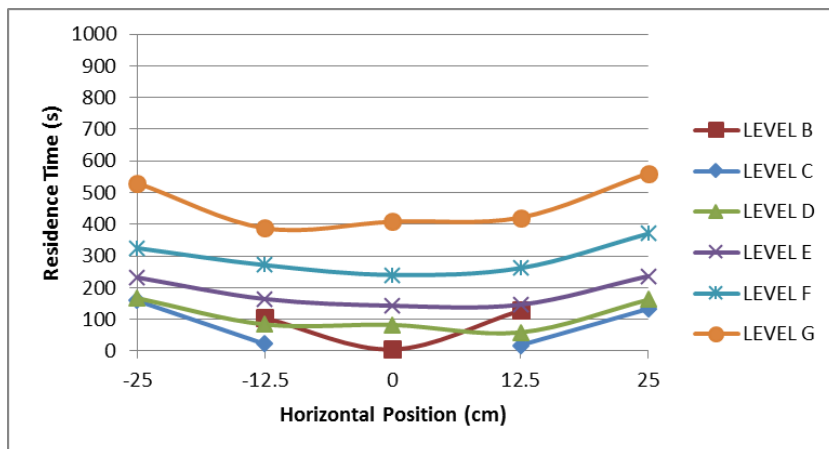
### South - North



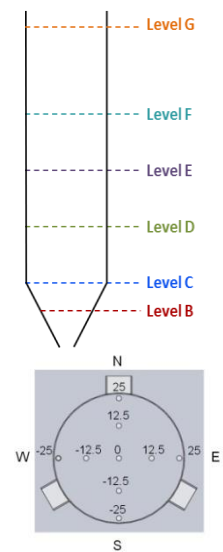
### TEST 2



### West - East

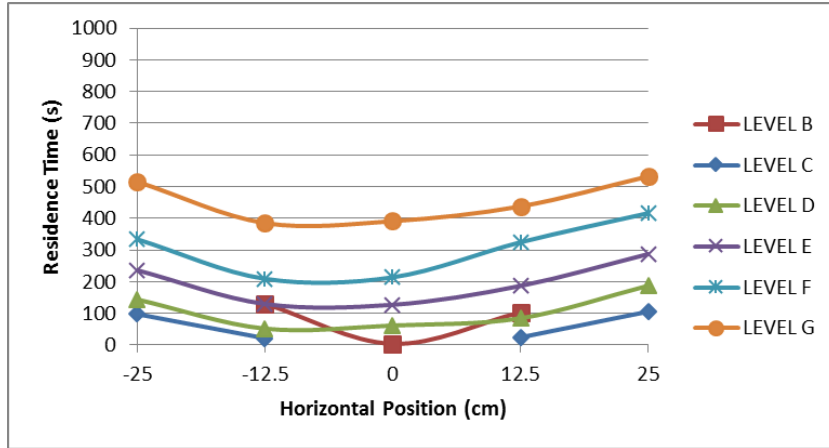


### TEST 2

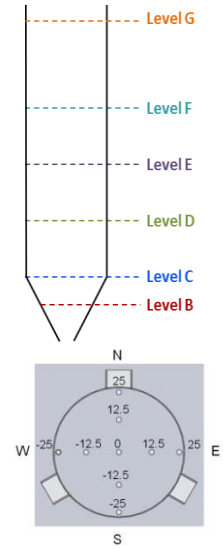


## Constant Head of Powder - Flow Pattern Results (Large Insert)

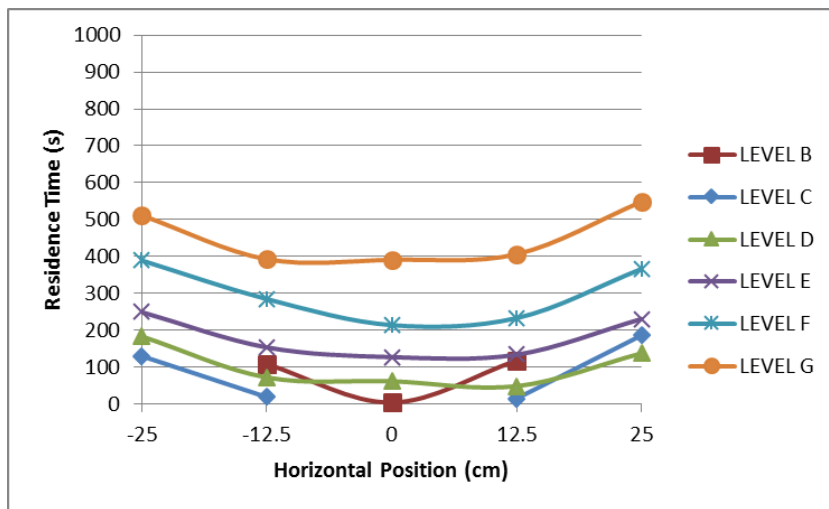
### South - North



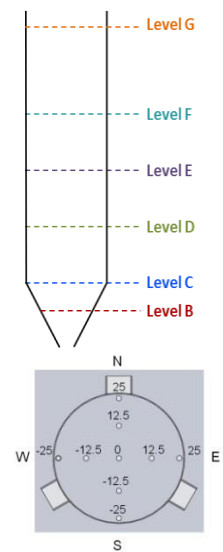
### TEST 3



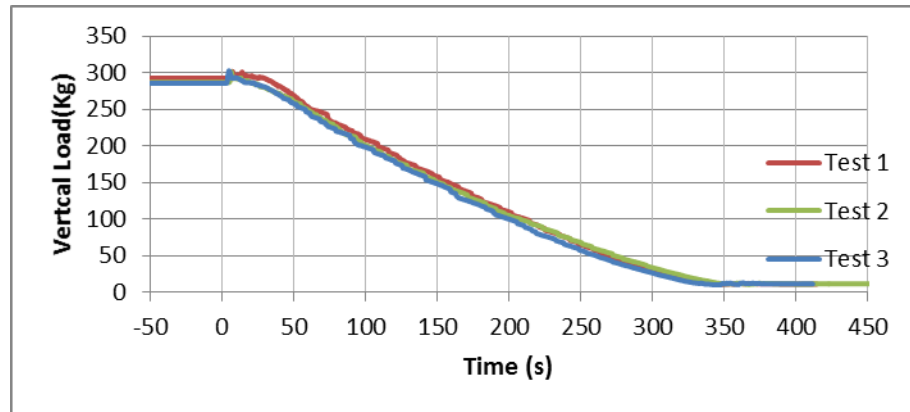
### West - East



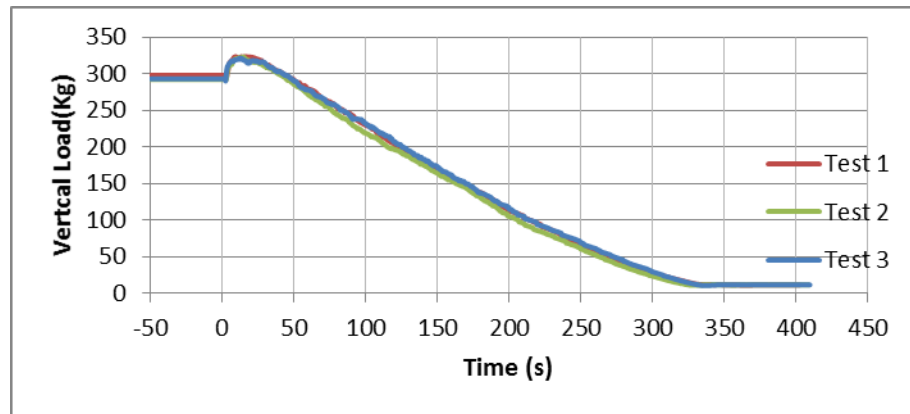
### TEST 3



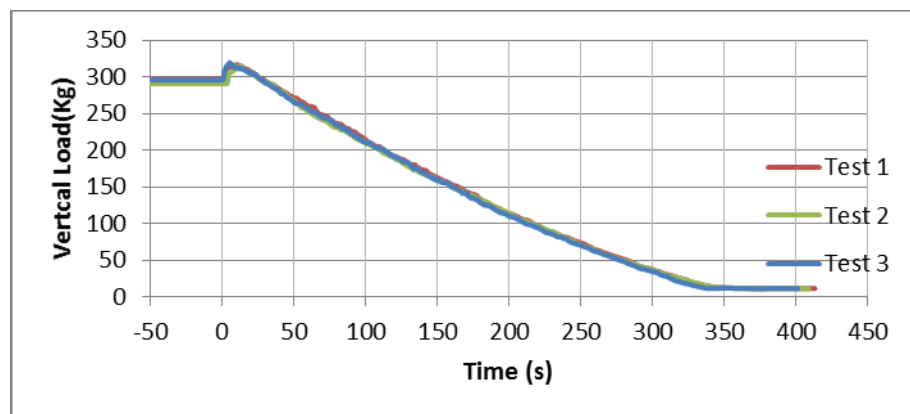
## Vertical Load Acting on the Cylindrical Section - Variable Head of Powder



No Insert

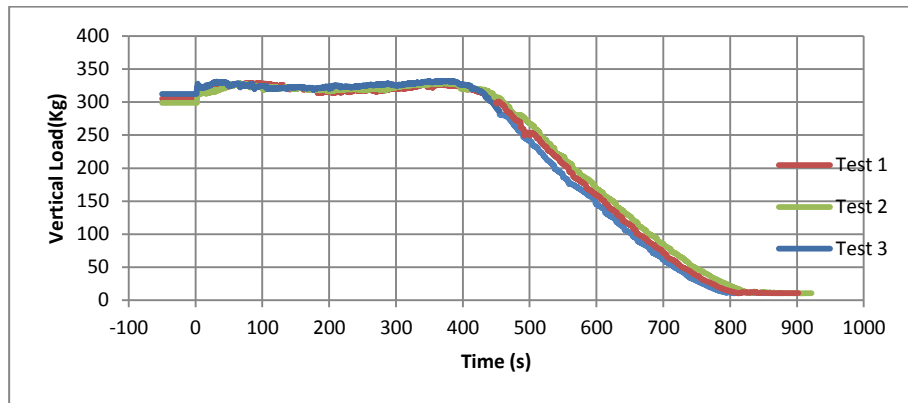


Small Insert

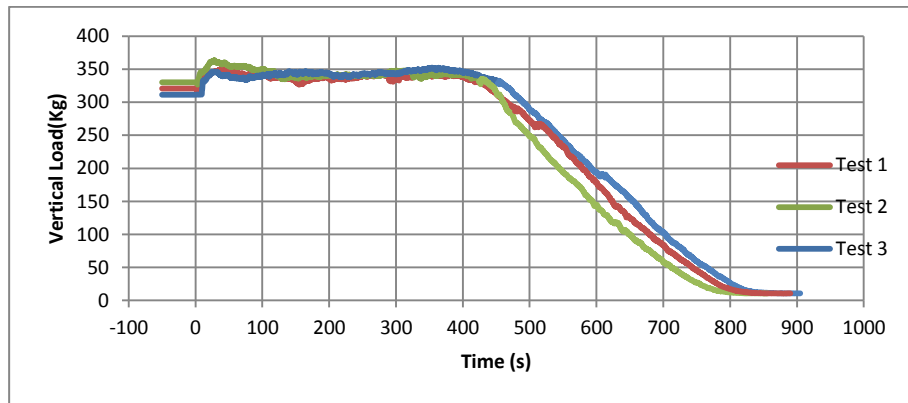


Large Insert

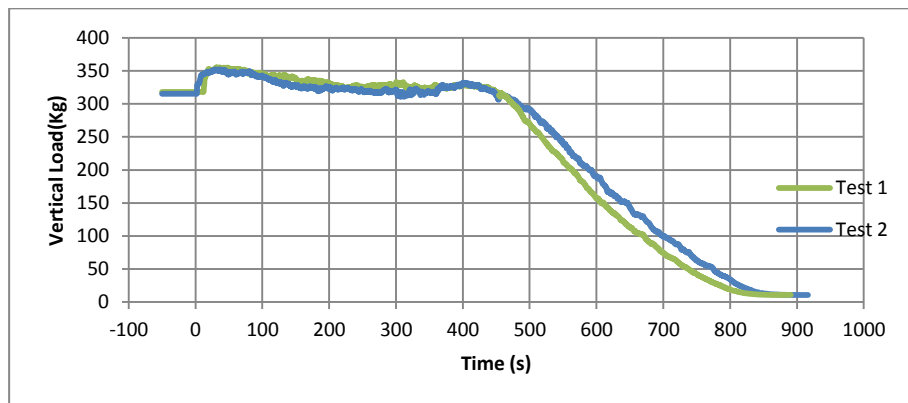
## Vertical Load Acting on the Cylindrical Section - Constant Head of Powder



**No Insert**

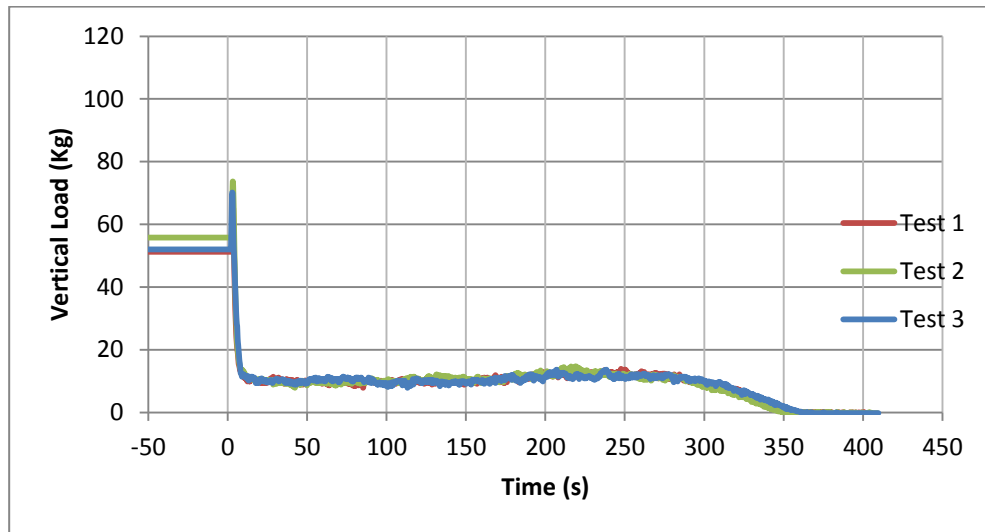


**Small Insert**

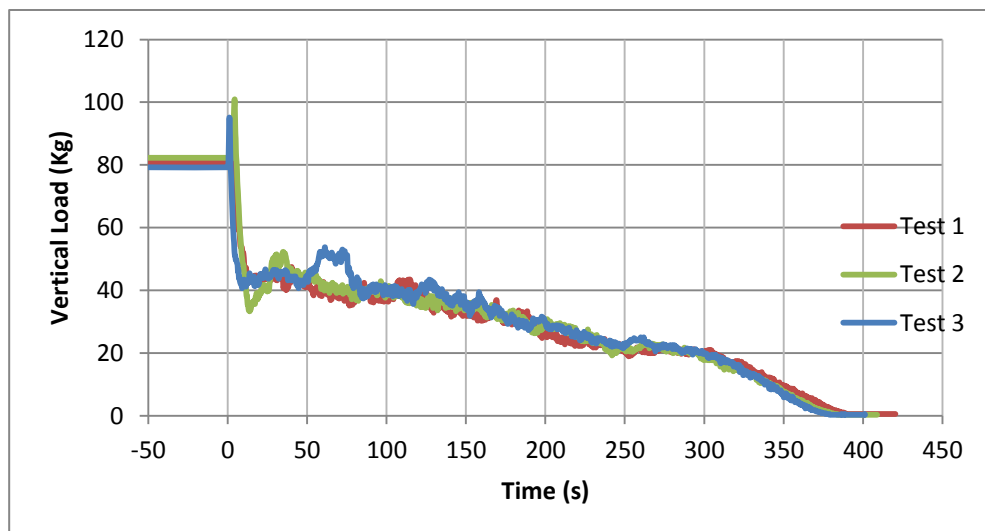


**Large Insert**

## Vertical Load Acting on the Insert - Variable Head of Powder

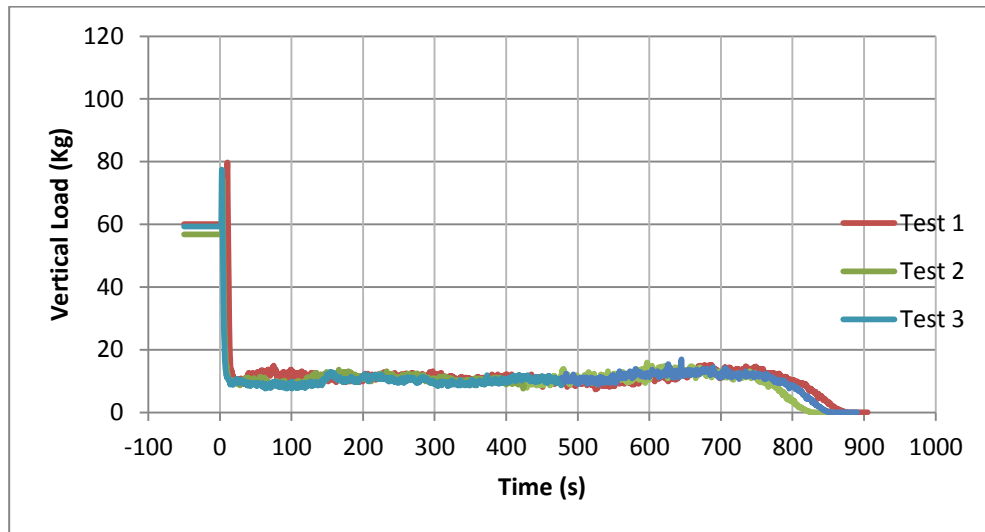


Small Insert

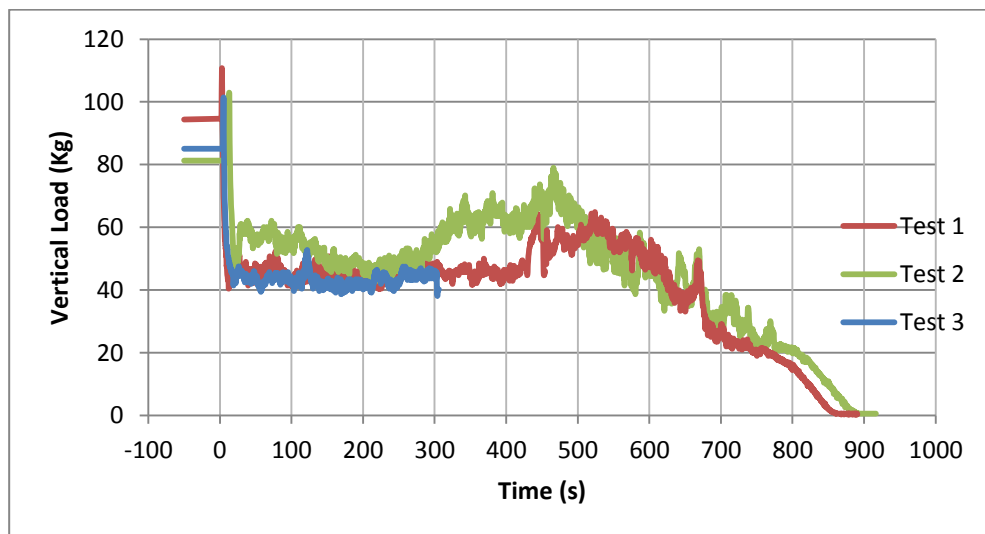


Large Insert

## Vertical Load Acting on the Insert - Constant Head of Powder



Small Insert



Large Insert